ROCKBURST HANDBOOK

FOR

ONTARIO HARDROCK MINES

D.G.F. Hedley

Mining Research Laboratories

CANMET Special Report SP92-1E

Available in Canada through

Authorized Bookstore Agents
and other bookstores

or by mail from

Canada Communication Group – Publishing
Ottawa, Canada K1A 0S9

Cat. No. M38–15/92-1E
ISBN 0–660–14549–9

Contributions have been made by:

D. Ames (*Ontario Ministry of Labour*), B. Arjang (*CANMET*), S. Bharti (*formerly Falconbridge Ltd.*), W. Blake (*Consultant*), M. Board (*Itasca*), W. Bromell (*Falconbridge Ltd.*), R. Brummer (*Golder Associates*), P. Campbell (*formerly Ontario Ministry of Labour*), C. Graham (*Mining Research Directorate*), D. Hanson (*formerly CANMET*), R. Hong (*Lac Minerals Ltd.*), P. Kaiser (*Geomechanics Research Centre, Laurentian University*), M. Kat (*Ontario Ministry of Labour*), L. Langdon (*Rio Algom Ltd.*), D. Lebel (*CANMET*), W. Logan (*Ontario Ministry of Northern Development and Mines*), P. MacDonald (*formerly Inco Ltd.*), A. Makuch (*Placer Dome Inc.*), S. Muppalaneni (*Rio Algom Ltd.*), M. Neumann (*formerly Placer Dome Inc.*), L. Ng (*Falconbridge Ltd.*), J. Niewiadomski (*formerly CANMET*), D. O'Donnell (*Inco Ltd.*), M. O'Flaherty (*Placer Dome Inc.*), M. Plouffe (*CANMET*), C. Pritchard (*Denison Mines Ltd.*), W. Quesnel (*Lac Minerals Ltd.*), P. Rochon (*CANMET*), T. Semadeni (*formerly CANMET*), A. Sheikh (*formerly Denison Mines Ltd.*), G. Swan (*Falconbridge Ltd.*), P. Townsend (*Denison Mines Ltd.*), J. Udd (*CANMET*), T. Villeneuve, (*Inco Ltd.*), B. Wetmiller (*Geological Survey of Canada*), P. Young (*Queen's University*).

PREFACE

Rockbursts, or sudden explosive rock fractures, occur when rock has been loaded beyond the failure point. In engineering terms, the stress in the rock exceeds its strength.

The stresses existing in rock masses naturally, as a result of tectonic processes, are disturbed by mined excavations such as tunnels or mine workings, or natural openings such as caverns. When such excavations are created, the state of equilibrium that previously existed is disturbed and a new equilibrium must be established. In essence, underground openings result in concentrations of stress around them. If these concentrations are less than the strength of the rock, a new equilibrium is established. If not, failure takes place.

Whether or not a rock will fail suddenly depends on its strength properties, the load applied to it, and the time during which the change of loading takes place. Contributing factors are the presence of weaknesses and stress concentrations in the rock mass, high pre-existing stresses, and shapes of excavations that result in particularly high stress concentrations. Long, narrow openings close to each other at great depth in hard brittle elastic rock have the greatest rockburst potential.

The rocks of the Canadian Shield and the conditions of mining in them have resulted in a high incidence of rockbursts on two occasions. In the early 1940s and beforehand, a significant part of Canada's mineral production was obtained from highly selective narrow-vein mining methods. The presence of many small openings at depth and a lack of knowledge of the stress concentrating effects of these upon each other led to a severe rockbursting problem, particularly in the gold mines of Ontario. The person responsible for my education as a mining engineer, the late Professor R.G.K. ("Bob") Morrison of McGill University in Montréal, was attracted to Canada from the Kolar Gold Field of India to address the problem. His knowledge of rockbursting in India, South Africa and elsewhere and the concept of sequential mining, which he introduced to Canadian practice, resulted in a much reduced frequency of rockbursting for many years.

In the 1970s, however, a new dimension was added to the problem. For reasons of cost efficiency and remaining competitive in international markets, the mining industry of Canada, and elsewhere, was being driven to use both larger underground production openings and bulk mining methods. Once again, in the early 1980s, rockbursting became a serious problem in Ontario mines.

In 1984, with leadership from the Canada Centre for Mineral and Energy Technology (CANMET), the Canada-Ontario-Industry Rockburst Project was initiated. The key feature of this $4.2-million, five-year initiative was that it was funded by the three partners on an equal basis and managed by tripartite technical and management committees. The model has been recognized very widely as being ideal for achieving partnership research.

In the first phase of the project, the Government of Canada, through CANMET, was responsible for providing human and supporting resources to the project. The Government of Ontario, though the Ministries of Labour and of Northern Development and Mines, was responsible for providing seismic monitoring equipment. The Ontario mining industry, through the Ontario Mining Association and, more recently, the Mining Research Directorate, was responsible for local installations in the mines requiring seismic monitoring equipment and for in-kind services. The contribution of each partner was valued at $1.4 million.

In 1984, when the project was initiated, the broad objectives were to improve the capabilities with which mining-induced seismic events could be monitored, to improve the accuracies of locating the sources of the events, and to study the causes of rockbursts and strategies for damage alleviation or control.

During the first five years, 1984 to 1989, much was achieved:

- Microseismic monitoring systems are now installed at all Ontario mines where these are required. Local coverage is now virtually complete.

- To complement the existing stations of the Eastern Canada Grid of the Geological Survey of Canada, seismograph stations were installed in four mining areas. Accuracies of locating events and response times have improved.

- Macroseismic monitoring systems, intermediate to the above, have been developed and installed in principal mines. These systems, which record waveforms, provide data for determinations of source mechanisms.

- Trials of destress blasting techniques and support systems for rockburst damage containment have been made.

Finally, Dr. David Hedley, CANMET's project leader for the Canada-Ontario-Industry Rockburst Project until mid-1990 when he retired, has produced this Rockburst Handbook as the final output for the first phase of the project. It is as complete a work as has been written on the subject and should be invaluable to the industry and others as a design manual. CANMET is proud of the role that it has played in the project, and the contribution of its staff, under the technical leadership of Dr. Hedley, in pushing back the frontiers of rockburst research in Canada.

John E. Udd
Director
Mining Research Laboratories
CANMET

Contents

1. ROCKBURST TERMINOLOGY

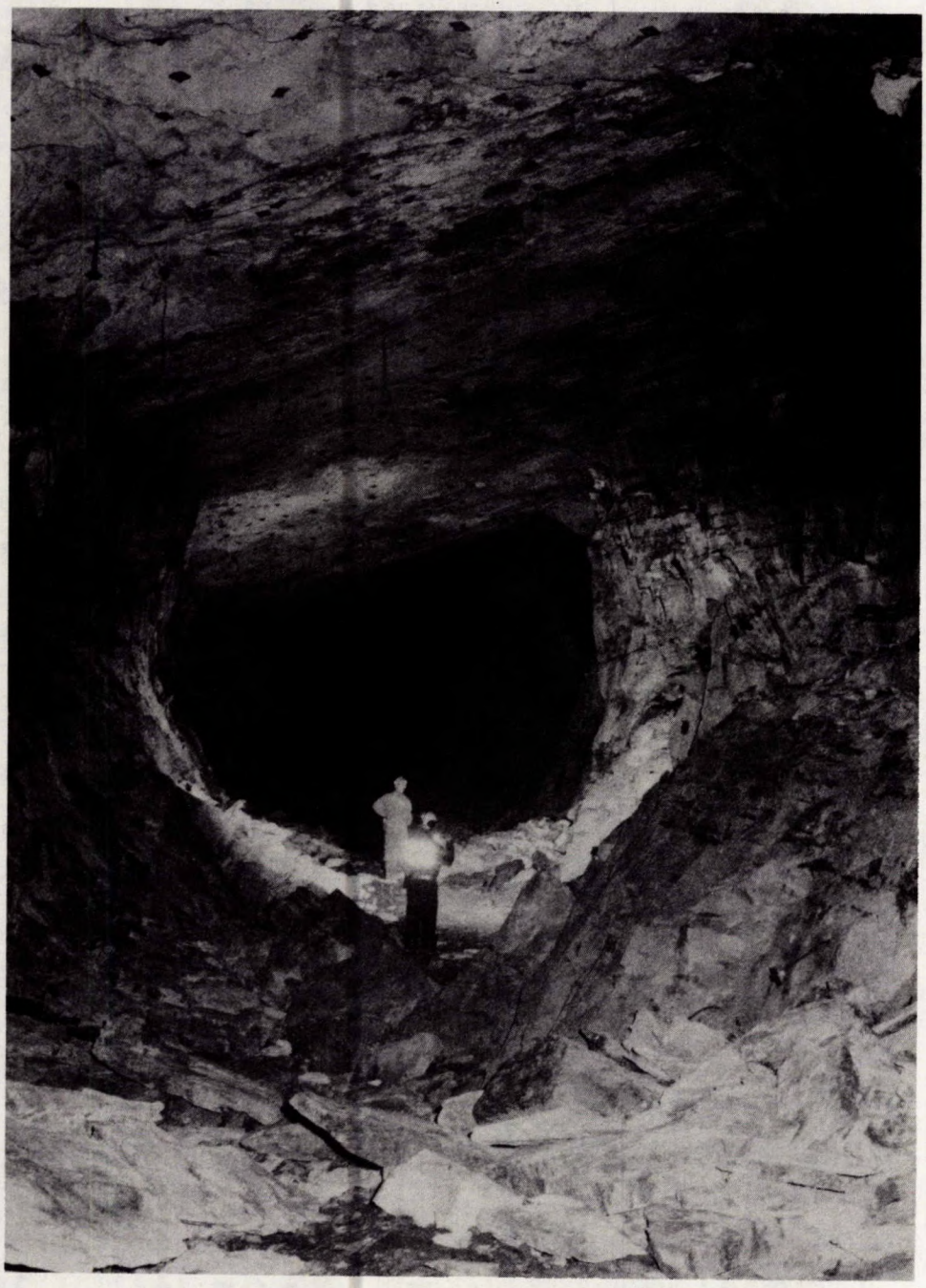

Failing pillars in a rockburst zone at Denison Mine.

1. ROCKBURST TERMINOLOGY

1.1 Introduction

A rockburst is the sudden and violent failure of rock. Sudden, in that failure occurs within a fraction of a second, and violent in that rock fragments are ejected into the mine opening. During the failure process, excess energy is liberated as seismic energy, which causes the surrounding rock mass to vibrate. It is these vibrations which are felt, both underground and on surface.

Rockbursts are 20th century phenomena. They first occurred at the turn of the century in the gold mines on the Witwatersrand in South Africa and on the Kolar Gold Field in India. A South African Commission in 1908 first established that the tremors being felt on surface were mining-induced, rather than from natural forces (i.e., earthquakes). The term 'rockburst' apparently was used to describe the 'shattering of support pillars' observed underground.

In Canada, rockbursts first became a problem in the mid-1930s in the hardrock mines at Kirkland Lake and Sudbury in Ontario. Subsequently, mines in other provinces of Canada also experienced rockbursts but to a lesser extent than those in Ontario.

1.2 Definition

Over the years a considerable amount of effort has been spent on finding an adequate definition for rockbursts. In the 1939 Ontario Mining Act, a rockburst was defined as:

> "a phenomenon causing a fall of ground into an excavated area, or a movement of ground in or about an excavated area and characterized/accompanied by a shock or tremor in the surrounding rock".

The 1978 Occupational Health and Safety Act for Ontario mines modified the

definition to:

> "an instantaneous failure of rock causing an expulsion of material at the surface of an opening or a seismic disturbance to a surface or underground mine".

There have been numerous other proposed definitions, generally referred to as sudden releases of energy or stress. They all suffer from the same ambiguity in that the term 'rockburst' is used to describe the damage or failure process as well as the sounds and vibrations emanating from the source. In some cases vibrations are felt but no damage can be found.

Over the past two decades, microseismic systems installed underground have indicated that the seismic events which cause damage are only a very small proportion of the total number recorded. This has led to the concept, initially in South Africa, of first defining a seismic event, then a rockburst as a sub-set of seismic events, which eliminated the ambiguity in the above definitions.

Based on the definitions used by the Chamber of Mines of South Africa (1982), the following definitions have been adopted.

A **seismic event** is a transient earth motion caused by a sudden release of potential or stored strain energy in the rock. As a result, seismic energy is radiated in the form of strain waves. The magnitude of a seismic event is usually determined from the peak amplitude of the strain wave, using a logarithmic scale (e.g., Richter Scale).

A **rockburst** is a seismic event which causes injury to persons, or damage to underground workings. The general and essential feature of rockbursts is their sudden, violent nature.

Consequently, all rockbursts are seismic events, but not all seismic events are rockbursts.

1.3 Classification

Initially, in Ontario, both the Kirkland Lake and Sudbury mines used a similar classification system for rockbursts. **Strain** bursts were caused by high stress concentrations at the edge of mine openings. Events ranged from small slivers of rock being ejected to the collapse of a complete wall. These small bursts were normally associated with development drifts including shafts.

Pillar bursts were the sudden failure of complete pillars when they became too small and overloaded. These tended to occur in extensively mined-out areas and the damage was significant. Multiple pillar failures were usually called **crush** bursts and, although few in number, they caused the most serious problems.

Subsequently, the Sudbury mines changed their classification systems. **Inherent** bursts replaced strain bursts to emphasize that the pre-mining stresses were high enough to cause failure when the initial development openings were driven. **Induced** bursts replaced pillar and crush bursts. These were caused by mining operations transferring and concentrating stress on the remaining structures such as pillars.

In the 1980s, a third type of rockburst was identified. When slippage suddenly occurs along a geological weakness plane a **fault-slip** burst is produced. This is the same mechanism as for an earthquake. Previously, a number of large seismic events were reported as unlocated. It is probable that these were fault-slip events.

1.4 Reporting

From 1928 to 1990, almost 4,000 rockbursts and 57 associated fatalities were reported to the Ontario Ministry of Labour or its predecessor, the Department of Mines, as shown in Figure 1.1. By the end of the 1930s, rockburst incidents and fatalities were increasing at an alarming rate. This led to an extensive research effort within the mining industry to develop methods to alleviate the problem. These methods were partially successful and the frequency of bursting declined during the 1940s. In the 1970s and '80s, the

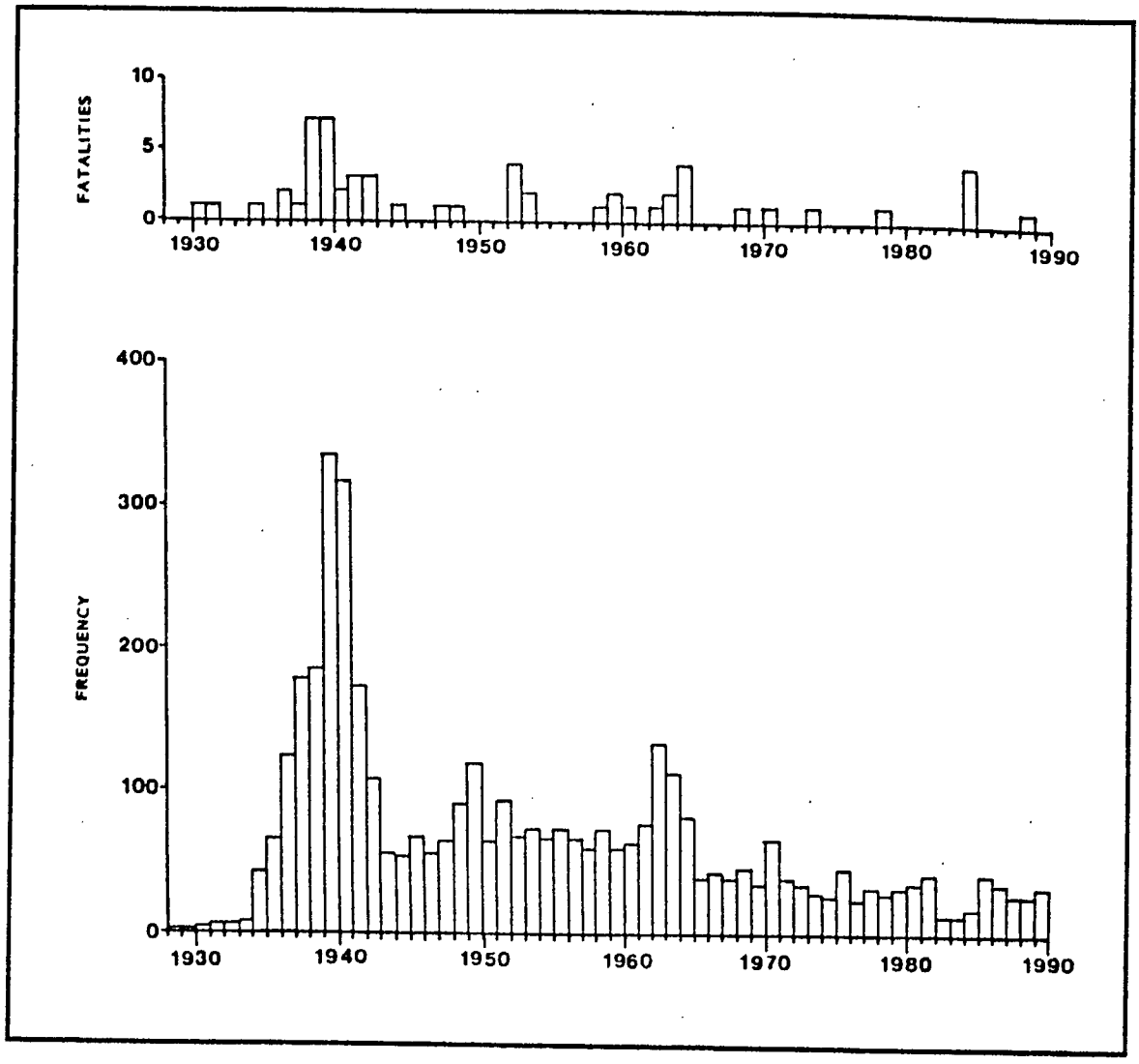

Fig. 1.1 - Reported rockbursts and fatalities in Ontario mines, 1928 to 1990.

reported level of rockburst activity was relatively low.

During this 60-year period, the criteria for reporting rockbursts have changed several times. Prior to 1939, there was no formal requirement to report rockbursts other than those causing injury to persons. However, the Ontario Mining Association had developed its own reporting procedure which included "noticeable damage to timber or other supports, or resulted in appreciable delays to operations". A modified form of this procedure was incorporated into the 1939 Ontario Mining Act, whereby it was necessary to report a rockburst if it was determined that it had occurred within the mine workings.

In the 1978 Act, the damage criteria were changed to: "where a rockburst occurs causing damage to equipment or the displacement of more than five tonnes of material".

Both the 1939 and 1978 Acts require a visual confirmation of damage. Consequently, seismic events that occur in abandoned areas of a mine, with no access for visual confirmation, are not reported. Similarly, fault-slip seismic events out in the wall rocks which produce no damage are not reported. During the 1980s, a significant number of large seismic events occurred either in abandoned areas of mines or out in the wall rocks. These events are not included in Figure 1.1.

Since 1984, all large seismic events in Ontario mines have been classified by magnitude, with a lower threshold of 2.0. These events are recorded on the Eastern Canada Seismic Network, operated by the Geophysics Division of the Geological Survey of Canada, who calculate the magnitude values.

1.5 References

Chamber of Mines of South Africa. (1982) Rockburst terminology: Circular No. 28/82, Johannesburg.

2. HISTORY OF ROCKBURSTS IN ONTARIO MINES

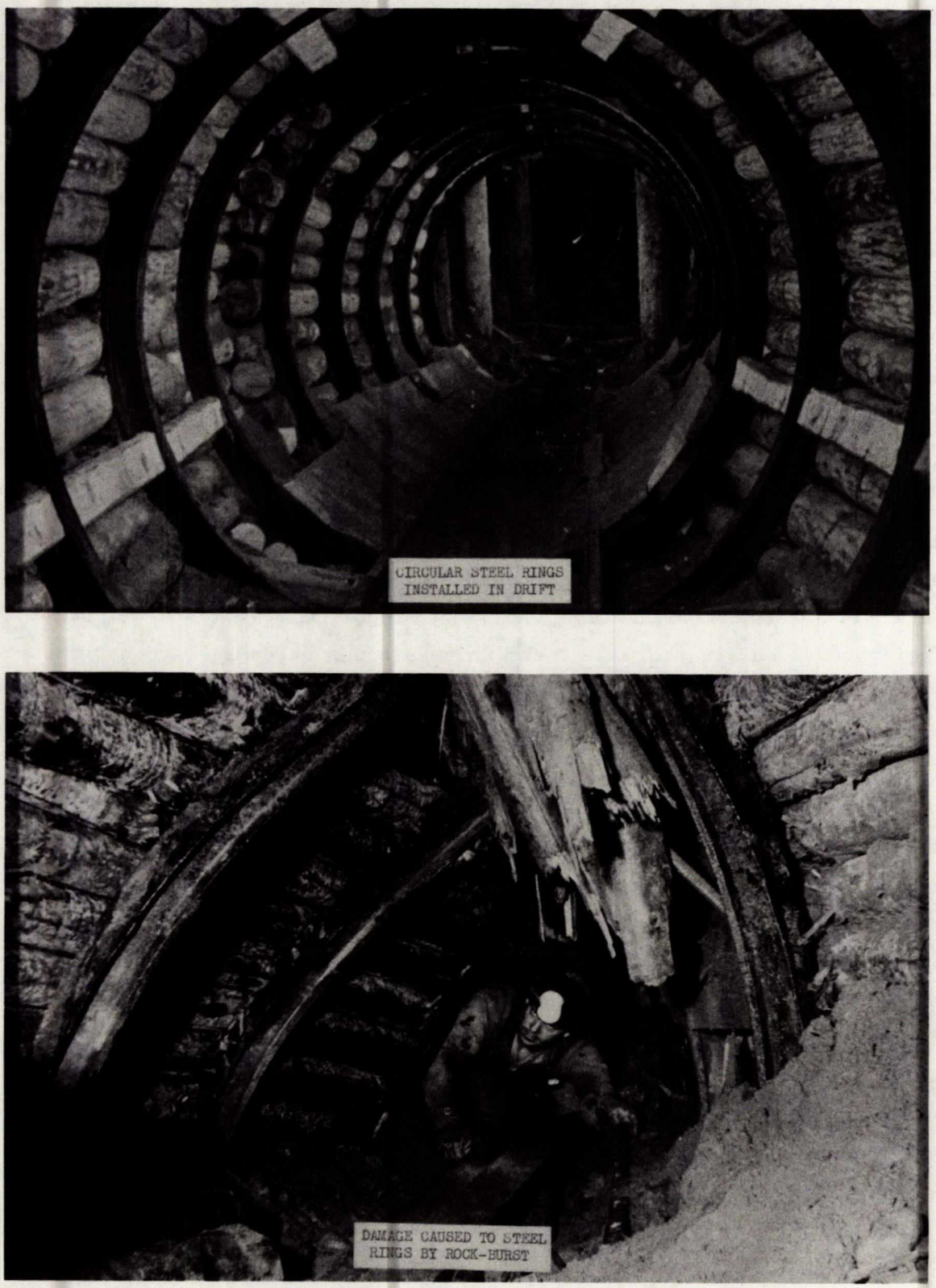

Steel rings used for support in rockburst-prone drifts at Lake Shore Mine in the 1940s.

2. HISTORICAL REVIEW OF ROCKBURSTS IN ONTARIO MINES

2.1 Introduction

The first reported rockburst in Ontario was in January 1928, at a depth of 670 m in the Mond Shaft of the Frood Mine in Sudbury. By the mid-1930s, significant rockburst activity was occurring in the Lake Shore, Teck-Hughes and Wright-Hargreaves mines in Kirkland Lake. In the Sudbury area, both Frood and Creighton mines were experiencing bursts.

Subsequently, other mining camps experienced bursts: gold mines at Red Lake and Virginiatown in the 1960s, and the Elliot Lake uranium mines in the 1980s. Gold mines in the Timmins area are of a similar age, depth and geometry as those at Kirkland Lake, but only the occasional, isolated rockburst has been reported.

In other provinces, so called mining-induced earthquakes have occurred above the potash mines in Saskatchewan. Rockbursts have been reported at some of the gold mines in the Val D'Or area of Quebec. The lead-zinc mines in New Brunswick have also experienced rockbursts. In 1958, a rockburst (called a bump) at the Springhill Colliery in Nova Scotia resulted in 75 fatalities. A fluorspar mine in Newfoundland has also experienced bursts at a depth of only 150 m.

2.2 Kirkland Lake Mines

At Kirkland Lake, the gold-bearing quartz veins are associated with several fault systems designated as the 'Main Break' or Kirkland Lake Fault. This fault extends across the whole mining camp in an east-west direction and dips steeply to the South. From east to west, the mines were Toburn, Sylvanite, Wright-Hargreaves, Lake Shore, Teck-Hughes, Kirkland Lake Gold and Macassa, of which only the last is still in production. Mining has progressed down to a depth in excess of 2000 m. Shrinkage methods were used at shallow depth, and then generally converted to cut-and-fill methods using waste rock, sand and gravel as backfill. At most mines, several sub-parallel veins are present,

typically 2 m wide. The host rocks are porphyry, tuff and basic syenite, all of which are hard and brittle.

Because of the increasing number of rockburst incidents, the Kirkland Lake Mine Operators' Rockburst Research Committee was formed in 1939. One of the first acts of this committee was the preparation of three papers dealing with the rockburst problems at Teck-Hughes (Christian, 1939), Wright-Hargreaves (Robertson, 1939), and Lake Shore (Robson et al., 1940). These papers give a good indication of the state-of-the-art of rockburst control methods employed at that time.

2.2.1 Factors Affecting Incidents and Severity of Rockbursts

Depth of Workings

The number and violence of rockbursts increases with depth. This was explained in terms of 'doming' theory. Stoping results in an arched area of disturbed and fractured rock in the hanging wall, and to a lesser extent, in the footwall. The size of the dome is controlled by the span of the excavation, properties of the wall rocks, method of support and depth. Rockbursts are attributed to the formation of these domes, and the more severe bursts to the merging of domes.

Structural Features

Hard brittle rocks are more susceptible to bursting than softer, weaker rocks. Joints, faults and dykes are lines of weakness and play some part in the incidence of rockbursts.

Dip of Orebody

Rockbursts are more apt to occur in steeply dipping deposits than in those that are gently dipping. The reason given for this is vague, being ascribed to the cumulative buildup of tangential stress in the wall rocks with depth.

Sequence of Stoping Operations

Scattered stoping operations result in the formation and merging of many domes. Sequencing should be designed to prevent the formation of remnant or promontory pillars and the sudden extension of domes from one area to another.

Rate of Mining

Settlement of ground goes on regardless of the rate of stoping, resulting in steadily increasing pressure. Under these conditions, stoping should be as rapid as possible.

2.2.2 Guidelines Developed

- Many rockbursts occur at the time of a blast, or shortly afterwards, which has led to the introduction of central blasting off-shift.

- Leaving small remnant pillars of ore or waste should be avoided to allow gradual and uniform subsidence of the hanging wall.

- Thin horizontal pillars are rockburst-prone and must be avoided, or mined as soon as possible.

- Vertical pillars, such as around shafts and the property boundary, are generally stable.

- Mining out remnants from two directions is not good practice.

- Steep rills avoid the formation of horizontal remnants and are less susceptible to bursts.

- Long rills extending from level to level and advancing towards unmined ground are less susceptible to bursts than those mined towards each other.

Many of the observations and guidelines presented in these reports are still relevant. However, some concepts have changed. Rockbursts in steeply-dipping orebodies are the result of high horizontal stresses, which are greater than the vertical gravitational stress. This was discovered in the 1960s when stress measurements were taken in a number of Ontario mines. The concept of 'doming' to explain rockbursts has been replaced by an energy balance approach. Domes, or expansion zones, do exist in the stope walls and small tensile stresses are present. However, the extent of these expansion domes decreases with increasing depth (Salamon, 1974). What was not recognized is

that when a pillar fails there is a sudden convergence of the wall rocks with a change in potential energy. This is the source of the energy liberated in a rockburst. Although faults, joint sets and dykes were considered to have an important effect on rockburst incidents, the concept was not recognized that slippage on these structures could be the cause and source of rockbursts. This, despite the fact that some of the large tremors were reported to have occurred deep-seated in the wall rocks, could only have occurred with a fault-slip mechanism.

2.2.3 Rockburst Sequence Wright-Hargreaves Mine

The most destructive rockburst sequence at Kirkland Lake occurred at the Wright-Hargreaves Mine in 1964 (Buckle). By that time most of the orebody had been extracted using a cut-and-fill mining method. All the major service openings including shafts, ventilation raises and ore passes were located in a shaft pillar near the centre of the mine. Limited mining in the shaft pillar triggered a series of rockbursts, the largest ever recorded in Canada having an estimated magnitude of at least 4.0.

Inspection of the workings revealed significant damage to the shaft pillar, and cross-cuts to the shaft were blocked off over a vertical distance of 400 m. The extent of the damage and the limited ore reserves resulted in the immediate closure of the mine.

2.3 Sudbury Mines

Although rockburst research and development was carried out in the Sudbury mines from the mid-1930s, there is no published literature until the late 1950s (Dickout, 1957, 1963).

2.3.1 Control Measures at the Creighton Mine

Creighton Mine first experienced rockbursts in the mid-1930s when mining below 600 m. The general pattern was for inherent bursts to occur during development. These were caused by the high, pre-mining field stresses and the brittle nature of the rock. After about 60 to 70% of a level had been mined,

induced bursts would occur in the crown pillars. This was followed by induced bursts in development openings in the wall rocks, and finally by unlocated bursts in the wall rocks.

The control methods adopted were based on the doming theory. Major development openings, such as shafts, were sunk in the footwall well outside subsequent domes produced as a consequence of mining. At depth, destressing techniques were used in driving development drifts which resulted in a large decrease in overbreak, working ground and spalling.

Below a depth of about 1200 m, square-set stoping was used exclusively with water-borne sand filling. Both primary stoping and pillar recovery were advanced upwards on a longwall front. Only one level was allowed to merge with the one above at any one time, so that the domes increased gradually. When the lead stope approached the level above, some bursting was experienced, but multiple and severe crown bursts were eliminated. Subsequently, the introduction of cemented backfill eliminated the square-sets, however, the sequence of mining was still retained.

2.4 Morrison's Report

The Ontario Mining Association formed its own Rockburst Committee in 1940. This committee retained R.G.K. Morrison, Superintendent, Nundydroog Mines on the Kolar Gold Field to investigate rockbursts in Ontario mines. Three months were spent visiting mining camps throughout Ontario (Kirkland Lake, Virginiatown, Timmins, Sudbury, Little Long Lac, Pickle Lake, Uchi Lake and Red Lake). A report on the rockburst situation in Ontario mines was published in the Transactions of the *Canadian Institute of Mining and Metallurgy* in 1942. In many respects this report formed the basis for implementing rockburst-control strategies at Ontario mines for the next 40 years.

2.4.1 Doming Theory

Rockbursts were attributed to the formation of 'domes', which was the prevalent theory being used on the Kolar Gold Field, the Witwatersrand, and at Kirkland Lake. Figure 2.1 illustrates this doming concept. Individual stopes

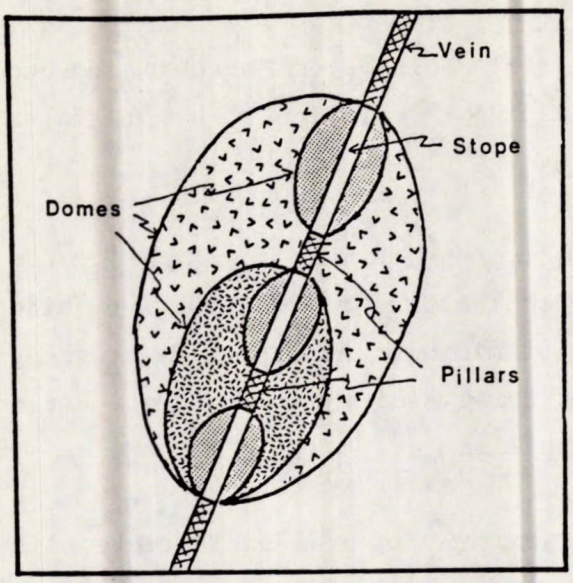

Fig. 2.1 - Concept of doming theory (after Morrison, 1942).

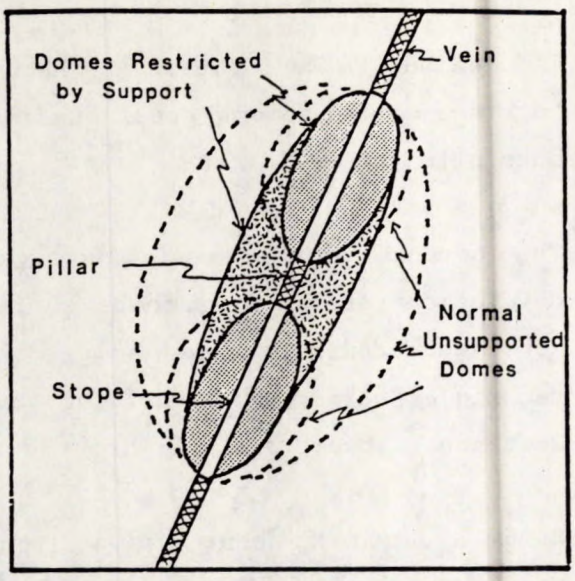

Fig. 2.2 - Effect of support on the size of domes (after Morrison 1942).

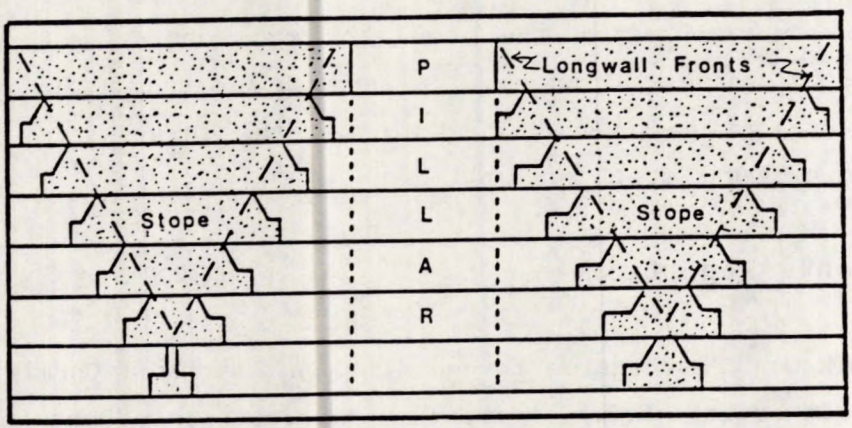

Fig. 2.3 - Longitudinal cut-and-fill layout with longwall configuration (after Morrison, 1942).

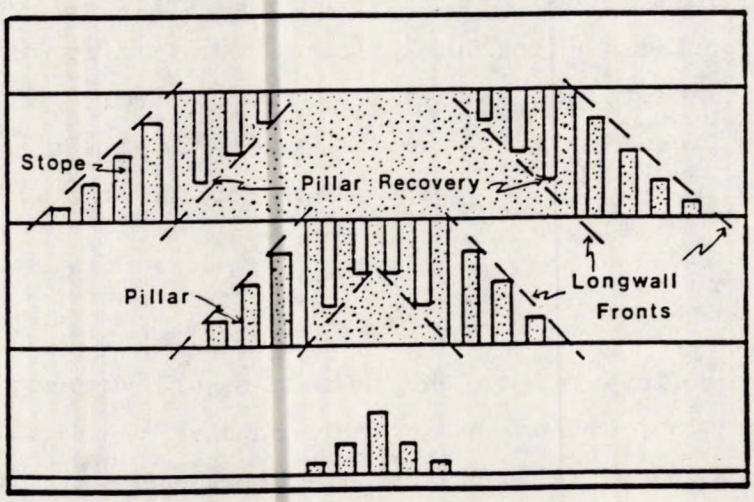

Fig. 2.4 - Transverse cut-and-fill layout with longwall configuration in primary stoping and pillar recovery (after Morrison, 1942).

are surrounded by a dome of fractured rock. As stopes approach each other the intervening pillars become increasingly stressed. If these pillars suddenly fail, the volume of the dome also suddenly increases (i.e., approximately quadruples for the merging of two equally sized stopes). The rupture of the large volume of rock between two or more initial domes, and the release of its accumulated energy results in a rockburst. The magnitude of the rockburst depends on the final size of the dome and the energy stored within it. This in turn is controlled by the areal extent of stoping, depth, and the physical properties of the wall rocks.

Although the formation of domes as a rockburst mechanism has been discredited, many of the characteristics associated with domes are still relevant to rockburst-control strategies. Areal extent of stoping, depth and elastic properties of the wall rocks also control convergence and change in potential energy of the surrounding rock mass. When a pillar fails between two equally sized stopes, the change in potential energy quadruples, similar to the volume of a dome.

The importance of support for controlling the number and severity of rockbursts was recognized, although again in terms of its effect on the size of domes, as illustrated in Figure 2.2. It was also recognized that some type of cushion was required. Although not implicitly stated, this was so the support could withstand the impact loading resulting from a rockburst.

2.4.2 Control Strategies

Morrison's main rockburst-control strategy was the use of mining layouts which eliminated small remnant pillars and allowed domes to gradually expand. In practice, this meant some form of longwall configuration. Figures 2.3 and 2.4 show two possible longwall stoping layouts for longitudinal and transverse cut-and-fill mining.

The effect of weakness planes such as faults, dykes, contacts, and major joint sets, was explained in terms of their effect on the formation of domes and stress concentrations. The concept of slippage along these structures was not recognized. It was recommended to mine away from major weakness planes, or to

mine through them at a perpendicular rather than an acute angle.

Many of the recommendations in Morrison's report were implemented by the Ontario mines and the number of rockbursts did substantially reduce in the 1940s.

2.5 Geophysical Research

During the 1930s, some of the larger rockbursts at Kirkland Lake were recorded 450 km away on the seismograph of the Dominion Observatory in Ottawa. This led to a proposal by Lake Shore Mines Ltd., in 1938, that a seismograph station be established at Kirkland Lake, and that geophysical research on rockbursts be undertaken at the mine. Direction of this research was assigned to Dr. E.A. Hodgson, Chief of the Seismological Division of the Dominion Observatory. The main objective of the geophysical research was to determine whether rockburst prediction was feasible. However, these rockbursts were also used as a convenient source for refraction profiles and crustal velocity models of the Canadian Shield. A detailed report on the rockburst research, between 1938 and 1945, was published by the Dominion Observatory in 1958.

A parallel research effort was also being done at Inco's Frood Mine at Sudbury. On a number of occasions the two research teams collaborated on the testing of new monitoring equipment.

The surface seismograph unit at Kirkland Lake was installed in December 1939, and was in almost continuous operation until the late 1950s. A number of devices were tested underground to monitor increasing stress. These included instrumentation to measure borehole and drift closure. Although some results were obtained, the instrumentation was cumbersome. Similarly, measuring an increase in temperature with increasing stress was not feasible, neither was measuring seismic velocity, since time could not be measured accurately enough.

A considerable effort was made to measure the frequency spectra of seismic events, blasting and other mining noises. Filters were made to try to eliminate non-seismic noises without noticeable success. Other factors also

affected or delayed the instrumentation program. In a wartime economy electronic components were scarce, and much of the equipment had to be custom built. Lake Shore Mine operated on 25 Hz power supply, with a fairly severe voltage fluctuation, whereas the electronic equipment was designed for a 60 Hz supply. Most of the electronic equipment was not designed to operate in a hot, dusty and damp underground environment.

In June 1942, Dr. L. Obert from the United States Bureau of Mines visited both Frood and Lake Shore Mines to demonstrate a microseismic monitoring system. Sub-audible noises up to 1000 Hz were recorded either using earphones or on a paper chart. Research in a Michigan mine had indicated that microseismic activity, as expressed in events per minute, increased before a rockburst. The demonstration tests at Frood and Lake Shore mines indicated that microseismic events could be readily detected with this equipment.

A comprehensive monitoring program was initiated in July 1942 at the Lake Shore Mine. Three of Obert's recording units were purchased and up to 100 geophones were installed underground to monitor microseismic activity. This program lasted approximately three years.

Since the background noise at the mine was so high, microseismic monitoring was eventually limited to off-shift periods. Monitoring at each site would be done over a 15-minute period using either earphones or a paper chart recorder. It was found that seismic events detection was limited to within 20 m of a geophone.

Initial tests indicated that an event rate of less than 20/min was no cause for concern. Over 20 events/min required close inspection of the affected stopes, and over 80 events/min meant withdrawing the labour force from the stope and, if possible, the next blast should be made abnormally heavy. Other observations were that various parts of a pillar would have higher event rates at different times, indicative of shifting stresses which could occur fairly rapidly. Also an increasing event rate would often be followed by a quiet period, just prior to a rockburst.

In many respects the monitoring program at Lake Shore Mine was the forerunner

of the present day microseismic systems. With electronics and computing devices being in their infancy it lacked the continuous recording ability, rapid evaluation of data and interconnected, multichannel aspects of the present systems. It appears from the reports that the research program became saturated with data.

2.6 Recent Seismic Activity and Research

During the 1950s, '60s and '70s, very little basic rockburst research was undertaken in Ontario. The main emphasis was on implementing and modifying the rockburst control strategies developed during the 1940s. This included adoption of longwall mining layouts, avoidance of remnant pillars and conversion of shrinkage to cut-and-fill at depth. The introduction of cemented backfill and rock bolts also assisted. It should be noted that by the mid-1960s all of the gold mines at Kirkland Lake, except the Macassa Mine, had closed, which significantly reduced the rockburst frequency in the province.

There was a significant increase in seismic activity in Ontario mines in the 1980s. Fourteen mines in the Red Lake, Elliot Lake, Sudbury and Kirkland Lake mining districts have experienced seismic events including rockbursts. The breakdown of the number of seismic events, of magnitude 2.0 and greater, by mining district and individual mines, for the years 1984 to 1990 is given in Table 2.1.

Quirke Mine at Elliot Lake dominated the statistics in 1984 and '85 and accounts for almost 50% of the total events. Other mines with significant seismic activity are the Campbell Mine at Red Lake, the Strathcona, Creighton and Copper Cliff North mines in Sudbury and, to a lesser extent, the Denison Mine at Elliot Lake and the Macassa Mine at Kirkland Lake.

A variety of ore deposits and mining methods are used in these mines. At Red Lake and Kirkland Lake, narrow steeply-dipping vein deposits are extracted by shrinkage and longitudinal cut-and-fill methods. At Elliot Lake gently-dipping reef deposits are mined by variations of room-and-pillar methods. At Sudbury, massive sulphide deposits are extracted by cut-and-fill and blasthole methods.

Table 2.1 - Distribution of seismic events of magnitude 2.0 and greater by mining camp, 1984 to 1990

Mining District	1984	1985	1986	1987	1988	1989	1990	Totals
Red Lake	18	3	6	0	0	0	0	27
Elliot Lake	46	74	13	8	1	4	2	148
Sudbury	15	20	35	56	36	10	23	195
Kirkland Lake	5	2	3	3	5	2	1	21
Timmins	0	0	0	0	0	3	0	3
Totals	84	99	57	67	42	19	26	394

Table 2.2 - Distribution of seismic events by individual mines, 1984 to 1990

Location	No.	Largest Magnitude	Location	No.	Largest Magnitude
SUDBURY			RED LAKE		
Falconbridge	7	3.5	Campbell	23	3.3
Fraser	1	2.5	Dickenson	4	2.1
Lockerby	2	2.6			
Strathcona	28	3.2	ELLIOT LAKE		
Copper Cliff South	1	2.5	Denison	11	2.8
Copper Cliff North	16	2.9	Quirke	137	3.4
Creighton	43	4.0			
Frood-Stobie	4	3.0	KIRKLAND LAKE		
Levack	3	2.6	Kerr Addison	3	3.3
Stobie	1	2.4	Macassa	15	3.1

One peculiarity in the recent increase in seismic activity is that it occurred in the same time period in mines across the province. These mines are in different geological settings with different life spans, depth and areal extent. Similarly, in the 1930s rockbursts started at the Kirkland Lake and Sudbury mines at the same time. The Precambrian Shield in Northern Ontario is considered to be a stable area with a low level of natural earthquake activity. Consequently, it is difficult to explain these coincidences.

Another feature of the recent seismic activity has been the multiple nature of the occurrences. Previously, rockbursts had occurred as isolated events followed by some microseismic activity. The exception was the rockburst incidents at the Wright-Hargreaves Mine in 1964, as described previously. In the 1980s multiple rockbursts occurred at the Campbell Mine (1983), the Falconbridge Mine (1984), the Creighton Mine (1984), and twice at the Quirke Mine (1982, 1984/85). The duration of these multiple rockbursts ranged from two hours at the Creighton Mine to five months at the Quirke Mine.

As mentioned previously, the geophysical research and seismic monitoring in the early 1940s floundered due to the primitive electronics, saturation with data and manual analysis and interpretation. All this changed by the 1980s with multichannel microseismic systems commercially available which give location of seismic events within a few seconds, usually at the engineering office on surface. In Ontario, the first microseismic system was installed at the Creighton Mine in 1980, followed by the Falconbridge Mine in 1981, and Quirke Mine in 1982. By 1990, sixteen microseismic systems, with up to 64 geophones per system, had been installed in Ontario mines.

In response to this increased seismic and rockburst activity, the Canada/Ontario/Industry rockburst project was initiated in 1985. It is a joint government-industry project organized on a tripartite footing with participation of the Canada Centre for Mineral and Energy Technology (CANMET), the Ontario Ministries of Labour and Mines, and the Ontario mining industry represented by Denison Mines Ltd., Falconbridge Ltd., Inco Ltd., Lac Minerals Ltd., Placer Dome Ltd., and Rio Algom Ltd.

2.7 References

Buckle, F. (1964), The rockburst hazard in Wright-Hargreaves Mine at Kirkland Lake; National Safety Congress, Chicago.

Christian, J.D. (1939), Rockbursts at Teck-Hughes Mine: Trans. CIM. vol. 42, pp. 550-567.

Dickout, M.H. (1957), Rockburst control at the Creighton Mine of the International Nickel company of Canada Limited; 6th Commonwealth Min. & Met. Congr., Canada, pp. 385-390.

Dickout, M.H. (1962), Ground control at the Creighton Mine of the International Nickel Company of Canada Limited; 1st Can. Rock Mech. Symp., McGill University, Montreal, pp. 121-139.

Hodgson, E.A. (1958), Dominion Observatory rockbursts research 1938-1945; Publication Dominion Observatory, vol. 20, No. 1, Ottawa, p. 248.

Morrison, R.G.K. (1942), Report on the rockburst situation in Ontario mines; Trans. CIM. vol. 45, pp. 225-272.

Robertson, A.F. (1939), Rockbursts at Wright-Hargreaves Mine. Trans CIM. vol. 42, pp. 583-392.

Robson, W.T., Adamson, J.C. and Selnes, W.E. (1940), Rockbursts at Lake Shore Mines. Trans. CIM, vol. 43, pp. 7-30.

Robson, W.T., Selnes, W.E. and Seymour, M.E. (1957), Rockburst control measures at Lake Shore Mines Limited. 6th Commonwealth Min. & Met. Congr. Canada, pp. 376-384.

Salamon, M.D.G. (1974, Rock mechanics of underground excavations. Proc. 3rd Congr. Int. Soc. Rock Mech., Denver, CO. vol. 1, Part B, pp. 951-1109.

3. ROCKBURST MECHANICS

Strain burst in a drift at Quirke Mine.

Slippage along a bedding plane in a pillar at Denison Mine.

3. ROCKBURST MECHANICS

3.1 Introduction

Since rockbursts are the result of a violent release of energy it is natural that an analysis of energy be used to explain the mechanics of violent rock failure. Mechanical energy is a force acting through a displacement. In the "International System of Units" energy is calculated in terms of joules (J) which are newton-metres (N.m). In the "Imperial System" the equivalent units are foot-pound-force (1 ft-lb = 1.36 J).

Initially only the energy stored within the rock was considered as the source of the liberated energy. Later it was realized that there was a change in potential energy of the surrounding rock mass because of mining operations. This led to the concept of an energy balance that was originally developed by Cook (1967) and later refined by Salamon (1974, 1984).

3.2 Energy Balance

When a mining excavation is enlarged the surrounding rock mass moves towards the excavation resulting in a change in potential energy (W_t). The rock removed during enlargement also contains stored strain energy (U_m). The term ($W_t + U_m$) represents the energy entering the mining operation as a result of the enlargement. This energy has to be dissipated somehow.

Stresses acting on the rock which was removed are transferred to the surrounding rock mass increasing its stored strain energy (U_c). If the excavations are internally supported (e.g., backfill, cribs, posts) then some energy is absorbed in deforming the support (W_s). Any excess energy is normally referred to as released energy (W_r). From the law of conservation of energy:

$$W_t + U_m = U_c + W_s + W_r \qquad \text{Eq 3.1}$$

In this analysis it is assumed that the rock behaves elastically and no energy is consumed in fracturing or non-elastic deformation.

There are a number of ways in which energy can be released. The stored strain energy (U_m) in the removed rock is obviously released. If the rock was removed instantaneously there would be oscillations in the rock mass. Equilibrium would be attained through damping and seismic (i.e., kinetic) energy (W_k) would be dissipated in the process. For elastic conditions there are no further alternatives, hence:

$$W_r = U_m + W_k \qquad \text{Eq 3.2}$$

It is the seismic energy (W_k) which is recorded by mine microseismic systems, and it is this energy component which is responsible for the damage caused by a rockburst. From Equations 3.1 and 3.2:

$$W_k = W_t - (U_c + W_s) \qquad \text{Eq 3.3}$$

In the case of unsupported excavations there is an inter-relationship between the energy components. This can be demonstrated by a simple example of two identical specimens under a constant load in a press, as shown in Figure 3.1(a). Both specimens would contain equal stored strain energy (U_m) as identified in Figure 3.1(b). If one specimen was removed, while still maintaining constant load, then the stress on the remaining specimen would double as would the displacement between the platens. The stored strain energy (U_m) in the removed specimen would be released (i.e., removed from the system) and the remaining specimen would carry the increase in stored strain energy (U_c). The platens of the press would follow the displacement of the remaining specimen, with a resultant change in potential energy (W_t). Areas representing various energy components are shown in Figure 3.1(b), with the following relationships:

$$U_c = 2U_m + U_1 \qquad \text{Eq 3.4}$$
$$W_t = 2(U_m + U_1) \qquad \text{Eq 3.5}$$
$$W_r = U_m + U_1 = W_t/2 \qquad \text{Eq 3.6}$$
$$W_k = U_1 \qquad \text{Eq 3.7}$$

where (U_1) is the increase in stored strain energy if the stress increase had occurred on an unstressed specimen. Salamon (1974) has shown, for elastic

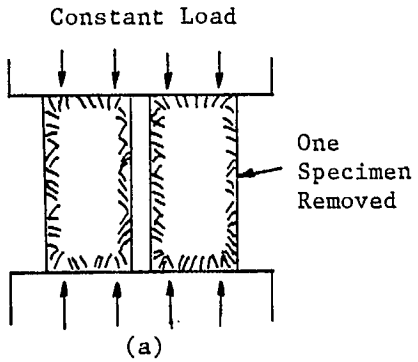

Area OAB = Um

Area BADE = Uc = 2Um + U_1

Area BCDE = Wt = 2Um + 2U_1

Areas OAB + ACD = Wr = Um + U_1

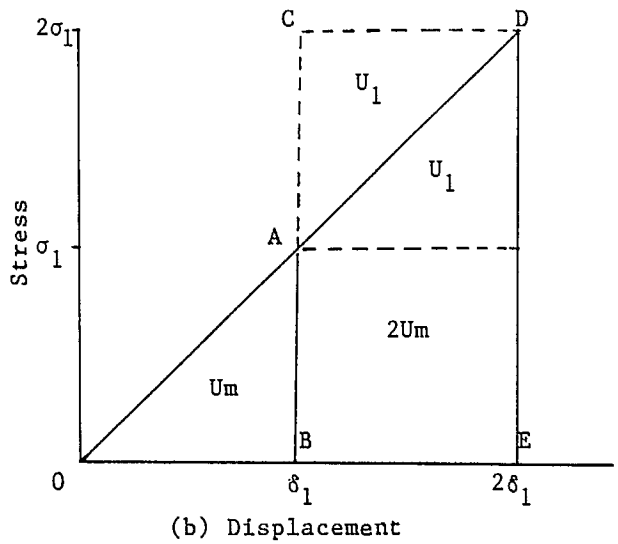

(b) Displacement

Fig. 3.1 - Energy components when one specimen is removed from a press under constant load.

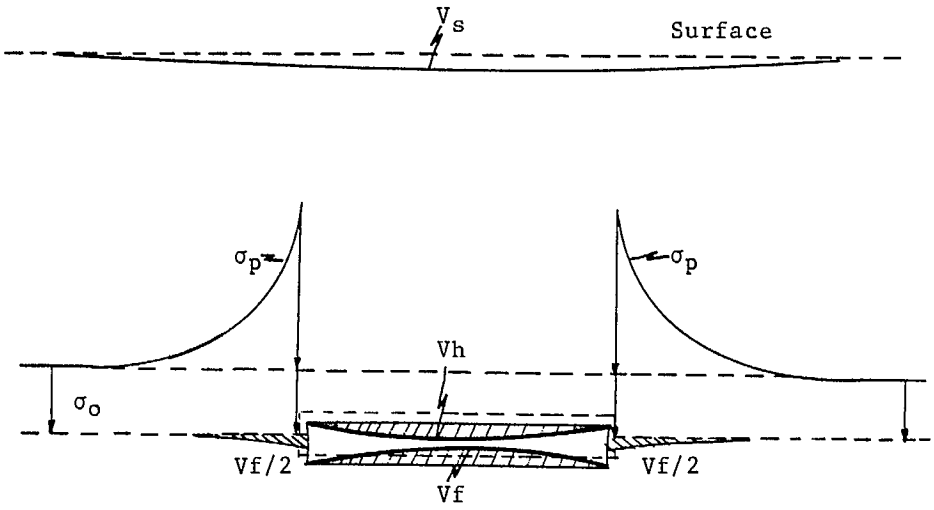

Fig. 3.2 - Section through a tabular excavation showing volumetric convergence and stress components (after Ortlepp 1983).

conditions, that Equations 3.4 to 3.7 apply to any mining configuration. Also, when mining takes place in very small steps the limiting conditions are:

$$\Delta W_t = \Delta U_c, \quad \Delta W_r = \Delta U_m \quad \text{and} \quad \Delta W_k = 0 \qquad \text{Eq 3.8}$$

Some fundamental deductions can be made from these energy relationships:

- Without support, all the energy components can be expressed in terms of two parameters (U_m) and (U_l). It is relatively easy to calculate these parameters using a variety of numerical models.

- When mining takes place in very small steps the process is stable and no seismic energy is released. In some cases this is contradictory since many mines employ incremental methods but still experience rockbursts. However, this means that some other sources of energy are being liberated due to non-elastic conditions, either fracturing of a pillar or slippage along a fault.

- The change in potential energy (W_t) is the driving force behind the other energy components. If it can be reduced the other energy components are correspondingly reduced.

- Support, such as backfill, has two beneficial effects. It will reduce the change in potential energy by reducing volumetric closure in the excavations, and by absorbing energy, less energy is available to be released as seismic energy.

There are some other energy terms in common use. Energy release rate is the stored strain energy in the rock to be removed per unit area ($\Delta U_m/\Delta A$). It is used in South African gold mines to rank rockburst potential of various mining layouts. There is a strong statistical relationship between energy release rate and damage in these mines (Hodgson and Joughin, 1967). Its use stems from Equation 3.8 and the concept of mining in very small steps.

Seismic efficiency is the ratio (W_k/W_r) and is usually expressed as a percentage. For a given set of circumstances, the higher the proportion of

energy released as seismic energy, the greater the rockburst potential.

3.3 Calculation of Energy Components

For simple geometrical mine openings it is possible to estimate the energy components using closed-form or approximate solutions. This has the benefit of identifying the parameters controlling the energy components. Complex mining geometry and multiple openings usually require more sophisticated numerical modelling techniques.

Thin tabular excavations have been examined in detail in a number of publications. Figure 3.2 shows an isolated horizontal narrow stope which prior to mining is subjected to a gravitational stress (σ_o). After mining the vertical stress on the hanging wall and footwall of the stope is zero, and an equivalent stress is transferred to the abutments. The hanging wall subsides downwards with a volumetric convergence (Vh), whereas the footwall lifts upwards with a volumetric convergence (Vf). The former represents a loss of potential energy and the latter a gain in potential energy, relative to the centre of the Earth. However, the increase in stress on the abutments depresses the footwall plane by a volume identical to the uplift of the footwall in the stope. Consequently, the net change in potential energy of the footwall is zero. Moreover, the hanging wall around the stope moves down by the same amount as the footwall is depressed. Thus the net volumetric convergence (Vc) of the hanging wall is the sum of the hanging wall and footwall convergence in the stope, which is relatively easy to calculate:

$$Vc = Vh + Vf = Vs \qquad \text{Eq 3.9}$$

For elastic conditions this volumetric stope closure also equals the volumetric subsidence (Vs) of the surface, although the latter is spread over a much larger area.

The change in potential energy of the hanging wall can now be expressed by:

$$W_t = \sigma_o \, Vc \qquad \text{Eq 3.10}$$

This equation is a valid approximation for thin tabular stopes. For more three-dimensional openings the changes in horizontal potential energy (W_h) as well as gravitational energy (W_g) have to be accounted for:

$$W_t = W_h + W_g \qquad \text{Eq 3.11}$$

and,

$$W_t = \sigma_o \, Vc + \sigma_a \, Va + \sigma_b \, Vb \qquad \text{Eq 3.12}$$

where, σ_a, σ_b = horizontal stresses
Va, Vb = volumetric convergence of the vertical walls.

Stopes in tabular deposits, of any orientation, can be considered as thin slits with rigid abutments. The convergence distribution across an isolated stope can be approximated by (Salamon, 1968):

$$C = \frac{4(1-\nu^2)\sigma_o}{E} \left(1 + \frac{\chi \sin \alpha}{2H}\right) \sqrt{s^2 - \chi^2} \qquad \text{Eq 3.13}$$

where, C = hanging wall to footwall convergence
E = elastic modulus
ν = Poisson's ratio
σ_o = virgin stress perpendicular to the orebody
α = dip of orebody relative to horizontal
H = depth below surface to stope centre
s = half span of stope
χ = distance from centre of span ($-s \leq \chi \leq s$)

Assuming the principal stresses are vertical and horizontal the perpendicular virgin stress is obtained from:

$$\sigma_o = \frac{\gamma H}{2} \left[(1+K) + (1-K) \cos 2\alpha\right] \qquad \text{Eq 3.14}$$

where, γ = unit weight of the rock mass
K = ratio of the horizontal to vertical stress.

In Equation 3.13 the term ($\chi \sin \alpha / 2H$) takes into account the variation in the virgin perpendicular stress on either side of the stope centre line. Unless

the stope span is very large the term is not significant and Equation 3.13 can be simplified to:

$$C = \frac{4(1-\nu^2)}{E}\ \sigma_o\ \sqrt{s^2-\chi^2} \qquad \text{Eq 3.15}$$

which is also the equation for a horizontal stope. Integrating Equation 3.15, with respect to (χ), gives the volumetric convergence per unit length along the stope:

$$Vc = \frac{2\Pi(1-\nu^2)\ \sigma_o\ s^2}{E} \qquad \text{Eq 3.16}$$

and from Equation 3.10 the change in potential energy is:

$$W_t = \frac{2\Pi(1-\nu^2)\ \sigma_o^{\,2}\ s^2}{E} \qquad \text{Eq 3.17}$$

The stored strain energy (U_m) in the rock to be removed is relatively easy to calculate. For a perfectly elastic material the stored strain energy is:

$$U_m = \frac{1}{2E}\ [\sigma_1^{\,2} + \sigma_2^{\,2} + \sigma_3^{\,2} - 2\nu(\sigma_1\sigma_2 + \sigma_2\sigma_3 + \sigma_3\sigma_1)] \qquad \text{Eq 3.18}$$

where, U_m = stored strain energy per unit volume

$\sigma_1, \sigma_2, \sigma_3$ = principal stresses.

Again for tabular deposits the perpendicular stress (σ_p) usually dominates and the stored strain energy can be approximated by:

$$U_m = \frac{\sigma_p^{\,2}(1-\nu^2)}{2E} \qquad \text{Eq 3.19}$$

Returning to the example of an isolated thin stope, the perpendicular stress profile into the abutment can be expressed by:

$$\sigma_p = \frac{\chi\sigma_o}{\sqrt{\chi^2-s^2}} \quad (\chi \geq s) \qquad \text{Eq 3.20}$$

and,

$$U_m = \frac{\sigma_o^{\,2}(1-\nu^2)\chi^2}{2E(\chi^2-s^2)} \qquad \text{Eq 3.21}$$

Equation 3.20 predicts infinite stress at the edge of the abutment (χ=s) which is unrealistic, also Equation 3.21 is in a form difficult to integrate. However, an engineering approach can be used by dividing the abutment into a series of unit slices and calculating the average stress on each slice. The stored strain energies are summed for those slices to be removed in the next mining step.

Having calculated the change in potential energy (W_t) by Equation 3.17, and the stored strain energy (U_m) in the material to be removed in the next mining step by Equation 3.21, the other energy components (U_c, W_r, W_k) can be calculated from Equations 3.4, 3.6 and 3.7.

3.4 Incremental Versus Bulk Mining

As indicated in Equation 3.6 half the change in potential energy has to be released. How this energy is released, either as stored strain energy (U_m) or seismic energy (W_k), depends on the number and size of the mining steps used to achieve the final shape of the opening. This can be demonstrated by the simple example of a circular tunnel or shaft subjected to a hydrostatic stress (p), for which a closed-form solution exists (Salamon, 1974).

The ratios (W_k/W_r) and (U_m/W_r) can be expressed by:

$$\frac{W_k}{W_r} = \frac{(1 - a^2/c^2)}{2(1-\nu)} \qquad \text{Eq 3.22}$$

and,

$$\frac{U_m}{W_r} = \frac{(1 - 2\nu + a^2/c^2)}{2(1-\nu)} \qquad \text{Eq 3.23}$$

when the radius of the tunnel is enlarged from (a) to (c). Figure 3.3 shows how the energy is released as the tunnel is increased in radius to its final size. If the tunnel is created instantaneously (i.e., one mining step) then 62.5% of the released energy would be in the form of seismic energy and 37.5% as stored strain energy. However, if the radius was increased in 64 equal increments only 3.4% of the released energy is seismic energy and 96.6% is stored strain energy.

In Canadian hard rock mines there is an increasing tendency to the use of bulk

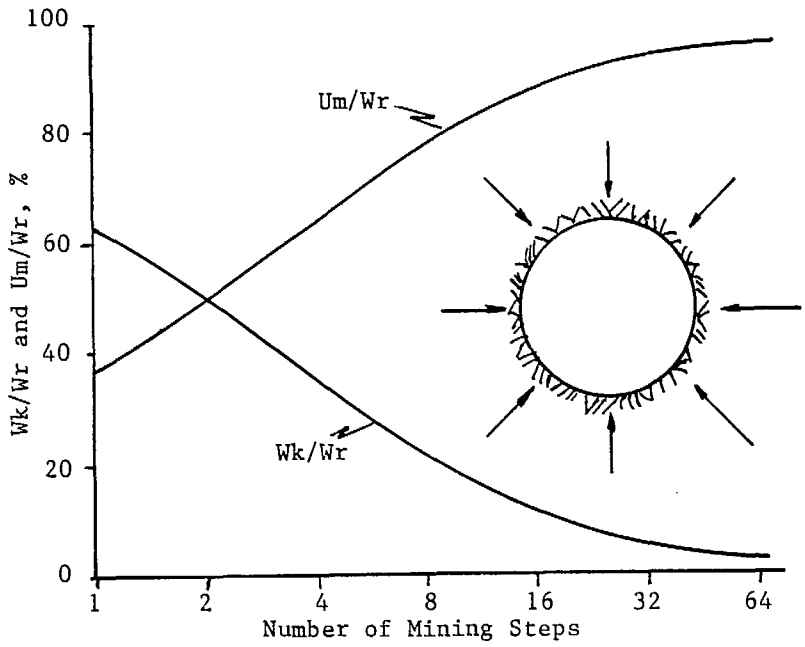

Fig. 3.3 - Variation in how energy is released with number of mining steps (after Salamon 1983).

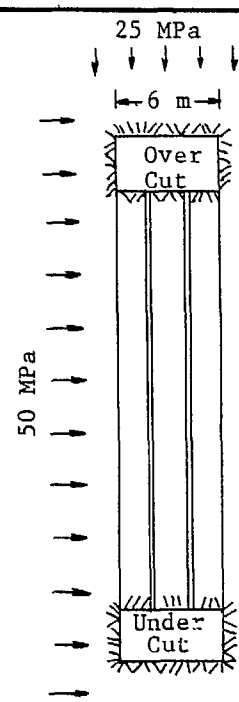

Fig. 3.4 - Blasthole stoping.

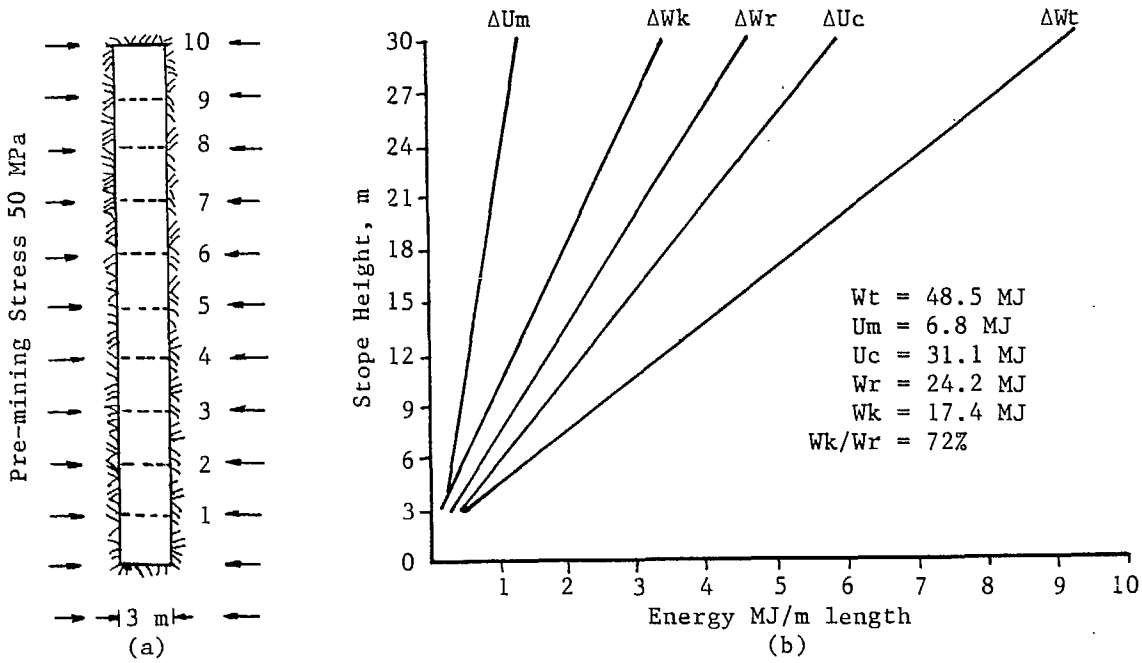

Fig. 3.5 - Energy components per cut during mining of a vertical stope.

mining techniques, wherever possible, due to the economics of scale. Figure 3.4 shows a typical layout of a blasthole stope in a vertical orebody. A 3 m high overcut and undercut are developed first, then the intervening orebody (26 m) is removed with large hole blasting techniques. The pre-mining horizontal and vertical stresses are taken as 50 MPa and 25 MPa, respectively, with the rock mass having an elastic modulus of 70 GPa and a Poisson's ratio of 0.2. A boundary element model was used to calculate the energy components which are listed in Table 3.1.

Table 3.1 - Energy components in a blasthole stope (in MJ/m in length)

Mining Stage	ΔW_t	ΔU_m	ΔU_c	ΔW_r	ΔW_k	$\Delta W_k/\Delta W_r$
Overcut and undercut	3.2	0.6	2.2	1.6	1.0	62%
Blasthole	52.8	2.9	29.8	26.9	24.0	89%

These results indicate that when the blasthole section is mined a significant amount (about 90%) of the released energy is in the form of seismic energy.

Figure 3.5(a) shows a vertical unsupported stope which is mined upwards in 10 incremental cuts. The stope is 3 m wide and each cut is 3 m high. Only the pre-mining perpendicular stress of 50 MPa is used in this example, together with Equations 3.17 and 3.21. The incremental change in potential energy (W_k) for each cut is obtained by subtracting the total change in potential energy of the previous cut from the present cut. The rock in the top abutment was divided into three horizontal 1 m slices to calculate the stored strain energy removed in the next cut.

Figure 3.5(b) shows the change in all energy components for each cut. Except for the first cut (not a good representation of a thin slit), there is a linear increase in all energy components as the stope progresses upwards. The total energy changes after 10 cuts are given at the bottom of Figure 3.5(b). Although the method of extraction could be classified as incremental, about 72% of the released energy is still in the form of seismic energy, even for these elastic conditions.

Suppose on the 10th cut in Figure 3.5(a) that three incremental slices are taken. This would more closely resemble horizontal drilling and breasting operations employed at many mines. In this case the boundary element model was used, because of the infinite stress at the face assumption in Equation 3.20. The results are presented in Table 3.2.

Table 3.2 - Energy components for three 1 m slices on the last cut (in MJ/m in length)

Slice	ΔW_t	ΔU_m	ΔU_c	ΔW_r	ΔW_k	$\Delta W_k/\Delta W_r$
1	2.52	0.52	1.78	1.26	0.74	59%
2	2.61	0.54	1.84	1.30	0.77	59%
3	2.69	0.56	1.90	1.35	0.79	59%

Reducing the mining enlargement from 3 to 1 m reduces the seismic efficiency from 72% to 59%. However, this is still a long way from a seismic efficiency approaching zero (i.e., $W_k = 0$). For this to happen the mining steps would have to be infinitesimally small, and probably equivalent to tunnel boring operations.

Theoretically, the seismic energy release in all these examples should occur within a fraction of a second following the blast. In practice it appears that the rock mass takes a longer time to adjust to the new stress regime. In a number of Canadian mines, rockbursts occur within a few seconds to hours after blasting. However, the longer the time interval the more probable that the cause of the rockburst is a breakdown of the rock mass rather than a purely elastic reaction.

3.5 Types of Rockbursts

The previous sections have dealt with the elastic reactions of the rock mass to mining. However, in most cases rockbursts are caused by the non-elastic rock behaviour during the failure process. Salamon (1983) has listed the pre-existing conditions necessary to initiate a rockburst. Part of the rock mass

must be at the point of unstable equilibrium because either:

a) changing stresses are driving a volume of rock to sudden failure;
b) a system of pillars is approaching a state of imminent collapse;
c) geological weakness planes are on the point of slipping.

These three categories can be conveniently labelled: strain, pillar, and fault-slip bursts, which are familiar terminology in mining.

Another condition is, that a change in stress is required to trigger the rockburst. This can be either an increase or decrease in stress depending on the type of rockburst. To initiate seismic waves an appreciable stress change must accompany the rockburst. Finally, there must be a substantial amount of energy available to provide the source of the seismic energy. This reservoir of energy can be either stored strain energy in the surrounding rock mass or a sudden change in potential energy.

One grey area in rockburst mechanics is the time element. From seismic records, rockbursts occur instantaneously or in a matter of milliseconds. It is not known whether the failure process will be violent if it is over seconds or even fractions of a second.

3.5.1 Strain Bursts

Strain bursts are caused by high stress concentrations, at the edge of mine openings, which exceed the strength of the rock. Events can range from small slivers of rock being ejected from the walls to collapse of a complete wall as it tries to achieve a more stable shape. These types of rockbursts are normally associated with development drifts including shafts.

Originally, it was thought that the source of the liberated energy was the stored strain energy in the rock that had failed. This concept changed in the 1960s with the advent of stiff testing machines.

The mechanical equivalent of a compression testing machine is a mass resting on a spring in contact with a rock specimen as shown in Figure 3.6(a). As the

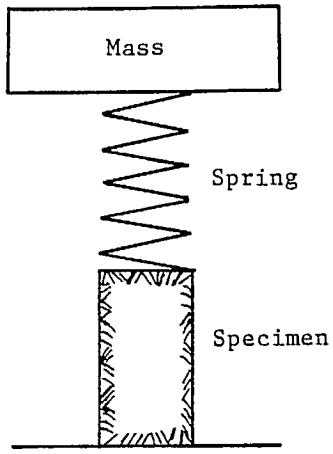

(a) Testing machine components.

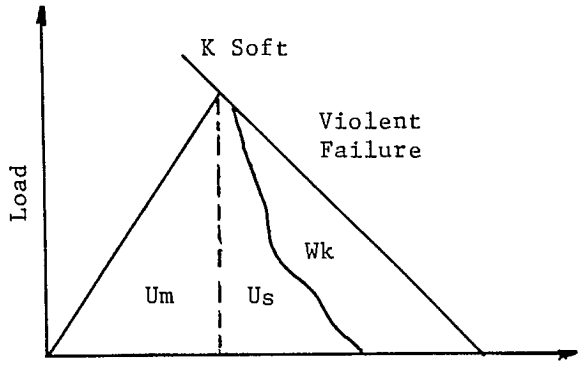

(b) Soft Loading.

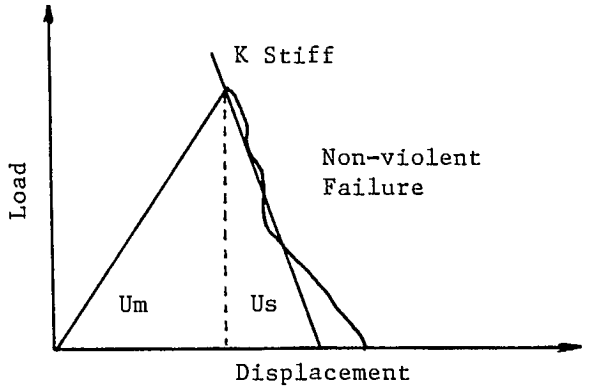

Fig. 3.6 - Violent and non-violent failure in soft and stiff testing machines.

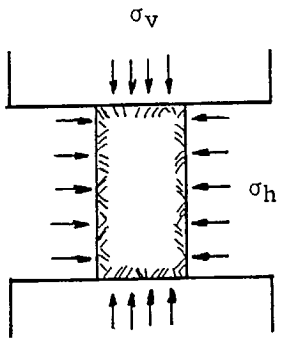

(a) Specimen under triaxial stress.

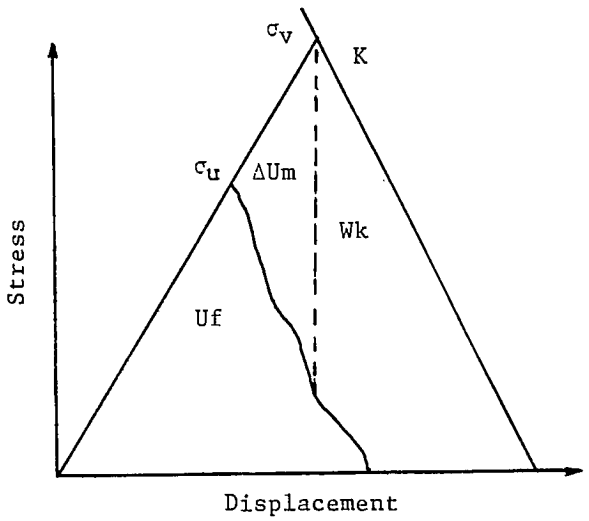

(b) Stress displacement behaviour due to release of lateral stress.

Fig. 3.7 - Release of stored strain energy due to loss of confinement.

mass is increased, energy is stored in both the rock specimen and spring. After the rock fails the load has to be reduced on both the failed rock specimen and the spring, and they will have different unloading curves. The gradient of the spring's unloading curve is called the spring constant (k). Figure 3.6(b) shows the load-displacement with a relatively soft spring (i.e., low k value). After failure, the load the spring applies to the specimen is greater than it can withstand and failure will be sudden and violent. The area between the spring and specimen unloading curves represents the energy that has to be released seismically (W_k). Figure 3.6(c) shows the same load-displacement curve for the specimen, but this time with a stiff spring (i.e., high k value). In this case, after failure, the load applied by the spring is less than what the specimen can withstand and the failure process will be gradual and non-violent with no excess energy being released seismically.

The area under the specimen load-displacement curve is made up of two components: the stored strain energy (U_m) of the specimen at its peak strength and part of the energy (U_s) that was stored in the spring. These two components represent the energy ($U_f = U_m + U_s$) consumed in the fracturing process. Consequently, the violence of rock failure is a property of the testing machine. The concept of loading and pillar stiffness is explored further under pillar bursts.

In some special cases part of the stored strain energy has to be released seismically. This occurs when a rock under triaxial stress conditions is suddenly reduced to a biaxial or uniaxial stress condition. The amount of energy stored in a rock under triaxial conditions was given in Equation 3.18. When mining an opening, one stress (say σ_3) is reduced to zero. Assuming the other stresses remain constant the reduction in stored strain energy (ΔU_m) is:

$$\Delta U_m = \frac{1}{2E}[\sigma_3^2 - 2\nu(\sigma_2\sigma_3 + \sigma_3\sigma_1)] \qquad \text{Eq 3.24}$$

Even more stored strain energy could be released if the rock, under triaxial stress, was just below its compressive strength. Figure 3.7(a) shows a specimen under triaxial stress in a testing machine, with a vertical stress (σ_v). If the lateral stresses are suddenly reduced to zero, the maximum uniaxial compressive stress the specimen can withstand is (σ_u) and ($\sigma_u < \sigma_v$).

As shown in Figure 3.7(b) the specimen will fail along its unloading curve, whereas the testing machine will unload, from the higher stress (σ_v) along its unloading curve of gradient (k). Again the area between these two unloading curves represents the energy that is released seismically (Es). The area identified at (ΔU_m) in Figure 3.7(a) is that proportion of the seismic energy which was originally stored as strain energy in the rock. In addition, the stored strain energy associated with the lateral stresses would also be released.

Strain bursts often occur when a drift is driven through a contact between a brittle and relatively soft rock. Damage is normally confined to the brittle side of the contact. Previously it was thought that the brittle rock, with a higher compressive strength and elastic modulus, would contain more stored strain energy. This is not necessarily the case as illustrated in Figure 3.8. Brittle rocks tend to have steeper unloading curves than soft rocks. In Figure 3.8, the area under both brittle and soft load-displacement curves are roughly the same, hence both rocks consume the same stored strain energy in the fracturing process. Again, the stiffness of the loading system (k) is less than that of the brittle rock and greater than the soft rock. Hence, the former fails violently and the latter non-violently, in this example.

Another mechanism that could be in operation is slippage along the contact. For the simple example of a circular tunnel excavated in a hydrostatic stress field (p) the radial displacement (u) of the circumference is given by:

$$u = \frac{rp}{E} (1 + \nu) \qquad \text{Eq 3.25}$$

where, r = radius of opening.

If the elastic modulus of the soft rock is half that of the brittle rock then the radial displacement is double for the soft rock. This would generate shear stresses along the contact with a chance of slippage.

Figure 3.9 shows a rectangular shaft which was subjected to a very high horizontal stress (70 MPa) across its short axis. At a depth of 1000 m one of the short walls burst in a semi-circular shape, at a contact between a brittle

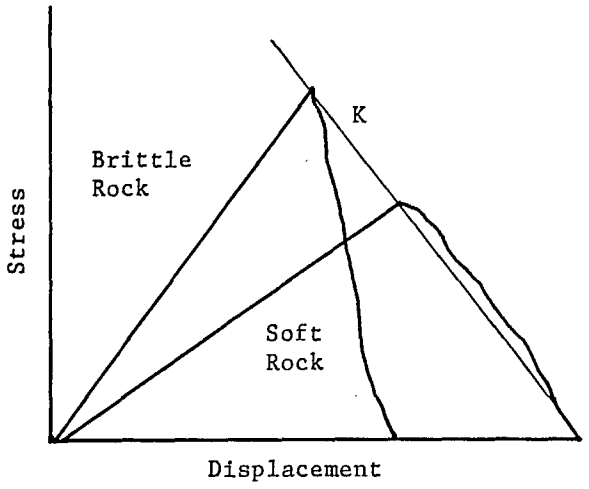

Fig. 3.8 - Stress-displacement characteristics of brittle and soft rocks.

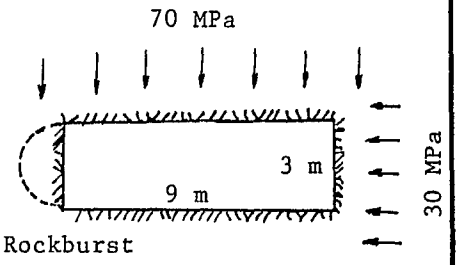

Fig. 3.9 - Rockburst in a rectangular shaft.

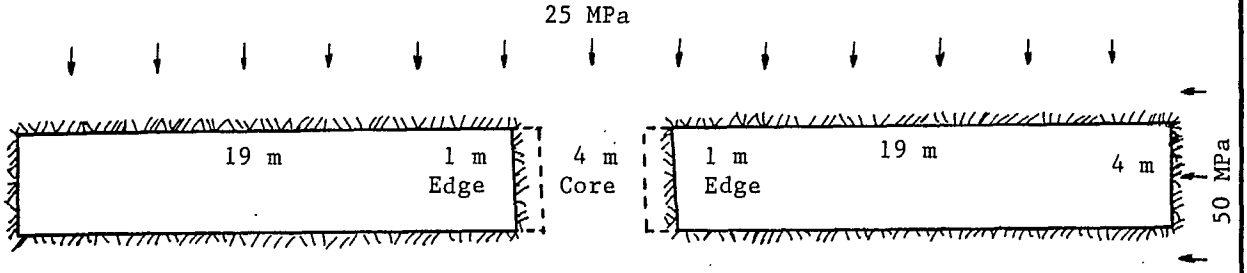

Fig. 3.10 - Stope and pillar model with two stages of pillar failure.

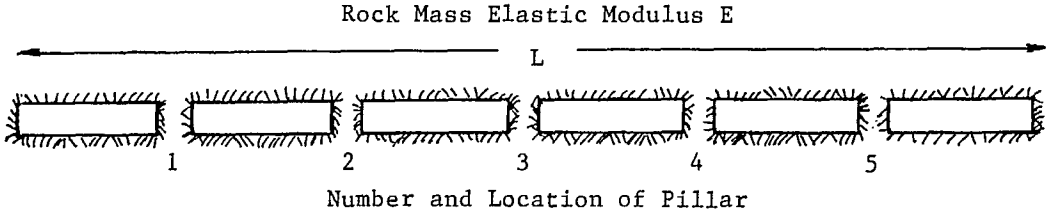

Fig. 3.11 - Factors affecting loading stiffness.

quartzite and a soft dyke. A boundary element model was run to determine the energy component due to the wall going from a straight to a semi-circular shape. These components are listed in Table 3.3.

Table 3.3 - Energy components for a burst in a shaft (in MJ/m in length)

ΔW_t	ΔU_m	ΔU_c	ΔW_r	ΔW_k	$\Delta W_k/\Delta W_r$
2.46	0.50	1.73	1.23	0.73	59%

Somewhat surprisingly, 59% of the released energy is seismic energy.

It appears that for strain bursts, energy can be released from a number of sources. If the rock goes from a triaxial to biaxial or uniaxial stress condition, some of the stored strain energy is released as seismic energy. Instantaneous failure of this rock will enlarge the opening and seismic energy will be released due to the elastic reactions of the rock mass (i.e., as in the example of the rectangular shaft). Finally, if brittle and soft rocks are present, then minor slippage could occur along the contact.

3.5.2 Pillar Bursts

Severe rockbursts, involving thousands of tonnes, have been caused by the complete collapse of support pillars. In some cases the collapse of one pillar can overstress adjacent pillars and a chain-type reaction ensues. In recent times, the most significant chain reaction occurred in an old stope-and-pillar area of Quirke Mine in Elliot Lake. Significant pillar bursts have also occurred in steeply-dipping vein-type orebodies at Red Lake and Kirkland Lake. These normally occur when sill/crown pillars of shrinkage or cut-and-fill stopes reach a critical size.

The source of the liberated seismic energy can be demonstrated by the simple example of two stopes separated by a pillar as shown in Figure 3.10. Two cases are examined: the edge of the pillar failing, followed by the central core. In both cases it is assumed that the stress on the failed portion

reduces immediately to zero (i.e., a vertical unloading line from peak strength). The boundary element model was used to calculate the energy components for the two stages of failure, which are given in Table 3.4.

Table 3.4 - Energy components for partial and complete pillar failure (in MJ/m in length).

Failure Stage	ΔW_t	ΔU_m	ΔU_c	ΔW_r	ΔW_k	$\Delta W_k/\Delta W_r$
Edges	1.62	0.30	1.11	0.81	0.51	63%
Core	10.73	0.93	6.29	5.36	4.44	83%

These results indicate a seismic efficiency ($\Delta W_k/\Delta W_r$) of 63% during failure of the pillar edges, which increases to 83% when the core fails. It appears that one of the characteristics of pillar bursts is that a very high proportion of the released energy (W_r) is seismic energy (W_k). The source of this liberated energy is the large change in potential energy (W_t) when the pillar fails. Equation 3.17 indicates that the change in potential energy is proportional to the square of the stope span. In this case, when the pillar core fails, the stope span more than doubles, hence the change in potential energy more than quadruples.

Whether a pillar fails violently or not depends on the stiffness of the loading system compared to that of the pillar, as explained in an elementary way in Figure 3.6. If the stiffness of the loading system is (k) (defined as always positive) and that of the pillar is (λ) then the condition for stability is:

$$k + \lambda > 0 \qquad \text{Eq 3.26}$$

If the pillar is on its loading curve, (λ) is positive and conditions are stable. It is only when the pillar exceeds its peak strength and its unloading curve (λ) is negative and exceeds the loading stiffness (k) that instability occurs.

In underground mines the stiffness of the loading system is influenced by many factors as illustrated in Figure 3.11. The areal extent or span of the mine workings has a strong influence. As the span increases loading stiffness decreases and eventually approaches a dead-weight loading system (i.e., k=0). The elastic modulus of the rock mass controls the amount of movement towards the excavations. The size, number and location of the pillars influence loading stiffness. Also, pillars cannot be treated in isolation since the presence of one pillar influences the loading stiffness on all other pillars.

The concept of local mine stiffness was introduced by Starfield and Fairhurst (1968). Suppose in Figure 3.11, that one of the pillars is replaced by a hydraulic jack which exerts the same load as the original pillar. The local mine stiffness, at that location, would be the unloading curve for the jack as the pressure is released. It can be envisaged that each pillar in turn is replaced by a hydraulic jack, thus obtaining the profile of loading stiffness across the panel. For a systematic layout of stopes and pillars the results would show that the loading system has its lowest stiffness at the centre of the panel and its highest stiffness next to the abutments. It follows that if one pillar fails the loading stiffness on all the remaining pillars is reduced.

A family of stress-displacement curves can be obtained by testing specimens in a compression testing machine, as shown in Figure 3.12. As either width/height ratio or confining stress increases the post-failure gradient (i.e., pillar stiffness λ) becomes flatter. This indicates that slender pillars, with a low width/height ratio are more prone to bursting than squat pillars, since their unloading gradient has a high negative value. However, experience underground suggests the complete reverse; slender pillars tend to yield and fail non-violently, whereas squat pillars fail violently. This apparent contradiction was resolved by Salamon (1970), in that loading and pillar stiffness cannot be treated in isolation, but must be considered in terms of all the pillars. Equation 3.26 only applies to testing single specimens in a press and its correct formulation is:

$$K + \Lambda > 0 \qquad \text{Eq 3.27}$$

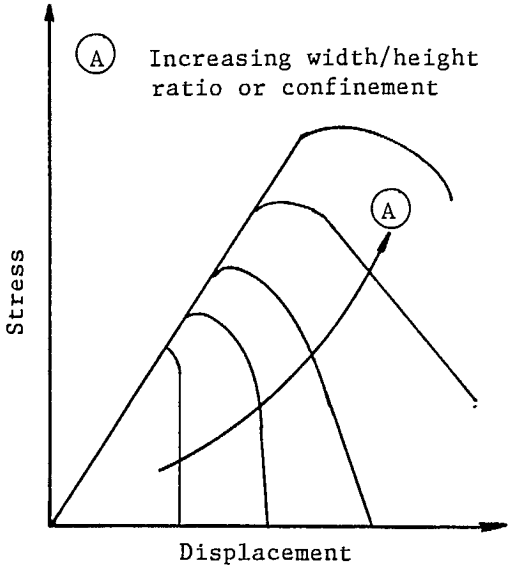

Fig. 3.12 - Factors affecting the post-failure stiffness of pillars.

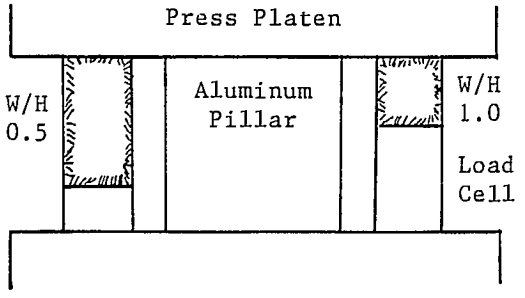

Fig. 3.13 - Multiple specimen testing.

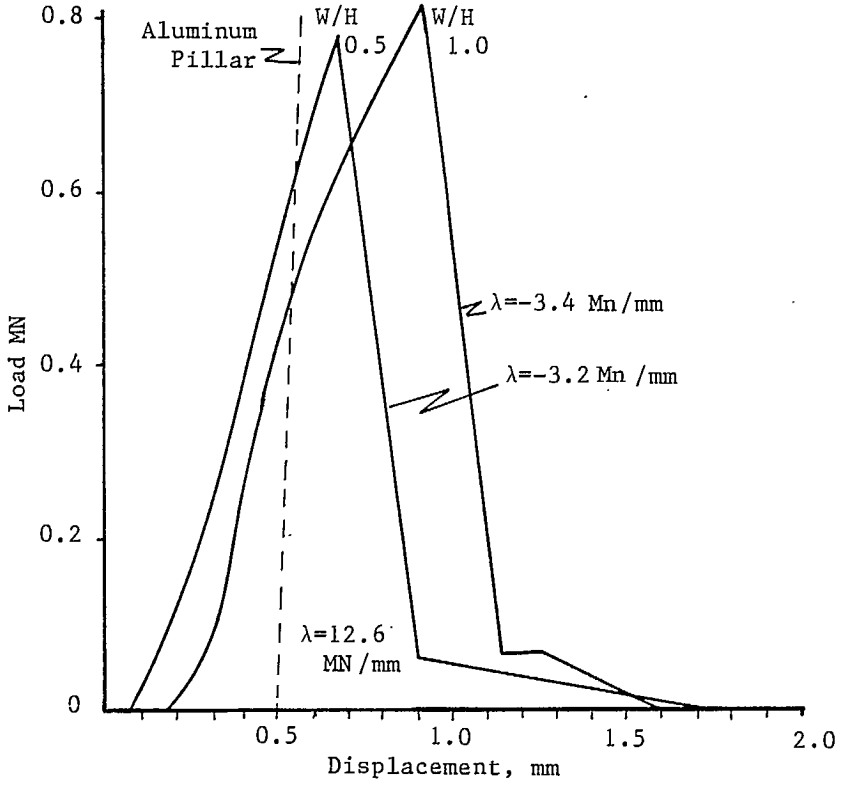

Fig. 3.14 - Load-displacement history of two specimens and aluminum pillar loaded simultaneously.

where (K) is the loading stiffness matrix on all the pillars and (Λ) is the slope matrix for all the pillars. It can be seen that for a mixture of slender and squat pillars, the slender ones would fail first, as indicated in Figure 3.12. Their slope would become negative, but the squat pillars would still be on their loading curve with a positive slope and ($K + \Lambda$) would still be greater than zero. With the slender pillars failing the loading stiffness would decrease and eventually, with increasing stress the squat pillars would fail violently.

This concept was demonstrated, in the laboratory, by loading multiple specimens at the same time, Swan (1985). As shown in Figure 3.13, a central aluminum pillar was surrounded by nine rock specimens of varying width/height ratios. Each specimen had its own load cell to measure its complete load-displacement history. Figure 3.14 shows the load-displacement curves for two of the specimens, of width/height ratios 0.5 and 1.0, as well as the central aluminum pillar. It was difficult to make each specimen the same height so their loading curves start at different displacements of the platen. By design the aluminum pillar was made slightly shorter so that the load capacity of the press was not used up compressing it.

The slender specimen failed first non-violently. Its slope became negative (λ = -3.2 Mn/mm), but the remaining specimens plus the central pillar were still on their loading curves with positive slopes. The squatter specimen failed next, again non-violently, with a similar negative slope (λ = -3.4 Mn/mm). In all, six of the nine specimens failed non-violently at peak strengths ranging from 175 to 235 MPa. At this point the test was terminated due to tilting of the platen. Although, in this test, the loading stiffness of the testing machine is constant, it did show that the slope matrix (Λ) for all of the specimens including the central aluminum pillar controls whether the specimens fail violently or not.

In summary, it appears that pillar bursts are caused by a sudden change in potential energy as the hanging wall and footwall rapidly converge during the failure process. Whether a pillar fails violently or not depends on the post-failure stiffness of the pillar compared to the stiffness of the loading system. However, pillar and loading stiffness cannot be treated in isolation,

but must be considered in regional terms involving whole stope-and-pillar panels and in some cases the whole mine.

3.5.3 Fault-Slip Bursts

Slippage along a fault has long been recognized as the mechanism of an earthquake. Only recently has the same mechanism been recognized as the cause of some rockbursts in Canadian hardrock mines, especially those in Sudbury.

A simple mechanical model which demonstrates fault-slip mechanics is shown in Figure 3.15(a). A block under a normal stress (σ_n) rests on a flat surface. A tangential stress (τ) is applied through an elastic spring (spring constant k), to the edge of the block. After the normal stress is applied the frictional force between the block and the flat surface is ($\mu_s \sigma_n$), where (μ_s) is the static coefficient of friction. The system is in stable equilibrium so long as:

$$\mu_s \sigma_n - \tau > 0 \qquad \text{Eq 3.28}$$

Unstable equilibrium is achieved when:

$$\tau = \mu_s \sigma_n \qquad \text{Eq 3.29}$$

Movement of the block will occur if there is a very small increase in (τ) or a decrease in (σ_n) or (μ_s). Once movement occurs the lower dynamic coefficient of friction (μ_d) comes into operation and an initial force of:

$$(\mu_s - \mu_d)\sigma_n$$

accelerates the block. Stable equilibrium is achieved when the shear stress reduces to:

$$\tau' = \mu_d \sigma_n \qquad \text{Eq 3.30}$$

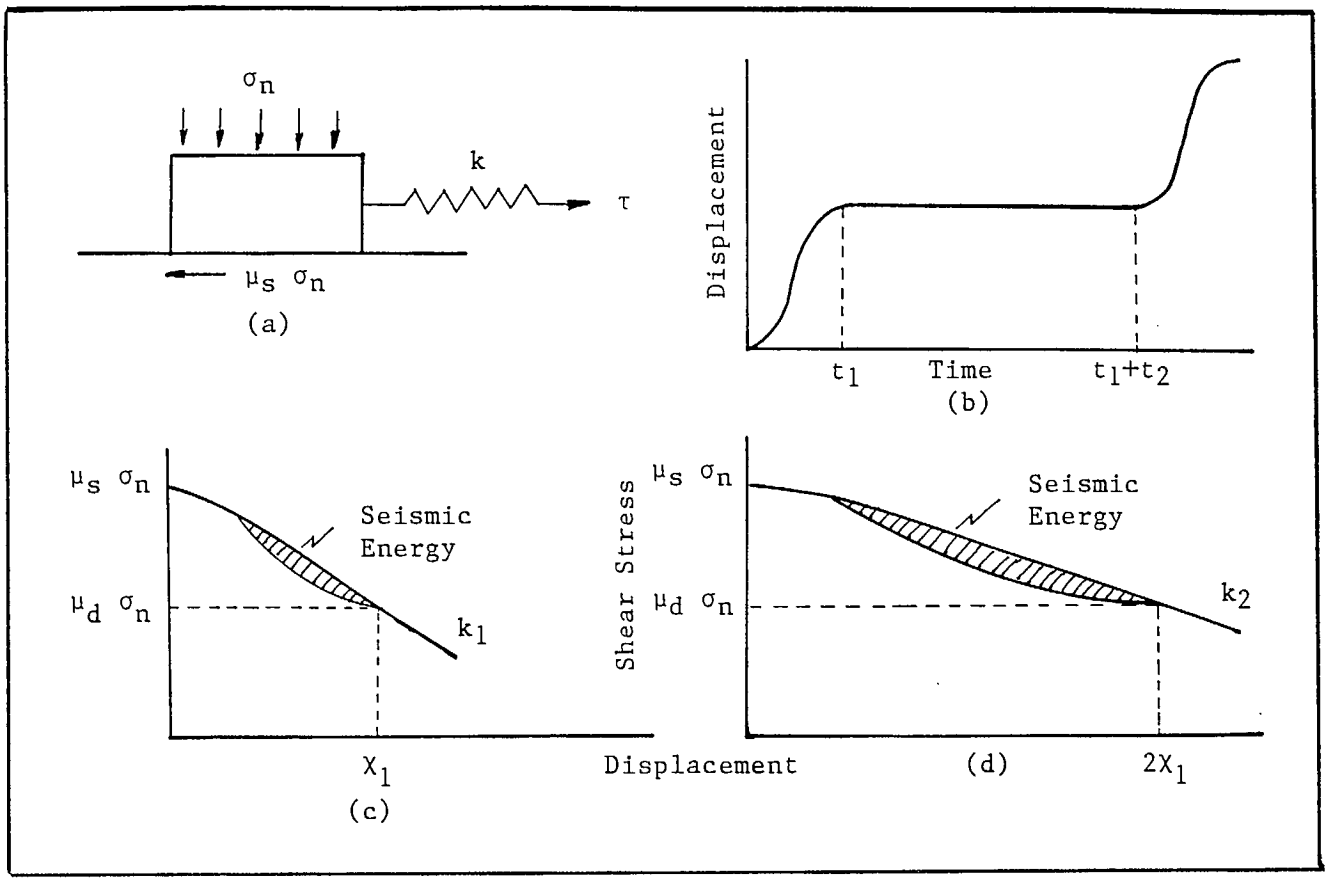

Fig. 3.15 - Displacement, time, shear stress history of fault-slip model.

and the resultant stress drop is:

$$(\tau - \mu_d \sigma_n) \qquad \text{Eq 3.31}$$

The dynamic history of the block movement is shown in Figure 3.15(b) (Jaeger and Cook, 1969). Here it is assumed that the free end of the spring moves at a constant velocity away from the block. Replacing the normal stress (σ_n) by a force (N) pressing on a mass (M), then the displacement (χ) of the block with respect to time (t) is:

$$\chi = (\mu_s - \mu_d) \frac{N}{k} (1 - \cos\alpha t) \qquad \text{Eq 3.32}$$

where $\alpha^2 = k/M$.

The block comes to rest at time (t_1):

$$t_1 = 2\Pi/\alpha \qquad \text{Eq 3.33}$$

after a displacement (χ_1):

$$\chi_1 = 2 (\mu_s - \mu_d) \frac{N}{k} \qquad \text{Eq 3.34}$$

If the end of the spring continues to move at a constant velocity then after an additional time (t_2) the spring is recharged and the whole slippage cycle repeats itself.

Figure 3.15(c) shows the stress-displacement history of the block. Again, displacement starts when the shear stress equals ($\mu_s \sigma_n$) and stops when it reduces to ($\mu_d \sigma_n$). The curve of block displacement can be non-linear as illustrated, whereas the spring has a linear unloading curve of gradient (k_1). The area between the two curves represents the energy that has to be dissipated kinetically. This is analogous to the specimen and loading machine stiffness concepts discussed earlier. The total kinetic energy (W_k) released can be expressed by:

$$W_k = \frac{N^2\Pi}{2k\alpha} (\mu_s - \mu_d)^2 \qquad \text{Eq 3.35}$$

Figure 3.15(d) shows the stress-displacement history if the spring constant is reduced by a half ($k_2 = k_1/2$). In this case the displacement of the block is doubled (from Equation 3.34) and the area between the two curves is increased. This emphasizes the importance of the stiffness of the loading system on both the amount of slippage and seismic energy released in fault-slip rockbursts.

The mechanics of slippage on a fault with a circular area have been developed in rock mechanics by Salamon (1974), and in seismology by Brune (1970). Using Salamon's terminology, the drop in the shear stress is:

$$\tau - \mu_d \sigma_n$$

For a circular fault of radius (R) in homogeneous isotropic ground, the tangential slip (ψ), is given by:

$$\psi = \frac{4(1 - \nu)(\tau - \mu_d \sigma_n)(R^2 - r^2)^{1/2}}{\Pi G (1 - \nu/2)} \qquad \text{Eq 3.36}$$

where, r = distance from centre

ν = Poisson's ratio

G = modulus of rigidity (shear modulus).

The energy components can be expressed as follows:

$$\text{Potential Energy, } W_t = \frac{8(1 - \nu)R^3\tau(\tau - \mu_d \sigma_n)}{3G(1 - \nu/2)} \qquad \text{Eq 3.37}$$

$$\text{Released Energy, } W_r = \frac{4(1 - \nu)R^3(\tau + \mu_d \sigma_n)(\tau - \mu_d \sigma_n)}{3G(1 - \nu/2)} \qquad \text{Eq 3.38}$$

$$\text{Heat Energy, } W_x = \frac{8(1 - \nu)R^3 \mu_d \sigma_n(\tau - \mu_d \sigma_n)}{3G(1 - \nu/2)} \qquad \text{Eq 3.39}$$

$$\text{Seismic Energy, } W_k = W_r - W_x = \frac{4(1 - \nu)R^3(\tau - \mu_d \sigma_n)^2}{3G(1 - \nu/2)} \qquad \text{Eq 3.40}$$

The seismic efficiency can be calculated from these relationships:

$$\frac{W_k}{W_r} = \frac{\tau - \mu_d \sigma_n}{\tau + \mu_d \sigma_n} \qquad \text{Eq 3.41}$$

Just before slip initiation the shear and frictional forces are in equilibrium:

$$\tau = \mu_s \sigma_n \qquad \text{Eq 3.42}$$

Hence,

$$\frac{W_k}{W_r} = \frac{\mu_s - \mu_d}{\mu_s + \mu_d} \qquad \text{Eq 3.43}$$

This analysis indicates that seismic efficiency is independent of depth, stress drop, fault dimensions or amount of slippage and is only dependent on the frictional properties of the fault. Typically the dynamic coefficient of friction is 90 to 95% of the static coefficient (Jaeger & Cook, 1969), giving seismic efficiencies of 5% to 2.5%. This is completely the reverse of the seismic efficiencies, of about 90%, encountered in pillar rockbursts.

In most mining operations the faults, on which slippage is occurring, intersect the mine openings. A full circular fault model may not be applicable in these cases and a semi-circular or quadrant model may be more appropriate. In some cases the aftershock pattern from microseismic monitoring systems gives a good indication of the areal extent over which slippage occurred.

In most cases, the damage caused by fault-slip rockbursts in Ontario mines is minimal. There is one example of a 2.2 Mn magnitude rockburst at the Falconbridge Mine near Sudbury where no damage was found, although 10 to 20 mm of slippage could be observed on the fault. Normally what damage is observed is away from the fault where the radiated seismic energy has triggered a critically loaded structure. In one case a 3.4 Mn fault-slip rockburst caused a backfill mat to collapse in an undercut-and-fill stope some 20 m away.

3.6 References

Brune, J.N. (1970), Tectonic stress and the spectra of seismic shear waves from earthquakes; J. Geophys. Res., vol. 75, pp. 4997-5009. Correction: J. Geophys. Res. vol. 76, (1971), p. 5002.

Cook, N.G.W. (1967), Design of underground excavations; 8th U.S. Rock Mech. Symp., Minnesota, pp. 167-193.

Hodgson, K. and Joughin, N.C. (1967), The relationship between energy release rate, damage and seismicity in deep mines; 8th U.S. Rock Mech. Symp., Minnesota, pp. 194-209.

Ortlepp, W.D. (1983), The mechanism and control of rockbursts; Chapter 12: Rock Mechanics in Mining Practice, S. Budavari (Editor), S. Afr. Inst. Min. Met., Mono Series No. 5, pp. 257-281.

Salamon, M.D.G. (1968), Two-dimensional treatment of problems arising from mining tabular deposits in isotropic or transversely isotropic ground; Int. J. Rock Mech. Min. Sci., vol. 5, pp. 159-185.

Salamon, M.D.G. (1970), Stability, instability and design of pillar workings; Int. J. Rock Mech. Min. Sci., vol. 7, pp. 613-631.

Salamon, M.D.G. (1974), Rock mechanics of underground excavations; Proc. 3rd Congr. Int. Soc. Rock Mech., Denver, Colorado, vol. 1, Part B, pp. 951-1099.

Salamon, M.D.G. (1983), Rockburst hazard and the fight for its alleviation in South African gold mines; Rockbursts: Prediction and Control, IMM, London, pp 11-36.

Salamon, M.D.G. (1984), Energy considerations in rock mechanics: fundamental results, J. S. Afr. Inst. Min. Met. vol. 84, No. 8, pp. 233-246.

Starfield, A.M. and Fairhurst, C. (1968), How high-speed computers can advance design of practical mine pillar systems; Eng. & Min. J., vol. 169, pp. 78-84.

Swan, G. (1985), Multiple pillar compression failure in brittle rock, Division Report MPR/MRL 85-103(TR), CANMET, Energy, Mines and Resources Canada.

4. SEISMIC MONITORING

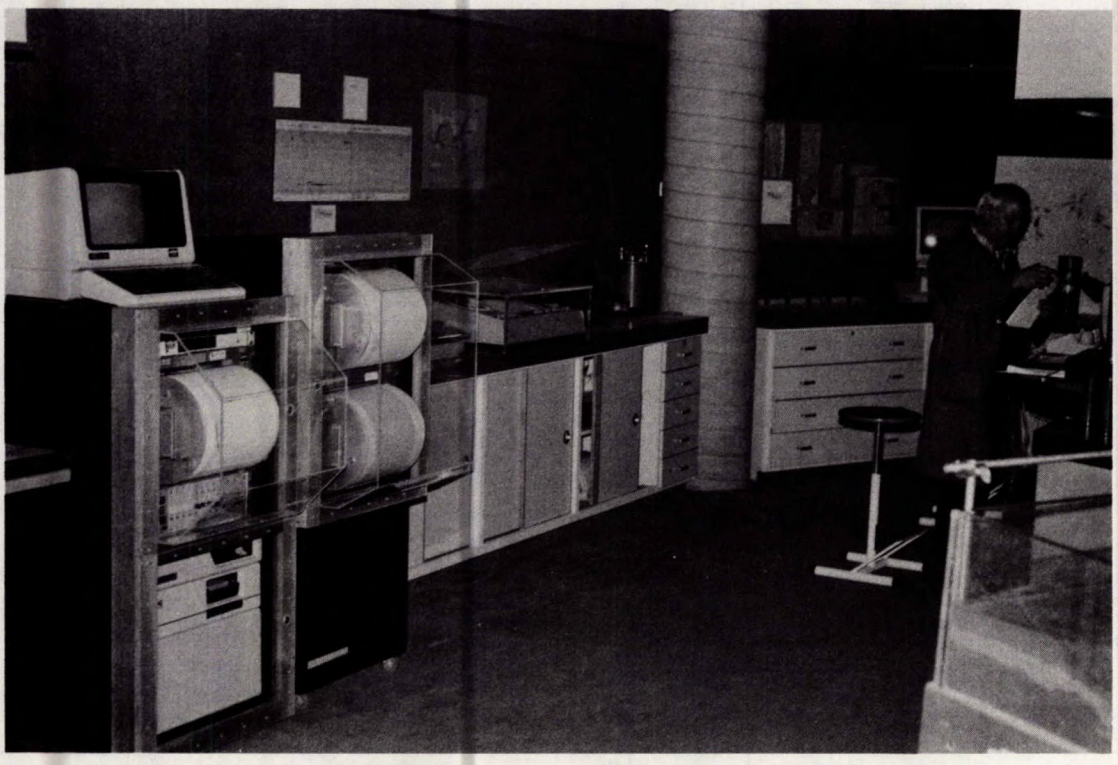

Three seismographs providing coverage of the Sudbury Basin from Science North.

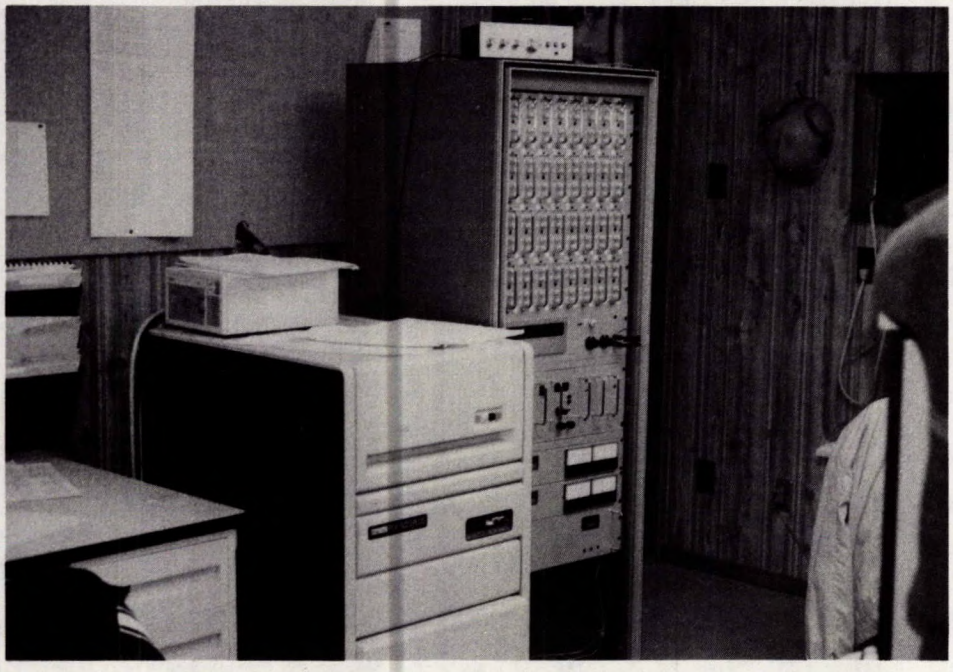

MP-250 microseismic system at Campbell Mine.

4. SEISMIC MONITORING

4.1 Introduction

There are three types of seismic monitoring equipment used to record and analyze seismicity in Ontario mines.

The Geophysics Division of the Geological Survey of Canada operates the Canadian Seismograph Network for earthquake detection. This network also records the larger rockbursts (i.e., >2.0 Mn). Additional regional seismograph stations have been installed at the mining camps experiencing rockbursts. All the stations are located on surface, usually tens of kilometers away from the mines. Magnitudes of the seismic events are obtained from this network.

Macroseismic systems are being used by research organizations to investigate the seismic source parameters of rockbursts. These systems have the capability of recording the seismic waveforms of events greater than 0.5 magnitude using triaxial sensors. The systems normally employ five sensors, located on surface and/or underground, usually within a kilometer of the mine workings. By 1991, five macroseismic systems were in operation at the most rockburst prone mines in Ontario.

Microseismic systems are used, by the mining companies, to detect both small and large seismic events. Source location is obtained in a few seconds and most mines have the capability of automatically plotting the events on digitized mine plans and sections. The first modern microseismic system was installed in Ontario at the Creighton Mine in 1980 and ten years later 15 systems were in operation at underground hardrock mines in Ontario.

4.2 Seismograph Systems

The Geological Survey of Canada has a network of almost 100 seismograph stations across Canada. These stations are grouped into four regions covering eastern, central and western Canada and the Arctic. Of particular interest for rockburst detection is the Eastern Canada Telemetered Network (ECTN) which

extends from Manitoba to the Atlantic provinces.

Originally this network was concentrated along the seismically active St. Lawrence river and adjacent areas. Subsequently, it was expanded to cover the Temiscaming - Kapuskasing areas.

Most hardrock mines in Ontario are located in the seismically stable Precambrian Shield, where earthquake activity is infrequent. Consequently, this region initially had poor coverage. The one exception was the seismograph station installed at Kirkland Lake in the 1940s, specifically to record rockburst activity in the local gold mines (Hodgson, 1958).

Coverage has improved since 1982 when the Canadian Nuclear Fuel Waste Management Program operated by Atomic Energy of Canada Ltd. supported the operation of six additional seismograph stations in Northern Ontario and Manitoba, to provide data for regional seismic hazard estimates. Since 1985, the Canada/Ontario/Industry Rockburst Project has expanded the Sudbury Local Telemetered Network (SLTN) and has installed local seismographs at Elliot Lake, Red Lake and Kirkland Lake. The location of the seismograph stations covering northern Ontario are shown in Figure 4.1.

All seismograph stations consist of a vertical single-component, one-second period, Teledyne-Geotech S13 seismometer, which usually records in a frequency range of 1 to 16 Hz. At some stations only the analog signal is recorded on a helicorder, the paper chart is changed once a day and sent to the Geophysics Division in Ottawa on a monthly basis. At other stations the seismic signal is digitized at source and transmitted to Ottawa over telephone lines or by UHF radio.

An example of the latter type of system is the SLTN network which provides coverage to mines in the Sudbury basin (Plouffe et al., 1988). The layout of this network is shown in Figure 4.2. It consists of three outstations located around the rim of the basin. The seismic signals are continuously digitized at each outstation and transmitted by dedicated telephone lines to Science North, a public science centre in Sudbury. Here a processor saves triggered seismic events using a simple short-term/long-term average algorithm. These

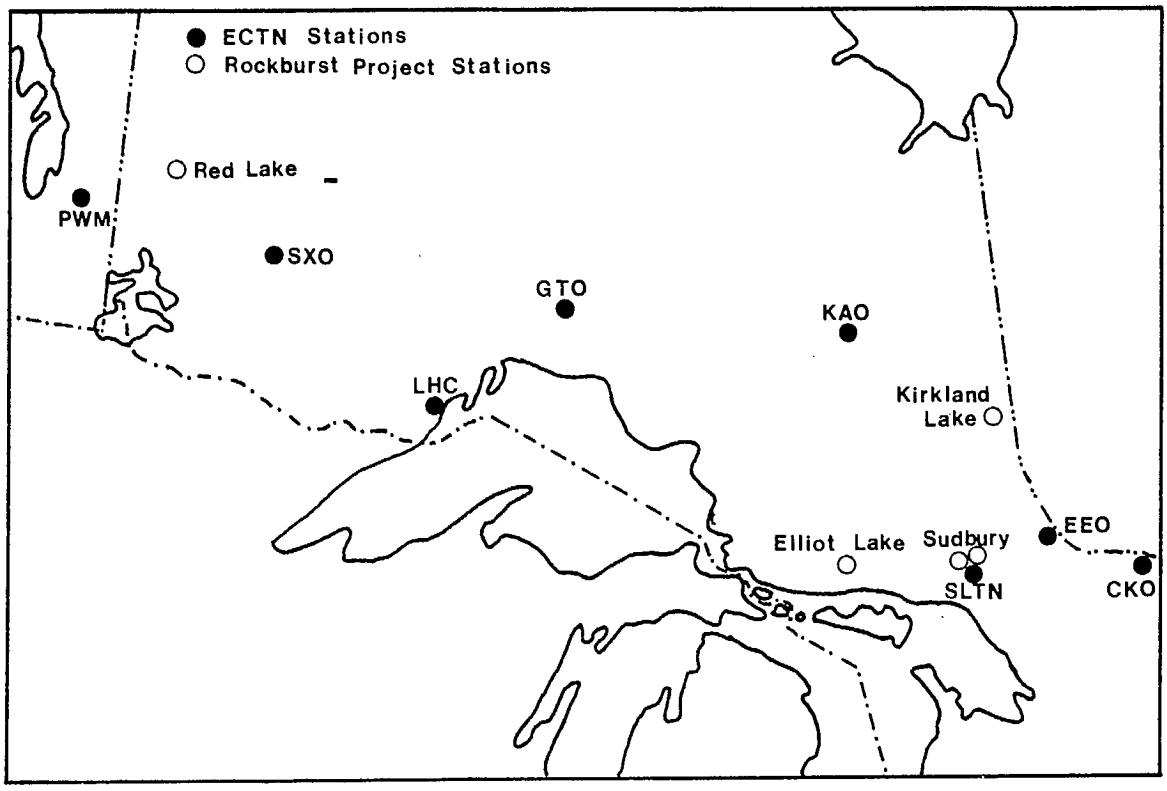

Fig. 4.1 - Location of seismograph stations in northern Ontario.

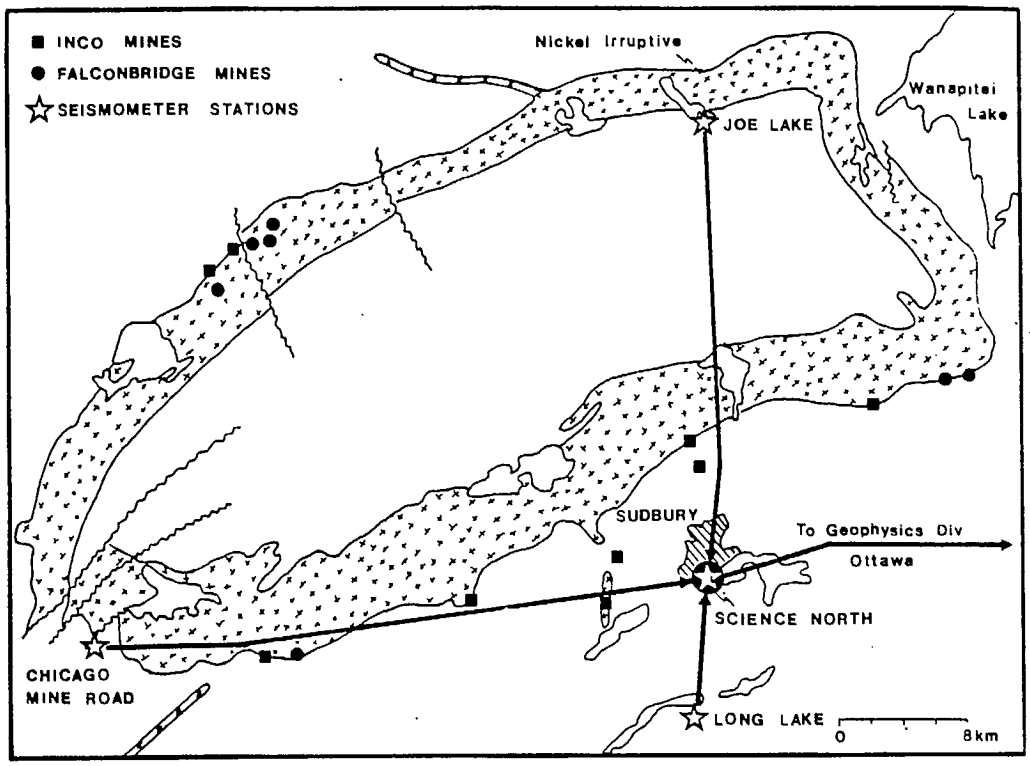

Fig. 4.2 - Location of the seismograph network around the Sudbury Basin.

triggered events are automatically transmitted over a dedicated telephone line to Ottawa and incorporated into the ECTN data base. In addition, the digitized signals from each outstation are converted back to analog signals and are recorded on helicorders, which are on public display at Science North.

Typically, this network records 200 events each month. Of these, about 28% are events emanating from outside the Sudbury Basin. Of the remaining 72%, about 60% are blasts and 12% are mining-induced seismic events within the Sudbury mines. All mining-induced seismic events and some blasts are identified with the collaboration of the mine operators.

In some cases it is possible to clearly differentiate between rockbursts and blasts from the seismic records, whereas in other cases it is difficult. Figure 4.3 shows the seismic signals from four events (two rockbursts and two blasts) recorded on the Elliot Lake Seismograph. Event A is a rockburst at a mine 12 km away which has a clear P-wave S-wave separation of 1.7 sec. Event B is a central blast at a mine 5 km away. The millisecond delays in the blast produce no clear P- and S-waves, besides which, central blasts only occur at specific times of the day and are usually clearly recognizable. Events C and D are a rockburst and a large blast in one of the Sudbury mines at a distance of about 80 km. In these cases there are no clear differences and the event would have to be confirmed by the mine operator.

The Geophysics Division of the Geological Survey of Canada publishes a quarterly report on mining-induced seismicity in Canada. The time of the event, the stations that recorded it, and the estimated magnitude are listed. Predominantly the coverage is for northern Ontario mines, but any events in New Brunswick and Quebec mines are also reported.

4.3 Macroseismic Systems

CANMET operates five macroseismic systems in Ontario mines. They are located at Rio Algom's Quirke Mine at Elliot Lake, Falconbridge's Strathcona Mine and Inco's Creighton Mine at Sudbury, Placer Dome's Campbell Mine at Red Lake and Lac Mineral's Macassa Mine at Kirkland Lake. Each system consists of five strong-motion triaxial sensors installed in boreholes underground and/or on

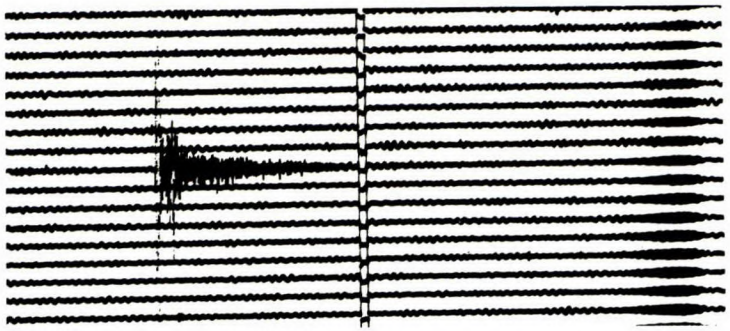

a) 1.8 Mn rockburst at Elliot Lake.

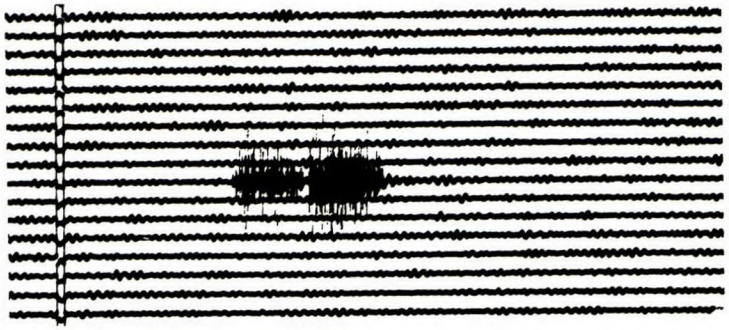

b) Central blast at Elliot Lake.

c) 2.9 Mn rockburst at Sudbury.

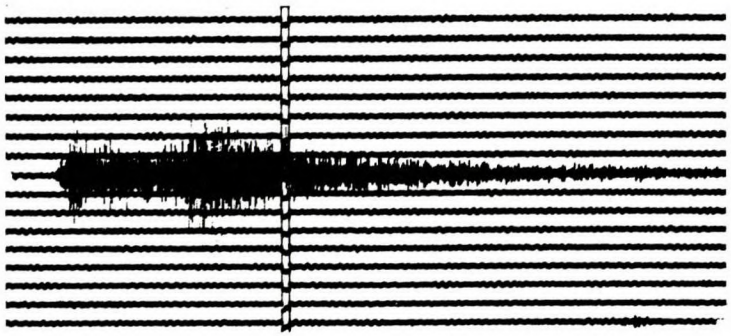

d) Blast at Sudbury.

Fig. 4.3 - Seismograph records of rockbursts and blasts.

surface. They are designed to capture the complete seismic waveforms to allow source location determination as well as seismic source parameters and mechanisms.

All five systems have basically the same hardware components as illustrated in Figure 4.4. Four systems use velocity gauge triaxial sensors with a sensitivity of 0.30 V/cm/sec and a frequency response range between 1 and 2700 Hz. The system at the Strathcona Mine uses accelerometers with a sensitivity of 20 V/g and a frequency range of 0.01 to 2000 Hz.

The seismic signals are amplified at each sensor. In the case of the Creighton system there is dual amplification to provide a larger dynamic range and prevent saturation for the larger seismic events. At the Strathcona, Campbell and Macassa Mines the seismic signals are transmitted through electric cable. At the Quirke Mine the system is totally fibre optics, and at the Creighton Mine the shaft cable is fibre optics. In the latter case a multiplexer and demultiplexer are located at either end of the fibre optics cable. Both Quirke and Strathcona Mines have surface sensors which have lightning protection (the Quirke system has electric cable in the fibre optics cable to power the sensors).

All processing units are located on surface, where the seismic signals are first conditioned (anti-aliasing filters) and then passed on to the data acquisition system located in the host computer. The signals are then digitized at a rate varying from 1024 to 4500 samples/sec/channel for the five systems.

A sophisticated triggering controller has been developed to eliminate the recording of very small seismic events, machine noise or electrical spikes which would saturate the system. The controller has the following features: selectable trigger windows, selectable number of channels for a valid trigger, short-term integration for spike suppression, selectable trigger thresholds, and individual channel enable/disable switches. If the trigger controller determines that a valid event has occurred then two seconds of seismic data are stored for each channel (i.e., 15 channels) including half a second of pre-trigger data. For the Strathcona, Campbell and Macassa systems, data

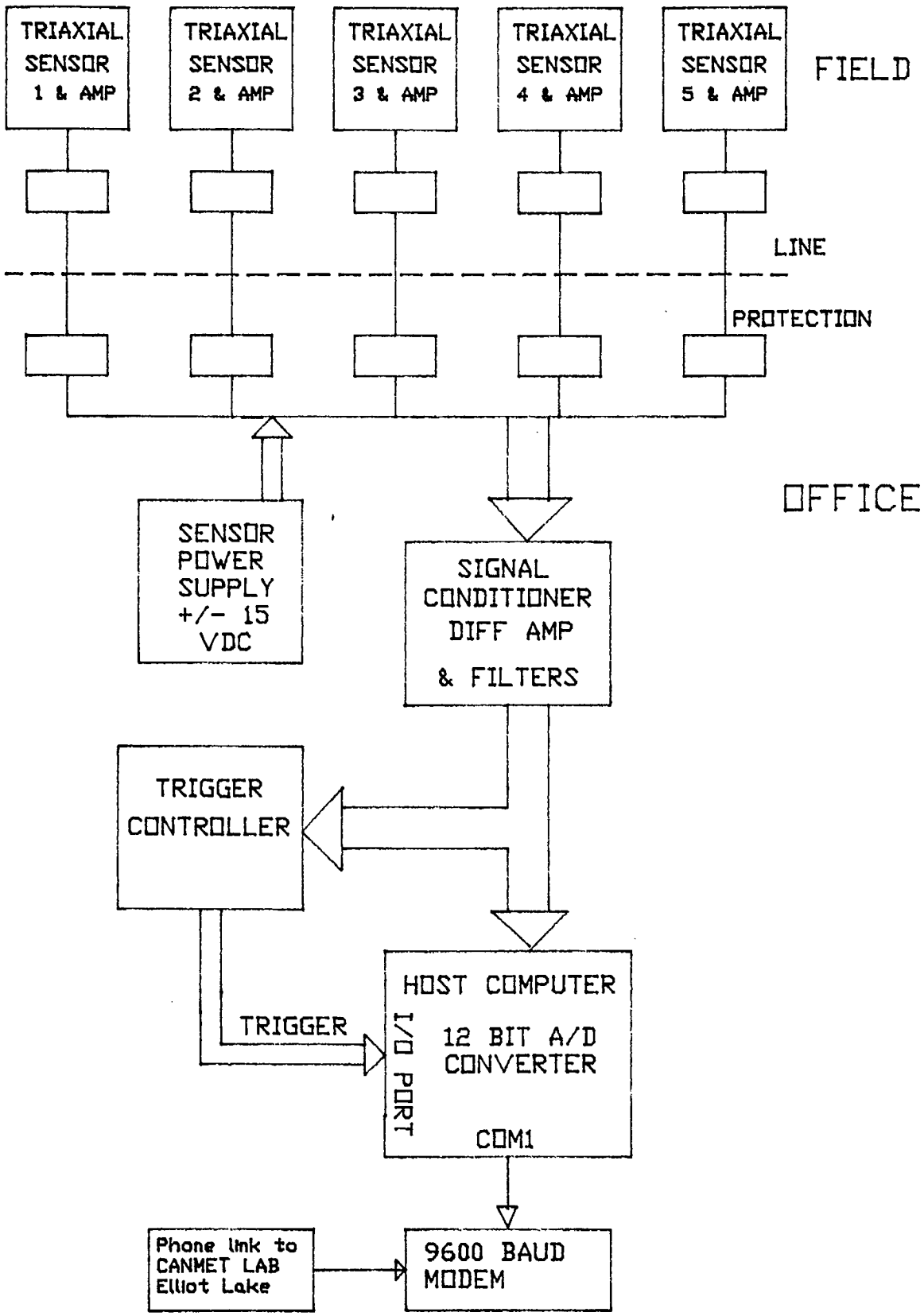

Fig. 4.4 - Components of a macroseismic system.

acquisition is interrupted for about 200 milliseconds while the data is down-loaded to the hard disk. In the Quirke and Creighton systems, data acquisition and down-loading can occur at the same time.

All macroseismic systems are connected via modems to CANMET's Elliot Lake Laboratory. From here the data files can be edited and transferred to Elliot Lake and some functions of the trigger controller can be altered.

4.4 Microseismic Systems

Mining-induced microseismicity (i.e., sub-audible noise) was accidentally discovered, in the late 1930s, while taking seismic velocity measurements at an underground mine in the United States (Obert, 1975). Soon afterwards the microseismic technique was tested at the Lake Shore Mine at Kirkland Lake and at Inco's Frood Mine in Sudbury. These early efforts lapsed due to inadequate electronic components.

The first modern day microseismic system was installed in a South African gold mine in the 1960s (Cook, 1963 and 1964), followed by mines in the Coeur d'Alene district, United States (Blake and Leighton, 1970). By the late 1970s commercial systems became available and all of the systems installed in the 1980s in Ontario mines were manufactured by Electro-Lab Inc. of Spokane, Washington, U.S.A. Basically these systems give the time of an event, the source location and a relative value which can be related to the seismic energy of the event.

The design of underground microseismic systems has been described by Blake (1974, 1982), Malott (1981) and Green (1982), and use of the systems in Ontario mines has been described by MacDonald and Muppalaneni (1983), Davidge (1984), Neumann (1985), and Oliver and MacDonald (1985).

The basic components of a microseismic system consist of an array of geophones and amplifiers wired to a processing unit normally located on surface.

Two types of geophones are in general use: velocity gauges and accelerometers. Both types have high sensitivities of 40 V/mm/sec and 950 V/g. Velocity

gauges record over the lower frequency ranges of 10 to 2500 Hz compared to accelerometers at 100 to 10,000 Hz. Either type of geophone is installed in short boreholes (e.g., 2 m) and is screwed into a metal or plastic plug cemented to the end of the borehole. Accelerometers can be installed in any hole direction, whereas velocity gauges are manufactured for either vertical or horizontal holes. Since the geophone output levels are very low, in the order of millivolts, amplifiers are installed inside the geophones to boost the signal. Seismic signals are transmitted over shielded electrical cables to the processing unit. Power (28 volts D.C.) is also normally provided via the processing unit over the same shielded cables.

The processing unit basically consists of signal filters and selectable threshold detectors for each geophone, a date clock, a selectable time window, an energy integrator, a microprocessor and a printer. Arrival times are recorded with a precision of ± 0.00005 sec. The time window is normally selected as the time taken for the P-wave to travel between the geophones furthest apart in the array, typically 0.1 to 0.2 sec. The energy integrator is the output from one of the geophones integrated over the length of the time window. Since seismic energy is proportional to particle velocity, the signals from accelerometers are integrated twice, once at the sensor then at the processing unit.

The system operates in a continuous monitoring mode. As soon as the voltage exceeds a preset threshold at any one geophone the time window is opened and the energy integrator activated. If a further minimum of four geophones exceed their threshold voltage, within the time window, the event is accepted and processed. Otherwise the data are discarded and the system returns to its monitoring mode.

Trigger threshold levels can vary up to 5 volts, but are typically set around 0.75 to 1.0 volts. More recent microseismic systems have the option of a floating threshold level to eliminate continuous triggering by machine noise. The background noise is continuously averaged over 2 second periods, and the threshold level (e.g., 1 volt) has to exceed this background level.

The printout of a seismic event from the processing unit first prints the

Julian day and time (h, min, sec) at which the first geophone was triggered. Then the sequency and arrival times of the triggered channel (up to 16) are listed in order of their occurrence relative to the first triggered channel. This is followed by the energy value from the integrator. Finally, up to four estimates of source location are calculated based on the 'direct solution method', which is described later. Many mining companies now by-pass the printer and feed the information from the processing unit directly into a computer for storage and analysis.

Since the microseismic systems are very sensitive they tend to record many events (e.g., blasts) that are not mining-induced seismic events. For mines that have a central blasting system at specific times (e.g., Elliot Lake mines), the events that are recorded during the blast are discarded from the microseismic records. At another mine only the seismic activity occurring during off-shift and weekends was analyzed.

After large seismic events (over 3.0 Mn) the geophones tend to be saturated when the time window closes which hangs-up the system. As an example, after a 4.0 Mn event at the Creighton Mine, the microseismic system was hung-up for four seconds before recording the next event. For slightly smaller seismic events (over 2.0 Mn) the geophones are still vibrating when the time window closes and it immediately reopens and records a second event which in reality is a continuation of the first event.

To obtain a more realistic indicator of seismic energy, the energy value given by the integrator should be multiplied by the distance from the energy phone to the source (i.e., seismic energy is directly proportional to distance squared and particle velocity squared, Equation 5.8). However, for the larger seismic events the energy channel is wholly or partially saturated and tends to produce similar numbers. In these cases it is better to rely on the seismograph and macroseismic systems to provide values of magnitude and seismic energy.

The Department of Geological Sciences, Queen's University at Kingston has developed a full waveform recording microseismic system. It is usually connected to the existing Electro-Lab systems. The seismic signals are

digitized, similar to the macroseismic systems, and stored on a computer. Accurate arrival times can be determined, rather than threshold values. Also, source parameters of the smaller seismic events can be investigated.

4.5 Source Location Techniques

Seismic monitoring systems basically measure the arrival times of the seismic waves. Knowing the coordinates of the sensors and assuming a uniform velocity at which the seismic signals travel through the rock, an estimate of the source location can be determined. Various mathematical techniques have been developed to determine source location (Cook, 1963), (Leighton and Duvall, 1972), (Blake, et al. 1974), (Godson, et al. 1978), (Gendzwill and Prugger, 1978), (Prugger and Gendzwill, 1988), and comprehensive reviews by (Lee and Stewart, 1981), and (Niewiadomski, 1986).

There are two general methods of source location based on the arrival times of the P-waves alone, or the arrival times of both the P- and S-waves. The latter method can only be used when the complete seismic waveforms are measured, as in the seismograph and macroseismic systems. The former method is generally used when only threshold values are measured, as in the microseismic systems.

The mathematical techniques can also be divided into two groups, either direct or iterative solutions. The former include the methods developed by United States Bureau of Mines (USBM) and the modifications made by Mt. Isa, and the latter include the Block and Simplex methods.

4.5.1 Direct Solutions

The direct technique was first developed by the USBM and presented by Leighton and Duvall (1972), and a least-squares technique was developed by Blake, Leighton and Duvall (1974). The three-dimensional coordinates of the source are unknown and can be represented by a system of linear algebraic equations as follows:

$$D_i = \sqrt{(X-a_i)^2 + (Y-b_i)^2 + (Z-c_i)^2} \qquad \text{Eq 4.1}$$

where, D_i = distance from the source to the ith sensor
X,Y,Z = coordinates of the source
a_i,b_i,c_i = coordinates of the ith sensor.

Also, $$D_i = V_p\ T_i \qquad \text{Eq 4.2}$$

where, V_p = P-wave velocity
T_i = time taken for the P-wave to travel from source to the ith sensor.

The seismic monitoring system only measures the arrival time relative to the first sensor triggered, hence,

$$D_i = V_p(t_i + T_1) \qquad \text{Eq 4.3}$$

where, T_1 = travel time to the first sensor
t_i = trigger time of the ith sensor,

and, $$D_i = d_i + D_1 \qquad \text{Eq 4.4}$$

where, D_1 = distance from the source to the first sensor triggered,
d_i = D_i, less the distance to the first sensor triggered.

The distance, D_1, to the first sensor triggered is expressed by:

$$D_1 = \sqrt{(X-a_1)^2 + (Y-b_1)^2 + (Z-c_1)^2} \qquad \text{Eq 4.5}$$

and the incremental distance, d_i, can be calculated from:

$$d_i = V_p\ t_i \qquad \text{Eq 4.6}$$

Consequently,

$$V_p t_i + \sqrt{(X-a_1)^2 + (Y-b_1)^2 + (Z-c_1)^2} = \sqrt{(X-a_i)^2 + (Y-b_i)^2 + (Z-c_i)^2} \qquad \text{Eq 4.7}$$

To solve this simultaneous equation at least five sensors have to be triggered if the P-wave velocity is known, or six sensors if the velocity is unknown.

Generally, the mines conduct blast calibrations at known locations to determine an average P-wave velocity.

If both the P- and S-wave arrival times are known, then

$$D_i = \Delta t_i^{S-P} / (\frac{1}{V_s} - \frac{1}{V_p}) \qquad \text{Eq 4.8}$$

where, Δt_i^{S-P} = difference in arrival times of S- and P-waves at the sensor. The equivalent of Equation 5.7 becomes:

$$\Delta t_i^{S-P} / (\frac{1}{V_s} - \frac{1}{V_p}) = \sqrt{(X-a_i)^2 + (Y-b_i)^2 + (Z-c_i)^2} \qquad \text{Eq 4.9}$$

In this case, the triggering of the first sensor is not critical, and only four sensors need to be triggered to calculate the source location.

In both methods, if more than the minimum number of sensors are triggered then a least-squares solution can be applied to the data, as described by Blake, et al. (1974), which increases the accuracy of the solution.

At some of the Inco mines in Ontario a multiple direct-solution is used for source location. Using Equation 4.7, all possible combinations of six arrival times are analyzed. Hence, if sixteen geophones are triggered there are 8008 possible solutions. Those which have a velocity below 3660 m/s or above 7920 m/s are discarded. A statistical analysis is made on the remaining locations to obtain modal values of the source coordinates.

Godson, et al. (1979) modified the USBM least-squares direct solution and developed a Mt. Isa method. The importance of the first sensor triggered is removed and a new variable, T_1, is introduced, being the travel time from the source to the first sensor triggered. Equation 5.7 now becomes:

$$V_p(T_1 + t_i) = \sqrt{(X-a_i)^2 + (Y-b_i)^2 + (Z-c_i)^2} \qquad \text{Eq 4.10}$$

Also, the P-wave velocity is assumed to be known and constant.

4.5.2 Iterative Solutions

In the iterative solutions the space around a mine is systematically searched to find the location which produces the smallest error in the measured arrival times. This is done in the following manner:

- the seismic event is assumed to occur at a known location;
- distances from the location to each sensor triggered are calculated;
- these distances are divided by the P-wave velocity to obtain theoretical arrival times at each sensor;
- the arrival time to the first sensor triggered is subtracted from the other arrival times;
- measured and theoretical arrival times are compared at each sensor and a least-squares time error is calculated;
- this time error is multiplied by the P-wave velocity to give a distance error;
- the program moves on to the next assumed source location and repeats the calculation.

The Block and the Simplex methods use this iterative technique. The only difference between them is the geometrical shape used in the search pattern: a shrinking cube for the Block method, and a tetrahedron for the Simplex method.

In the Block method a large cube, with sides of about 300 m, is first defined. This cube is divided into 15 smaller cubes with sides of 60 m. The program calculates the distance errors for source locations at the corners of each small cube and the centre of its sides. A second cube is then constructed around the source location with the least distance error. This second cube has sides of 150 m and is divided into 15 smaller cubes with sides of 30 m,

and the calculations are repeated. This process of shrinking the cube is automatically repeated until a cube size of about 5 m is achieved.

The accuracy of source location, using the Block method, is dependent on a smooth conical shaped error function centered on the actual location. If the error function is not smooth and contains valleys then the Block can be locked in the valley, resulting in a gross error. This can be overcome by dividing the initial large cube into 5 m small cubes, and avoiding the shrinking process, but it takes much more computing time.

In the Simplex method only the three sets of coordinates of the initial tetrahedron are defined, typically 100 m apart. The logic of the Simplex model is given by Gendzwill and Prugger (1978) as follows. An error function is calculated for each of its vertices and the maximum and minimum error identified. The one with the largest error is moved to the opposite side of the tetrahedron (i.e., its reflected position) and the error recalculated. If the error is less than the minimum error, the reflected distance is doubled expanding the tetrahedron. If the error is less than the original, the vertex with the second largest error is reflected. If the error is more than the original maximum, the reflected distance is halved contracting the tetrahedron. In this way, the tetrahedron can tumble through space both expanding and contracting until a minimum error condition is met.

Fewer calculations are made with the Simplex method, compared to the Block method, and source location is obtained much faster. The Simplex can also be trapped within error valleys. This can be overcome by starting a second tetrahedron at completely different coordinates.

Both the Block and Simplex methods are interactive with the computer operator. In these cases, the data can be manipulated by either rejecting geophones with poor arrival times, changing the P-wave velocity on individual geophones, or identifying those geophones which have triggered on the S-wave.

4.6 Accuracy of Source Location

The accuracy of source location is dependent on a number of factors including:

variations in seismic velocity, errors in choosing the arrival times of the P- and S-waves, the geometrical layout of the sensor and whether the event occurs inside or outside the array, and the method used to calculate source location.

Usually, average values are used for the P- and S-wave velocities. These can well vary by ±5% by fractured zones around mine openings and the waves being diverted around the openings.

With waveform recording equipment, it is usually possible to accurately pick the P-wave arrival. The S-wave arrival is more difficult to identify, especially if the sensor is close to the event when the P- and S-waves overlap each other. Systems using threshold triggering are inherently less accurate in picking the P-wave arrival. In addition, single-axis sensors are used, which may be oriented in a direction insensitive to recording the P-wave.

Ideally, the layout of the sensors should be a three-dimensional array around the mine. This is sometimes difficult in tabular orebodies, where access is not available in one dimension. Consequently, the accuracy perpendicular to the orebody tends to be poor.

Some methods of calculating source location are more sensitive to errors in the input data, especially when the event occurs outside the sensor array.

The Eastern Canada Telemetered Network can be used to calculate source location if three or more seismographs record the event. However, only the horizontal coordinates can be calculated. Accuracy is usually about 5% of the distance to the third closest station and the errors are typically 10 km (Hedley and Wetmiller, 1985). This allows only identification of the mining camp at which the seismic event occurred.

The three seismograph stations in the Sudbury Basin allow better resolution for the Sudbury mines. Accuracy is typically 2 km which allows, in most cases, identification of the mine at which the event occurs, except when the mines are adjacent to each other (e.g., Falconbridge's Strathcona and Fraser Mines).

The triaxial sensors of the macroseismic systems are usually installed 500 to 1500 m away from the mine workings. Source locations can be determined either using the P-wave arrival times, or the difference between the P- and S-wave arrivals. The errors in source location of seven large events at the Strathcona Mine are listed in Table 4.1, for three location techniques. Comparison is with the locations obtained from the mine's microseismic system, which itself will be subject to some error. The best accuracy is obtained with the Block methods using the P-wave arrival times, with an average error of 50 m. S-P arrival times, again using the Block method gave an average error of 100 m, mainly due to the difficulty of picking the S-wave arrival times for the underground sensors close to the source. The largest error, averaging 300 m, was obtained with the USBM Direct method using the P-wave arrival time. This method tended to locate events much deeper in the mine.

Table 4.1 - Accuracy of source location using a macroseismic system

Event No.	P-wave Block	S-P-wave Block	P-wave USBM Direct
1	57 m	86 m	716 m
2	32 m	46 m	93 m
3	88 m	183 m	680 m
4	37 m	41 m	364 m
5	18 m	75 m	204 m
6	60 m	88 m	133 m
7	35 m	156 m	25 m
Average	50 m	100 m	300 m

Microseismic systems are the main source of source location, since the sensors are the closest to the event. As an example of the errors in source location, two calibration blasts at the Macassa Mine were analyzed. These blasts were recorded by a 12-channel Electrolab microseismic system of which eight channels were also connected to waveform recording equipment. This allows a comparison between manually picked P-wave arrivals from the waveforms and threshold triggered values. One calculation blast was inside the geophone

array while the other was 130 m outside the array. The four methods described in Section 4.5 were used, varying the P-wave velocity between 5200 and 7900 m/s. Only the geophones connected to the waveform equipment were used in the analysis. One geophone had to be deleted from the calibration blast within the array, using threshold values, as the arrival time was extremely late compared to the waveform arrival.

The errors in source location for the two blasts are presented in Figures 4.5 and 4.6, separated into waveform arrivals and threshold values.

For the calibration blast within the array, reasonable errors of less than 10 m are obtained from both waveform and threshold arrival times, for all four solution techniques. An exception is the Mt. Isa method for the threshold arrival times which has an almost constant error of about 17 m. In general, the errors from the USBM and Mt. Isa methods are insensitive to changes in P-wave velocity over a fairly large range. The Block and Simplex methods have an error function more in the shape of a trough with the largest errors occurring at the lower velocities.

For the calibration blast outside the array, the errors are larger and more inconsistent. The error functions for the USBM and Mt. Isa methods are completely different for the waveform compared to the threshold arrival times. In the former, the errors are high at low velocities and decrease almost linearly to low errors at velocities approaching 8000 m/s. In the latter, the errors increase slightly with increasing velocities and average about 80 m. This implies that both methods are sensitive to small changes in arrival times (i.e., the threshold arrival times were generally within 10% of the waveform arrival times). The error functions for the Block and Simplex methods are similar, being a steep trough for the waveform arrivals, and a shallower trough for the threshold arrivals. In the former, the error is less than 20 m for velocities around 6000 m/s and in the latter, the error is about 60 m at somewhat higher velocities.

Although the errors from the preceding examples are site specific, as a general rule of thumb, the accuracy of the various seismic monitoring systems are as listed in Table 4.2.

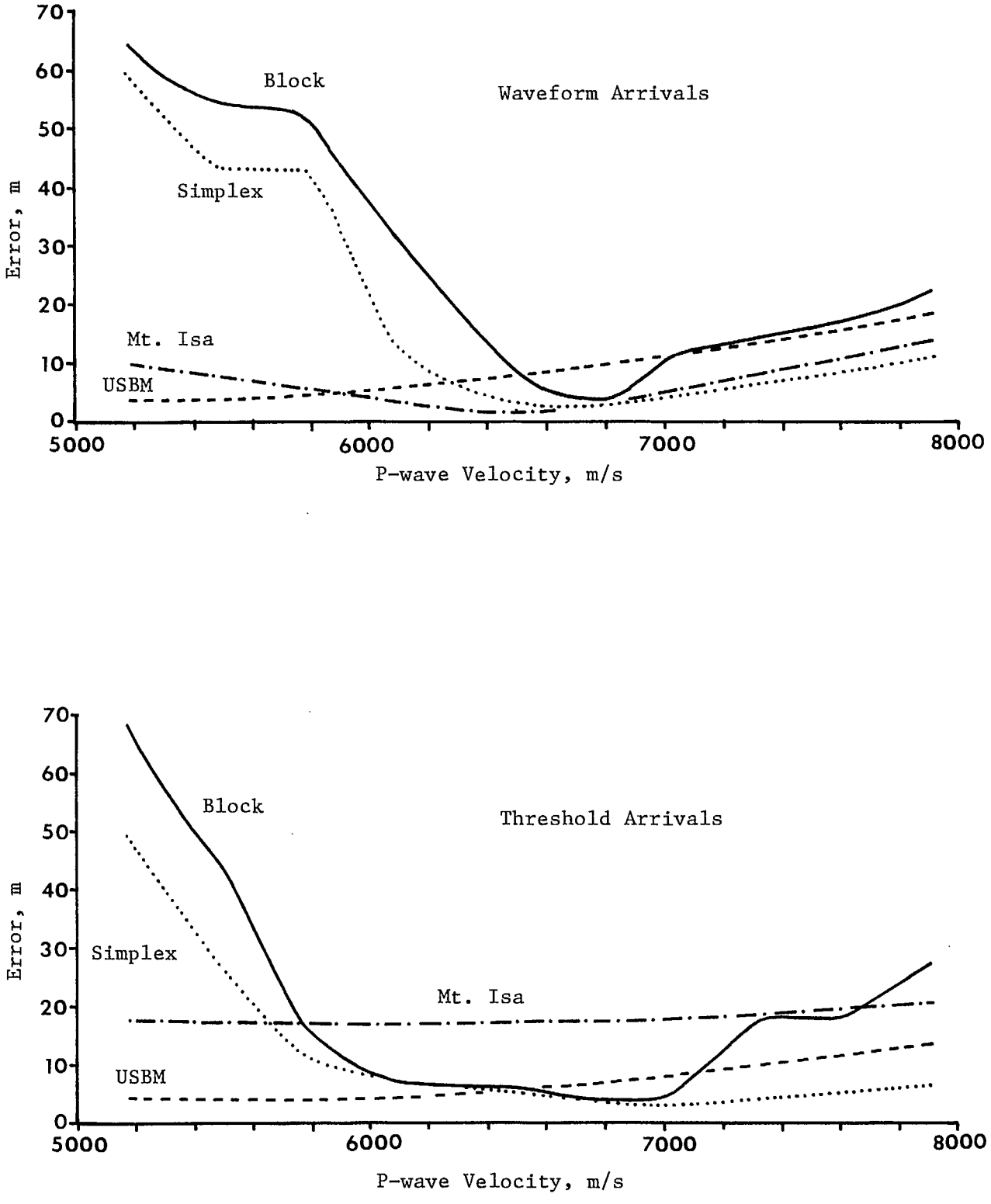

Fig. 4.5 - Accuracy of source location techniques for a calibration blast within the array.

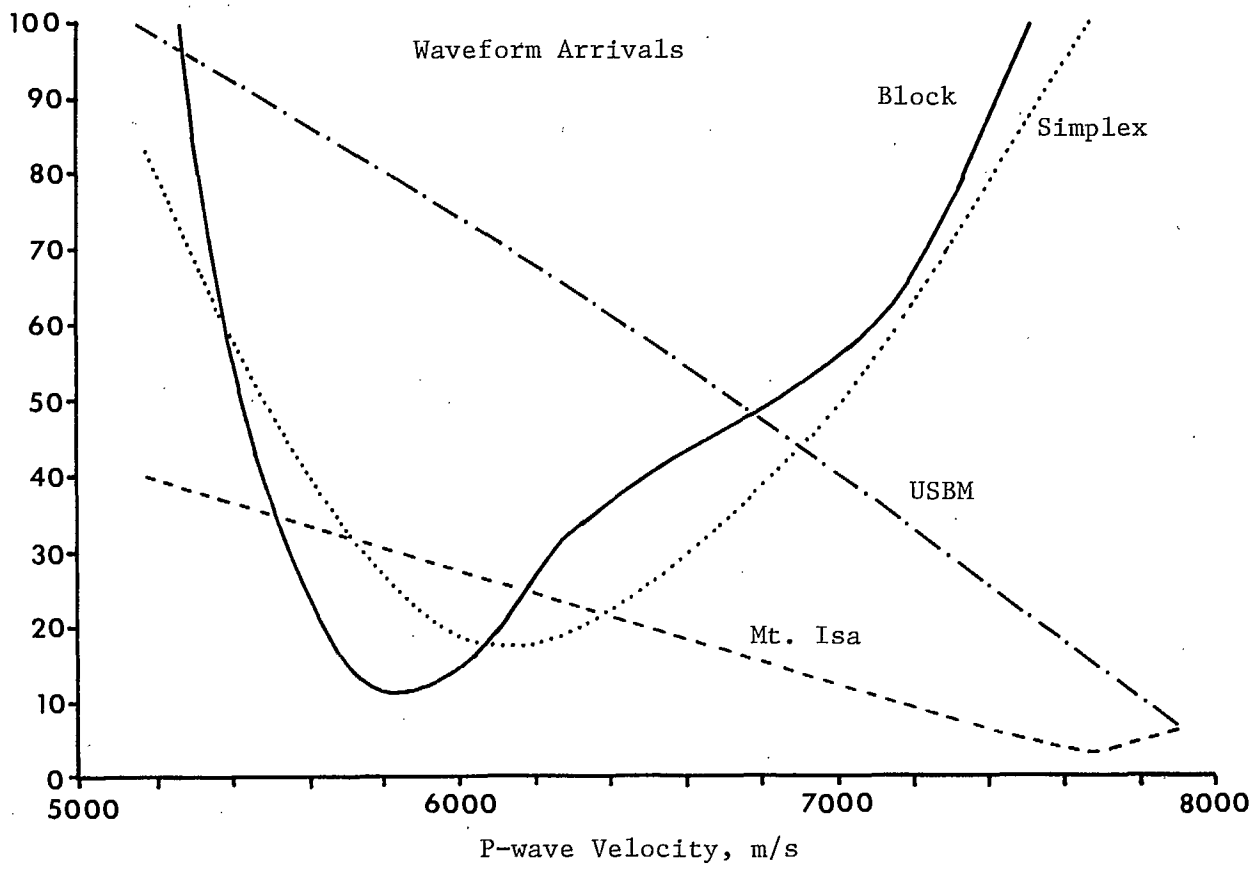

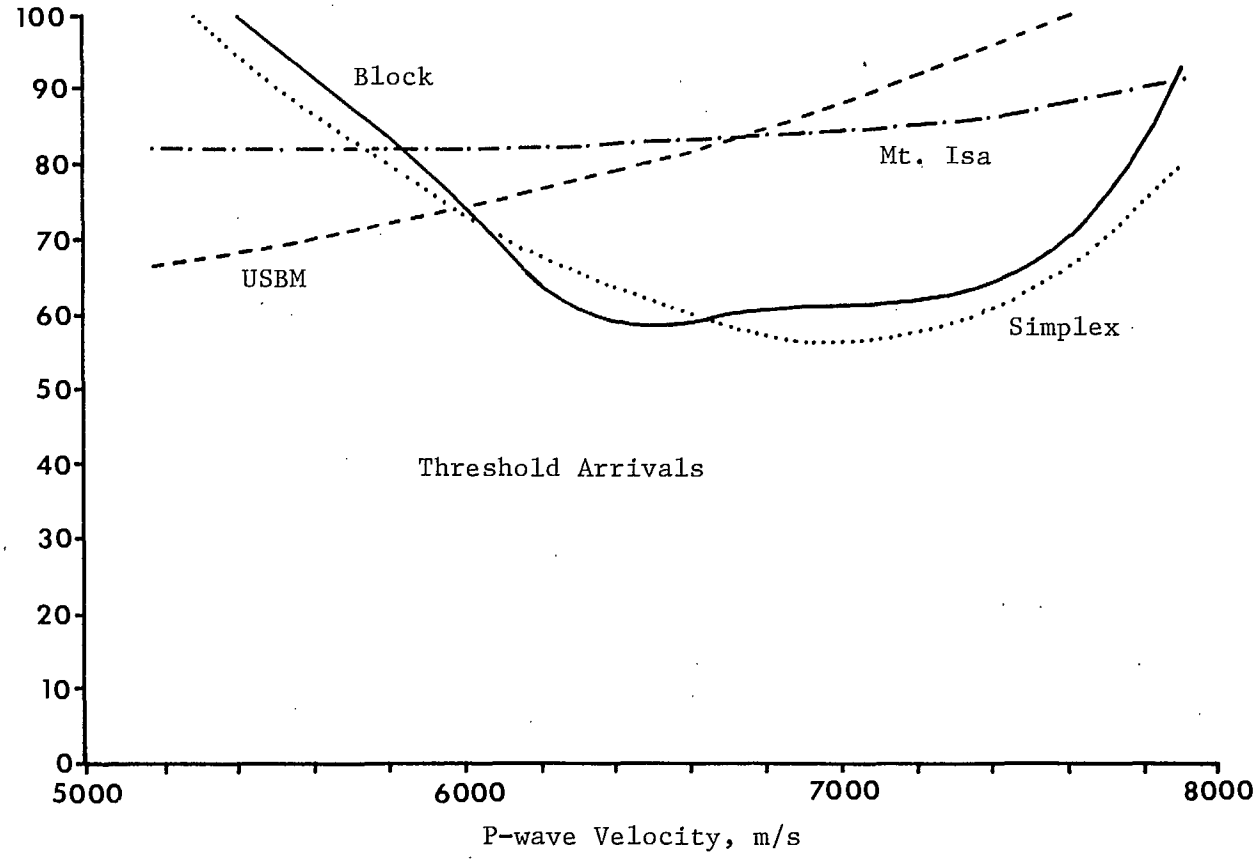

Fig. 4.6 - Accuracy of source location techniques for a calibration blast outside the array.

Table 4.2 - Accuracy of seismic monitoring systems

System	Error in Location
Regional Seismograph Network	±10 km
Sudbury Seismograph Network	±2 km
Macroseismic	±50 m
Microseismic, outside array	±60 m
Microseismic, within array	±10 m

Some mines, such as Creighton Mine, have a dense microseismic array surrounding part of the orebody. In this case, errors in the order of 5 m may be achievable within the array.

4.7 References

Blake, W. and Leighton, F.W. (1964), Recent developments and applications of the microseismic method in deep mines. In: Theory and Practice, AIME, pp. 429-443.

Blake, W., Leighton, F.W. and Duvall, W. (1974), Microseismic techniques for monitoring the behaviour of rock structures. Bull. 665, U.S. Bureau of Mines.

Blake, W. (1982), Design considerations for seismic monitoring systems. Proc. 1st Int. Symp. Rockbursts and Seismicity in Mines, Johannesburg, pp. 79-82, South African Inst. Min. Met Symp. Series No. 6.

Cook, N.G.W. (1963), The seismic location of rockbursts. Proc. 5th U.S. Symp. Rock Mechanics, Minnesota, pp. 493-516.

Cook, N.W.G. (1964), The application of seismic techniques to problems in rock mechanics. Int. J. Rock Mech. Min. Sci., vol. 1, No. 2, pp. 169-179.

Davidge, G.R. (1984), Microseismic monitoring at Falconbridge Mine, Falconbridge, Ontario. CIM Bull., vol. 77, No. 868, pp. 45-49.

Gendzwill, D. and Prugger, A. (1978), Algorithms for micro-earthquake location. Proc. 2nd Conf. on Acoustic Emission/Microseismic Activity, Penn. State University.

Godson, R.A., Bridges, M.C. and McKavanagh, M. (1978), A 32-channel rock noise source location system. Proc. 2nd Conf. on Acoustic Emission/Microseismic Activity, Penn. State University.

Green, R.W.E. (1982), Design considerations for an underground seismic network. Proc. 1st Int. Symp on Rockbursts and Seismicity in Mines, Johannesburg, pp. 79-82.

Hedley, D.G.F. and Wetmiller, R.J. (1985), Rockbursts in Ontario mines during 1984. Special Report SP85-5, CANMET, Energy, Mines and Resources Canada.

Hodgson, E.A. (1958), Dominion observatory rockburst research 1938-1945. Publication Dominion Observatory, Ottawa, vol. XX, No. 1.

Lee, W.H.K. and Stewart, S.W. (1981), Principles and applications of microearthquake networks. Academic Press, New York.

Leighton, F.W. and Duvall, W.I. (1972), A least squares method of improving the source location of rock noise. U.S. Bureau of Mines, Report of Investigations 7626.

MacDonald, P. and Muppalaneni, S.N. (1983), Microseismic monitoring in a uranium mine; rockbursts prediction and control, pp. 141-146. IMM, London, U.K.

Malott, C. (1981), Theoretical limitations of microseismic transducer systems. Proc. 3rd Conf. on Acoustic Emission/Microseismic Activity, Penn. State University, pp. 681-693.

Neumann, M. (1985) Microseismic monitoring at Campbell Red Lake Mines Ltd. 54th Annual Meeting, Mines Accident Prevention Association, Ontario.

Niewiadomski, J. (1986), Source-location techniques using P-wave arrivals. Special Report SP86-15, CANMET, Energy, Mines and Resources Canada.

Obert, L. (1975), The microseismic method: discovery and early history. Proc. 1st Conf. Acoustic Emission/Microseismic Activity, Penn State University, pp. 11-12.

Oliver, P.H. and MacDonald, P. (1985), The monitoring system at Creighton Mine, Inco Ltd., Proc. 4th Conf. Acoustic Emission/Microseismic Activity, Penn. State University.

Plouffe, M., Cajka, M.G., Wetmiller, R.J. and Andrew, M.D. (1988), The Sudbury local telemetered seismograph network. Proc. 2nd Int. Symp. Rockbursts and Seismicity in Mines, Minneapolis.

Prugger, A.F. and Gendzwill, D.G. (1988), Micro-earthquake location: a non-linear approach that makes use of a Simplex stepping procedure. Bull. Seism, Soc. Am., vol. 78, No. 5, pp. 340-362.

5. ROCKBURST SEISMOLOGY

Damage from a 3.2 Mn pillar burst at Quirke Mine.

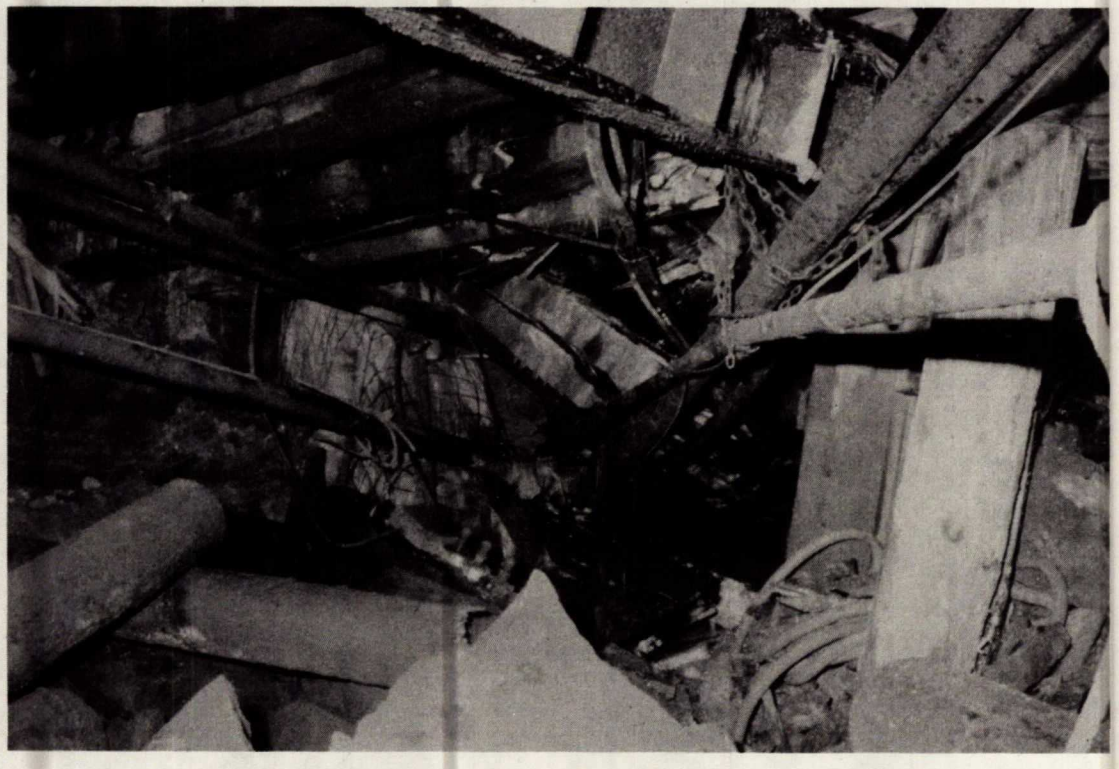

Damage from a 3.3 Mn fault-slip burst at Falconbridge Mine.

5. ROCKBURST SEISMOLOGY

5.1 Introduction

Scientific observations on earthquakes have taken place over a much longer time period than rockbursts. Consequently, the scientific discipline of seismology has progressed on both a theoretical and empirical basis. Much of the instrumentation, focal mechanisms and empirical relationships developed in seismology are applicable to the study of rockbursts, especially those related to slippage along faults.

One of the first applications of seismology techniques to rockbursts was by E. Hodgson of the Dominion Observatory in the Kirkland Lake gold mines in the early 1940s. Since that time, most of the investigations have been carried out in the South African gold mines, notably by A. McGarr and S.M. Spottiswoode, and in the Polish mines by S.J. Gibowicz.

5.2 Seismic Waves

When a seismic event occurs underground, strain waves radiate from the source in a spherical pattern. There are two types of waves. P or compressional waves are radial vibrations in the same direction as the wave front. S, or shear waves are transverse vibrations perpendicular to the wave front. The velocity of propagation of the S-wave (β) is always less than the P-wave (α) and generally two-thirds. A geophone located in the rock records these two waveforms, first the direct transmission, then reflections from discontinuities such as the surface.

Besides these two waves, there are other waves which travel along the surface. The most common of these are Rayleigh and Love waves. In underground applications, however, these surface waves are not important.

Measurements of P-wave (α) and S-wave (β) velocities can be used to calculate the dynamic elastic modulus (E) and Poisson's ratio (ν) of the rock mass as

follows:

$$E = \beta^2\rho[3(\alpha/\beta)^2-4]/[(\alpha/\beta)^2-1] \qquad \text{Eq 5.1}$$

$$\nu = 0.05[(\alpha/\beta)-^2]/[(\alpha/\beta)^2-1] \qquad \text{Eq 5.2}$$

where, ρ = rock density

Also, $$G = \beta^2\rho \qquad \text{Eq 5.3}$$

where, G = shear modulus = $E/2(1+\nu)$

Some measured seismic velocities in Ontario mines and the elastic properties are listed in Table 5.1. In general, the P- and S-wave velocities are consistent between mines and agree well with the average values used in Northern Ontario by the Geophysics Division of the Geological Survey of Canada. The elastic moduli tend to be 20-30% higher than those obtained in loading tests.

5.3 Magnitude Relationships

5.3.1 Richter and Nuttli Scales

The magnitudes of mining-induced seismic events, including rockbursts, are calculated in the same manner as for earthquakes. Two scales are in general use: one developed by Richter (1958) for California, and the other by Nuttli (1973) for central and eastern North America. Both scales are logarithmic and are based on the maximum amplitude of the seismic signal, as measured on a seismograph, taking into account the distance from the source and the instrument characteristics.

For mines in the Canadian Shield, the Nuttli (Mn) is the primary local magnitude scale used by the Geophysics Division of the Geological Survey of Canada. This scale is expressed by:

$$Mn = -0.1 + 1.66 \log D + \log \left(\frac{A}{KT}\right) \qquad \text{Eq 5.4}$$

Table 5.1 - Typical seismic velocities and dynamic elastic properties of rocks in Ontario Mines

Mining District	Main Rock Type	Density kg/m^3	P Velocity m/s	S Velocity m/s	Elastic Modulus GPa	Shear Modulus GPa	Poisson's Ratio
Red Lake	Andesite	2840	6330	3740	98	40	0.23
Elliot Lake	Quartzite	2660	5900	3630	85	33	0.19
Sudbury	Norite	2770	6170	3460	84	33	0.27
Kirkland Lake	Syenite	2840	6250	3690	95	39	0.23
Average Northern Ontario		2700	6200	3570	86	34	0.25

where, D = epicentral distance to source, km

A = half the maximum peak to peak amplitude in the S-phase

K = instrument magnification factor

T = time period, sec.

This equation is used if the recording station is more than 50 km from the source, otherwise Richter's (M_L) local magnitude scale is used,

$$M_L = \log \left(\frac{A\ Kw}{K}\right) - \log Ao\ (D) \qquad \text{Eq 5.5}$$

where, Kw = magnification of a Wood-Anderson seismograph at period T.

Log Ao (D) is a calibration factor such that a standard seismograph will have a trace amplitude of 0.001 mm at a distance of 100 km for a magnitude zero event (or 1 mm for a magnitude 3.0 event). This calibration function is listed by Richter (1958, p. 342).

The Richter local magnitude scale is used for rockbursts in most of the world outside of eastern North America. Several studies have been done to relate the two scales (Hasegawa, 1983; Boore and Atkinson, 1987). The results are shown in Figure 5.1. Over the range of interest for rockbursts (i.e., M = 1.5 to 4.0) the Mn scale gives values 0.3 to 0.6 units higher than the M_L scale for the same event.

Seismograph stations located very close to mines are saturated by seismic events of relatively low magnitude. In these cases, the duration of the seismic signal can be used to estimate the magnitude. Figure 5.2 shows the relationship between duration at the Elliot Lake station and magnitude determined by the Eastern Canada Seismic Network. These seismic events occurred at the Quirke and Denison Mines, 12 km away. Duration was based on the time the seismic signal was greater than ± 1 mm on the analog record. There is reasonable agreement between the two parameters in the form,

$$Mn = 1.33 \log t + 0.12 \qquad \text{Eq 5.6}$$

where, t = duration of signal, sec.

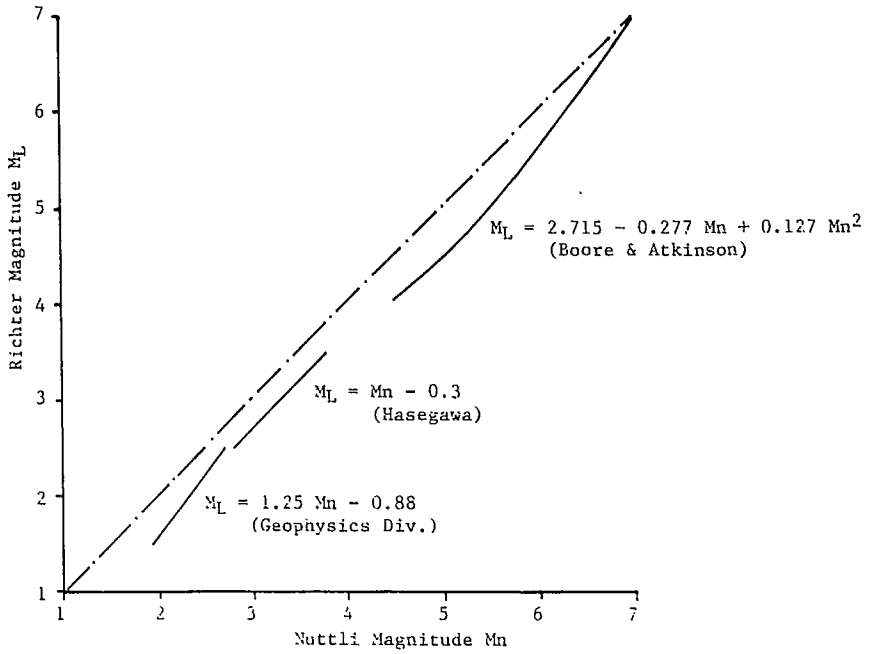

Fig. 5.1 - Relationship between Richter and Nuttli magnitude scales for eastern North America.

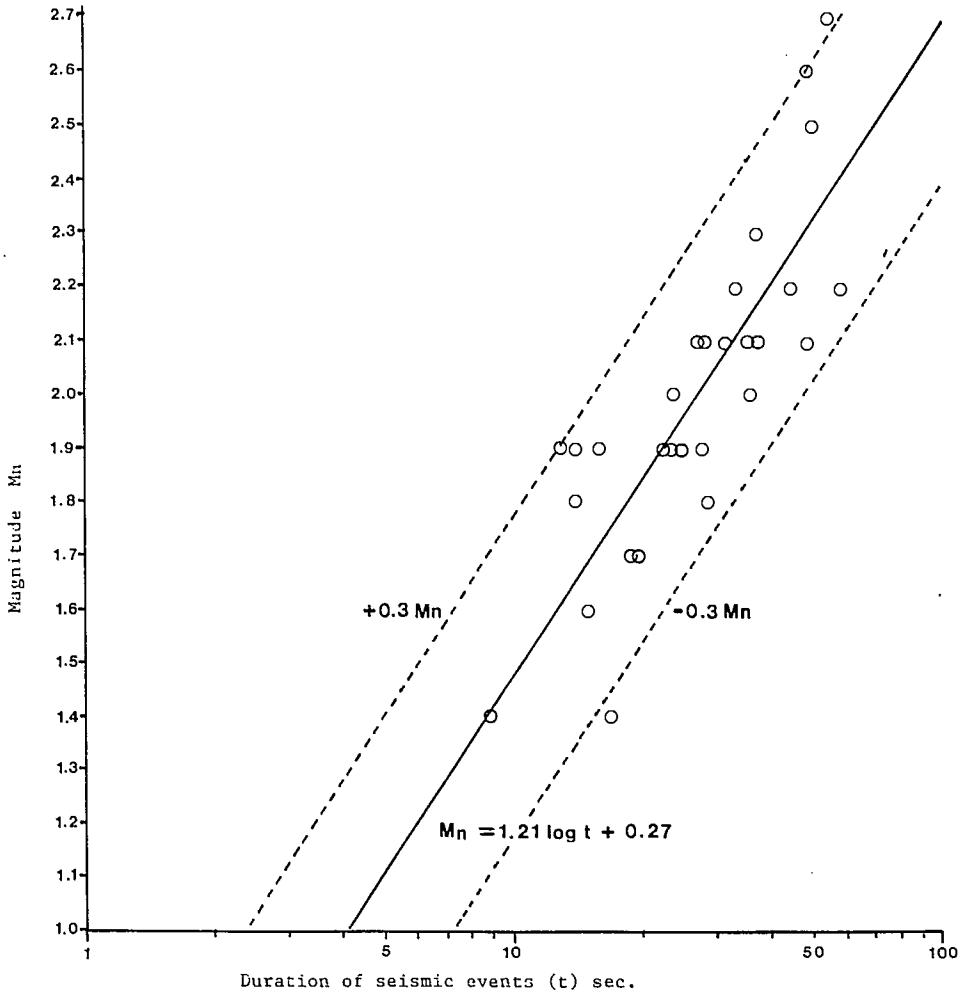

Fig. 5.2 - Relationship between magnitude and duration of seismic events at Quirke and Denison Mines.

This relationship is used to assign magnitudes for seismic events between 1.0 and 1.9, while still relying on the national network for events of 2.0 and greater. Equation 5.6 is site specific to the Elliot Lake station and Quirke and Denison Mines. Other relationships will be relevant to the other mining camps.

5.3.2 Magnitude Statistics

It has been observed that earthquakes and mining-induced seismic events usually follow a consistent relationship between magnitude and frequency of occurrence expressed by:

$$\log N = a - b\,Mn \qquad \text{Eq 5.7}$$

where, N = number of events greater than or equal to a given magnitude in a given time period

a and b = constants.

The gradient, b, is normally in the range of 0.5 to 1.5 (McGarr, 1982).

Figure 5.3 shows three different relationships using this format. Curve A is for naturally occurring earthquakes in eastern Canada for the years 1986-87, as recorded by the Eastern Canada Seismic Network. Curve B is of the seismic events at Quirke Mine in Elliot Lake for the years 1984-85, again using the national network for magnitude values. Curve C is of Quirke Mine for the years 1986-87, this time using the national network for magnitudes of 2.0 and greater and the relationship in Equation 5.6 for magnitudes 1.0 to 1.9.

In all cases, there is a linear relationship in the form of Equation 5.7, for the larger magnitude events. The number of small events tend to tail off due to the limits of detectability. However, this does not apply to the Quirke results in the 1986-87 period, when magnitudes down to 1.0 could be adequately measured. Below a magnitude of 1.8, there is still a linear relationship but with a much lower gradient. This may be a peculiarity of the mine with regard to depth, areal extent and failure mechanism (i.e., predominantly pillar failures).

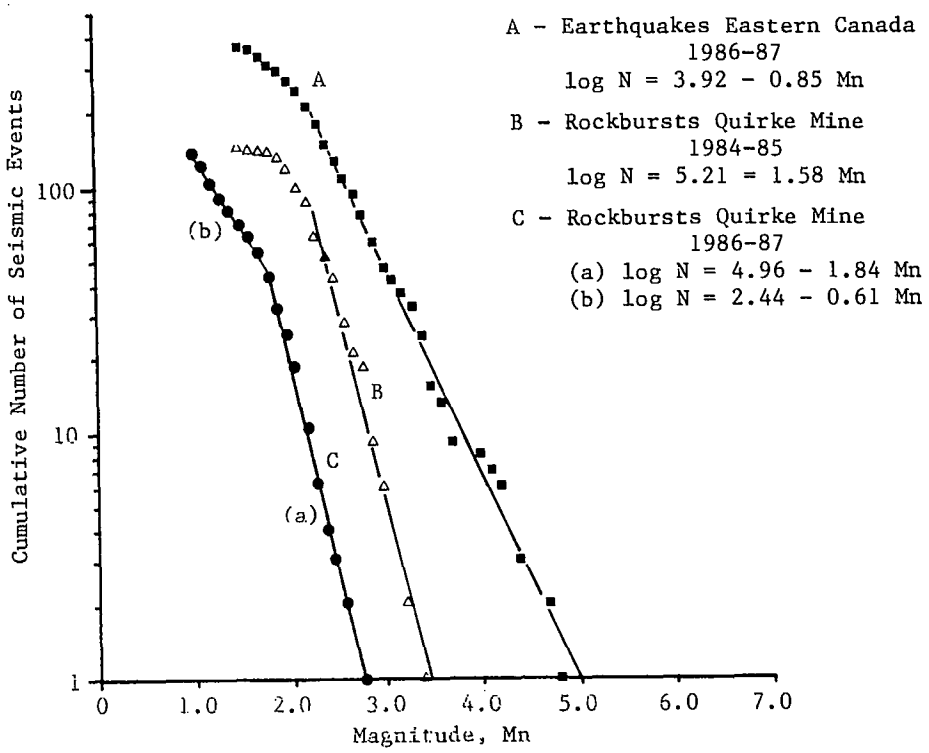

Fig. 5.3 - Example of the frequency of occurrence of earthquakes and rockbursts.

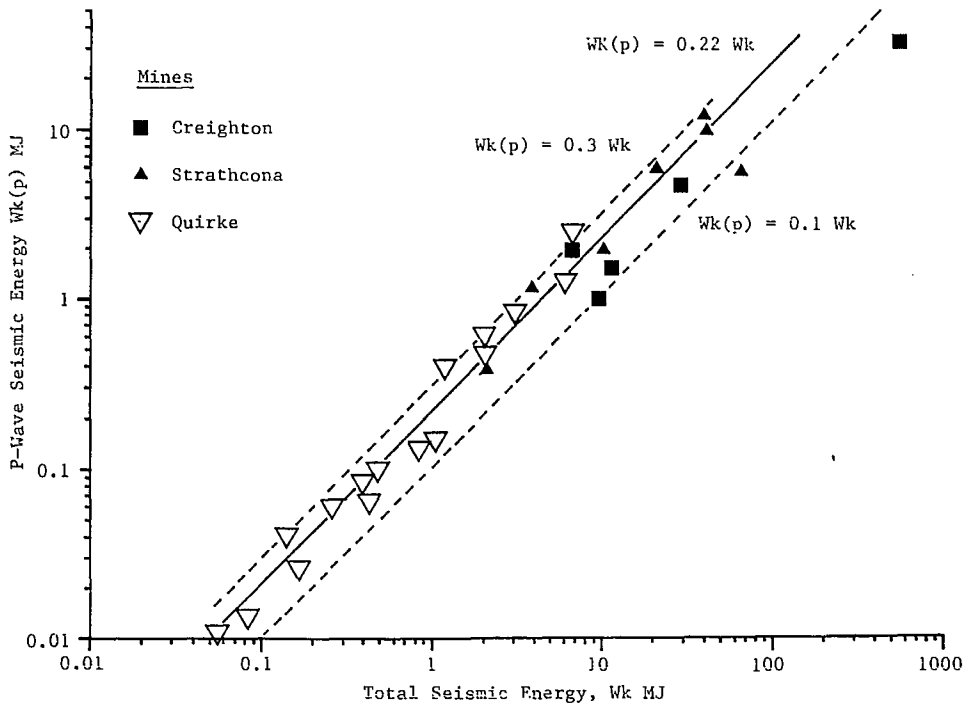

Fig. 5.4 - Proportion of seismic energy in the P-wave.

Sometimes the relationships shown in Figure 5.3 are used to predict seismic events in a broad sense, for instance, the number of events of a specific magnitude or greater expected in a given time period. This type of prediction seems to apply to the South African gold mines, where the rate and geometry of mining does not significantly change from year to year (McGarr, 1984). It does not apply to some Ontario mines where sections or the complete mine are closed down due to rockburst conditions, or when the loading conditions are radically altered. From the 1984-85 results at Quirke Mine, six seismic events of magnitude 3.0 or greater are predicted for a two-year period. However, in 1986-87, there were no events of 3.0 or greater at Quirke Mine. This was because the loading conditions had changed. During most of 1984-85 the hanging wall was spanning the affected area without major breakdown. By 1986-87 the hanging wall had fractured through to surface.

5.3.3 Seismic Energy

In an elastic medium and for a point source the seismic energy, W_k, radiating from a seismic event can be expressed by (Cook, 1964):

$$W_k = 4\Pi R^2 \rho(\alpha \int^{Tp} Vp^2 dt + \beta \int^{Ts} Vs^2 dt) \qquad \text{Eq 5.8}$$

where, R = distance from source
α and β = velocity of P- and S-waves
ρ = rock density
Vp and Vs = particle velocity in P- and S-waves
Tp and Ts = duration of the seismic waves in P- and S-phases.

Triaxial geophones with the three sensors mounted orthogonally will record the total seismic energy liberated.

Both Cook (1964) and Spottiswoode and McGarr (1975) observed that most of the seismic energy is contained in the S-wave, for mine tremors in South Africa. From this it was concluded that shear is the predominant failure mechanism. Typically they found that only about 10% of the seismic energy is contained in the P-wave and usually this component is ignored and analysis is confined to the S-wave.

Figure 5.4 shows the results obtained from triaxial sensors at the Quirke and Strathcona Mines. A log-log scale is used to enlarge the lower values. The seismic energy in the P-waves varies between 10 and 30% of the total energy and averages 22%. Under these circumstances, the energy in the P-wave cannot be ignored.

Since both magnitude and seismic energy are related to the particle velocity, it is natural that there is a relationship between the two parameters. Gutenberg and Richter (1956) first developed this relationship for earthquakes in California in the form:

$$\log W_k = 1.5\ M_L - 1.2 \qquad \text{Eq 5.9}$$

where, the energy units are megajoules (MJ). Subsequently, Spottiswoode and McGarr (1975) found that this equation also applied to mine tremors in South Africa.

The results obtained from Ontario mines are shown in Figure 5.5 with the relationship in the form:

$$\log W_k = 1.3\ Mn - 1.75 \qquad \text{Eq 5.10}$$

The lower seismic energy values obtained in Ontario compared to South African mines could be explained by the different magnitude scales being used (i.e., Nuttli scale in Ontario, Richter scale in South Africa).

5.3.4 Seismic Moment

Besides magnitude (M), the seismic moment (Mo) is preferred in seismology as a measure of the size of an earthquake. Seismic moment provides information on the fault dimensions and slippage, and is defined by:

$$Mo = G\ A\ \psi a \qquad \text{Eq 5.11}$$

where, G = shear modulus

A = area of fault on which slippage occurs

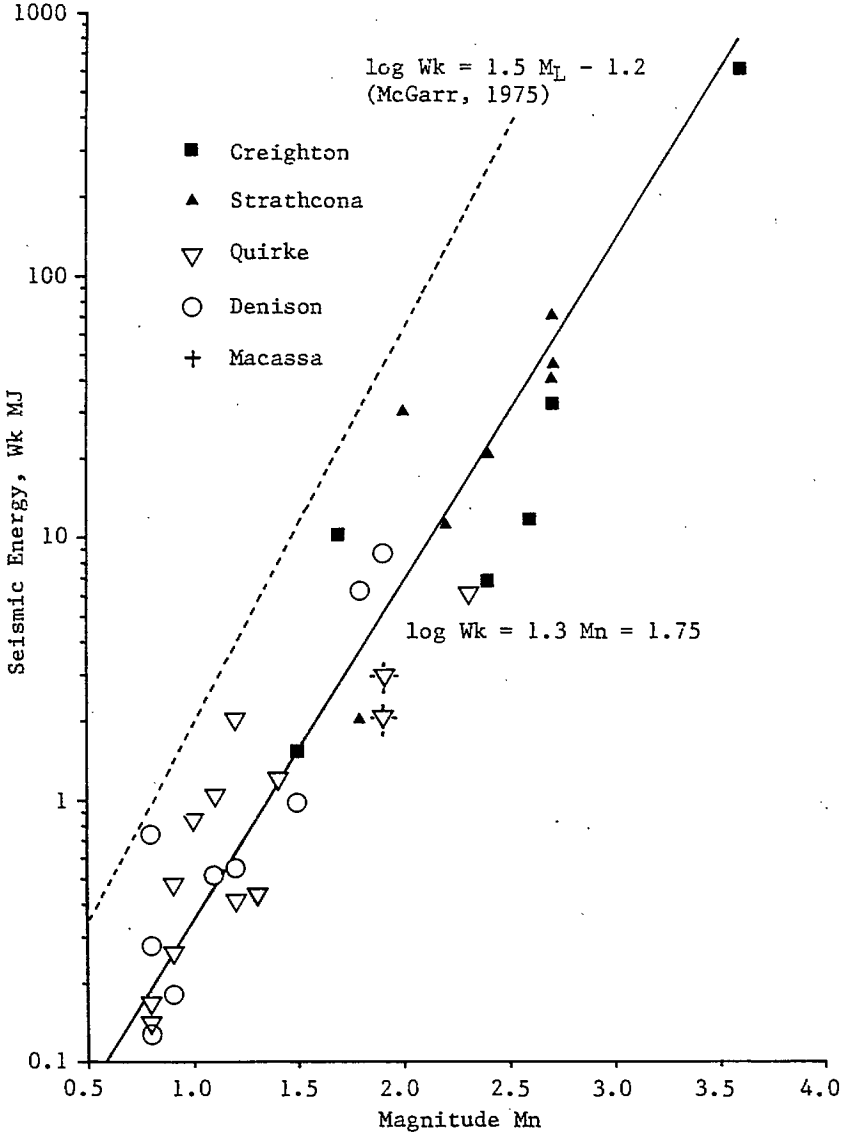

Fig. 5.5 - Relationship between seismic energy and magnitude for Ontario mines.

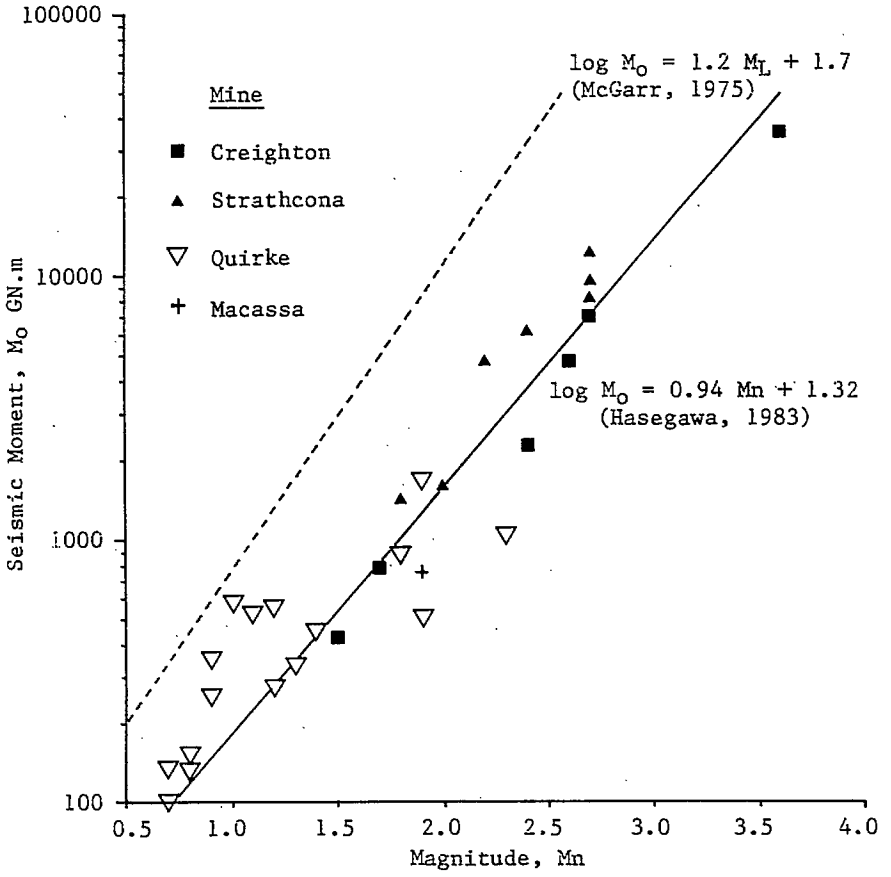

Fig. 5.6 - Relationship between seismic moment and magnitude for Ontario mines.

ψa = average slippage,

and has units of Newton metres (N.m). Generally, seismic moment is calculated from the spectral analysis of seismic waves as described in Section 5.4.2.

There is a strong empirical relationship between moment and magnitude. Spottiswoode and McGarr (1975) found that for tremors in South African gold mines that:

$$\log Mo = 1.2\ M_L + 1.7 \text{ in GN.m} \qquad \text{Eq 5.12}$$

Hasegawa (1983) found that for earthquakes in the Canadian Shield that:

$$\log Mo = 0.94\ Mn + 1.32 \text{ in GN.m} \qquad \text{Eq 5.13}$$

Again, the results from seismic events in Ontario mines are shown in Figure 5.6. They tend to follow the relationship of Hasegawa for the Canadian Shield.

The original concept of seismic moment is only applicable to fault-slip type of seismic events. For mining applications, McGarr (1976) has suggested that seismic moment can be expressed by:

$$Mo = G\ \Delta V \qquad \text{Eq 5.14}$$

where, ΔV = volumetric closure due to incremental mining.

However, Salamon (1983) questioned the validity of this concept since when mining occurs in very small steps, the energy associated with volumetric closure is dissipated non-violently. Also, it would be difficult to apply this concept to a mine such as Quirke, where no mining was taking place in the rockburst area.

5.4 Seismic Waveform Analysis

5.4.1 Time Domain

Velocity gauges or accelerometers record the seismic signal in the time domain. By integrating and/or differentiating the original signal it is possible to obtain the waveform as acceleration, velocity and displacement, as shown in Figure 5.7.

A number of pertinent details of the seismic event can be obtained from these records. The arrival of the P-wave and the time separation to the S-wave arrival can be used to calculate the distance of the sensors from the source and hence the location of the event as described in Section 4.5. The peak acceleration and particle velocity are used in assessing possible damage from a seismic event (Section 7). Integration of the velocity waveform is used to obtain the seismic energy as described in Section 5.3.3.

The direction of first motion of the sensors provides information on the failure mechanisms at the source. Arrival of the P-wave will produce either an initial ground motion towards the source (i.e., dilational wave) or away from the source (i.e., compressional wave). Different types of rockbursts will produce different ground motions around the source.

Hasegawa et al. (1988) identified six different types of mining-induced seismic events which would produce different ground motion distributions. Of these six types, two are more important: a double-couple fault model and a pillar implosion model.

Figure 5.8(a) illustrates the ground motion pattern that would be produced by slippage along a vertical fault. Sensors located in opposite quadrants of a sphere, centered on the event, would indicate either compression or dilation as indicated. Sudden collapse of a pillar is an implosion and all first motions would be towards the pillar as illustrated in Figure 5.8(b). Similarly, monitoring of blasts would indicate all first motions away from the blast, since it is an explosion.

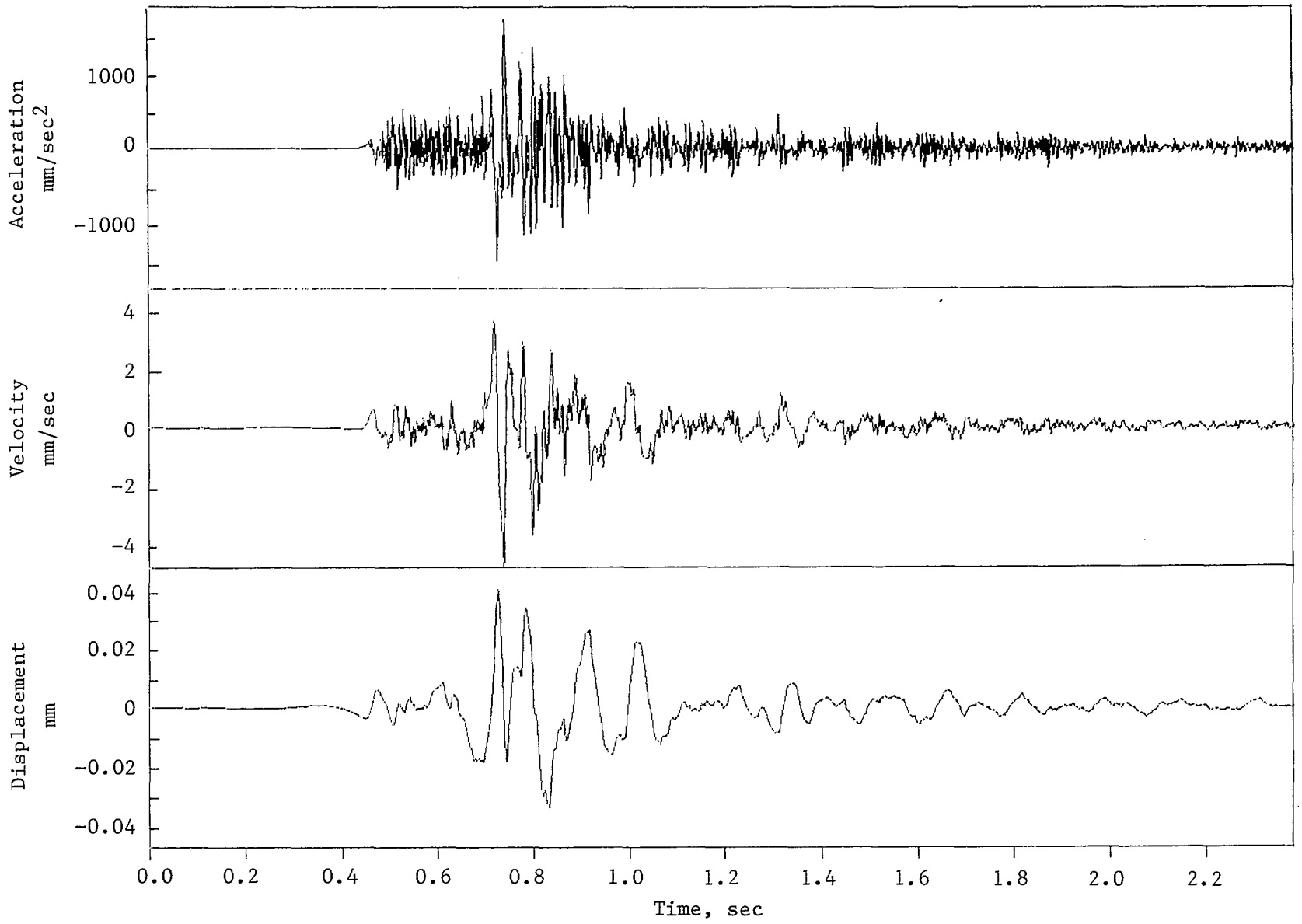

Fig. 5.7 - Acceleration, velocity and displacement waveforms for a 3.6 Mn rockburst at Creighton Mine.

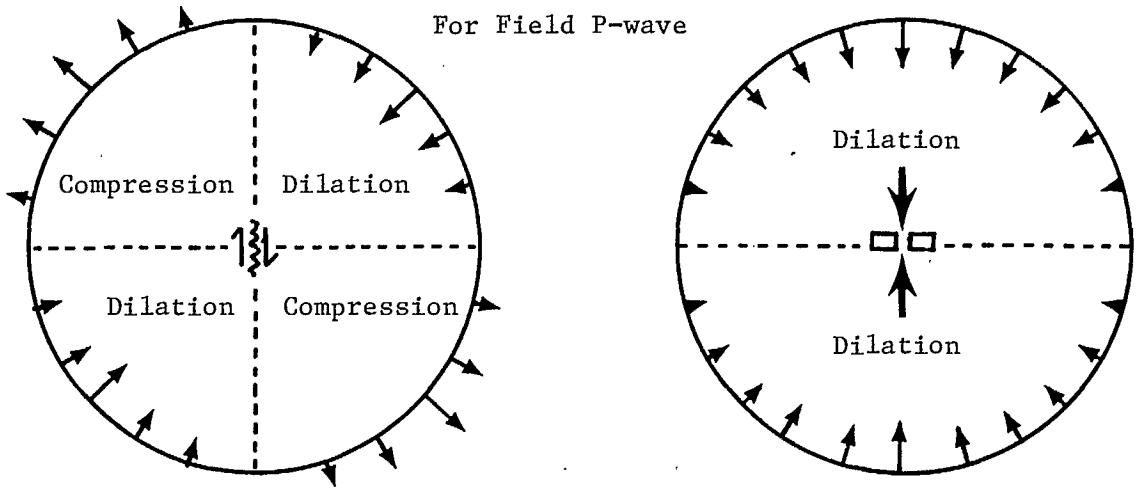

a) Double-Couple Fault Model b) Pillar Implosion Model

Fig. 5.8 - Direction of first ground motion for two types of seismic events. (After Hasegawa et al., 1988)

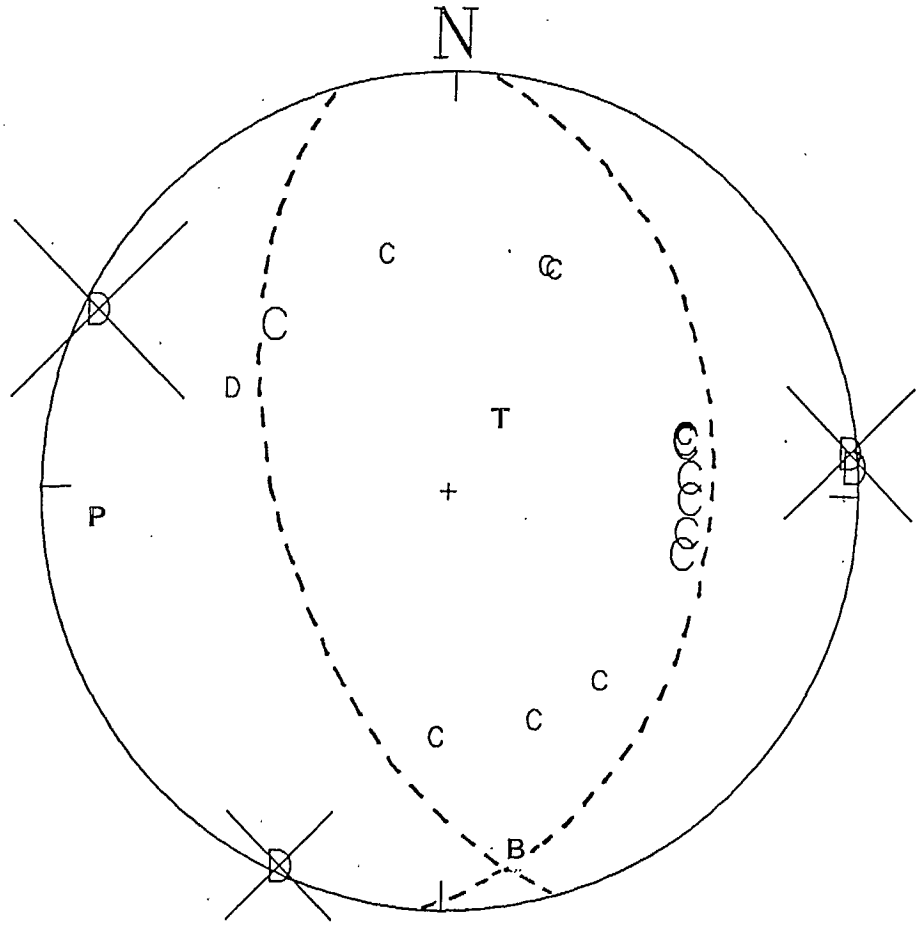

Fig. 5.9 - Fault-plane solution for a 3.7 Mn event at the Creighton Mine in 1987. (After Wetmiller et al., 1988)

So far, monitoring of mining-induced seismic events in South Africa and Poland has indicated only a double-couple fault mechanism, indicative of shear failure. Wong and McGarr (1988) investigated five possible cases of pillar implosions in coal mines. They concluded that in most cases, due to the poor spherical coverage, the first motion pattern could also be fitted to a double-couple mechanism. One of the main problems in first motion studies is to have adequate coverage of sensors in all four quadrants, surrounding the source.

Information on the dip and orientation of the faults on which slip is occurring can be obtained by plotting first motions on stereographic projections. The lower hemisphere equal area net is generally used. Figure 5.9 shows the first motions recorded by seismographs in the Eastern Canada Seismic Network for a 3.7 Mn event at the Creighton Mine near Sudbury in 1987 (Wetmiller et al. 1988). The two orthogonal lines separating compressional and dilational motion are the nodal planes separating the quadrants, one of which is the fault plane on which slippage is occurring. The axes at right angles to the two planes represent the pressure P and tension T axes, while the null motion axis B is the intersection of the two planes. These axes correspond to the direction of the maximum, minimum and intermediate principal stresses respectively.

5.4.2 Frequency Domain

Spectral analysis of seismic waveforms in the frequency domain is used in seismology to obtain information on source mechanisms and dimensions. The seismic signal, in the form of a displacement wave, is transformed into a frequency distribution using a Fast Fourier Transform.

Spectral density is plotted against frequency in a logarithmic format as illustrated in Figure 5.10. The resultant spectrum has several pertinent characteristics. At low frequencies, there is a flat plateau and at high frequencies, the spectrum decays at some power of frequency, usually between second and third power. The intersection of the plateau and the high frequency decay is called the corner frequency.

The magnitude of the plateau is a measure of the energy of the seismic event

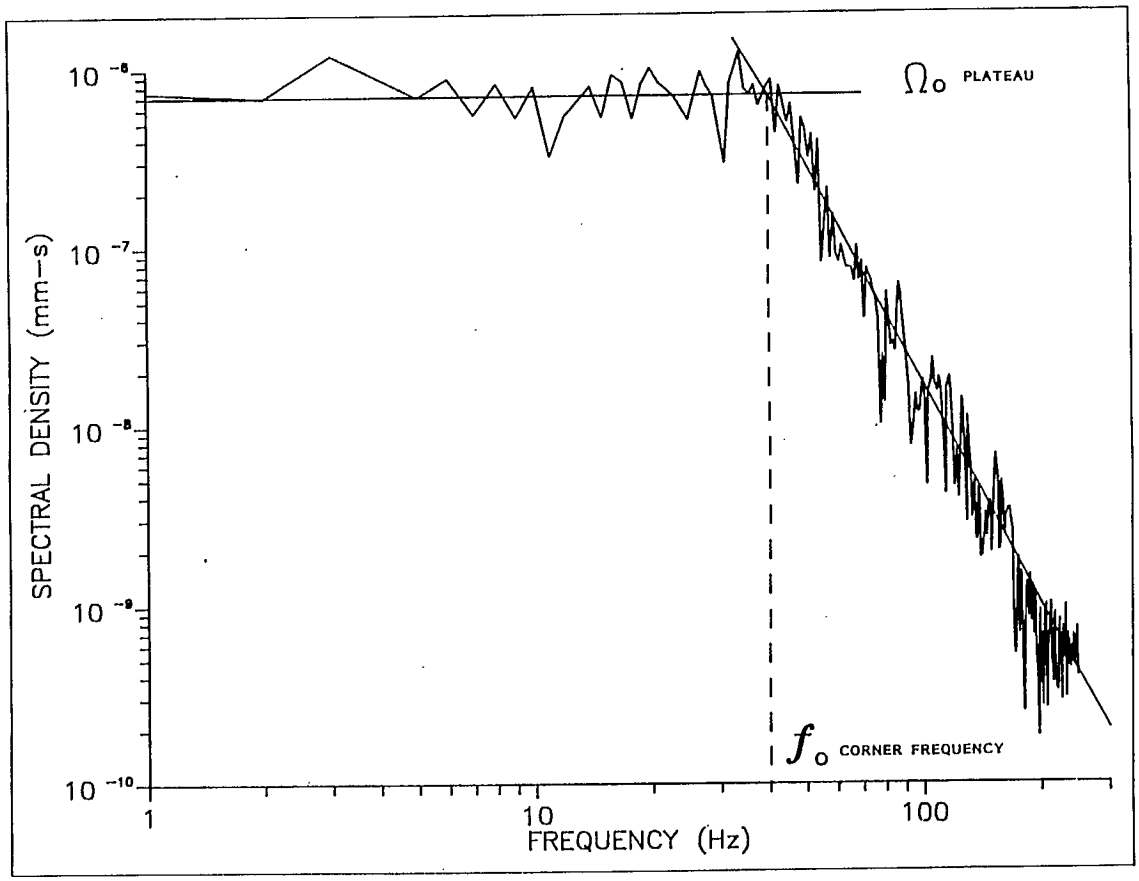

Fig. 5.10 - Typical seismic waveform plotted as spectral density in the frequency domain.

and is related to the seismic moment as follows:

$$Mo = \frac{4\Pi \rho C^3 R \Omega o}{f^c r^c} \qquad \text{Eq 5.15}$$

where, Ωo = low frequency plateau

ρ = rock density

C = velocity of either the P-wave, α, or S-wave, β

R = distance from source

f^c = radiation pattern coefficients

r^c = free-surface effects (for surface sensors only).

The radiation coefficients are usually assigned average values of 0.39 for P-waves and 0.57 for S-waves (Spottiswoode and McGarr, 1975). The free-surface effect is always 2 for the horizontal shear wave, SH, whereas for the SV and P-waves, the correction factors depend on the angle of incidence of the incoming wave (Aki and Richards, 1980). In seismology, usually only the seismic moment from the SH wave is calculated, since the surface effects are known and constant. In underground mining (McGarr et al. 1981, and Gibowicz, 1988), the vector sum of the low frequency plateau, obtained from triaxial gauges, is used to calculate the seismic moment.

The calculated seismic moment is an independent measure of the magnitude of the event, based on the far-field radiation pattern. Other parameters on the fault size are dependent on the type of model used.

5.4.3 Seismic Models

The circular fault model developed by Brune (1970) is the most commonly used model for earthquakes and mining-induced seismic events. The mechanics of stress and displacement are identical to the circular fault model developed by Salamon (1974), described in Section 3.5.3.

Source radius is related to the corner frequency of the spectral density

diagram:

$$ro = \frac{2.34\ \beta}{2\Pi\ fo} \qquad \text{Eq 5.16}$$

where, ro = source radius
fo = corner frequency
β = shear wave velocity

The reduction in shear stress along the fault is assumed to be constant, and from Salamon's model:

$$\Delta\tau = \frac{3(2 - \nu/2)Mo}{8(1 - \nu)ro^3} \qquad \text{Eq 5.17}$$

where, $\Delta\tau$ = stress drop
ν = Poisson's ratio

For a Poisson's ratio of 0.25, Eq 5.17 reduces to the Brune model:

$$\Delta\tau = \frac{7\ Mo}{16\ ro^3} \qquad \text{Eq 5.18}$$

Average slippage, ψ, along the fault is given by,

$$\psi a = \frac{16\Delta\tau\ ro}{7\Pi\ G} = \frac{2}{3}\ \psi\ max \qquad \text{Eq 5.19}$$

where G = shear modulus.

For the circular fault model, there is a direct relationship between seismic energy liberated, W_k, and seismic moment, Mo. From Eq 3.40 and using a Poisson's ratio of 0.25:

$$W_k = \frac{8\Delta\tau^2\ ro^3}{7\ G} \qquad \text{Eq 5.20}$$

Combining with Eq 5.18 produces:

$$W_k = \frac{\Delta\tau\ Mo}{2\ G} \qquad \text{Eq 5.21}$$

5.4.4 Scaling Relationships

For large earthquakes, it has been found that the stress drop is more or less independent of the seismic moment, and values of 1 to 10 MPa are typical. A similar trend has been found for seismic events in South African gold mines (Spottiswoode and McGarr, 1975). This means that corner frequency decreases and source radius increases with increasing seismic moment.

The corner frequencies calculated for seismic events at Quirke and Strathcona Mines as a function of seismic moment are plotted in Figure 5.11. In this case, the trend of lower corner frequency for larger seismic moments is weak and is not consistent with a constant stress drop model. Also the range of source radius is limited from 36 to 70 m. A similar observation has been made for small mine tremors in Polish copper mines (Gibowicz, 1988) and for some small earthquakes in southern California.

The results from Quirke Mine are particularly difficult to rationalize. It is strongly suspected that these events were pillar failures. Section 3.5.2 on pillar bursts showed that when a pillar fails the compressive stress usually goes to zero. Consequently, the shear stress drop across the pillar diagonals should be in the order of 60 MPa, source radius 3 m and corner frequencies over 400 Hz, according to a circular fault model. Obviously the results of the seismic analysis are nowhere near these values, which throws doubt on the validity of the circular fault model in these circumstances.

It has been shown that high frequency seismic radiation is strongly attenuated close to the source, especially for small seismic events (Anderson, 1986). This means that the corner frequency can be seriously underestimated. Figure 5.12 shows the apparent corner frequencies that can be obtained for different seismic moments. The factor, k, is obtained from the decay slope of the acceleration spectra and is related to the attenuation effects. For small seismic moments, the apparent corner frequency can be about 1% of the true corner frequency.

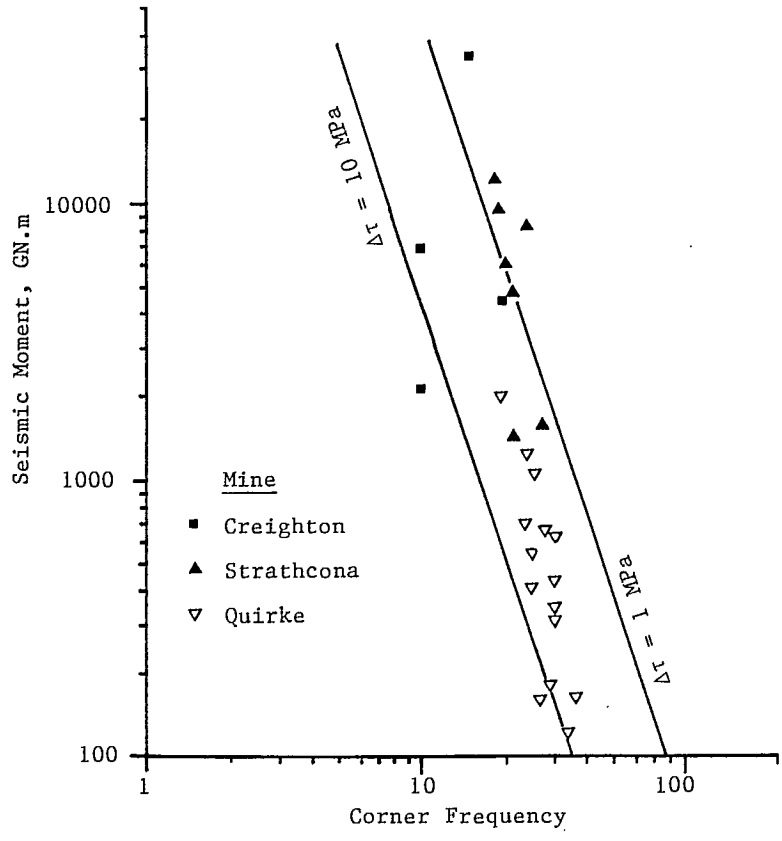

Fig. 5.11 - Seismic moment as a function of corner frequency at Quirke and Strathcona Mines.

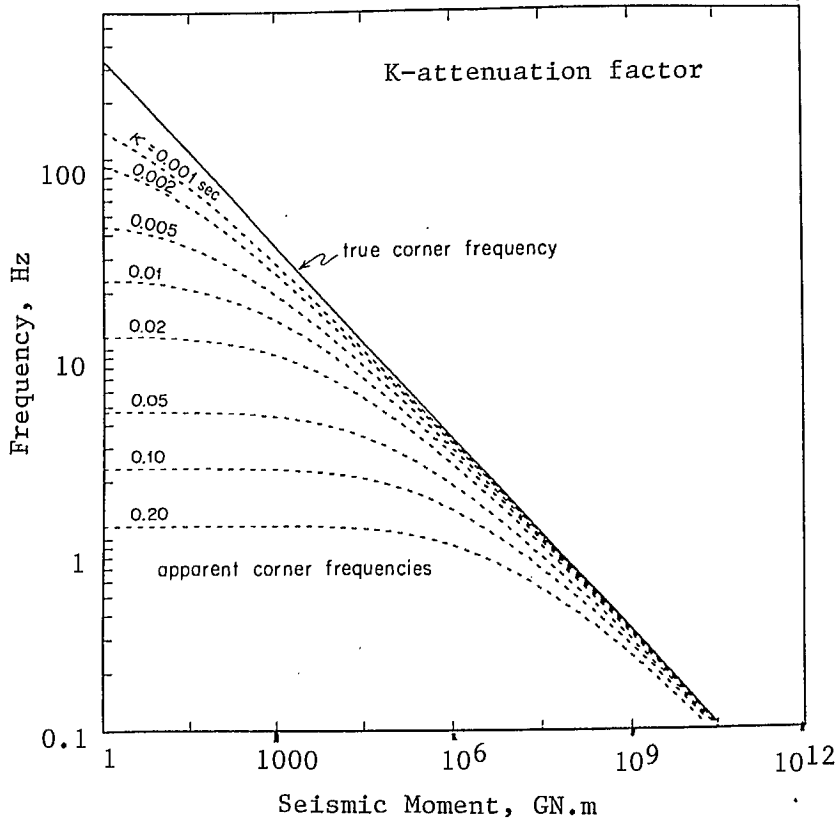

Fig. 5.12 - Effect of attenuation of the apparent compared to the true corner frequency. (after Anderson, 1986)

5.5 References

Aki, K. and Richards, P.G. (1980), Quantitative seismology: theory and methods. W.H. Freeman and Co., San Francisco.

Anderson, J.G. (1986), Implication of attenuation for studies of the earthquake source. Earthquake Source Mechanics Geophys Mon. 37, Am. Geophys. Un., Washington, D.C.

Boore, D.M. and Atkinson, G.M. (1987), Stochastic prediction of ground motion and spectral response parameters at hard-rock sites in eastern North America. Bull. Seism. Soc. Am. vol. 77, No. 2, pp. 440-467.

Brune, J.N. (1970), Tectonic stress and the spectra of seismic shear waves from earthquakes. J. Geophys. Res. 75, pp. 4997-5009. Also Correction, J. Geophys. Res. 76, p. 5002.

Cook, N.G.W. (1964), The application of seismic techniques to problems in rock mechanics, Int. J. Rock Mech. Min. Sci., vol. 1, No. 2, pp. 169-180.

Gibowicz, S.J. (1988), The mechanism of seismic events induced by mining: a review. 2nd Int. Symp. Rockbursts and Seismicity in Mines, Minneapolis, Minnesota.

Gutenberg, B. and Richter, C.F. (1956), Magnitude and energy of earthquakes. Ann. Geofis. (Rome), 9, pp. 1-15.

Hasegawa, H.S. (1983), Lg spectra of local earthquakes recorded by the eastern Canada telemetered network and spectral scaling. Bull. Seism. Soc. Am., vol. 73, No. 4, pp. 1041-1061.

Hasegawa, H.S., Wetmiller, R.J. and Gendzwill, D.J. (1988), Induced seismicity in mines in Canada - an overview, seismicity in mines. Pure App. Geophys.

McGarr, A (1976), Seismic moments and volume changes. J. Geophys. Res., vol. 81, No. 8, pp. 1487-1494.

McGarr, A., Green, R.W.E. and Spottiswoode, S.M. (1981), Strong ground motion of mine tremors: some implications for near-source ground motion parameters. Bull. Seism. Soc. Am., vol. 71, No. 1, pp. 295-319.

McGarr, A. (1984), Some applications of seismic source mechanism studies to assessing underground hazard. 1st Int. Symp Rockbursts and Seismicity in Mines, Johannesburg, S. Afr. Inst. Min. Met. Symp. Series 6, pp 199-208.

Nuttli, O.W. (1973), Seismic wave attenuation and magnitude relations for eastern North America. J. Geophys. Res., vol. 78, pp. 876-885.

Richter, G.F. (1958), Elementary seismology. W.H. Freeman, San Francisco.

Salamon, M.D.G. (1974), Rock mechanics of underground excavations. Proc. 3rd Congr. Int. Soc. Rock Mech., Denver, Colorado, vol. 1B, pp. 951-1099.

Salamon, M.D.G. (1983), Rockburst hazard and the fight for its alleviation in South African gold mines. Rockbursts: Prediction and Control, IMM, London, pp. 11-36.

Spottiswoode, S.M. and McGarr, A. (1975), Source parameters of tremors in a deep-level gold mine. Bull. Seism. Soc. Am., vol. 65, No. 1, pp. 93-112.

Wetmiller, R.J., Plouffe, M., Cajka, M.G. and Hasegawa, H.S. (1988), Natural and mining-related seismic activity in northern Ontario. 2nd. Int. Symp. Rockbursts and Seismicity in Mines, Minneapolis, Minnesota.

Wong, I.G. and McGarr, A. (1988), Implosional failure in mining-induced seismicity: a critical review. 2nd Int. Symp. Rockbursts and Seismicity in Mines, Minneapolis, Minnesota.

6. ALLEVIATION OF ROCKBURSTS

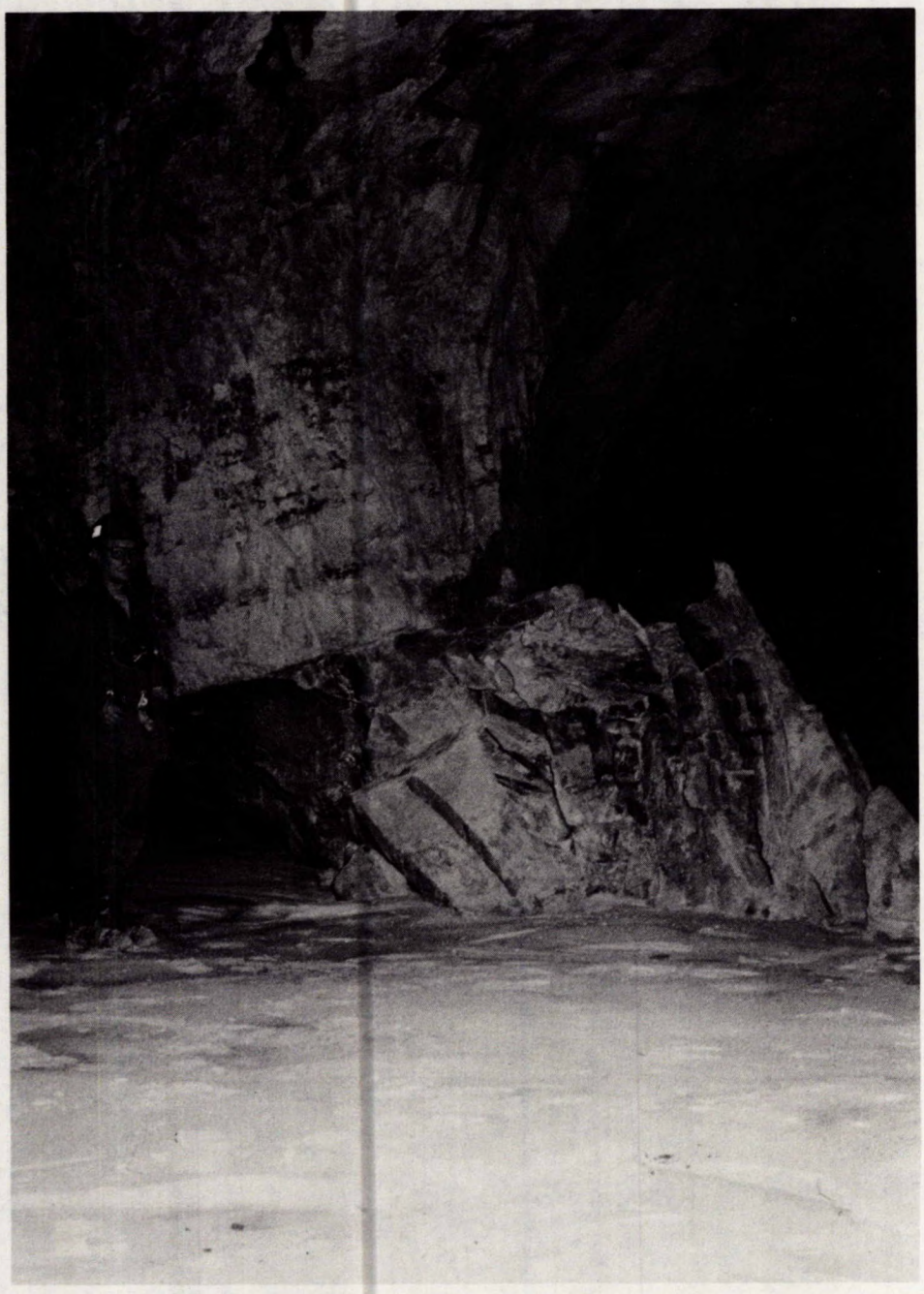

Backfill used to stabilize pillars at Denison Mine.

6. ALLEVIATION OF ROCKBURSTS

6.1 Introduction

There are two approaches to the alleviation of rockbursts which can be termed 'strategic' and 'tactical' (Salamon, 1983). The strategic approach is to diminish the possibility of encountering rockburst-prone ground, or to reduce the severity of the rockbursts. Techniques include altering the shape and orientation of development openings to minimize stress concentrations; sequencing of extraction to minimize large energy releases; layout of permanent pillars to reduce volumetric closure and the change in potential energy; and the use of backfill to both limit closure and to absorb energy otherwise liberated as seismic energy. The benefits of these techniques are only realized in the long term.

The tactical approach is to accept that some rockbursting is inevitable, but seeks to limit the extent of the damage or to control the timing of a rockburst. Techniques include design of support systems which can survive dynamic loading, destress blasting to soften the rock and change the potential energy, and large-scale production blasts scheduled just prior to a weekend shutdown. The benefits of these techniques are realized in the short term and are described separately in Chapters 7 and 8.

Over the years, a number of strategic practical solutions have been developed to reduce the number and severity of rockbursts. Examples of the measures used in the 1940s in Ontario mines were described in Chapter 2. Recently these have been augmented by theoretical studies which have identified the critical parameters which have to be controlled, such as 'energy release rate' and 'excess shear stress' concepts developed in South Africa.

6.2 Energy Release Rate

Studies in South African gold mines indicated that the damage from rockbursts could be empirically related to the energy release rate (Hodgson and Joughin, 1967). This was defined as the stored strain energy per square metre in the rock to be extracted in the next mining step. These values could readily be

obtained from computer models such as MINSIM. The relationship between energy release rate, number of damaging bursts and rock conditions for longwall operations in South African gold mines is illustrated in Figure 6.1 (Jaeger and Cook, 1976). The graph indicates negligible damage below 15 MJ/m^2, ranging up to extreme damage above an energy release rate of 100 MJ/m^2.

The energy release rate is essentially a measure of the theoretical stress concentration on the rock to be mined in the next step. For plane strain conditions and just considering the perpendicular stress, then (Salamon, 1983):

$$\sigma p = \sqrt{\frac{2E}{(1-\nu^2)h} \frac{\Delta Um}{\Delta A}} \qquad \text{Eq 6.1}$$

where, σp = perpendicular stress
E = elastic modulus
ν = Poisson's ratio
h = height of the stope
$\Delta Um/\Delta A$ = energy release rate.

It was realized that the stress values from Equation 6.1 were fictitious. For example, given a modulus of 70 GPa, a stoping height of 1 m, an energy release rate of 50 MJ/m^2, this equation would yield a theoretical perpendicular stress of 2700 MPa. Rocks are not able to withstand these high stress values and they would fracture at much lower values and transfer the stress into the solid abutment. Nevertheless, the empirical relationship shown in Figure 6.1 can still be used in South Africa to compare different mining layouts and to evaluate the likely degree of damage at the working face (i.e., for strain energy and pillar types of bursts).

However, Figure 6.1 is specific to longwall operations in South African gold mines. It cannot be used in other mines with different mining methods and different geometries. In the Elliot Lake, Red Lake and Kirkland Lake mines, severe pillar bursts occur when the stress levels approach 150 MPa. Stoping height is typically 3 m at these mines, which gives an energy release rate of about 0.5 MJ/m^2, or only about 1% for similar damage conditions in South Africa.

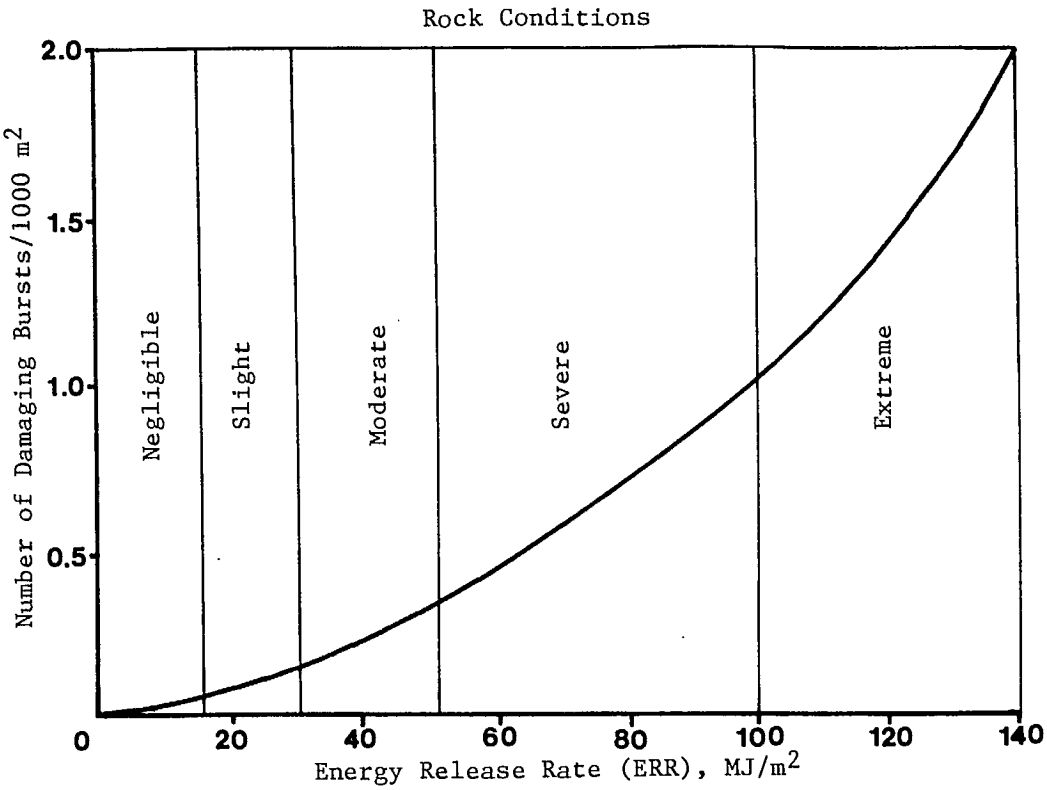

Fig. 6.1 - Damage criterion as a function of energy release rate for South African gold mines (after Jaeger and Cook, 1976).

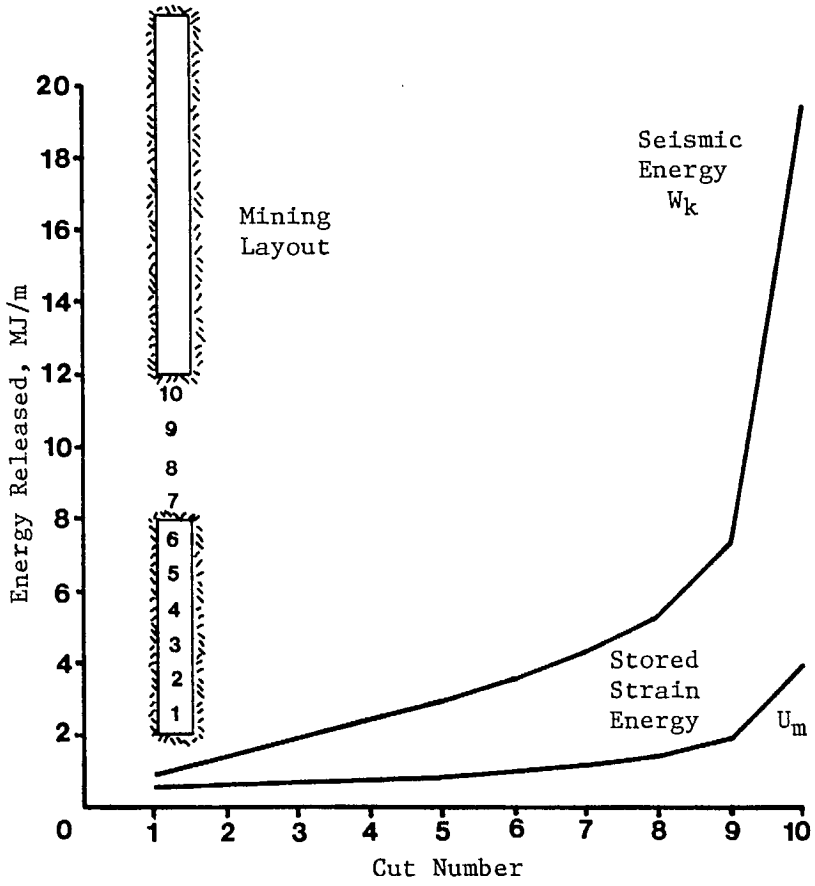

Fig. 6.2 - Energy released during mining of a vertical stope in ten cuts.

An alternative to the energy release rate is to calculate the seismic energy released at different mining stages. Figure 6.2 shows an example of a vertical stope being mined in ten successive cuts towards a mined-out stope above, essentially forming a crown/sill pillar situation. The stored strain energy, Um, in the rock mined (equivalent to energy release rate) increases gradually, whereas the seismic energy, W_k, liberated increases at a much greater rate. These values are also fictitious, since they assume linear elasticity for the rock, and the rock in each cut is mined instantaneously rather than in a series of discrete steps. Also the intervening pillar would probably fail well before the last cut. However, it does provide a means of comparing different mining layouts to determine which one would liberate the least seismic energy.

6.3 Excess Shear Stress

The energy release rate, or the seismic energy release, only relates to the rockburst potential within the mine workings. It does not provide information on likely seismic activity along prominent geological structures. Slippage along these structures can produce large rockbursts, at some distance from the mine workings and cause mine-wide damage. All the large rockbursts above a magnitude of 3.0 Mn, in the Sudbury mines are believed to be caused by fault-slip, and are essentially mining-induced mini-earthquakes.

Chapter 3 introduced the mechanics of slippage along a circular fault with only frictional properties. In this case the reduction in shear stress, or stress drop, is proportional to the difference between the static and dynamic coefficients of friction on the fault. Ryder (1986) expanded on this concept and developed an 'excess shear stress' criterion for assessing potential slippage on a fault.

At the point of slippage, the balance between shear and clamping forces on a fault can be expressed by:

$$\tau_s = C_s + \mu_s \sigma_n \qquad \text{Eq 6.2}$$

where, τ_s = static shear stress, or strength

C_s = cohesion

μ_s = static coefficient of friction

σ_n = normal stress.

Once slippage is initiated the dynamic coefficient of friction, μ_d, comes into operation, and generally the cohesion is eliminated and the shear stress becomes:

$$\tau_d = \mu_d \sigma_n \qquad \text{Eq 6.3}$$

The difference in the static and dynamic shear stresses is the excess shear stress, τ_e,

$$\tau_e = \tau_s - \tau_d = C_s + \mu_s\sigma_n - \mu d\ \sigma_n \qquad \text{Eq 6.3}$$

Ryder (1986) suggested preliminary values for excess shear stress, in the order of 5 to 10 MPa for existing weakness planes, and 20 MPa for rupture through intact rock. Values for the static coefficients of friction are typically 0.6, or a 30^o angle of friction. In his analysis the dynamic coefficient was taken to be the same as the static, and hence the excess shear stress, or stress drop, reduces to the cohesion (assuming the normal stress remains constant).

Ryder's concept of triggering slippage on a fault is illustrated in Figure 6.3. The fault plane will have an irregular static strength distribution, due to asperities and varying frictional properties, as shown in the top curve. After slippage the dynamic shear strength drops to a lower smooth curve. If the profile of static shear stress touches any point on the static shear strength distribution, then slippage is initiated at that point with an immediate stress drop to the lower dynamic shear strength. High stress concentrations at the tip of the rupture surface drive the slippage along the fault into areas of lower excess shear stresses, and can overshoot into areas where the static shear stress is lower than the dynamic shear strength.

The procedure used in South Africa to assess the potential of fault slippage is as follows. A number of numerical models can be used to calculate the

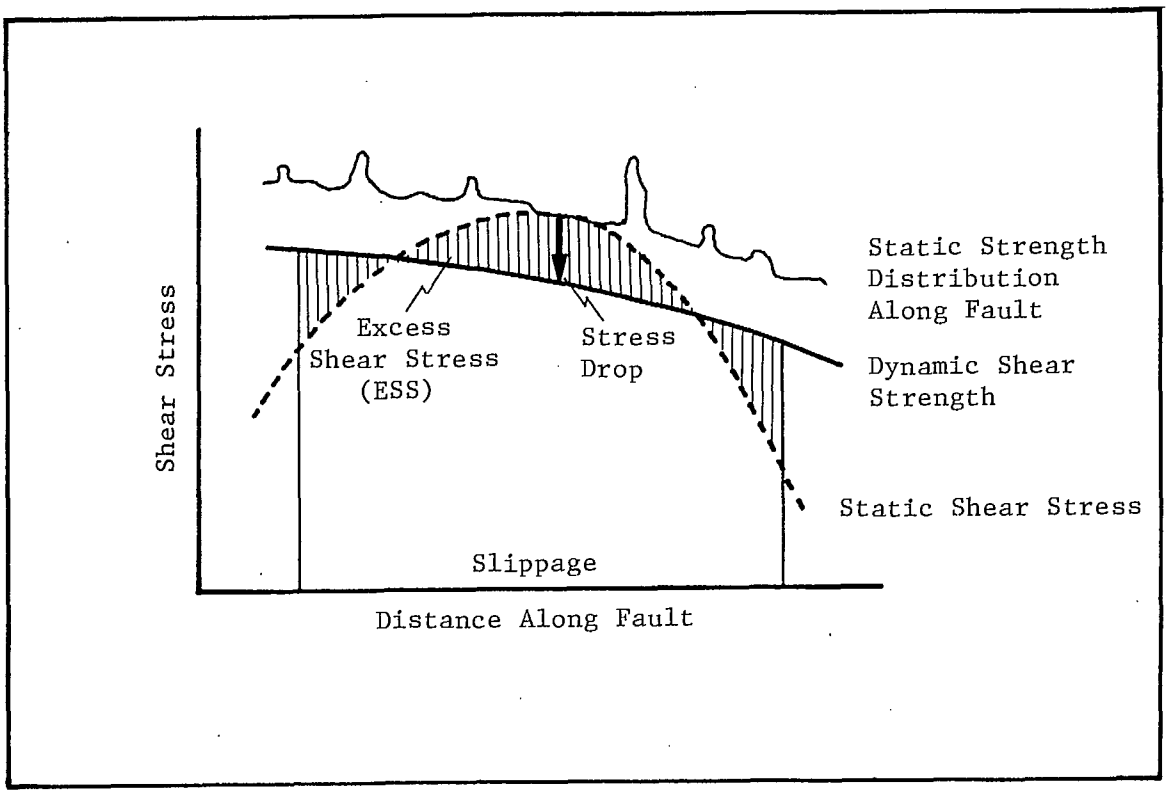

Fig. 6.3 - Concept of excess shear stress and initiation of slippage on a fault (after Ryder, 1986).

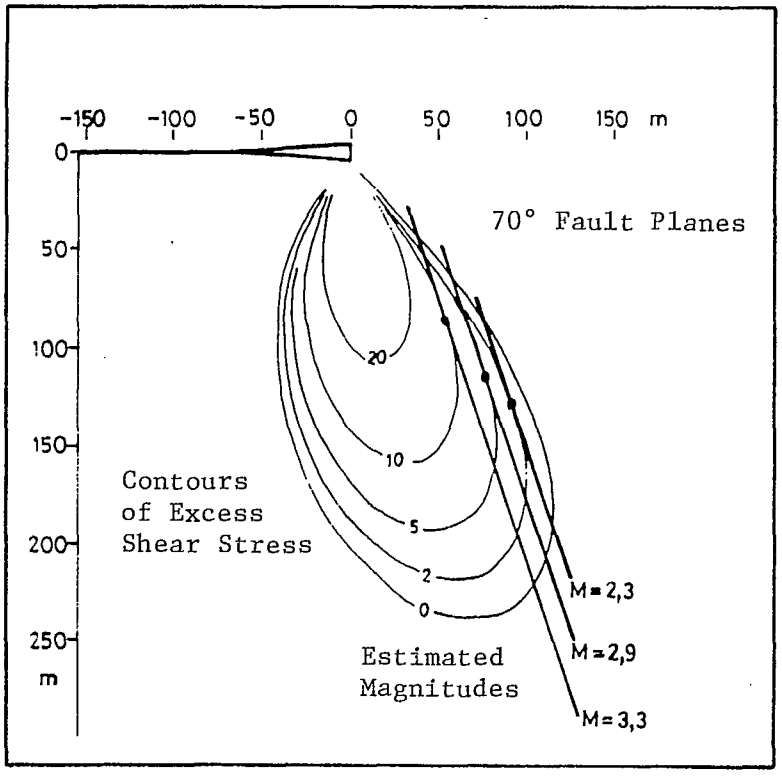

Fig. 6.4 - Contours of excess shear stress, intersecting 70° fault planes and anticipated seismic events (after Ryder, 1987).

shear and normal stresses on a fault plane. If the static shear stress exceeds the dynamic shear strength, then the area of excess shear stress on the fault plane is calculated. If the maximum excess shear stress is in the order of 5 to 10 MPa, then slippage is assumed to occur and the displacement, or ride, distribution along the fault is calculated. Standard seismology equations, introduced in Chapter 5, are then used to estimate the magnitude of the potential seismic event. First, the seismic moment is calculated as being the product of the shear modulus, average slippage and area over which slippage occurs (i.e., area of excess shear stress). Richter magnitudes are obtained from the empirical relationship to seismic moment. Other parameters, such as seismic energy liberated, average stress drop and peak particle velocity close to the source can also be calculated.

Figure 6.4 shows an example of this technique for an isolated longwall stope (Ryder, 1987). Lobes of excess shear stress are plotted in the footwall and assumed fault planes, dipping at 70^{o}, intersect these lobes. Slippage is initiated where these planes touch the individual lobes (i.e., 10, 5 and 2 MPa in the example). Displacement would occur over the area where the excess shear stress is positive (i.e., over 0), resulting in seismic events of magnitudes of 3.3, 2.9 and 2.3, respectively. Ryder found that faults dipping around 70^{o} or 130^{o} were the most susceptible for South African longwall stoping and virgin stress conditions.

Ryder (1987) observed that the excess shear stress criterion tends to produce conservative results, in that high levels often do not result in any seismic activity. Also the criterion is very sensitive to the virgin stress levels and the friction properties of faults. However, more success has been obtained in using the excess shear stress criterion in back analysis of major fault-slip rockbursts (Brummer and Rorke, 1988; Holmes and Reeson, 1988). Reasonable estimates of magnitude and seismic moments were obtained in these studies. In many cases it is practically impossible to eliminate slippage on a fault. Control measures, such as leaving strategically placed pillars, backfill and sequence of extraction can only be used to limit the size of the seismic event.

Some mines in Ontario have a further complication, namely intermittent water

on the fault surfaces. At some mines there is an increase in seismic activity during the spring run-off, and at others there is an apparent correlation between pouring hydraulic backfill and increased seismic activity. Biskup and Kaiser (1990) have investigated the properties of several prominent faults in the Sudbury mines. They found that the dry static angle of friction was 33^{o} which reduced to 26^{o} under wet conditions. This order of reduction affects the seismic efficiency. This term was introduced in Chapter 3 as being the proportion of the released energy liberated as seismic energy. For dry faults with only frictional properties, the dynamic coefficient of friction is typically 95% of the static, producing seismic efficiencies of about 5%. Using the values for dry and wet faults increases the seismic efficiency to about 14%. Biskup and Kaiser (1990) also introduced cohesion into the seismic efficiency equation which becomes:

$$W_k = \frac{\frac{C_s}{\sigma_n} + (\mu_s - \mu_d)}{\frac{C_s}{\sigma_n} + (\mu_s + \mu_d)} \qquad \text{Eq 6.4}$$

When the cohesion is half the normal stress, seismic efficiencies approach 40%.

The original friction model produced relatively low stress drops which meant that slippage had to occur over large areas to explain the seismic energy liberated. The introduction of cohesion and a wet angle of friction result in a much higher stress drop and a corresponding slippage over a smaller area. This is more in line with observations in Ontario mines where damage from suspected fault-slip rockbursts is restricted to fairly small areas.

6.4 Mining Layout and Sequence of Extraction

When bursting first began to occur in the Kirkland Lake and Sudbury mines in the 1930s, it was soon realized that mining method, layout of stopes and pillars, and the sequence of extraction played an important role in their occurrence.

The strategies developed at the Lake Shore Mine in Kirkland Lake are

particularly well documented (Robson et al. 1940, 1946 and 1957). At the mine there were two parallel and steeply-dipping veins, 1 to 3 m wide and extending to a depth of 2500 m. Down to the 1600 level (370 m) shrinkage stoping was employed. Bursting started in the thin sill pillars on the 1200 level (370 m) as the shrinkage stopes approached the mined-out level above.

Below the 1600 level stoping was converted to flat-back longitudinal cut-and-fill, using sand and waste rock as the backfill material. A typical layout of these stopes is shown in Figure 6.5a). Bursting occurred below the 2200 level (670 m) when the sill pillars approached a 12 m thickness. To assist in the mining of these thin sill pillars, they were divided up by additional raises and extracted in vertical slices. This compounded the problem and there were many bursts in these small pillars, followed by failure of the adjacent sill pillars over distances up to 75 m.

The next step was to mine only half the stope with flat cut-and-fill methods, then to convert to sub-vertical rill mining. With increasing depth these larger sill pillars began to burst.

Below the 2700 level (825 m) it was decided to convert completely to rill stoping, with square-sets and backfill. Rill stopes were established over multi-levels and their line of advance was rigidly controlled, as illustrated in Figure 6.5b). Successive stopes were opened up in a triangular configuration before the stope below was started. This resulted in the stopes advancing, from a central raise, in a 'V' type formation. The purpose was to prevent the formation of isolated remnant pillars or pillars projecting out into the mined-out areas.

This type of stoping layout reduced the number of pillars but did not entirely eliminate them, since eventually the rill stoping blocks approached each other. Fig. 6.5c) shows the layout and location of a particularly large rockburst which caused extensive damage to the pillars and drifts over two levels. In this case the standard procedure was not being followed, in that small pillars were being formed.

A similar strategy was also being used in the Sudbury mines. Figure 6.6 shows

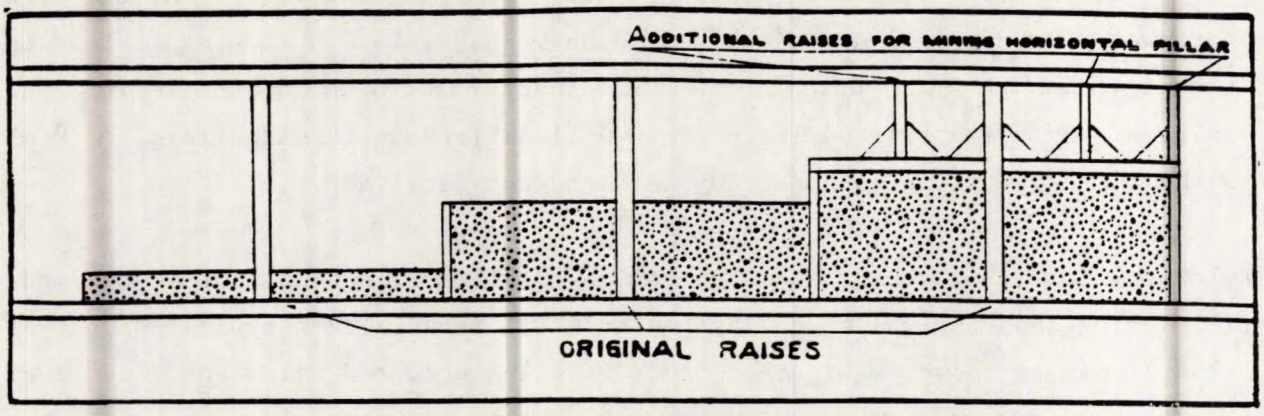

a) Flat-back cut-and-fill mining.

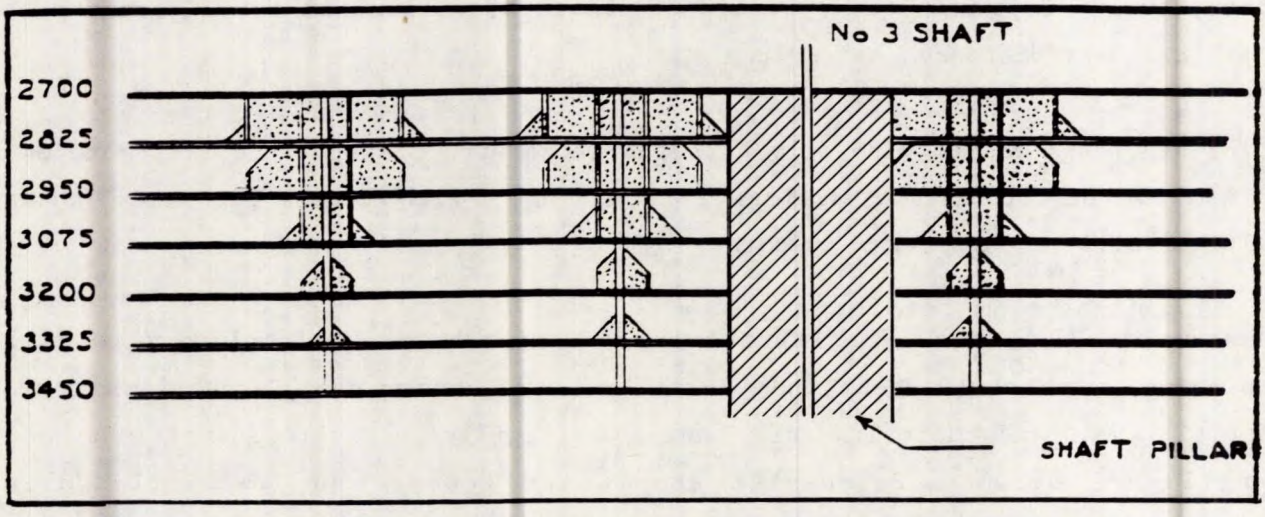

b) Planned system of rill stoping below the 2700 level.

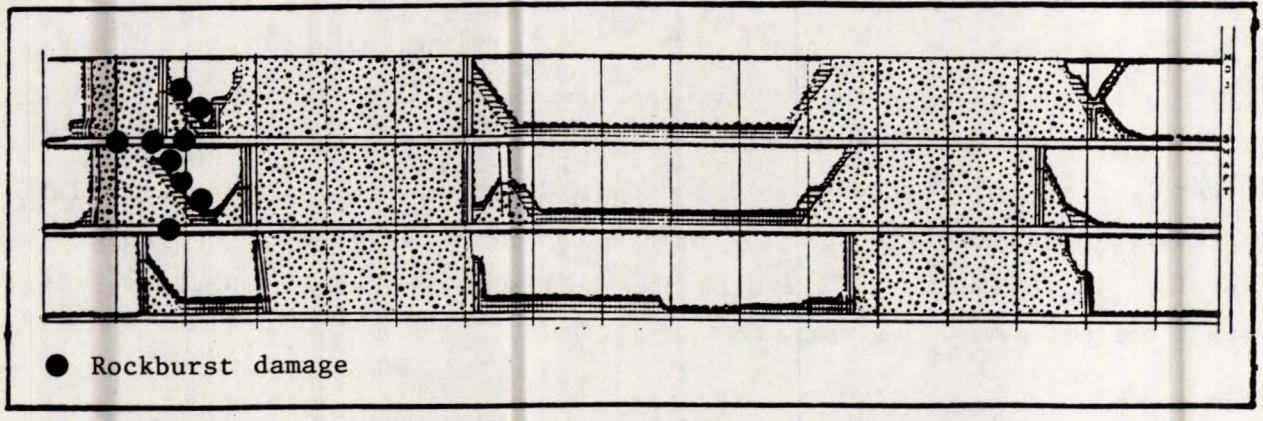

c) Mining layout at the time of a major rockburst.

Fig. 6.5 - Changes in mining layouts and sequence at Lake Shore Mine (after Robson, 1940).

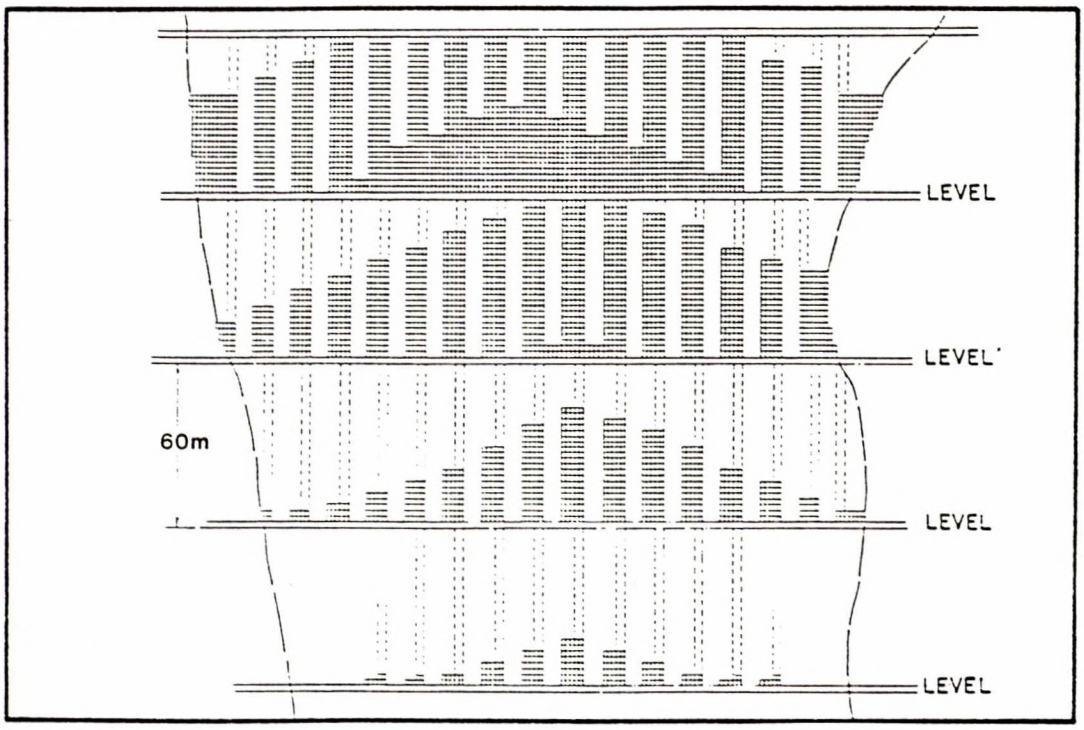

Fig. 6.6 - Mining sequence with square-set stoping and backfill (after Dickout, 1962).

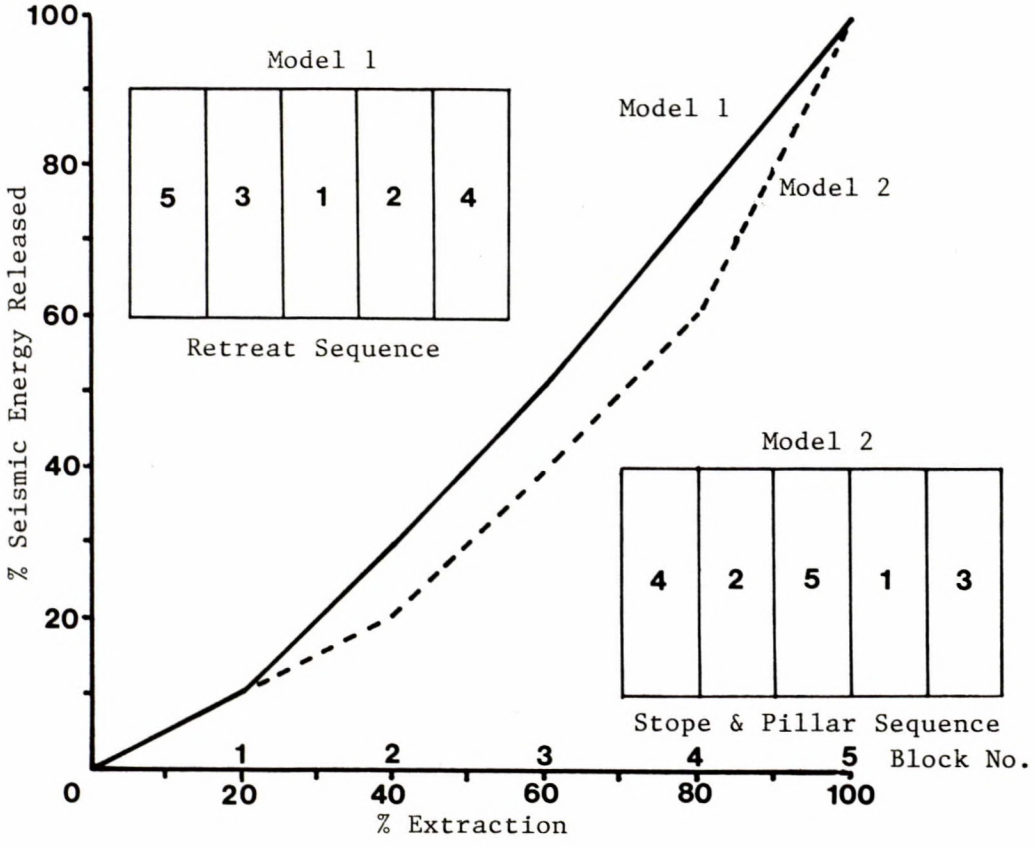

Fig. 6.7 - Seismic energy released as a function of extraction for two alternative mining sequences.

the standard layout for transverse cut-and-fill stopes with square sets at the Creighton Mine (Dickout, 1962). Both primary stoping and pillar recovery were advanced upward on an inverted 'V' front. Only one level was allowed to merge with the one above at any one time. When the lead stope approached the level above some bursting was experienced, but multiple and severe crown bursts were eliminated. Subsequently, the introduction of cemented backfill eliminated the square sets, however, the sequency of mining was still retained.

Essentially, these mines were adopting mining layouts where they could control the change in potential energy of the wall rocks. The wall rocks were allowed to converge continuously in a gradual manner, rather than suddenly at the end of the mining cycle (i.e., in a sill pillar situation). By controlling the change in potential energy they also had some control over the release of seismic energy.

This can be demonstrated by the simple example of a block of five stopes which can either be mined starting at the centre and retreating outwards, or in a stope and pillar configuration. Figure 6.7 shows the two alternative mining sequences and the resultant release of seismic energy, if each block is mined instantaneously. Starting at the centre and retreating has a more uniform rate of seismic energy release, with the last 20% of extraction resulting in 24% of the total seismic energy released. In the stope and pillar layout, initially the release of seismic energy is lower, until the final centre pillar is removed. In this case the last 20% extraction is responsible for 40% of the seismic energy released.

If the centre pillar is left as a permanent stabilizing pillar, then the overall release of seismic energy is reduced. This is one of the main methods used in South African gold mines to reduce the severity and number of rockbursts (Salamon and Wagner, 1979). Regional stabilizing pillars have only been used in a planned systematic manner at Rio Algom's Stanleigh Mine at Elliot Lake. Barrier pillars 30 m wide were left at 250 m centres, with a stope and pillar layout in between taking about 67% extraction. This layout was used only below a depth of about 1000 m, essentially to prevent any pillar failures in one panel spreading to other panels, such as that which happened at Quirke Mine.

Stabilizing pillars have also been left in other Ontario mines, but in an unplanned fashion. These usually took the form of regional sill pillars separating the upper and lower levels of a mine, or shaft pillars. The intention was to recover these pillars towards the end of the mine's life. More often than not rockbursts started to occur in these pillars and they were abandoned.

One of the practical solutions developed in the 1940s was that it was better to start stoping next to a major fault or dyke and retreat away from it, rather than advance towards it (Morrison, 1942). The rationale was explained in terms of the doming theory and stress concentrations, rather than where slippage was initiated on the fault and its location relative to the working face.

Figure 6.8 shows the layout of a two-dimensional numerical model, where mining either retreats away from or advances towards a prominent fault, in eleven mining steps. The fault was given both cohesion and frictional properties. Stress drop, displacement and distance over which displacement occurred were determined for each mining step, from which the seismic energy could be calculated.

Retreating away from the faults resulted in a more even distribution in seismic energy released, as shown in Figure 6.8. However, it is not a smooth distribution, but varies up and down in successive mining steps. It was observed that the larger releases of seismic energy coincided with large stress drops when sections of the fault first slipped. When the same sections of the fault slipped a second time the stress drops were much less.

Advancing towards the fault resulted in no release of seismic energy for the first six mining steps. Further mining steps resulted in moderate releases of seismic energy until the stope intersected the fault, resulting in a very large release of seismic energy. Also the total release of seismic energy in the advance sequence was about 25% greater than the retreat sequence.

These results suggest that retreating away from a fault results in a larger number of small seismic events. Advancing towards the fault is characterized

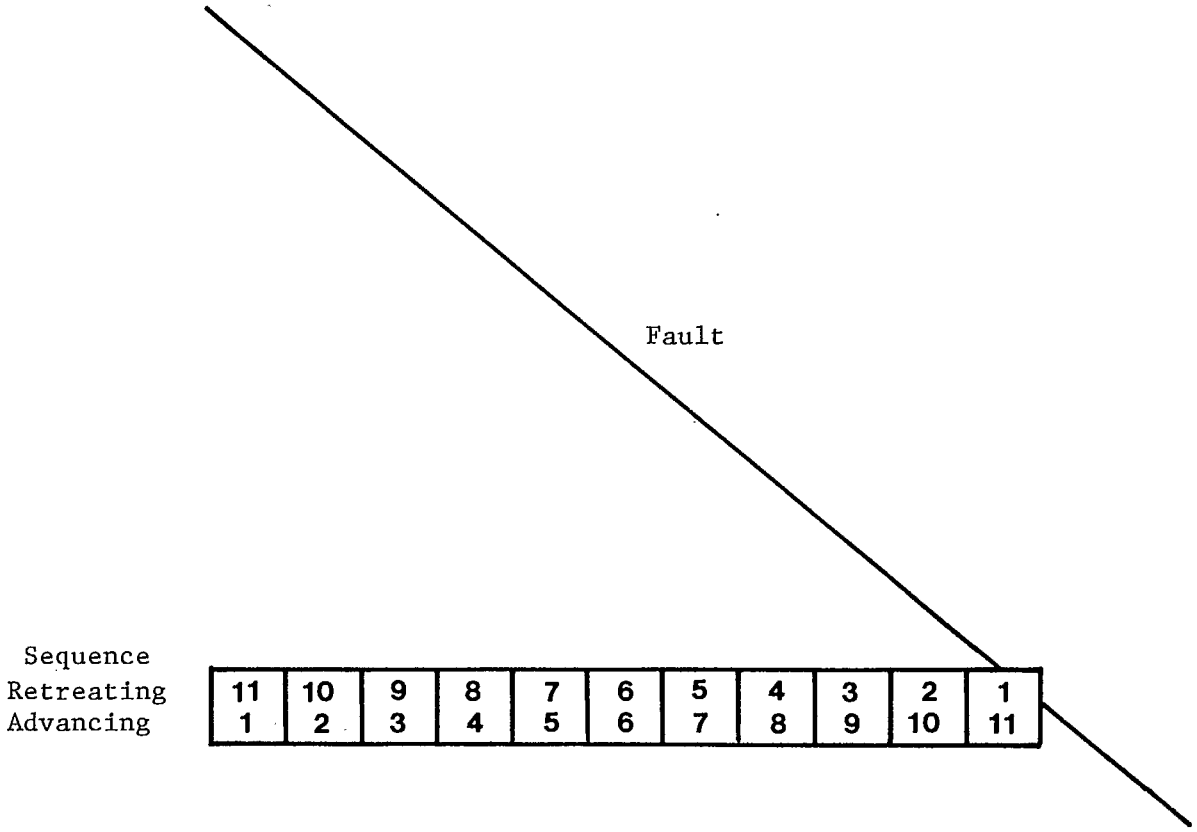

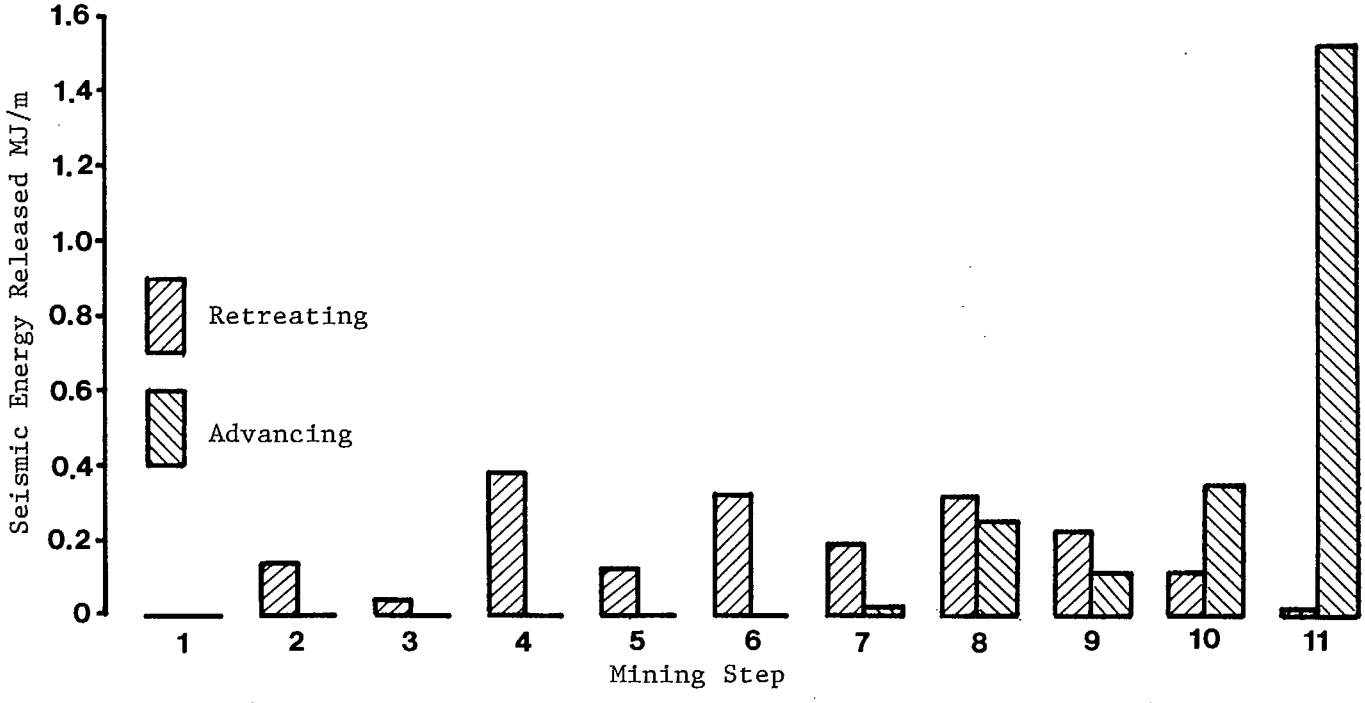

Fig. 6.8 - Seismic energy released when retreating from, or advancing towards a fault.

by one major seismic event when the stope intersects the fault. This major event would probably occur in close proximity to the working face. It should be mentioned that slippage on a fault is probably a chaotic behaviour, in that small changes in fault properties or stresses produce completely different results (Scholz, 1991).

6.5 Utilization of Backfill to Alleviate Rockbursts

Backfill is used in many mining methods, either concurrently with stoping as in longitudinal and transverse cut-and-fill, or delayed at the completion of stoping as in blasthole and vertical retreat methods. Other than its own body weight, backfill is a passive support system, in that it has to be compressed before exerting a reaction force against the wall rocks. The magnitude of the reaction force is dependent on the amount of stope closure, the time of backfill placement in the mining sequence and its stiffness characteristics.

Compared to an unfilled stope, backfill will reduce the volumetric closure of the stope walls, decrease the stress transfer to the rock abutments, increase the strength of the wall rocks by its confining effect and absorb energy which would otherwise be released as seismic energy. Some of these effects will be small, unless the stope is at great depth (i.e., 2000 m) or the backfill is very stiff (i.e., 3 GPa).

6.5.1 Effect of Backfill on the Energy Balance

The energy balance incorporating backfill was given in Chapter 3.2, and is repeated below:

$$W_t + U_m = U_c + W_s + W_r$$

where, $W_r = U_m + W_k$

hence, $W_k = W_t - (U_c + W_s)$

where, W_t = change in potential energy

U_m = stored strain energy in material mined

U_c = increase in stored strain energy in remaining rock
W_s = energy absorbed by backfill
W_r = released energy
W_k = seismic energy.

Hedley (1984) developed an algebraic model to investigate the effect of backfill on the energy components, including its time of placement. Subsequently, this model was updated and expanded by Brummer (1991).

A single isolated stope was represented as a two-dimensional thin slit. It was assumed that the backfill did not alter the closure distribution in the stope but rather that closure was imposed on the backfill generating a stress in the backfill. Both the rock and backfill behaved as linear elastic materials.

The convergence distribution across a thin slit and the stress distribution into the abutments were given in Section 3.3 and are repeated below:

$$c = \frac{4(1-\nu^2)}{E}\ \sigma_o\sqrt{S^2-X^2}$$

$$\sigma_p = \frac{X\sigma_o}{\sqrt{X^2-S^2}}$$

where, c = convergence
σ_o = virgin perpendicular stress
S = half span of stope
X = distance from centre of span
E = elastic modulus
ν = Poisson's ratio.

The energy absorbed by the backfill was expressed by:

$$W_s = \frac{\Delta\ V_f^2\ E_f}{2Lh(1-u^2)}$$

where, $\Delta\ V_f$ = incremental volumetric compression of backfill
E_f = deformation modulus of backfill

L = height of backfill
h = width of backfill
u = Poisson's ratio of backfill.

A stope 3 m wide, at a depth of 1000 m, was mined vertically, either up or down, in 13 3 m cuts for a total stope height of 39 m. The horizontal perpendicular stress was taken as twice the vertical, and the rock had an elastic modulus of 70 GPa. Three mining methods were investigated:

i) Overhand cut-and-fill with uppers drilling, where backfilling lags behind stope advance by one cut.

ii) Overhand cut-and-fill using horizontal drilling (i.e., breasting) where the backfill is poured to within 1 m of the stope back before the next cut is mined.

iii) Underhand cut-and-fill where the backfill is poured tight before the next cut is mined beneath.

The utilization of the convergence to compress the backfill, for the three mining methods, as mining progresses through the 13 cuts, are illustrated in Figure 6.9. After the 13th cut, 46% of the convergence was utilized in compressing the backfill for overhand cut-and-fill with upper drilling, which increased to 59% for breasting and 69% for undercut-and-fill.

Figure 6.10 shows the energy components for the undercut-and-fill method, as a function of mining cut, for a backfill stiffness of 3 GPa. The stored strain energy in the material mined, U_m, increases linearly with each cut. This is equivalent to the energy release rate (ERR) discussed previously. Released energy, W_r, and seismic energy, W_k, are slightly non-linear, the rate of increase diminishes with each cut. The energy absorbed by backfill, W_s, is also non-linear, but in this case the rate of increase becomes slightly larger for each cut.

The efficiency of backfill to absorb energy can be expressed as a proportion of the seismic energy released, since most of the energy it absorbs would

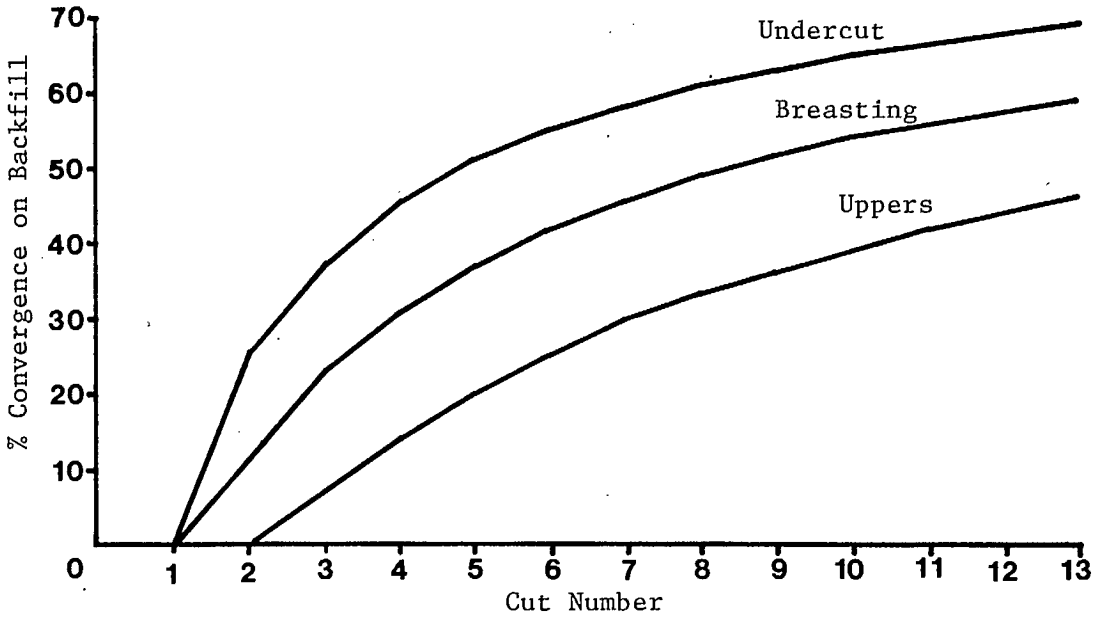

Fig. 6.9 - Utilization of convergence to compress backfill.

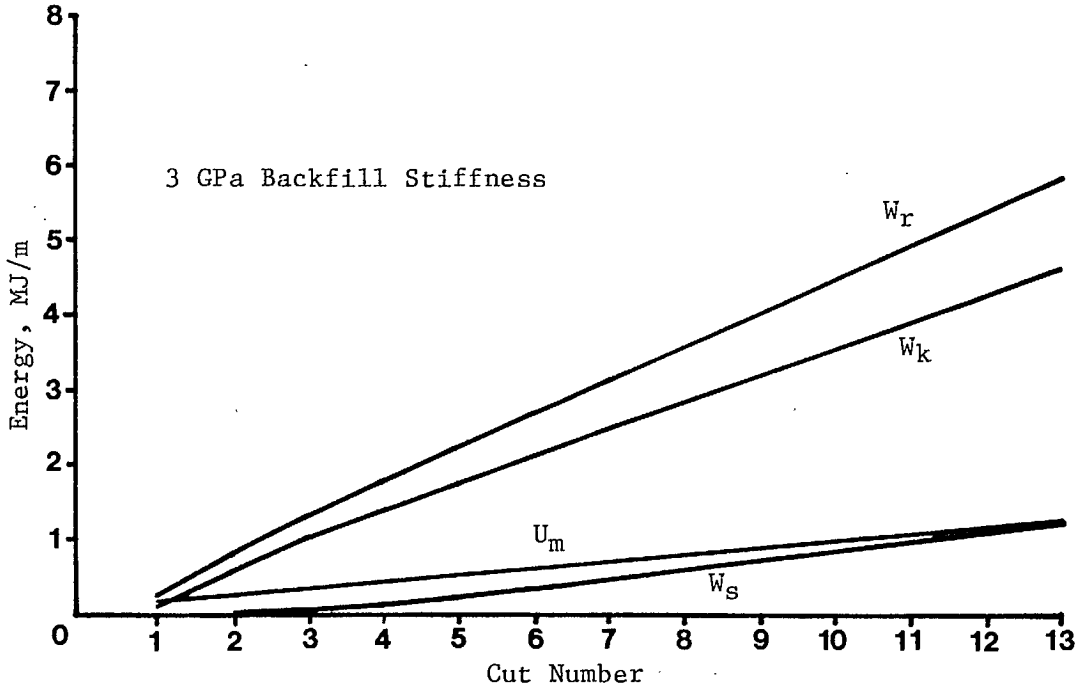

Fig. 6.10 - Energy components in undercut-and-fill, algebraic model.

otherwise be released as seismic energy. This is illustrated in Figure 6.11 for the three mining methods and a backfill stiffness of 3 GPa. After the 13th cut, the backfill efficiency is 26% for undercut-and-fill, which reduces to 21% for breasting, and 16% for overhand cut-and-fill with uppers drilling. Backfill efficiencies for undercut and breasting are under-estimated since the model removes each cut instantaneously over an infinite length. In practice, material is mined in small incremental steps of about 3 x 3 m in these two methods. This would increase the stored strain energy in the material removed, and hence, slightly reduce the seismic energy liberated. Figure 6.11 illustrates the importance of placing the backfill as early in the mining cycle as possible, so that the maximum amount of convergence is utilized in compressing the fill. For undercut-and-fill it is equivalent to having a backfill about 60% stiffer compared with overhand cut-and-fill with uppers.

Backfill efficiency can also be plotted as a function of backfill stiffness as illustrated in Figure 6.12. These results are after the 13th cut in each of the three mining methods. For underhand cut-and-fill the energy absorbed by the backfill equals the seismic energy (i.e., backfill efficiency of 100%) at a backfill stiffness of about 7 GPa, and somewhat higher values for the other two mining methods. These stiffnesses can probably only be achieved by using cemented rockfill for typical stoping layouts in Ontario mines. However, at these stiffnesses the algebraic model is probably no longer valid in that the backfill starts to affect the convergence distribution.

To investigate the effect of backfill on stope closure a displacement discontinuity model was used. The same stope geometry as with the algebraic model was used for a base case of undercut-and-fill with a 3 GPa backfill stiffness. For comparison purposes the model was first run with no backfill.

The effect of the stiff backfill on the energy components is shown in Figure 6.13 a), b) and c). After the 13th cut, backfill reduced the change in potential energy, W_t, by 37%. Hence, volumetric stope closure was also been reduced by this amount.

The stored strain energy in the material removed, U_m, was reduced by 21%. This is because the backfill was reducing the stress concentration on the

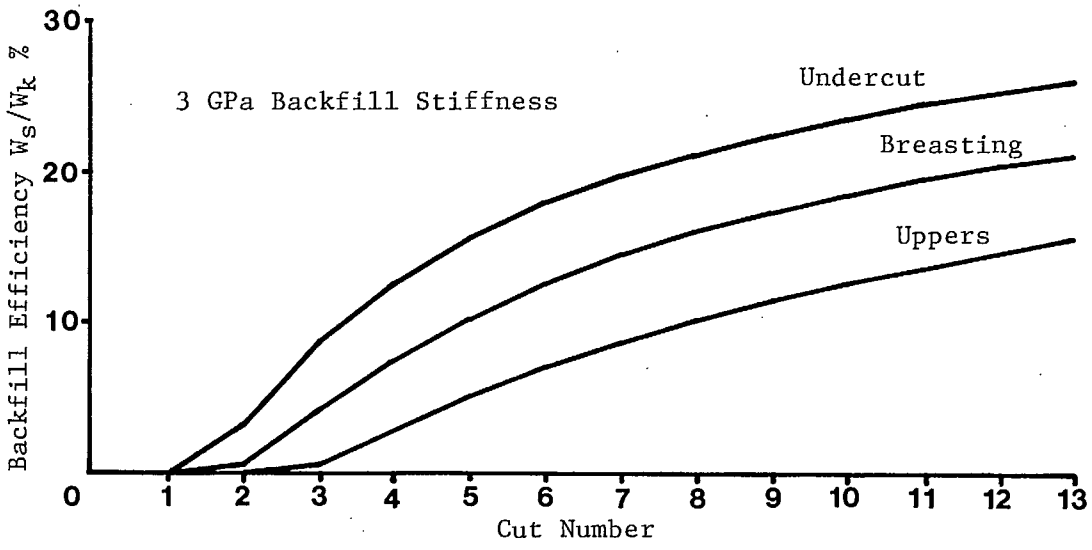

Fig. 6.11 - Energy absorbed by backfill as a proportion of seismic energy released, algebraic model.

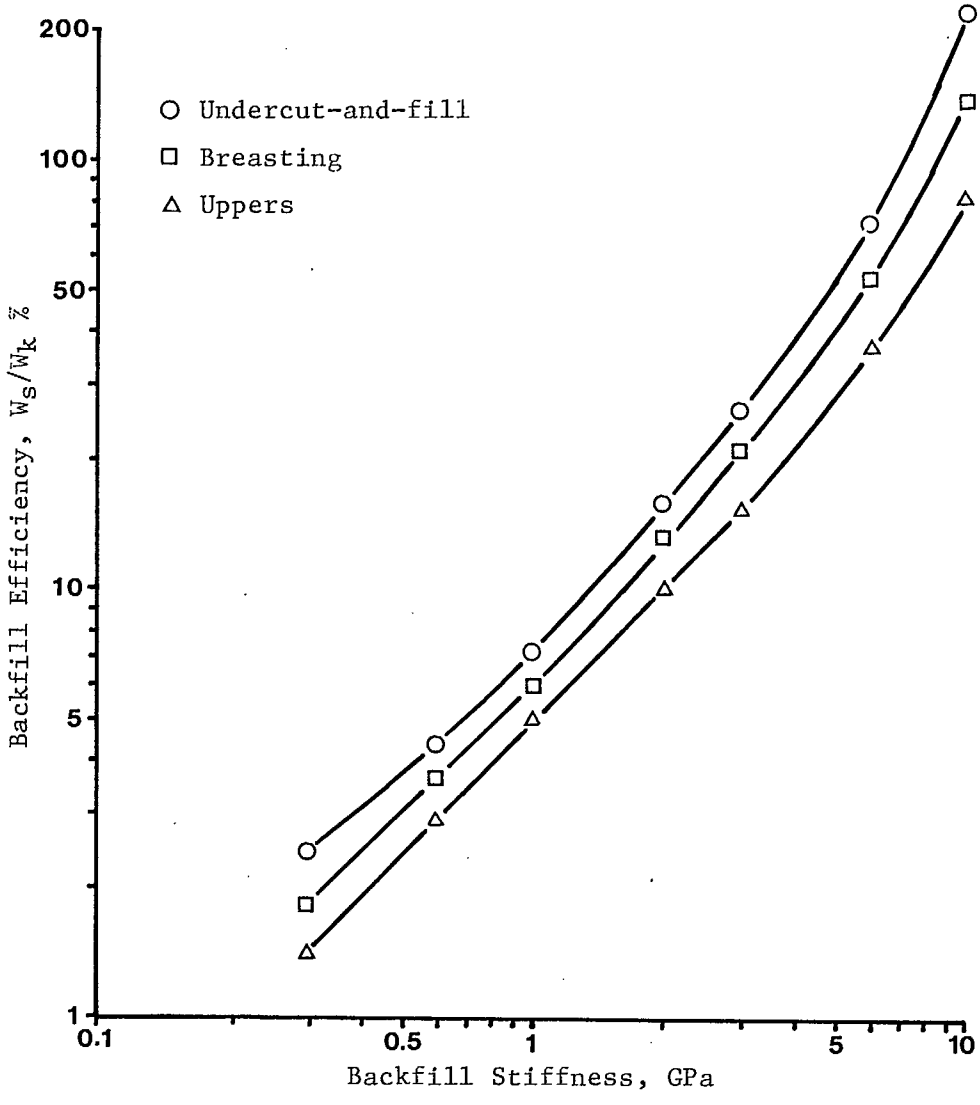

Fig. 6.12 - Variation in backfill efficiency with backfill stiffness, algebraic model.

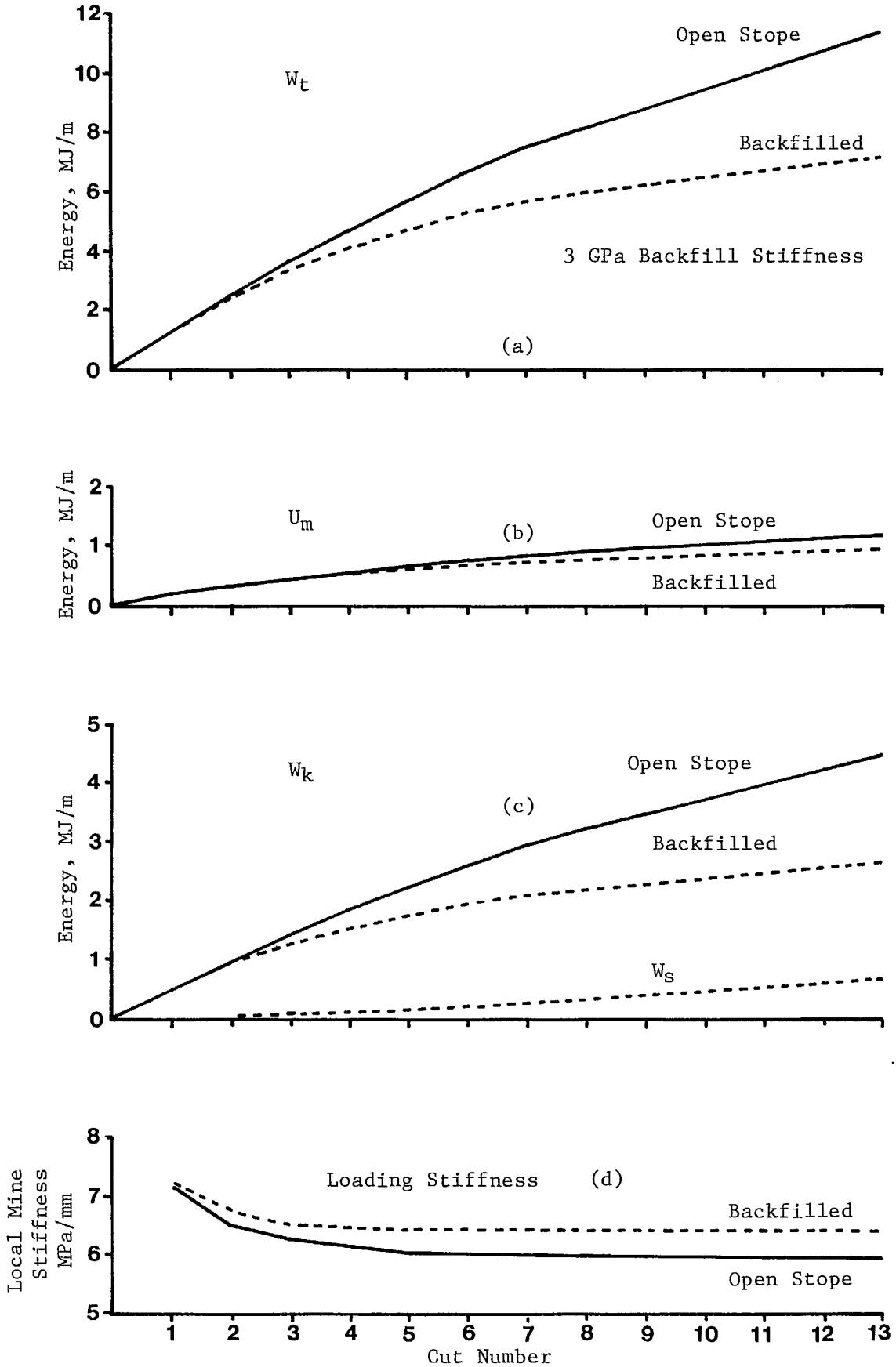

Fig. 6.13 - Energy components for a stope mined with and without backfill, numerical model.

working face. On the 13th cut, this theoretical stress was reduced from 148 MPa with no backfill to 122 MPa with backfill.

The seismic energy released, W_k, showed the largest reduction at 41%. Somewhat surprisingly the energy absorbed by the backfill, W_s, was also reduced by about 37% compared to the corresponding algebraic model (see Figure 6.10), since the convergence had been reduced by this amount. This means that the energy absorbed by the backfill is not as important as previously thought. Rather, the effect of backfill on the change in potential energy is the critical parameter. This in turn reduces the energy released, W_r, and the seismic energy, W_k. However the backfill efficiency (W_s/W_k) in this model is 26%, the same as in the algebraic model.

Since the backfill is affecting the stress on the face, as well as the convergence, it will also have some effect on local mine stiffness. This is defined as the stress on the element just to be mined, divided by the net convergence as the result of mining it. Figure 6.13d) shows the local mine stiffness for both the backfill and open stope cases. After the 13th cut the backfill had increased local mine stiffness by 7%.

The displacement discontinuity model was used to conduct a sensitivity analysis, whereby each of the important parameters are varied in turn and its effect on the energy components determined. The results are summarized in Table 6.1, using as a base case the undercut-and-fill mining method at the 13th cut with a backfill stiffness of 3 GPa.

Doubling the stope width reduces the energy absorbed by the backfill (W_s) by 47%, but also reduces the seismic energy (W_k) by 23%.

Halving the modulus of the wall rocks increases W_s by 145% and W_k by 76%.

Halving the ore modulus has little effect on the backfill energy but decreases W_k by 23%.

Doubling the depth increases all energy components by almost 300%, but does not change their relative size with respect to each other.

Table 6.1 - Sensitivity of energy components to model parameters

Parameter	Potential Energy W_t	Stored Strain Energy U_m	Energy Absorbed by Backfill W_s	Released Energy W_r	Seismic Energy W_k
Double Stope Width, 3 to 6 m	+2%	+73%	-47%	+2%	-23%
Half Modulus Wall Rocks, 70 to 35 GPa	+55%	-3%	+145%	+55%	+76%
Half Ore Modulus, 70 to 35 GPa	+2%	+73%	+5%	+2%	-23%
Double Depth 1000 to 2000 m	+291%	+291%	+291%	+291%	+291%
Double Fill Modulus, 3 to 6 GPa	-21%	-11%	+27%	-21%	-25%

Doubling the fill modulus reduces the change in potential energy ($3W_t$) by 21%, increases the backfill energy (W_s) by 27% and reduces the seismic energy (W_k) by 25%.

Based on this analysis the following conclusions can be drawn regarding the possibility of rockburst occurrences:

- Of the three mining methods analyzed, undercut-and-fill with tight fill is the least rockburst prone, and overhand cut-and-fill with uppers is the most rockburst prone.

- Narrow stopes are more burst prone than wide stopes.

- Stopes where the orebody has a higher modulus than the wall rocks are more prone to bursting than the reverse.

- The likelihood of bursting increases dramatically with depth.

- Backfill can reduce the seismic energy liberated, and hence rockbursts, if it is installed early and has a high in-place stiffness.

Some of these observations are self-evident (i.e., incidents of rockbursts increase with depth) whereas others (i.e., stoping width and relative modulus of ore and wall rocks) are less obvious and need to be confirmed by experience.

6.5.2 Stiff Backfill Design*

Given that a requirement exists for the placement of a 'stiff' fill and that this requirement is able to specify the deformation characteristics of the fill, the question arises, how to achieve such a fill, practically, technically and economically? Clearly, adding cement to an aggregate unconditionally is unlikely to provide the correct or the acceptable answer.

---

*Prepared by G. Swan, Falconbridge Ltd.

With respect to a fill's in situ properties, placement technique alone may defeat the design objective. Some of the most important steps which should be observed in order to achieve an optimum in situ quality solution are now discussed.

Prior to a consideration of cement content and placement technique, the nature of the fill aggregate should be expressed in general terms. For a fill deformation modulus requirement much in excess of 1 GPa, it can be shown empirically that the aggregate size should constitute rockfill and not mine tailings, as illustrated in Figure 6.14. Where the rockfill is derived from underground drill/blast development waste, including Alimak raise muck, a maximum particle size of 150 mm with a Uniformity Coefficient of 20 to 30 is common. Bored raise cuttings exhibit a smaller maximum particle size (about 10 mm) and a much higher Uniformity Coefficient, which increases the surface area for cement coating. For this reason, it is not to be recommended as a cemented rockfill aggregate. This has been demonstrated in work conducted by Lac Minerals/Hemlo Mine, where a fines content (arbitrarily defined as -6 mm size particles) greater than 25% by weight of the total aggregate adversely affected the uniaxial compressive strength for a 5% cement content mix, Quesnel (1988). This raises the question of a theoretical optimum grading to maximize strength and stiffness.

For a given aggregate material, cemented or otherwise, it is possible to demonstrate by experiment that a grading or particle size distribution can be found which maximizes bulk density or minimizes void ratio. Strong laboratory evidence now exists which shows that minimizing the void ratio will tend to maximize the material stiffness in a confined or unconfined state (Uhle and van Zyl, 1990; Swan, 1991). This conclusion is based upon the existence of an empirical relationship between tangent modulus and void ratio for a wide variety of fill materials as shown in Figure 6.15. While theoretical criteria exist which specify a void-minimizing grading (e.g., a Uniformity Coefficient of 5, Nicholson and Wayment, 1964), none are yet sufficiently general to include the effects of particle shape and angularity. As a consequence it is generally still not possible to 'engineer' an optimum material without some experimentation. The simplest of these would involve trial placements with varying fines content of uncemented aggregate in a fixed volume. This raises

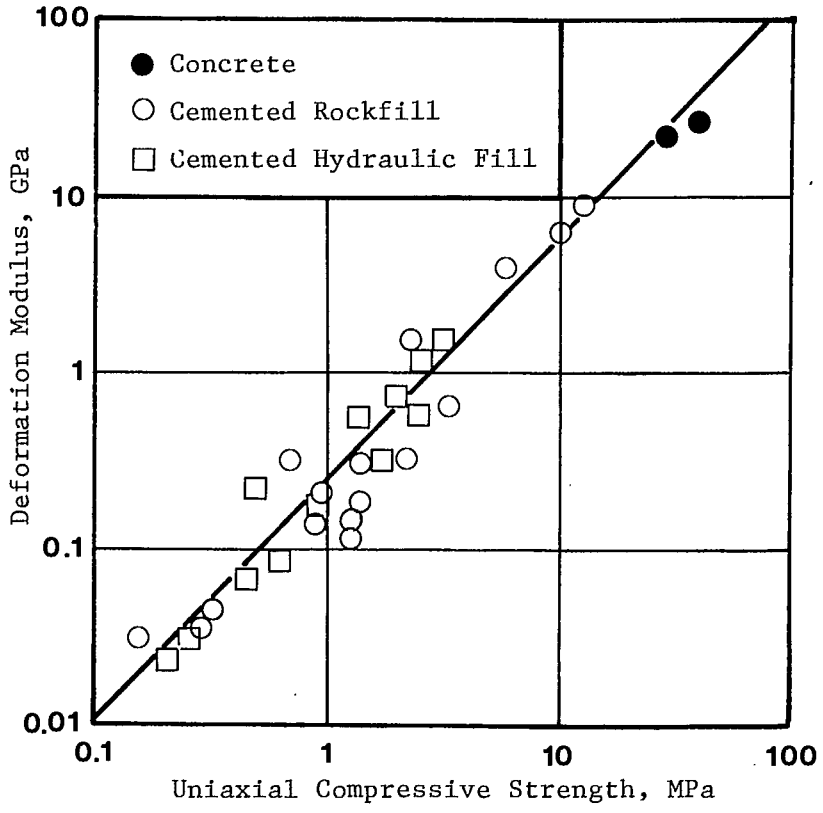

Fig. 6.14 - Compressive strength of various backfills versus deformation modulus.

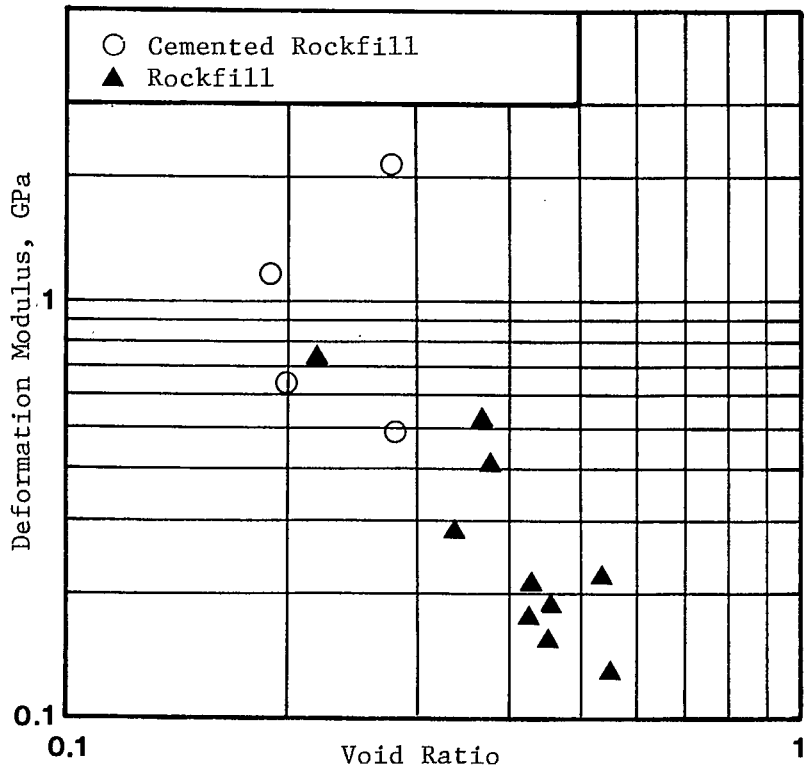

Fig. 6.15 - Modulus as a function of void ratio for a 2.5 MPa confining pressure (after Swan, 1991).

the issue of placement technique.

Methods of placing cemented rockfill in the underground environment vary depending on the mining method and equipment available. In narrow vein mining where a 'stiff' fill makes the most sense, conventional bulk truck hauling and dumping of the cemented fill material is impractical. With the object of achieving a reasonable degree of compaction and tightness to the back and walls of the excavation, the ideal fill handling system must be small and versatile. A trackless example of such a system is that used at Falconbridge's Deep Copper Mine in Sudbury, where grout tanks feed 1 and 2 cubic yard scooptrams carrying development waste to place in the order of 1000 tons/day cemented rockfill in 3 to 4 m wide stopes. The compaction and tight fill requirement is achieved in part using special 4 m long booms with swivel-action 1.4 m wide blades mounted on converted 2 cubic yard scooptrams. In this example, an in-transit mixing of cement slurry with rockfill has been found to provide significantly stiffer in situ properties than a flood and percolation method (Hopkins, 1988), presumably because of the compaction achieved by the placement technique.

The requirement for cement or fly ash addition to achieve a given rockfill stiffness may or may not be necessary when pillar recovery is not contemplated (i.e., excluding the case of undercut-and-fill or a blasthole pillar sequence). Fill design for the most part is based on uniaxial laboratory test data and this is likely a far too conservative indicator of stiffness for a confined stope placement. Unfortunately, only very limited triaxial data are available for cemented rockfills (Gonano et al. 1978), and until recently no assessment of triaxial data from civil work with rockfills had been made (Swan, 1991). While the results clearly demonstrate a disproportionate increase in strength and stiffness with increasing confinement, no data exist for confining pressures in excess of 5 MPa. In narrow vein mining, convergence-driven stresses have been shown to develop values well in excess of 5 MPa according to in situ measurement (Gurtunca et al. 1989), and numerical models (Swan et al. 1989). At the present time, the best available data relate void ratio to tangent modulus for a confining stress of 2.5 MPa on cemented and uncemented laboratory rockfill cylinders, as shown in Figure 6.15. At present, these data fail to demonstrate the value of cement in a

confined rockfill.

6.5.3 Use of Backfill to Control Violent Pillar Failure

The conventional role of backfill in alleviating rockbursts is that the fill should be as stiff as possible and placed as early as possible. In this way load is transferred to the fill and it can significantly affect the energy balance, as described in Section 6.5.1. In other words, it acts as a substitute pillar.

This concept of the support role of backfill has mitigated against its use in flat-lying, room-and-pillar mines, such as those at Elliot Lake because:

- stope closure is small and is mainly controlled by the elastic deformation of the pillars; and

- backfill can only be introduced at the end of the mining cycle after most of the closure has occurred.

The first indication that backfill could have another role in altering the post-failure behaviour of pillars was obtained by Blight and Clarke (1983) in South Africa. They conducted laboratory tests on quartzite samples confined with different types of fill. A soft backfill (i.e., cemented tailings) had no effect on the peak strength of the rock sample, but resulted in a high residual strength after failure. A stiff backfill (i.e., cemented rockfill), on the other hand, increased the strength of the rock sample as well as producing a progressively higher residual strength.

Swan and Board (1989) repeated these tests using quartzite samples and the type of cemented tailings available at Denison Mine in Elliot Lake. The testing set-up is shown in Figure 6.16, and the stress-closure curves are shown in Figure 6.17. Two types of tests were conducted: tight fill where both the rock and fill were loaded, and the rock protruding above the sill so that only the rock was loaded. The rock samples were 44 mm in diameter and 88 mm high.

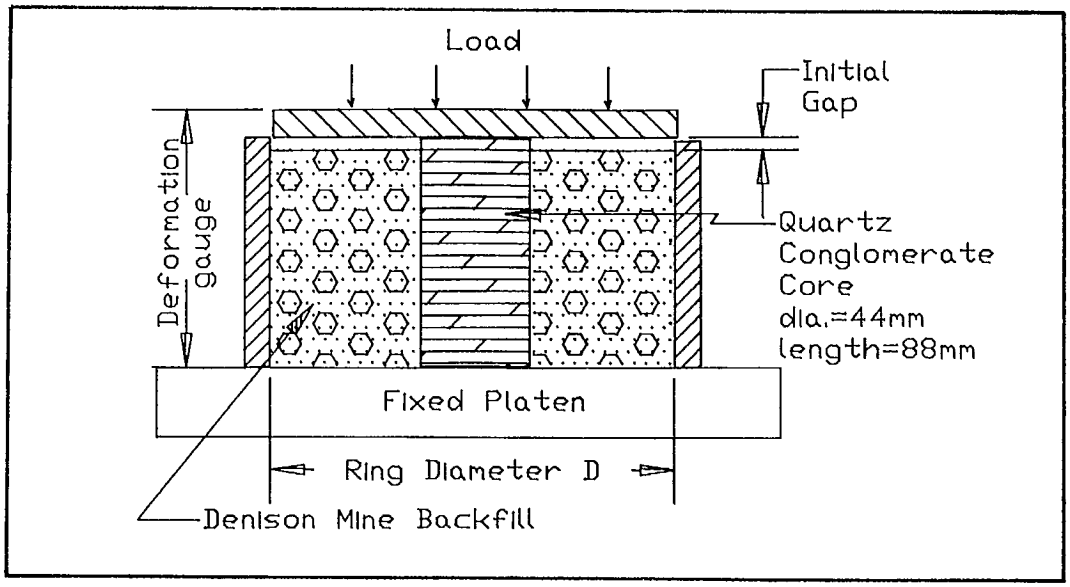

Fig. 6.16 - Laboratory set-up of rock/backfill tests.

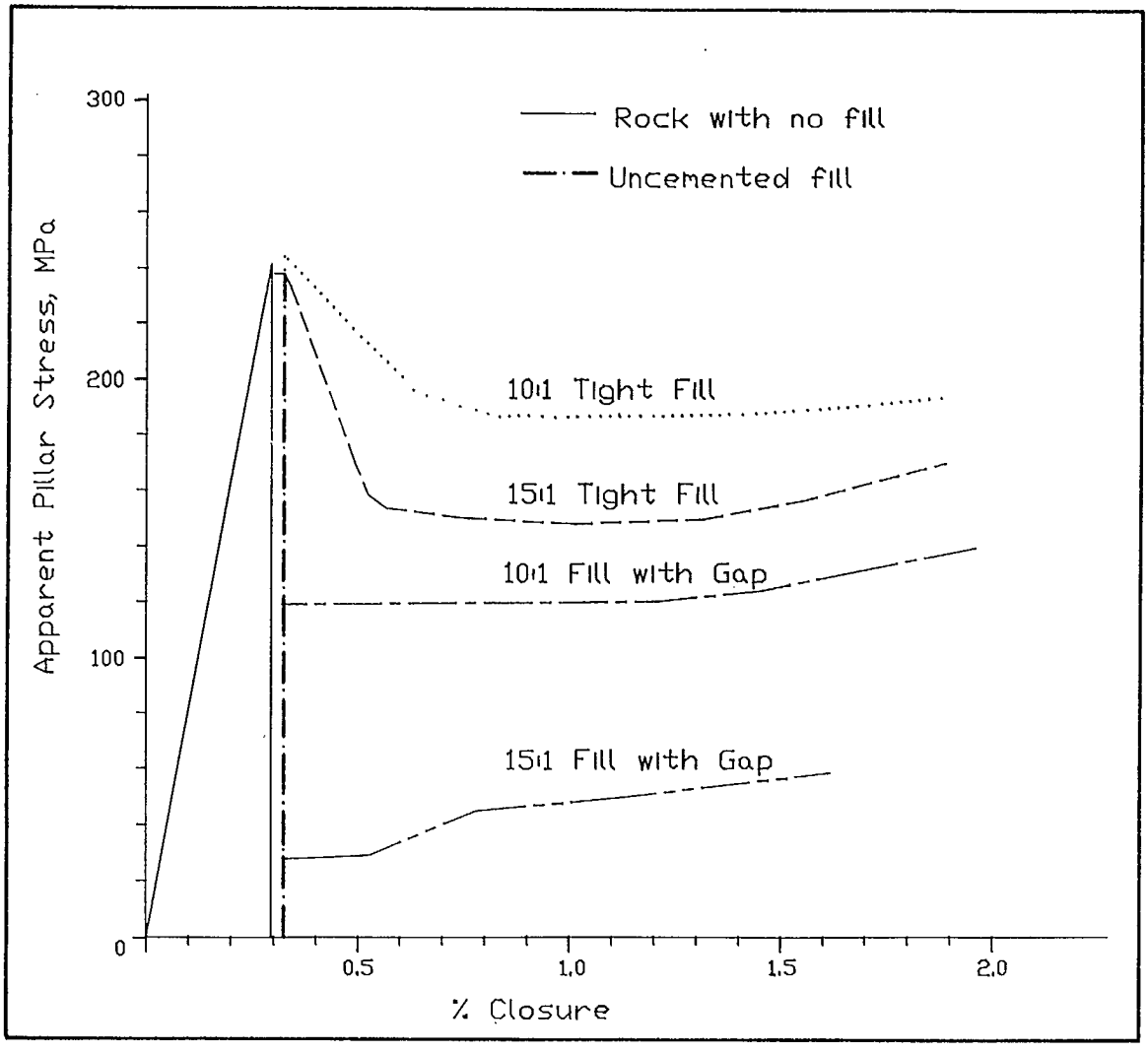

Fig. 6.17 - Stress-closure characteristics of rock surrounded by different types of backfill.

The graphs in Figure 6.17 show that the rock by itself failed violently, with an instantaneous reduction in stress from peak strength to zero. When the rock was surrounded by uncemented tailings the same violent failure was observed. Rock samples surrounded by 15:1 and 10:1 cemented tailings, with the rock protruding above the fill, still had an instantaneous reduction in stress from peak strength, but the stress stabilized at residual strengths of 6% and 50% of peak strength. The stress then increased slightly with increasing closure. Rock samples surrounded by 15:1 and 10:1 tight cemented fill showed a different type of post-failure behaviour. There was a gradual reduction in stress from peak strength which stabilized at 60% and 75%, respectively, of peak strength, and again increasing slightly with additional closure. In these two cases, failure occurred non-violently.

These tests confirmed the original conclusions of Blight and Clark (1983) that a cemented tailings backfill has no effect on the peak strength of the rock, but significantly increases its residual strength. However, this only applies to tight fill with high cement contents of 10:1 and 15:1. It was suspected that when scaling-up from small scale laboratory tests to underground conditions, the leaner cement mixes would produce similar results.

Subsequently, laboratory tests were repeated on quartzite from Denison Mine using larger samples, 133 mm diameter by 333 mm long, in a large 300 mm diameter cylinder (Arjang, 1991). Also, leaner cement mixes were used. The results are plotted in Figure 6.18 in the form of residual strengths as a function of cement contents. The 10:1 fill had an average residual strength of 71% of peak strength, similar to the previous tests. Leaner mixes of 20:1, 30:1, 40:1 and 50:1, and straight tailings had residual strengths, but they were progressively lower with decreasing cement contents. Samples surrounded with straight tailings and 50:1 fill still failed violently, and the 40:1 fill semi-violently. Otherwise the richer mixes of 30:1, 20:1 and 10:1 all failed non-violently. Also there was a slight indication that the samples surrounded by 10:1 fill had a higher peak strength than the other samples.

Fry and Hustrulid (1990) conducted tests on a weak limestone (i.e., uniaxial strength 60 MPa compared to over 200 MPa for quartzite), surrounded by loose sand. They found that the sand confined sample had a higher strength of about

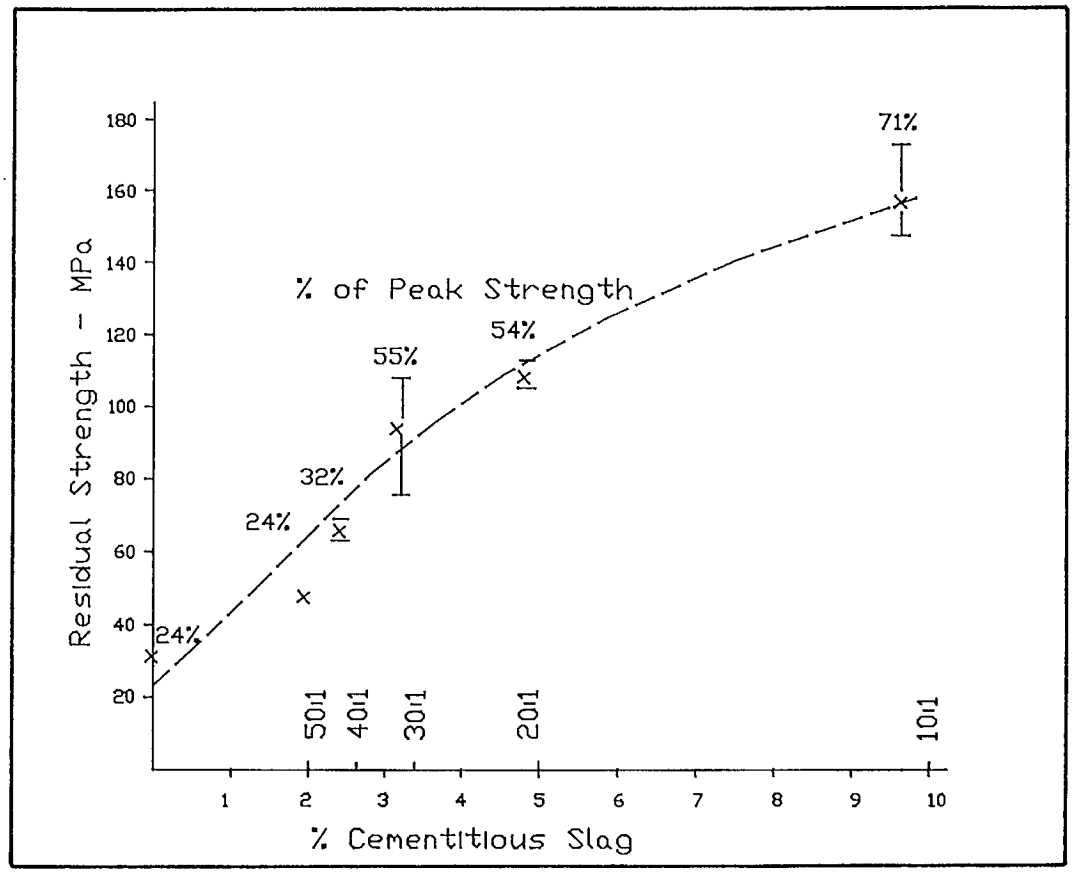

Fig. 6.18 - Variation of residual strength with cement content (after Arjang, 1991).

30% and failed non-violently with very little decrease in strength. Then the load bearing capacity continued to increase with additional closure. Also, after failure, significant lateral pressures were developed in the fill and there was a shift of stress to the centre of the rock sample.

These four sets of laboratory tests suggest that for weak rocks or weak pillars a fill with little or no cement is required. For strong rocks or strong pillars a stiffer backfill with higher cement content is required.

In the mid-1980s pillar deterioration began to occur at Denison Mine, in the boundary pillar area with Rio Algom's Quirke Mine and directly down dip from the main rockburst zone in Quirke Mine. To improve regional stability on Denison's side of the boundary pillar, backfilling was initiated in early 1985. Deslimed tailings and cementitious slag at a ratio of 30:1 at a pulp density of 55% were used to stabilize the pillars. Backfilling continued for six years to create a backfill corridor adjacent to the boundary pillar. A shared microseismic system had previously been installed to monitor seismic activity in the boundary pillar area (Pritchard et al., 1991).

In some cases the introduction of backfill coincided with an increase in microseismic activity. It is thought that the water in the backfill penetrated small fractures at the edge of the pillar, reducing friction and cohesion on these fractures. However, once the pillars were encased in backfill, seismic activity essentially ceased. This is illustrated by two examples shown in Figures 6.19 and 6.20. In May 1986 about 60 seismic events, up to a magnitude of 2.2 Mn, occurred in the 33 and 35 panels at Denison Mine. All of these events were located in pillars where the stopes had not been backfilled, whereas there was no seismic activity in the adjacent backfilled areas. The location of seismic events during 1989 is shown in Figure 6.20. Again the majority of events occurred at the edge of the backfilled area in pillars not surrounded by backfill. An exception is where pillars were being recovered between backfilled stopes. Since backfilling was initiated no seismic event of magnitude over 1.0 Mn has occurred in any pillar surrounded by backfill, whereas rockbursts up to a magnitude of 2.8 Mn have occurred in adjacent pillars which were not surrounded by backfill.

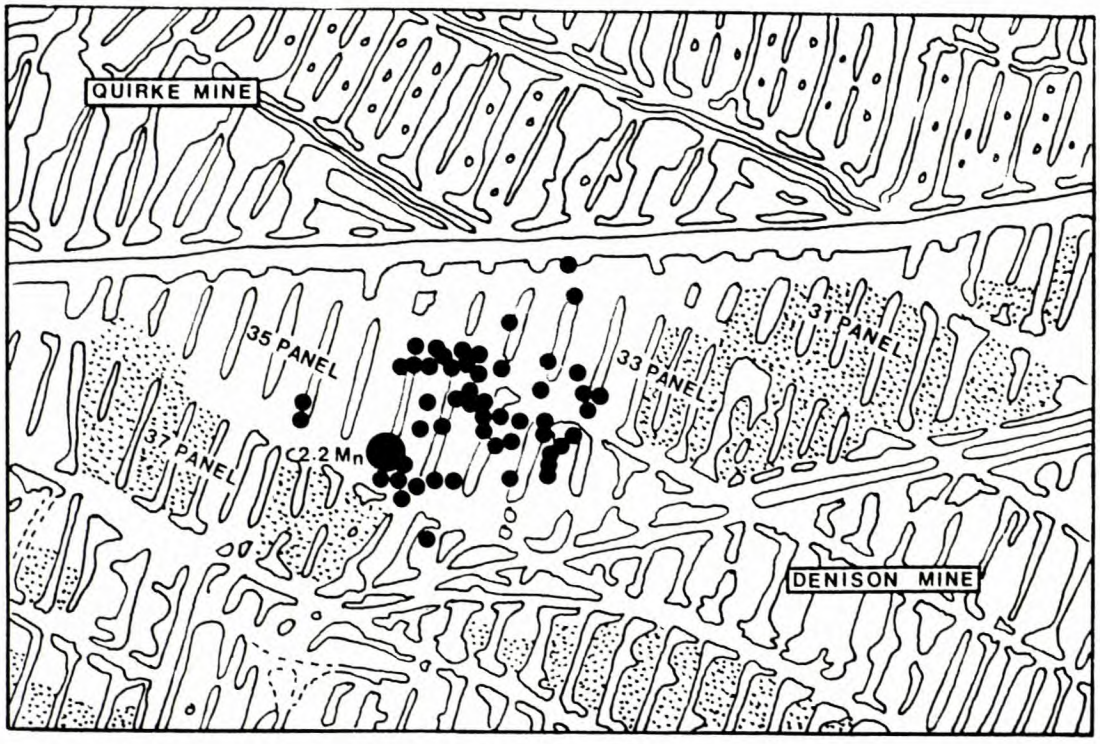

Fig. 6.19 - Location of seismic activity at Denison Mine during May 1987.

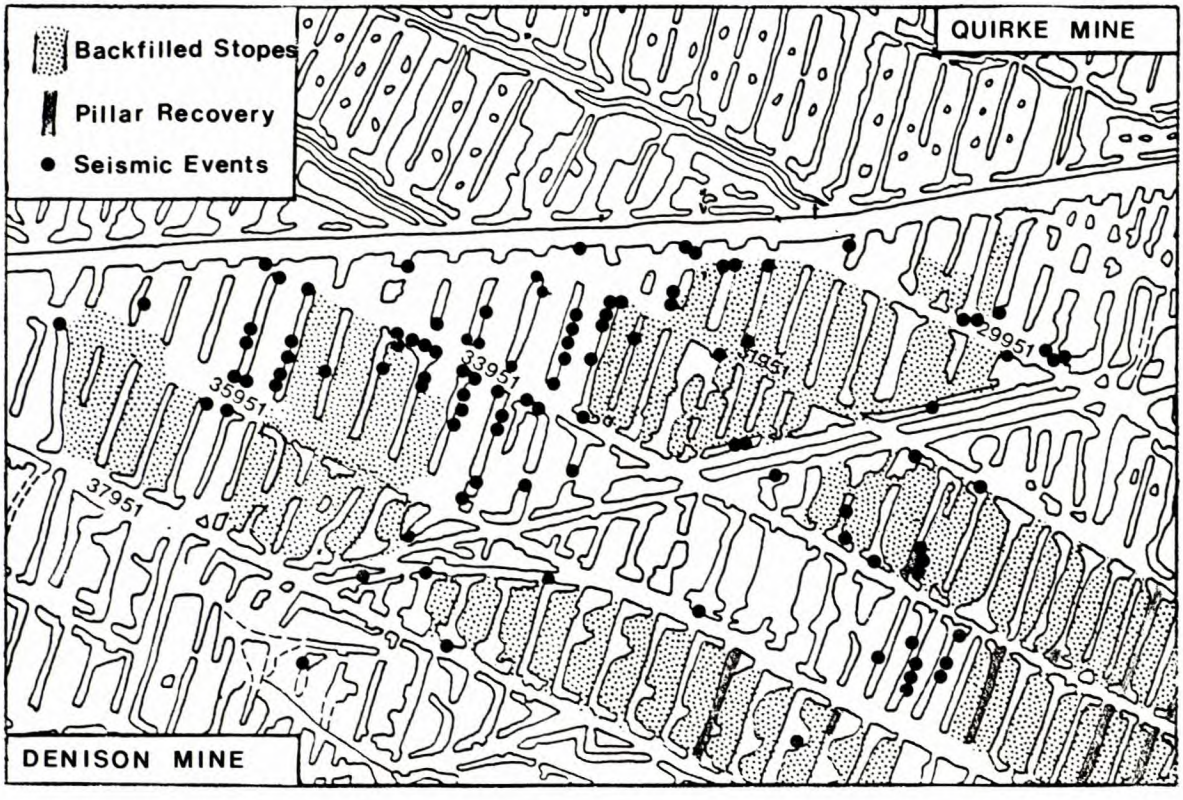

Fig. 6.20 - Location of seismic activity at Denison Mine during 1989.

It appears from the laboratory and underground observations that cemented backfill can control the release of seismic energy. This, in a conceptual way, is shown in Figure 6.21. Upon failure, a pillar by itself will have an instantaneous reduction in stress from peak strength to zero, represented by line AB in Figure 6.21. Upon failure, a pillar surrounded by cemented backfill will have a gradual reduction in stress and stabilize at a residual strength (taken as 50% of peak strength in the example), represented by line AD. Because of the pillar failure, the hanging wall and footwall will converge along the local mine stiffness curve, represented by line AC. Equilibrium is achieved at point D for the pillar surrounded by backfill, and at point C for the pillar by itself. The area under the local mine stiffness curve represents the seismic energy liberated. In the example shown, the pillar surrounded by backfill has only 8% of the seismic energy released compared to a pillar by itself. This would explain the almost complete elimination of seismic activity observed in pillars surrounded by backfill underground.

Since relatively weak backfill can control violent pillar failure in room-and-pillar mines, it should also apply to other mining methods where pillars are encased in backfill, such as post pillars and rib pillars in transverse cut-and-fill mining. As a general observation, rockbursts can occur in post and rib pillars on the first and second cuts when backfill has not yet been introduced. Pillar failure on subsequent cuts tends to be non-violent (Oliver et al., 1987). Morrison and Galbraith (1990) reported on a series of major rockbursts in transverse pillars. But in this case, backfilling had fallen behind and the adjacent stopes were only partially filled.

6.6 References

Arjang, B. (1991), Preliminary results of pillar-backfill confinement tests. Division Report MRL 91-063(TR), CANMET, Energy, Mines and Resources Canada.

Biskup, E. and Kaiser, P.K. (1990), Fault property determination at two Inco Mines. Geomechanics Research Centre, Laurentian University, Sudbury, Ontario.

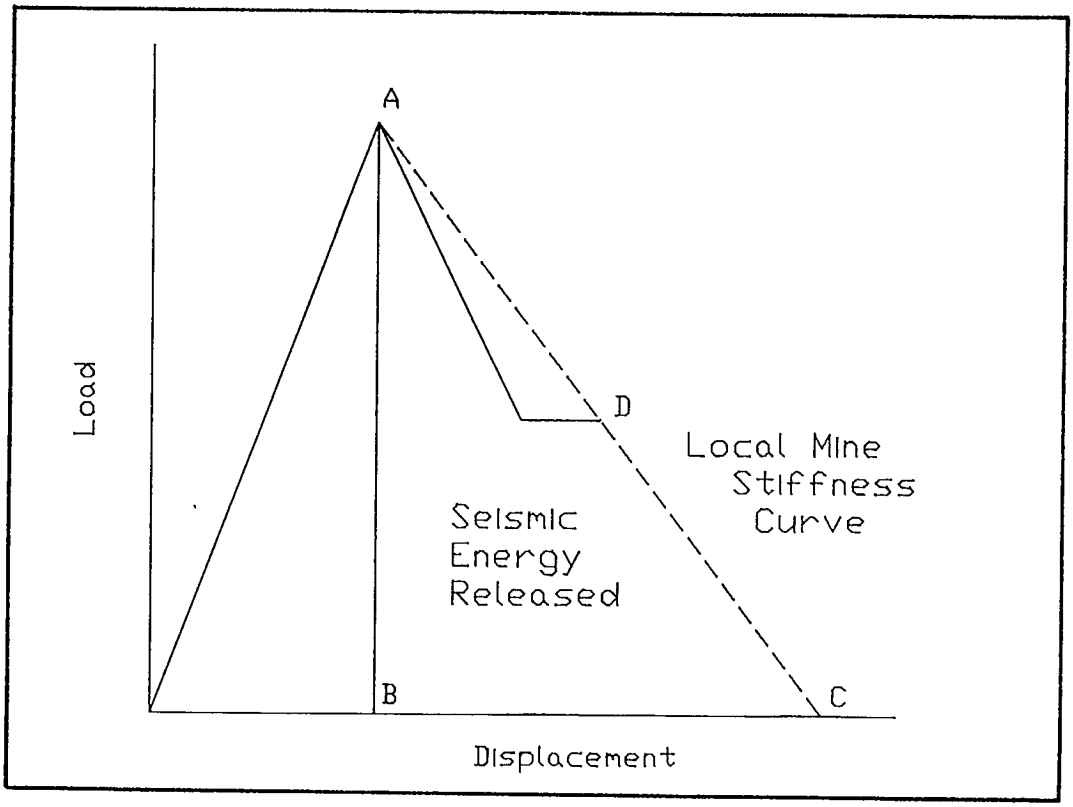

Fig. 6.21 - Concept of the reduction in seismic energy released when a pillar is surrounded by cemented backfill.

Blight, G.E. and Clarke, I.E. (1983), Design and properties of stiff fill for lateral support of pillars. Proc. Int. Symp. on Mining with Backfill, Lulea, Sweden, pp. 303-307.

Brummer, R.K. (1991), Algebraic modelling of energy balances in backfill/rock interaction. Golder Associates Report, Canadian Rockburst Research Program.

Brummer, R.K. and Rorke, A.J. (1988), Case studies on large rockbursts in South African gold mines. Proc. 2nd Int. Symp. Rockbursts and Seismicity in Mines, Minneapolis, 1990, Balkema, Rotterdam.

Dickout, M.H. (1962), Ground control at the Creighton Mine of the International Nickel Company of Canada Limited. Proc. 1st Can. Rock Mech. Symp., McGill University, Montreal, pp. 121-139.

Fry, M.F. and Hustrulid, W.A. (1990), Split platen results with application to backfill at great depths. Proc. Int. Deep Mining Conf., Technical Challenges in Deep Level Mining, Johannesburgh, S. African Inst. Min. Metall, pp. 1305-1314.

Gonano, L.P., Kirkby, R.W. and Dight, P.M. (1978), Triaxial testing of cemented rockfill. Tech. Report 72, SCIRO, Australia.

Gurtanca, R.G., Jager, A.J., Adams, D.J. and Gonlag, M.D. (1989), The in situ behaviour of backfill materials and the surrounding rockmass in South African gold mines. Proc. 4th Int. Symp. Mining with Backfill, Montreal.

Hedley, D.G.F. (1984), Utilization of backfill support in longitudinal cut-and-fill mining. Division Report MRL 84-76(TR), CANMET, Energy, Mines and Resources Canada.

Hodgson, K. and Joughin, N.C. (1967), The relationship between energy release rate, damage and seismicity in deep mines. Proc. 8th U.S. Rock Mech. Symp., Minnesota,, pp. 194-209.

Holmes, R.D. and Reeson, J.A. (1988), Excess shear stress (ESS) - a case study. Proc. 2nd Int. Symp Rockbursts and Seismicity in Mines, Minneapolis, 1990, Balkema, Rotterdam.

Hopkins, P. (1988), Strathcona deep copper zone consolidated rockfill option - background data. Internal Report, Falconbridge Ltd.

Jaeger, J.C. and Cook, N.G.W. (1976), Fundamentals of rock mechanics. 2nd edition, Methuen, London.

Morrison, D.M. and Galbraith, J.E. (1990), A case history of Inco's Copper Cliff North Mine. Proc. 31st U.S. Rock Mech. Symp., Golden, Colorado.

Morrison, R.G.K. (1942), Report on the rockburst situation in Ontario mines. Trans. C.I.M., vol. 45, pp. 225-272.

Nicholson, D.E. and Wayment, W.R. (1964), Properties of hydraulic backfills and preliminary vibratory compaction tests. Report of Investigations RI 6477, United States Bureau of Mines.

Oliver, P., Wiles, T., MacDonald, P. and O'Donnell, D. (1987), Rockburst control measures at Inco's Creighton Mine. Proc. 6th Conf. on Ground Control in Mining, West Virginia.

Pritchard, C., Townsend, P. and Hedley, D.G.F. (1991), Use of backfill to control violent pillar failure at Denison Mine.

Quesnel, W. (1988), Optimum grading for Hemlo Mine CRF. Internal Report, Lac Minerals.

Robson, W.T. (1946), Rock-burst incidence, research and control measures. Trans. C.I.M., vol. 49, pp. 347-374.

Robson, W.T., Adamson, J.C. and Selnes, W.E. (1940), Rock-bursts at Lake Shore Mines. Trans. C.I.M., vol. 43, pp. 7-30.

Robson, W.T., Selnes, W.E. and Seymour, M.E. (1957), Rockburst control measures at Lake Shore Mines Limited. Proc. 6th Commonwealth Min. & Met. Congr., Ottawa, Canada, pp. 376-384.

Ryder, J.A. (1986), Excess shear stress (ESS) assessment of geologically hazardous situations. In: Mining in the Vicinity of Geological and Hazardous Structures. S. African Inst. Min. Metall, Transvaal, S. Africa.

Ryder, J.A. (1987), Excess shear stress (ESS): an engineering criterion for assessing unstable slip and associated rockburst hazards. Proc. 6th ISRM Rock Mech. Congr., Montreal, pp. 209-218.

Scholz, C.H. (1991), Earthquakes and faulting: self-organized critical phenomena with a characteristic dimension. Proc. NATO ASI Spontaneous Formation of Space-Time Structures and Criticality. T. Riste (Ed.), Kluwer Acad. Publ.

Swan, G. (1991), On cemented vs. uncemented rockfill in overhand CAF mining. Internal Report, Falconbridge Ltd.

Swan, G. and Board, M. (1989), Fill-induced post-peak pillar stability. Proc. 4th Int. Symp. Innovations in Backfill Technology, Montreal.

Swan, G., Steed, C., Espley, S.J., O'Hearn, B. and Allan, G.R. (1989), Strathcona deep copper zone: geomechanics investigation. Internal Report, Falconbridge Ltd.

Uhle, R.J. and van Zyl, D. (1990), Shear strength and deformation parameters of rockfill related to particle size. Proc. 31st U.S. Rock Mech. Symp., Colorado.

7. CONTROL OF ROCKBURST DAMAGE

Lacing used in rockburst-prone areas at Strathcona Mine.

Damage to wooden posts and beams at Macassa Mine.

7. CONTROL OF ROCKBURST DAMAGE

7.1 Introduction

In some cases, it is impossible to prevent rockbursts from occurring, either because of very high stress conditions or past mining practices that may have created a layout which is rockburst prone. In these instances, to protect the labour force, it is necessary to install a support system capable of withstanding and controlling the damage from rockbursts.

Experimentation with different types of support systems was initiated in Ontario mines in the 1930s. Concrete lining and conventional timber posts and beams, being used at that time, were ineffective in controlling rockburst damage. The first concept was to install stronger and more rigid systems, especially with the introduction of mechanical bolts and rebar. These support systems were successful in controlling damage from the smaller magnitude rockbursts, but were ineffective against larger events. It was realized that the rigidity of the support was contributing to the problem. This led to the introduction of supports with yielding characteristics, for instance, the friction type supports. The importance of steel mesh, in conjunction with friction supports, was also realized.

The rockburst problem is much more severe in South African gold mines than in Ontario mines. By necessity, support systems capable of withstanding rockbursts had to be found. This led to the development of rapid-yielding hydraulic props for stope support which could accommodate closure of up to 2 m/s. These types of support are specific to South African gold mines (i.e., 1 m high stopes) and do not have general application to Ontario mines.

In haulage drifts a lacing support system was developed. This consists of grouted rebars in boreholes, wire mesh, and tensioned steel cables between rebars in a diamond configuration. This type of support has been very effective and has survived rockbursts of magnitude 4.0 only a few tens of metres away. This type of support system has general application in Ontario mines, and the first lacing installation was done at Falconbridge's Strathcona Mine (Davidge, et al. 1988).

The development of these support techniques has been done in an intuitive manner with trial-and-error testing to fit specific applications. It was only in the early 1980s that Wagner, in South Africa, developed the theoretical basis for designing support systems to withstand rockbursts.

Between 1984 and 1990, there were 391 recorded seismic events of magnitude 2.0 or greater in Ontario mines. The distribution by magnitude is shown in Figure 7.1. As expected there were many more small events than large events. The distribution can be split into three broad groups. Magnitudes between 2.0 and 2.4 accounted for 65% of the total, and the damage associated with these events was usually minor, involving a few tonnes of displaced rock. However, there were exceptions; two rockbursts of magnitude 2.0 produced over 800 tonnes of displaced rock in an isolated drift at the Strathcona Mine. Events of magnitude 2.5 to 2.9 accounted for 30%, and more damage would be expected in the order of tens of tonnes. Events of magnitude over 3.0 only accounted for 5% of the total, but the damage was usually more severe, typically involving hundreds, up to thousands, of tonnes of displaced rock. Over the seven-year period these large events averaged three per year in Ontario mines.

From a support design point of view, for large events greater than 3.0, probably only lacing would survive if it occurred close to the mine workings. For smaller events there is probably a range of support techniques which could control the damage.

7.2 Peak Particle Velocity, Acceleration and Displacement

In both blasting and rockburst studies, peak particle velocity, and to a lesser extent acceleration and displacement, are the main criteria for assessing damage to support systems and underground structures.

As mentioned in Section 5.2, there are two types of waves associated with rockbursts. P, or compressional waves, are radial vibrations in the same direction as the wave front, and travel at a velocity of about 6.2 km/s in hardrock mines. S, or shear waves, are transverse vibrations perpendicular to the wave front and have a velocity of about 3.6 km/s.

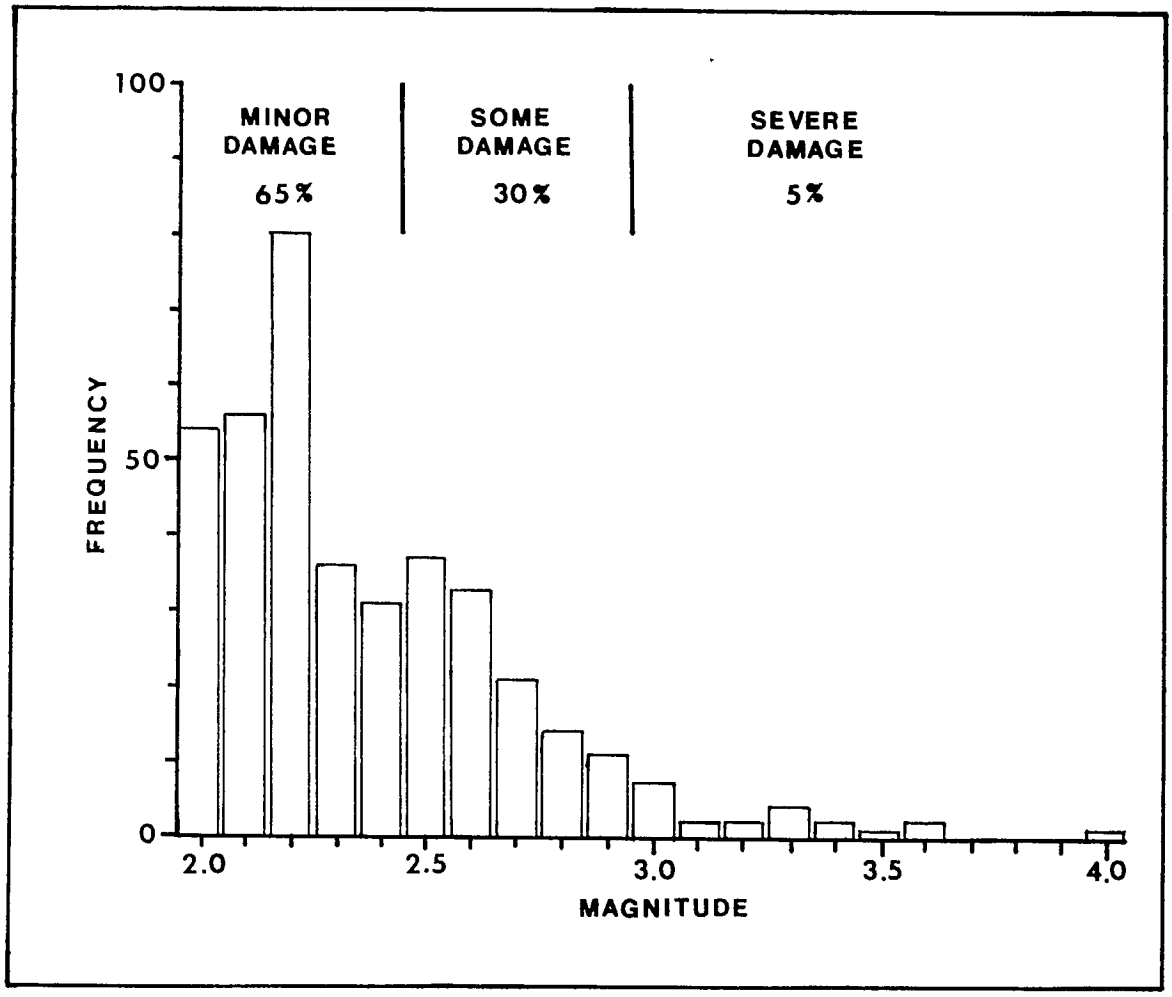

Fig. 7.1 - Distribution of seismic events in Ontario mines, 1984-1990.

Predominantly, the peak particle velocity of these vibrations is in the S-wave. From measurements taken on triaxial sensors at a number of Ontario mines, the maximum particle velocity in the P-wave is about 45% of the peak particle velocity in the S-wave.

Peak particle velocity, acceleration, and displacement are dependent on the magnitude of the rockburst and attenuate with distance from the source. In blasting studies a cube root scaling factor is generally used to take into account the distance from source, R, and the weight of explosive, W, in the form:

$$u = K\left(\frac{R}{W^{1/3}}\right)^n \qquad \text{Eq 7.1}$$

where, u = peak particle velocity, acceleration or displacement
n = attenuation or decay factor
K = constant.

The cube root scaling factor is used so that the ratio of distance to the volume of explosive (i.e., equivalent to weight) is dimensionless. To use this type of relationship for rockbursts a substitute has to be found for the weight of explosive. The chemical energy contained in an explosive is proportional to its weight. Similarly, the magnitude of a rockburst is proportional to the logarithm of its seismic energy. Consequently, as a first approximation Equation 7.1 can be transformed to:

$$u = K\left(\frac{R}{10^{M/3}}\right)^n \qquad \text{Eq 7.2}$$

where, M = rockburst magnitude
and the term in the brackets is referred to as the scaled distance.

Figure 7.2 shows the relationship between peak particle velocity, acceleration and displacement with the scaled distance. These measurements were taken on triaxial sensors at a number of Ontario mines and a vector sum product was calculated. Accelerations and velocities were measured directly, whereas some velocities and displacements were obtained by integration of the acceleration

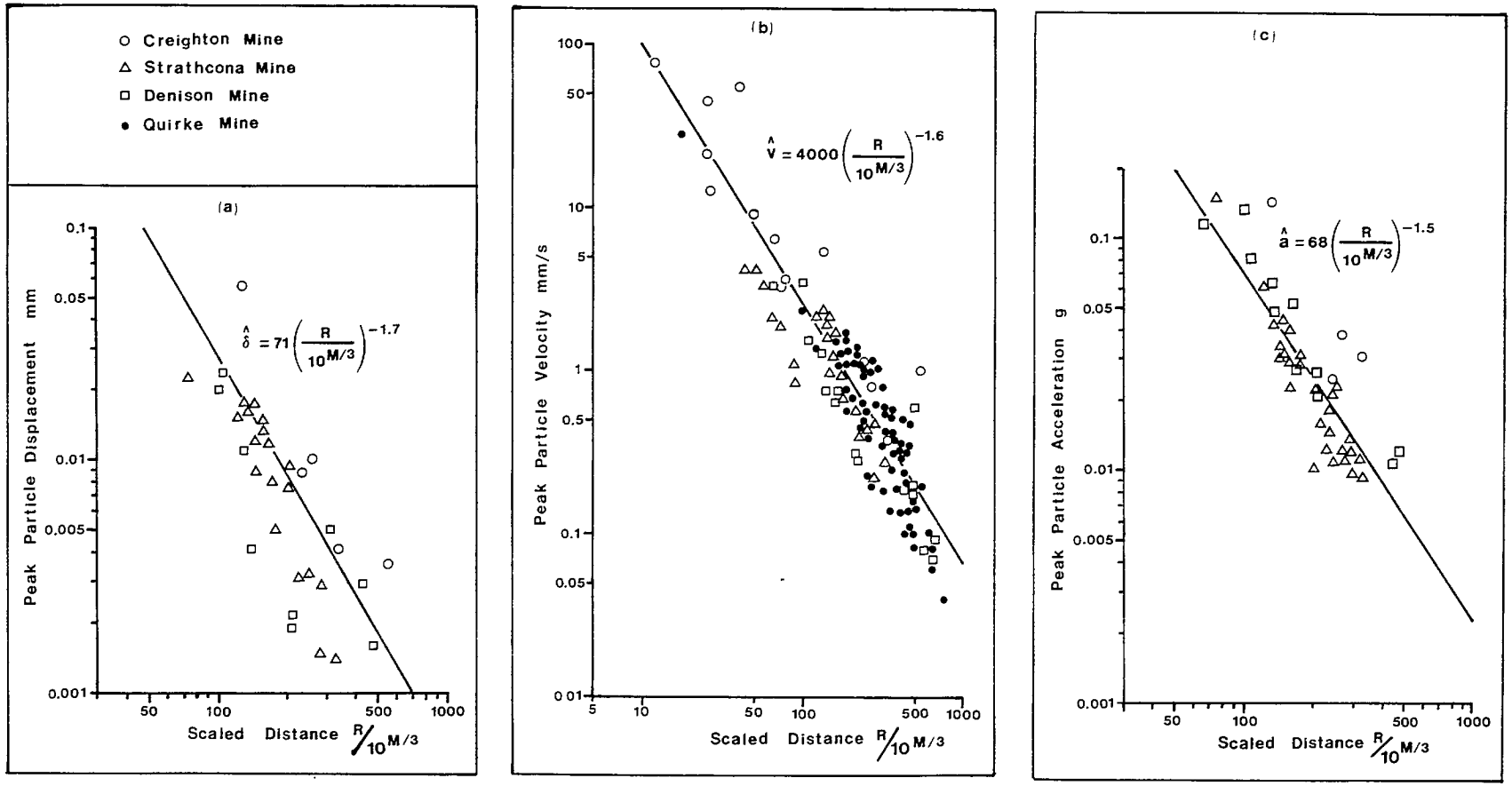

Fig. 7.2 - Peak particle displacement, velocity and acceleration as a function of scaled distance.

and velocity waveforms.

The average scaled distance attenuation relationships for displacement, velocity and acceleration can be expressed by:

$$\hat{\delta} = 71\left(\frac{R}{10^{M/3}}\right)^{-1.7} \qquad \text{Eq 7.3}$$

$$\hat{v} = 4000\left(\frac{R}{10^{M/3}}\right)^{-1.6} \qquad \text{Eq 7.4}$$

$$\hat{a} = 68\left(\frac{R}{10^{M/3}}\right)^{-1.5} \qquad \text{Eq 7.5}$$

where, $\hat{\delta}$ = peak particle displacement in mm

$\hat{v}$ = peak particle velocity in mm/s

$\hat{a}$ = peak particle acceleration in g (gravity)

R = distance from source in m

M = rockburst magnitude using the Nuttli scale.

The attenuation coefficients for displacement velocity and acceleration are very similar varying over a narrow range of 1.5 to 1.7.

A different type of equation is used in the South African gold mines to relate peak particle velocity, rockburst magnitude and distance (McGarr, 1981; Spottiswoode, 1984; and Gibbon, 1986).

$$\log (R\hat{v}) = 0.5\ M + 2.81 \qquad \text{Eq 7.6}$$

In this equation, $\hat{v}$ is expressed in mm/s and R in m. It can be rearranged into a blasting type format as follows:

$$\hat{v} = 645\left(\frac{R}{10^{M/2}}\right)^{-1} \qquad \text{Eq 7.7}$$

In this case the R^{-1} relationship represents purely geometrical spreading with no inelastic behaviour of the rock mass, and as such represents the far-field velocity.

If the vibrations can be approximated by sinusoidal waves, then displacement, velocity and acceleration are inter-related by the frequency, f, as follows:

$$\hat{v} = 2\pi f \hat{\delta} \qquad \text{Eq 7.8}$$

$$\hat{a} = 2\pi f \hat{v} \qquad \text{Eq 7.9}$$

These relationships are normally plotted on four-axis tripartite paper to produce a response spectra. Figure 7.3 shows the spectra of three rockbursts: a 2.7 magnitude event at a distance of 87 m, a 3.6 event at 2080 m, and a 2.6 event at 1800 m. The shapes of the spectra are similar being a truncated triangle, although the amplitudes vary according to magnitude and distance. Predominant frequencies are defined by the constant velocity section, and for these events, cover a range of 15 to 50 Hz. The intersection of the peak displacement and velocity lines, in these cases, is very close to the corner frequency determined from spectral density analysis. This intersection also represents the frequency at which the peak seismic energy is liberated.

7.3 Damage Criteria

Damage criteria, based on peak particle velocity, usually come from blasting investigations in tunnels. Lenhardt (1988) used blasting studies by Langefor and Kihlstrom (1963) to assess rockburst damage at the Western Deep Levels gold mine in South Africa. Blake and Cuvelier (1988) used similar criteria at Hecla's Lucky Friday Mine in the United States.

Falls of loose ground occurred at velocities as low as 50 mm/s. Fracturing of intact rock started at about 300 mm/s, and severe damage at 600 mm/s. These damage criteria are expressed in Figure 7.4 in terms of the magnitude-velocity-distance relationship given in Equation 7.4.

Damage reports from rockbursts at some Ontario mines can be used to check these criteria. At Inco's Creighton Mine a 3.6 Mn magnitude rockburst caused severe damage to a drift over a distance of 31 m, local falls of ground up to 57 m away, and falls of loose up to 100 m. Also at the Creighton Mine severe damage occurred 30 m away from a 2.9 Mn rockburst. At Falconbridge's

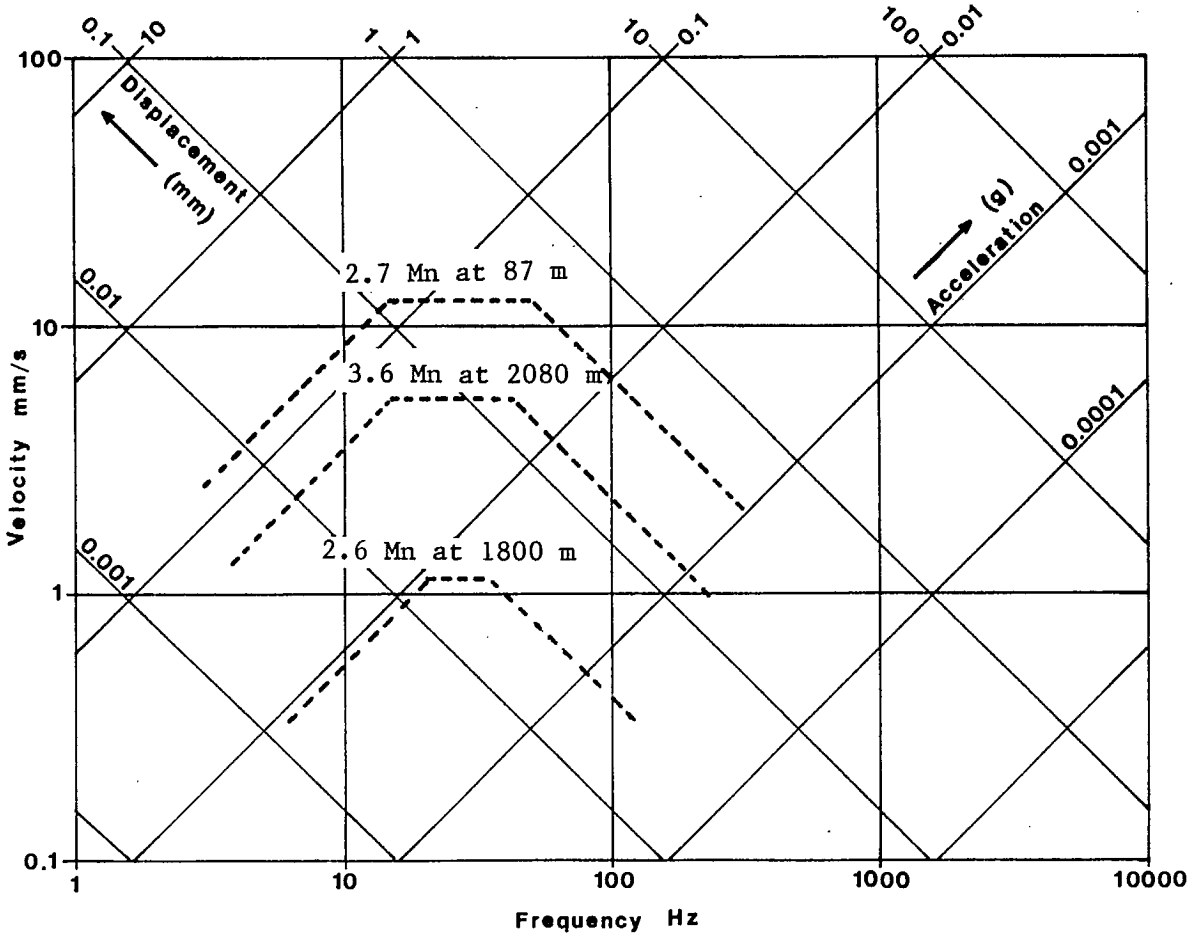

Fig. 7.3 - Response spectra of rockbursts of different magnitude and distance.

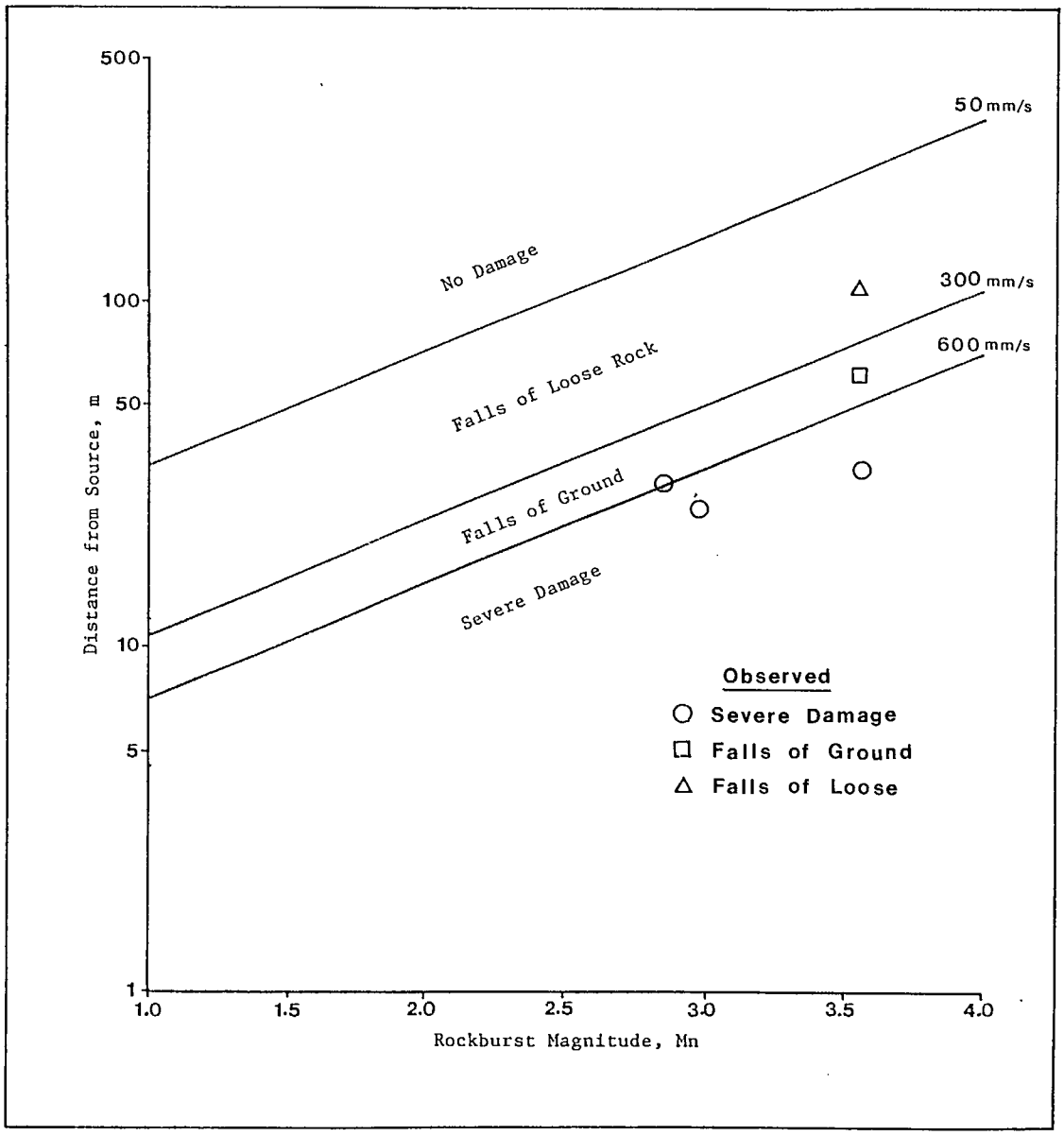

Fig. 7.4 - Damage criteria from blasting studies and some observed rockburst damage.

Strathcona Mine severe damage occurred 25 m from a 3.0 Mn rockburst.

These few instances are plotted in Figure 7.4 and are in good agreement with the damage criteria, at least for the larger magnitude events. However, the damage criteria for the low magnitude events are suspect, in that no damage has ever been observed for a 1.0 Mn event. The problem probably is caused by overestimating the peak particle velocity close to the source. The format of Equation 7.4 predicts infinite peak particle velocity at the source for any rockburst magnitude, whereas at the source the peak particle velocity should be finite and related to magnitude.

The damage criteria will also be affected by the type of support being used. For instance, rock supported by lacing techniques will be able to survive much higher peak particle velocities without severe damage, compared to rock supported by mechanical bolts.

7.4 Mechanics of Dynamic Loading

The first theoretical study on the design of support systems in rockburst-prone ground was done by Wagner (1984) in South Africa. Subsequently, Roberts and Brummer (1988) elaborated on these design concepts. Figure 7.5 shows a drift supported by rockbolts in the walls and roof. At depth, the high stresses produce a fractured zone around the drift, typically 1 m deep. Consider a slab, in the roof and side walls, of mass Mr detached from the surrounding rock and being held by the bolts. When a rockburst occurs the work done by the slab at peak particle velocity, $\hat{V}$, equals the energy consumed in stressing and stretching the bolts. This can be expressed by:

$$\frac{Mr\ \hat{V}2}{2} + Mr\ g\ c = 1/2 \int_o^c Fs(x)dx \qquad \text{Eq 7.10}$$

where, Fs = force exerted by the bolt
c = amount of bolt stretch
g = gravity.

For slabs in the roof, subject to gravitational forces, Equation 7.10 becomes:

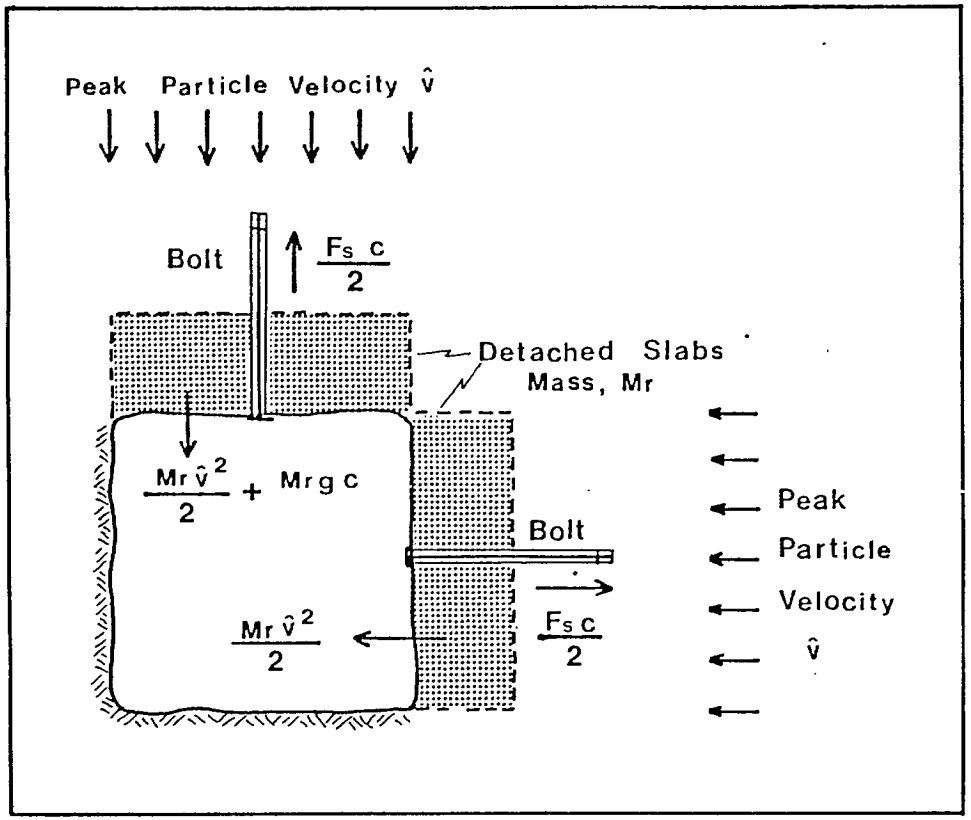

Fig. 7.5 - Forces imposed on rock slabs and the reaction of bolts during a rockburst.

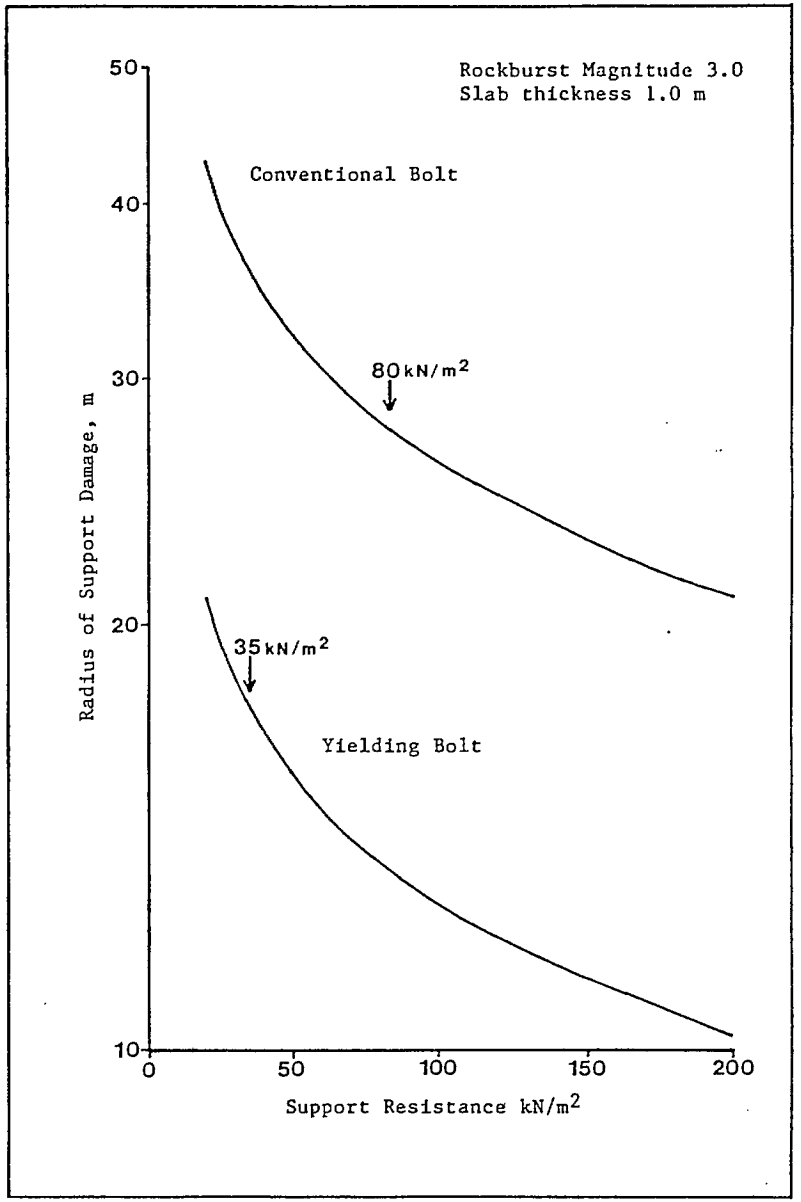

Fig. 7.6 - Radius of support damage as a function of support resistance for conventional and yielding bolts.

$$Mr = \frac{Fs\ C}{2\ (\frac{V^2}{2} + gc)} \qquad \text{Eq 7.11}$$

For slabs in the side walls, not affected by gravity:

$$Mr = \frac{Fs\ C}{\dot{v}^2} \qquad \text{Eq 7.12}$$

Equations 7.11 and 7.12 apply to support systems with a predominantly linear load-deformation characteristic (e.g., rockbolts). If the support has a constant yielding load, Fy (e.g., friction support) then:

$$Mr = \frac{2\ Fy\ C}{\dot{v}^2} \qquad \text{Eq 7.13}$$

The mass of the slab supported by the bolts can be expressed by:

$$Mr = \frac{\rho t}{A} \qquad \text{Eq 7.14}$$

where, ρ = rock density

A = support density in bolts/m^2

t = slab thickness.

These equations can be used to compare different types of support systems under rockburst conditions. Suppose a rock slab 1 m thick with a density of 2700 kg/m^3 is being pinned on the side of a drift. Assuming that conventional mechanical rockbolts have a failure load, under dynamic loading conditions of 120 kN, and a maximum elongation of 20 mm, whereas yielding friction type supports slip at a constant 50 kN over 100 mm. Rearranging Equations 7.12, 7.13 and 7.14 gives:

$$\dot{v} = \sqrt{\frac{Fs\ Ac}{\rho t}} \qquad \text{Eq 7.15}$$

for conventional bolts, and

$$\dot{v} = \sqrt{\frac{2Fy\ Ac}{\rho t}} \qquad \text{Eq. 7.16}$$

for yielding bolts.

The terms Fs A and Fy A are the support resistance expressed in kN/m^2. Substituting the relevant support characteristics into Equations 7.15 and 7.16

gives the maximum particle velocity the support system can withstand. Equation 7.4 can then be used to calculate the distance from the source over which the support system would be severely damaged for different rockburst magnitudes.

Figure 7.6 shows the radius of support damage as a function of support resistance for a rockburst magnitude of 3.0. The area under the curves represents the conditions where the support system will suffer damage. The radius of support damage is much less for the yielding bolts because of their ability to absorb more energy. Increasing the support resistance decreases the extent of the damage but with reduced effectiveness at higher resistance. Greater improvement is obtained by increasing the yielding characteristics even at a lower failure or slippage load.

In Ontario, bolts are usually installed at 1.2 m (4 ft) centres. For the above examples, this gives a support resistance of 35 kN/m^2 for the yielding bolts, and 80 kN/m^2 for the conventional bolts, as indicated by the arrows in Figure 7.6. Although the yielding bolts have less than half the resistance, their radius of damage is 18 m compared with 28 m for the conventional rockbolts.

Wagner (1984), and later Roberts and Brummer (1988), put forward a set of conditions that support systems have to satisfy under dynamic loading. Those relevant to Ontario hardrock mines are as follows:

- The support elements must be capable of yielding at 2 m/s and preferably 3 m/s.

- The support system must be capable of accommodating wall displacements of not less than 60 mm in drifts.

- The support resistance should not be less than 60 kN/m^2 in drifts.

- The ability of support systems to do work against the dynamic rock movement is as important as its load-bearing capacity.

- The support system must be able to maintain the integrity of the rock mass surrounding the excavation during the entire yield process.

As mentioned previously, one of the greatest uncertainties in support design is the peak particle velocity near the source. Kirsten and Stacey (1988) suggested using a value of 10 m/s to provide a safe design criterion. Brune (1970) calculated the particle velocity, at the source, for fault-slip type earthquakes, where:

$$V_{source} = \frac{\Delta\tau\ \beta}{G} \qquad \text{Eq 7.17}$$

where, $\Delta\tau$ = drop in shear stress along the fault
β = shear wave velocity $\simeq$ 3600 m/s
G = shear modulus $\simeq$ 30,000 MPa

Stress drops for earthquakes rarely exceed 10 MPa which give a particle velocity at source of 1.2 m/s. For pillar rockbursts, the perpendicular stress on the pillar typically 120 MPa, can be reduced to zero instantaneously. Assuming a shear stress of half this value produces a particle velocity at source of 7.2 m/s. It is not surprising that in Ontario mines the damage associated with pillar bursts is much more severe than fault-slip bursts of comparable magnitude.

7.5 Laboratory and Underground Tests

Slow and rapid loading tests on rockbolts have been done in both Canada (Hedley and Whitton, 1983), and South Africa (Hepworth and Heins, 1983). An underground trial using conventional and yielding rockbolts subject to dynamic loading from explosives has been described by Ortlepp (1969). At Placer Dome's Campbell Mine, measurements were made on how different supports responded to dynamic loading produced by explosive charges detonated at fixed distances from the support. Also similar to the Ortlepp trial, sections of a drift were reinforced with different types of supports, which were then subject to close-in explosive charges (Hedley et al., 1991).

7.5.1 Laboratory Testing

Some broken mechanical rockbolts from the rockburst area at Quirke Mine in Elliot Lake indicated only about half the stretch normally obtained in laboratory testing. It was thought that the rockbursts were subjecting the bolts to dynamic loading which resulted in a lower failure load with less stretch. Tests were done in the laboratory on 0.76 m long bolts, 15 mm diameter. The maximum displacement velocity achieved with the testing machine was 60 mm/sec. It was found that the failure load of 129 kN was independent of the loading rate and the stretch at failure was also constant at about 61 mm. Fatigue tests on the same type bolts indicated that the failure load decreases with the number of loading cycles and a reduction to 102 kN was achieved. However, the bolt stretch at failure decreased marginally to 57 mm. None of these tests duplicated the lack of bolt stretch observed underground. Ortlepp (1969) has suggested that in post-yield, plastic deformation of steel cannot occur at very high displacement velocities and failure will be abrupt with reduced stretch.

Tests were done by the South African Chamber of Mines on two types of high tensile steel bolts and one low tensile steel rebar. In addition a yielding device attached at the bolt head was tested. Displacement velocities of 0.5 mm/s (slow), and up to 1.9 m/s (fast), were used. A summary of the results is shown in Table 7.1.

The effect of high displacement velocity was to slightly increase the failure load on all the bolts and the stretch remained more or less the same. Bolts with a yielding collar accommodated about 100 mm more displacement without affecting the failure characteristics. Low tensile steel rebar, with a larger diameter, had a greater failure load and stretched about 40% more than the high tensile steel bolts.

It appears that a velocity of 1.9 m/s is still not high enough to affect the yield characteristics of the bolts during plastic deformation.

Table 7.1 - Bolt characteristics at slow and fast loading rates (after Hepworth and Heins, 1983)

Displacement Velocity	Failure Load		Stretch	
	Slow	Fast	Slow	Fast
H.T. steel bolt 13.5 mm dia.	108 kN	115 kN	33 mm	32 mm
H.T. steel bolt 13.5 mm dia. with yielding collar	109 kN	114 kN	131 mm	138 mm
H.T. steel bolt 18.5 mm dia. with yielding collar	--	198 kN	--	146 mm
L.T. steel rebar 16 mm dia.	129 kN	137 kN	46 mm	47 mm

H.T. - High tensile; L.T. - Low tensile; Bolts 1.2 m long.

7.5.2 ERPM Mine Trials

A comprehensive underground trial using conventional and yielding rockbolts was done at the ERPM Mine in South Africa. The yielding bolts had an extra 225 mm threaded portion at the anchor end. A smooth-bored die of internal diameter less than the threads was fitted to the bolts. Slippage occurred at a constant load as illustrated in Figure 7.7.

An isolated drift 2.7 m high by 3 m wide was bolted with 1.2 m long conventional and yielding bolts at 0.76 m centres, on opposite sides of the drift. A double layer of 8 gauge linked, 50 mm wire mesh was also installed under the rockbolt plates. A 3 m length of drift was supported in this manner. Holes for the explosives were drilled 3 m long at 430 mm centres, parallel to the drift axis and about 600 mm from the perimeter of the drift. These holes were loaded with 100 mm by 22 mm cartridges of 40% dynamite, uniformly spaced to fill 15% of each borehole (i.e., 0.60 kg/hole, 24 holes, total charge 14 kg). This instantaneous explosive charge completely destroyed both the conventional and yielding support systems.

In a second test, the length of the yielding bolts was increased to 1.5 m and the explosive charge reduced to 8% of each borehole (i.e., 0.32 kg/hole, 24 holes, total charge 7.6 kg). Figure 7.8 shows the layout of the bolts and

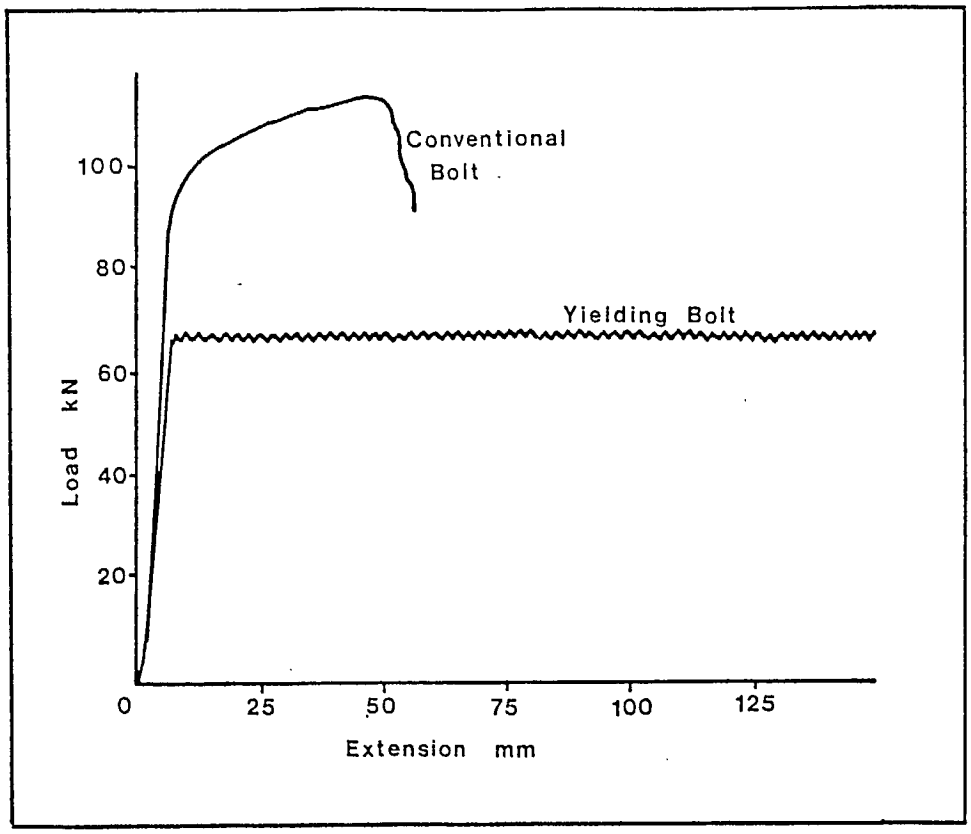

Fig. 7.7 - Load-extension characteristics of conventional and yielding bolts (after Ortlepp, 1969).

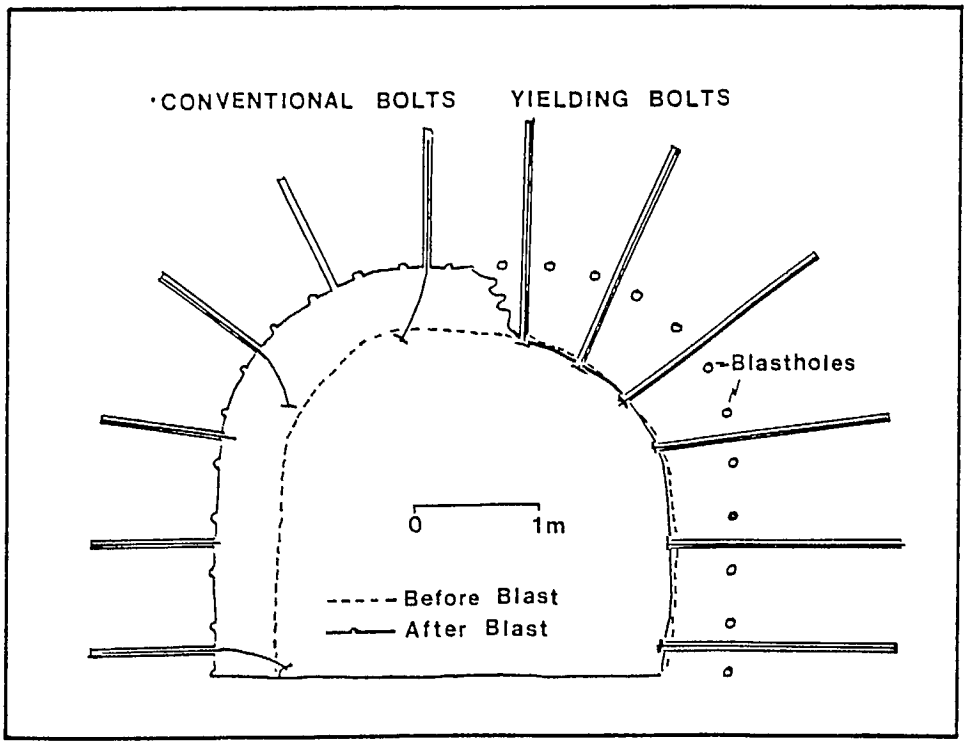

Fig. 7.8 - Layout of supports and drift profile after a blasting trial (after Ortlepp, 1969).

explosive holes, and a profile of the drift after the blast. In this case the side of the drift supported by conventional rockbolts was destroyed, whereas the yielding bolts survived with minor cracking of the rock.

7.5.3 Placer Dome, Campbell Mine Trials

The layout of the dynamic response of the supports trial is shown in Figure 7.9. Different types of supports were installed horizontally in a 1 m by 1 m section of the drift roughly 0.3 m apart. In the drift at right angles to the test drift, boreholes were drilled at distances of 3.0 m, 4.5 m and 6.0 m from the heads of the supports. Explosive charges (0.06 kg) were detonated in these boreholes directly behind the supports.

The different types of supports tested included tensioned mechanical bolts, split sets, swellex, grouted rebars, grouted cable bolts, grouted smooth rebar, grouted dywidag bolt, and a tensioned and grouted pipe bolt. Velocity gauges were attached to the heads of the supports as well as cemented to the rock face.

Figure 7.10 shows the typical recorded vibrations on the supports from a blast at a distance of 4.5 m. There are significant differences in the response of various supports and the rock face, in terms of amplitude of the vibrations, duration and to a lesser extent frequency.

The duration of the vibrations in the cable bolt, pipe bolt and mechanical bolt was longer than in the rock face itself, whereas the other supports had much shorter vibration durations. For this particular blast the rock face, smooth wall rebar, cable bolt, mechanical bolt and pipe bolt exhibit free vibrations ranging from 1500 to 2400 Hz. This corresponds to wave lengths of 2.4 to 3.6 m.

A support can be characterized by a mechanical model consisting of a spring and dashpot connected in series. The spring represents the elastic characteristics, and the dashpot the damping characteristics. It appears from the waveform records that the cable bolt, mechanical bolt and pipe bolt are acting mainly as springs with a weak damping component, whereas the grouted

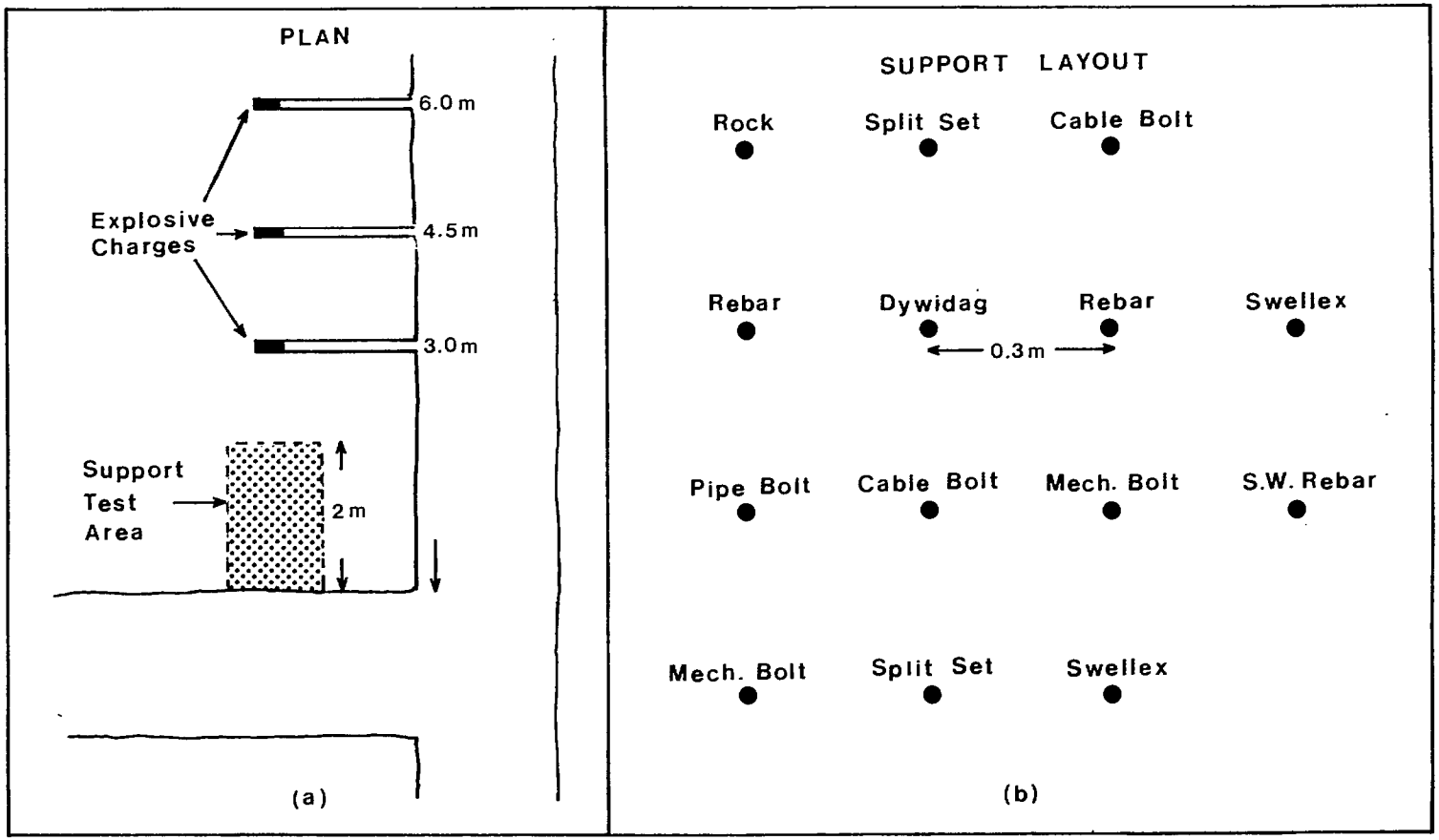

Fig. 7.9 - Layout of the support dynamic response trial at the Campbell Mine.

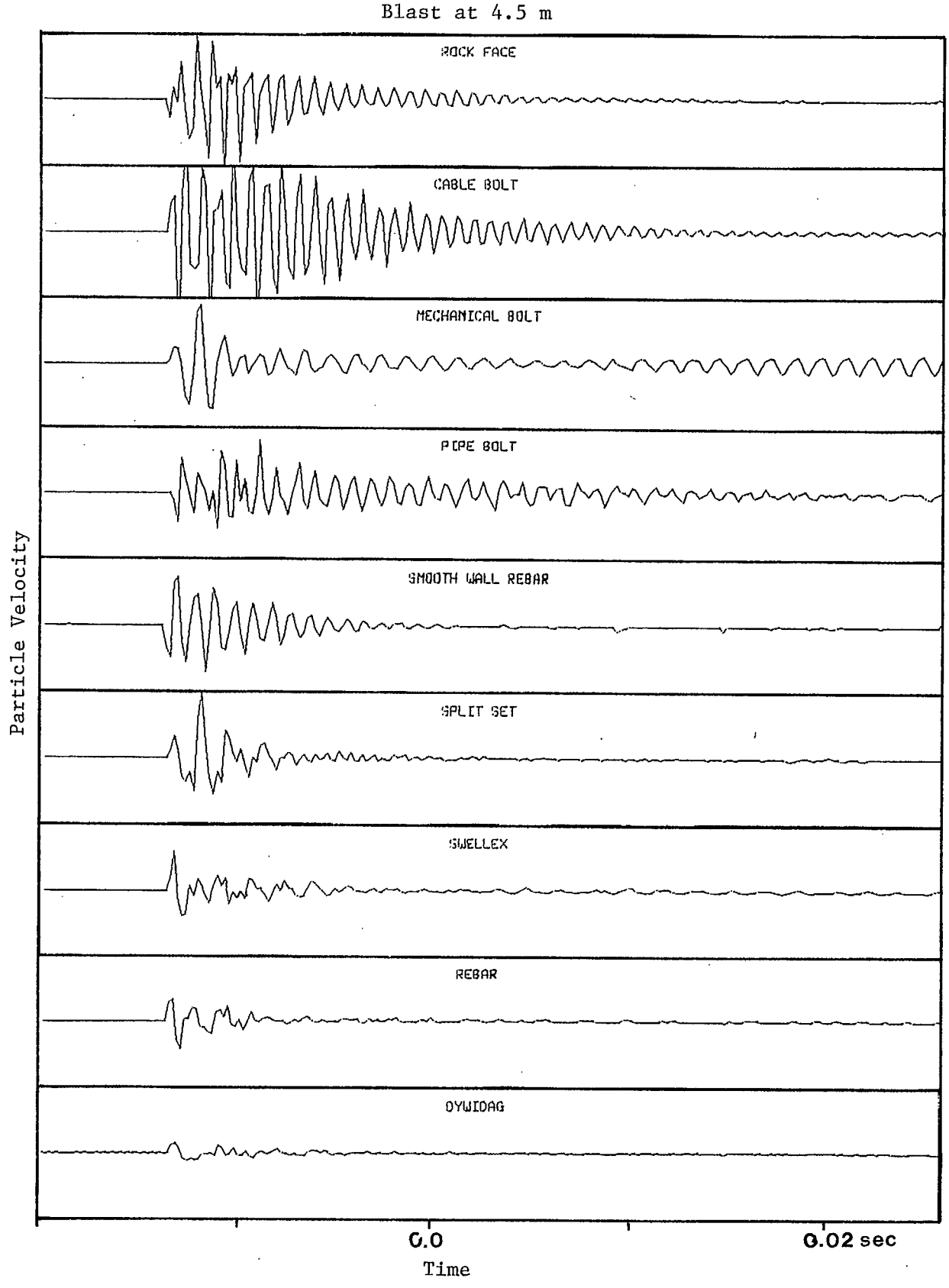

Fig. 7.10 - Recorded waveforms on supports.

rebar, dywidag, split set and swellex bolts are acting as springs with a strong damping component. The smooth wall rebar falls somewhere in between, since it exhibits free vibrations which are damped fairly quickly.

Peak particle velocity measured on the rock face and supports exhibited a large degree of scatter, probably because of varying detonation pressures of the explosive charges. Average values, excluding some of the extreme (high and low) values are plotted as a function of distance in Figure 7.11 a). Originally, it was thought that the peak particle velocity in the rock would be imposed on the supports with minor variations. This is not the case; the range is from 25% of the rock peak particle velocity for the dywidag bolt to almost double that for the cable bolt.

From peak particle velocity, the peak stress pulse in the supports and rock can be calculated as:

for steel bars $$\sigma = \frac{\hat{v}\ E}{Cp} \qquad \text{Eq 7.18}$$

and for the rock $$\sigma = \frac{\hat{v}\ E(1-\nu)}{Cp(1+\nu)(1-2\nu)}$$

where, σ = peak stress pulse
$\hat{v}$ = peak particle velocity
E = elastic modulus (steel rods 200 GPa, steel cable 70 GPa, rock 98 GPa)
Cp = compression wave velocity (steel 5950 m/s, rock 6300 m/s)
σ = Poisson's ratio (rock 0.23).

From peak stress, the peak force in each support can be obtained by multiplying by the cross-sectional area. Peak stress and force are plotted as a function of distance in Figures 7.11 b) and c). In terms of peak force, the results are much more closely bunched together; for example, the force exerted on the rebar, cable bolt and mechanical bolt are almost identical for each blast distance. Consequently, as a first approximation, a blast and by extension a rockburst, produces a constant peak force on a support. The cross-sectional area and elastic modulus of the support determines the

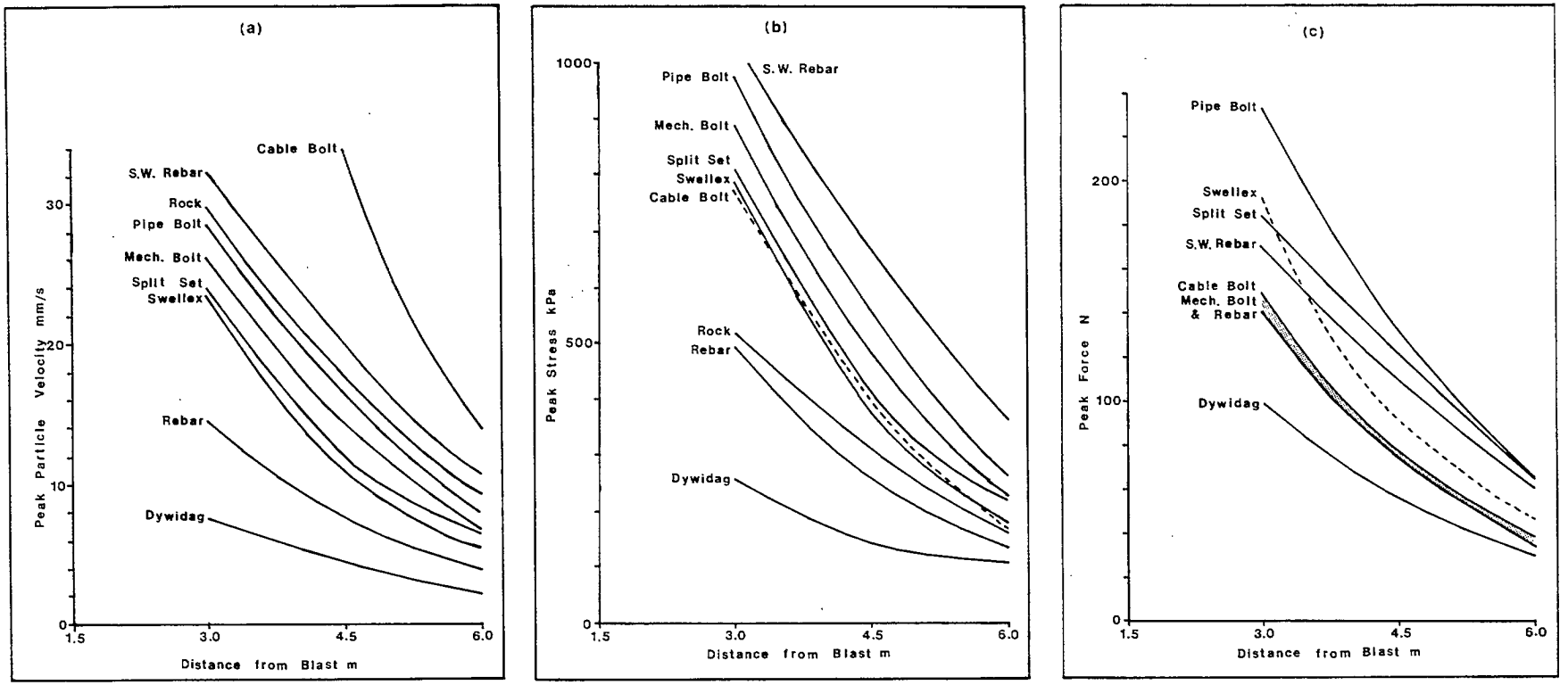

Fig. 7.11 - Peak particle velocity, stress and force on different supports.

corresponding peak stress and particle velocity. This concept conforms with Wagner's model (Section 7.4), which is defined in terms of the force exerted by a support.

In the second test at Campbell Mine, 4 m sections of a drift were reinforced with various types of supports, mesh and lacing, which were then subjected to close-in blasting. The layout of the drift and blastholes is shown in Figure 7.12. The types of supports installed in each area were as follows:

Area 1 - conventional lacing consisting of grouted mild steel rebar, chain-link screen and tensioned cable between rebars in a diamond pattern;
Area 2 - split set lacing with chain-link screen and tensioned cable between split-sets in a polygon pattern;
Area 3 - split-sets and chain-link screen;
Area 4 - grouted rebars and chain-link screen;
Area 5 - mechanical bolts and chain-link screen;
Area 6 - mechanical bolts and welded wire mesh.

The blastholes were loaded with approximately 2.3 kg of explosives in the centre of each support area for a total charge of 23 kg. All the explosive charges were detonated instantaneously. After the blast, most of the damage occurred in the areas supported by the mechanical bolts with welded wire mesh and chain-link screen. Many of the bolts were broken or blown out of their holes with major fracturing and spalling of the rock. The areas supported by the split-sets and grouted rebar with chain-link mesh held up fairly well, with a minor amount of fracturing and loose rock being contained by the screen and mesh. The two lacing areas stood up the best with regard to the containment of the loose rock. It was observed that slippage had occurred on some of the split-sets.

7.6 Underground Observations on Support Systems

Over the last 50 years, the reaction of various support systems to rockbursts has been fairly well documented in Ontario mines. The following sub-sections illustrate the failures and successes of different support systems.

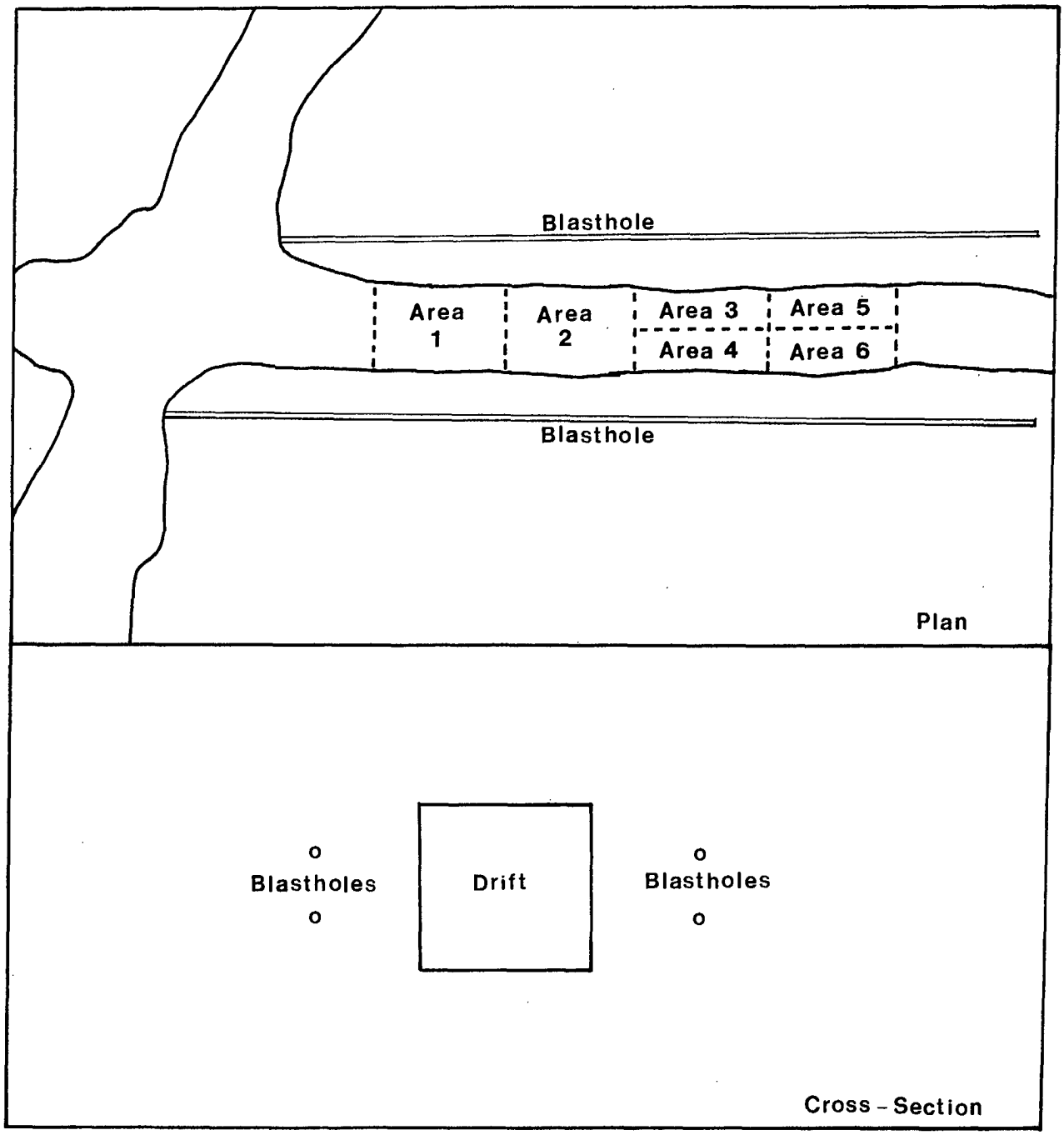

Fig. 7.12 - Layout of drift and blastholes in support trials.

7.6.1 Timber Posts and Beams

Although wood is a relatively soft material, posts and beams to not stand up well to rockbursts as they buckle readily. It is not known whether this buckling is due to impulse loading or the closure of the drift following a rockburst. On the other hand, wooden cribs stand up fairly well to rockbursts, perhaps because their aspect ratio and load-bearing capacity are much greater.

7.6.2 Steel Sets

Steel sets, either of circular or elliptical shape, were used in some hardrock mines in the 1940s and '50s. Generally, wood lagging was placed behind them and any space with the wall rock was backfilled with sand. Their use comes from coal mining, with the concept of evening out the pressure over the whole support system rather than at a point load. This type of support was effective in controlling damage from small seismic events but did not prevent extensive damage from large rockbursts.

7.6.3 Tendon Supports

Support tendons include mechanical bolts, rebar and cable bolts. They typically have support capacities of 110 kN, 150 kN and 260 kN, respectively.

Mechanical bolts are used extensively in Ontario mines with either a forged or nut head. Failure of these bolts is significant in rockburst areas, especially in the mines of Elliot Lake. Three types of failure are observed: tensile failure at the threads on the anchor end, shear failure due to lateral displacement of the borehole, and tensile failure about 2 cm behind the forged head. One common observation in the Elliot Lake mines is that failure at the forged head occurs before there is any major damage to the drift or stope. In other words, bolt failure is being caused by small seismic events. Metallurgical investigations on these bolts suggest that they are failing from fatigue.

Grouted rebar, using resin or cement, is a rigid support system and would be expected to behave similarly to mechanical bolts when subjected to dynamic

loading. However, very few rebar failures have been observed. Rebar has a larger diameter and hence is stronger. Also failures may be concealed by the resin or cement retaining the broken rebar in the borehole.

Grouted cable bolts are used in the Sudbury mines. Failures have occurred but it is difficult to tell whether they are caused by structure/gravity factors or rockbursts. However, the vibrations from seismic events could be a contributing factor even for gravity falls. Generally, failure occurs at the cement/cable bond which allows the rock to unravel. Only rarely has breakage of the cables been observed. It has been found that the use of high pulp density grout improves the effectiveness of the support system (MacDonald, 1988).

Mechanical bolts, rebar and cable bolts are more effective against rockbursts when used with steel wire mesh, although some failures still occur. At one mine, a drift had one wall supported by wire mesh as well as 2.4 m long mechanical bolts. The wall with mesh survived a rockburst of magnitude 2.4, although the rock behind the mesh was extensively fractured. The wall without mesh failed completely.

7.6.4 Friction Supports

Two types of friction supports are used in Ontario mines. A steel tube with a longitudinal slit which is hammered into a borehole (trade name, Split Set) and a sealed steel pipe which is pressurized against the borehole (trade name, Swellex). The split sets typically yield at about 50 kN and can slip in excess of 100 mm. Swellex bolts have a typical load capacity of 130 kN but their slippage characteristics are unknown since, during pull tests, failure occurs at the collar prior to slippage in the borehole.

Friction supports installed by themselves do not prevent spalling of a drift when subject to rockbursts. In conjunction with wire mesh, they are much more effective. At one mine, a haulage drift was rehabilitated with split sets and wire mesh. Subsequent rockbursts extensively fractured the rock behind the mesh and slippage of at least 100 mm was observed on some split sets.

7.6.5 Lacing

Lacing is a three-tiered support system with grouted rebar inside a borehole, wire mesh and steel cable between rebars in a diamond pattern. The steel cable acts like an automobile seat-belt and absorbs a considerable amount of energy radiating from a rockburst. Present day lacing is a South African gold mining innovation, however, a forerunner of lacing was used in the Lakeshore Mine at Kirkland Lake in the 1940s. In drifts opposite highly stressed pillars, two steel cables were run down the roof and anchored at 5 m intervals with 2 m long rock bolts. Round wood lagging was placed between the cable and the roof. The wooden mat/steel cable formed a yielding membrane which cushioned the impact of a rockburst. Sometimes this technique was also used in the walls.

In South African gold mines mild steel rebar 13 mm in diameter is used as the support tendon. Wire mesh is generally chain-linked and the steel cables are 13 mm diameter slusher cables tensioned to about 40 kN. This type of support system has survived a rockburst of magnitude 4.0 a few metres away.

Falconbridge's Strathcona Mine has also installed the same type of support system (Davidge et al., 1988). A footwall development drift and accesses to the overcut of a blasthole stope were laced. Subsequently, a rockburst of magnitude 3.0 occurred in the area. The conventionally supported overcut (grouted rebar and wire mesh) which was about 25 m away was severely damaged. The nearest lacing was about 40 m from the burst and suffered no damage. The same area was subjected to a series of rockbursts in June 1988 up to a magnitude of 2.7. This time, in places, the rock fractured and had 'bagged' behind the mesh and one broken rebar was observed.

At Inco's Copper Cliff North Mine, a different design of lacing has been installed. In this case, welded wire screen is held against the rock using 2 m long split sets. Steel cable in a square pattern is tensioned against the wire screen by driving a short 45 cm long split set inside the longer split set.

7.7 Design of Support Systems

From theoretical considerations and underground observations, the effectiveness of various support systems to rockburst conditions can be evaluated, in at least a qualitative sense. Mechanical bolts are the most prone to failure and lacing is the most effective. In between these two extremes, different types of supports can be used, based on the likely maximum rockburst magnitude to which they are subjected and the distance from the source.

The characteristics of tendon, friction, mesh and cable supports are listed in Table 7.2. Unfortunately, most of the information on load capacity and stretch comes from semi-static pull tests which may not represent their characteristics under dynamic loading.

The peak particle velocity a support can withstand and especially the energy it can absorb are the two most important parameters for rockburst conditions. These parameters more or less follow the ranking obtained from underground observations. Mechanical bolts absorb the least energy followed by cable bolts and regular rebar. The friction type supports, smooth mild steel rebar, and those that yield at a fixed load, have the best energy absorbing properties. Wire mesh and the steel cables used in lacing have similar energy absorbing abilities.

The use of wire mesh and steel cables, in two- and three-tiered support systems does not increase the support resistance of the system. This is controlled by the member installed in the borehole, although the mesh and cables may average out the resistance over a number of supports. However, the ability of a support system to absorb energy is the summation of each of its components. For instance in lacing, the smooth rebar, chain link mesh and three steel cables can absorb 9.4 kJ/m^2, compared to just 3.4 kJ/m^2 for smooth rebar itself. It is this energy parameter which best explains the underground observations and forms the basis for designing support systems for rockburst conditions. Consequently, another requirement can be added to Wagner's 'set of conditions', that the support system be capable of absorbing 9.0 kJ/m^2 (i.e., preliminary value).

Table 7.2 - Possible support characteristics under dynamic loading

Type of Support	Load Capacity kN	Stretch or Slip mm (1)	Support Resistance kN/m^2 (2)	Peak Particle Velocity m/s (3)	Energy Absorbed kJ/m^2 (2)
Mechanical bolts	120	20	83	0.46(4)	0.6(4)
Yielding bolts (5)	65	200	45	2.6	9.0
Rebar, regular	150	25	104	1.0	1.3
Rebar, smooth	130	75	70	1.6	3.4
Cable bolts	230	15	160	0.9	1.2
Split sets	50	100	35	1.6	3.5
Swellex, annealed (6)	100	50	70	1.6	3.5
Welded wire mesh (7)	30	200	20	1.2	2.1
Chain link mesh (7)	35	270	25	1.5	3.3
Steel cable, lacing	90	30	62/cable	0.8	0.9/cable

Notes: (1) 2 m long supports; (2) supports at 1.2 m (4 ft) centres;
(3) from Equations 7.15 or 7.16 using a slab thickness of 1 m;
(4) bolts installed with 60 kN tension and 10 mm stretch;
(5) Ortlepp, 1969; (6) Herron, 1988; (7) Pakalnis and Ames, 1983.

This concept of support requirements is illustrated in Figure 7.13 which relates the type of support system that can be used for a given rockburst magnitude at varying distances. At present, the ranking of the support systems is realistic but the scale of the magnitude and distance axes is doubtful.

The three instances of severe damage given in section 7.3 were supported by mechanical bolts and welded wire mesh at the Creighton Mine and grouted rebar and welded wire mesh at the Strathcona Mine. Rockburst magnitudes ranged from 2.9 to 3.6, and severe damage occurred 25 to 31 m away. From Figure 7.13, for tendon supports with mesh, damage would be expected over distances of 16 to 28 m, for the same range of rockburst magnitudes. Consequently, this particular curve at the higher rockburst magnitudes should be moved to the right.

At magnitudes below 2.0, probably the reverse is true and some of the support curves should intersect the magnitude axis at zero distance. The main reason for this is the over-estimation of the peak particle velocity close to the source. As mentioned previously, the blasting format used in Equation 7.4 predicts an infinite peak particle velocity at the source for any rockburst magnitude. Modifications are required to this equation so that the peak particle velocity at source is finite and related to magnitude.

7.8 References

Blake, W. and Cuvelier, D.J. (1988), Developing reinforcement requirements for rockburst conditions at Hecla's Friday Mine. Proc. 2nd Int. Symp. Rockbursts and Seismicity in Mines, Minneapolis, June 1988, pp. 589-598.

Brune, J.N. (1970), Tectonic stress and the spectra of seismic shear waves from earthquakes. J. Geophys. Res., vol. 75, No. 26, p.4997.

Davidge, G.R., Martin, T.A. and Steed, C.M. (1988), Lacing support trial at Strathcona Mine. Proc. 2nd Int. Symp. Rockbursts and Seismicity in Mines, Minneapolis, Minnesota.

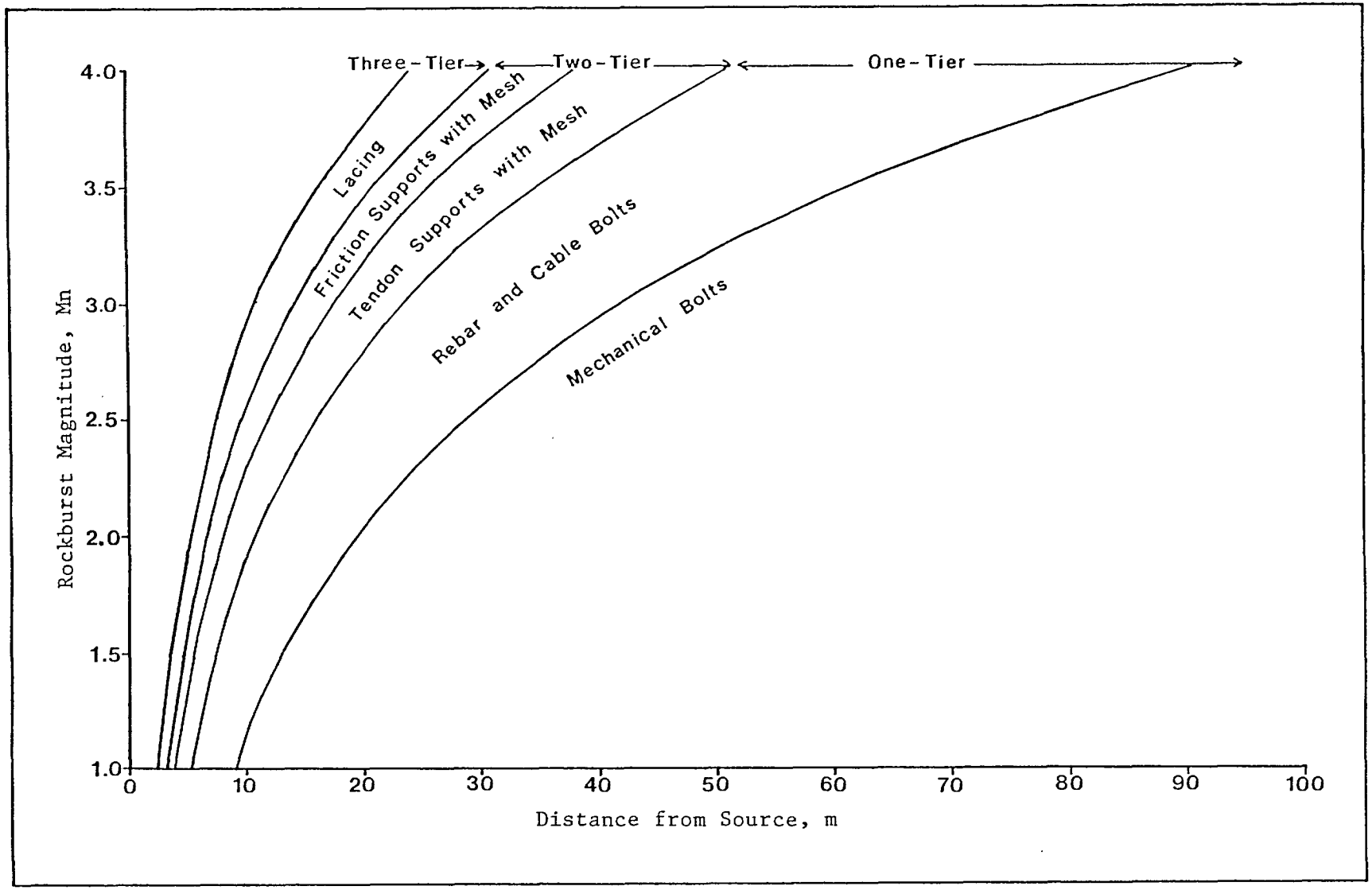

Fig. 7.13 - Conceptual support requirements for rockburst conditions.

Gibbon, G.J., De Kock, A. and Mokebe, J. (1986), Monitoring of peak ground velocity during rockbursts. Proc. 8th West Virginia University Int. Min. Electrotechnology Conf., Morgantown.

Hedley, D.G.F. and Whitten, N. (1983), Performance of bolting systems subject to rockbursts. CIM Seminar Underground Support Systems, Sudbury, CIM Special volume 35, pp. 73-79.

Hedley, D.G.F. (1988), Peak particle velocity for rockbursts in some Ontario mines. Proc. 2nd Int. Symp. Rockbursts and Seismicity in Mines, Minneapolis, pp. 503-512.

Hedley, D.G.F., Nelson, M., O'Flaherty, M. and Makuch, A. (1991), Evaluation of support systems subject to moderate rockbursts. Contract Report, Mining Research Directorate.

Hepworth, N. and Heins, C. (1983), Slow and rapid extension tests on support tendons and yielding collars. South African Chamber of Mines Internal Report.

Kirsten, H. and Stacey, T.R. (1988), Destabilizing effects of seismic disturbances on fractured rock surrounding tabular stopes. Proc. 2nd Int. Symp. Rockbursts and Seismicity in Mines, Minneapolis, pp. 541-555.

Langefors, H. and Kihlstrom, B. (1963), Rock Blasting. John Wiley and Sons Inc., New York.

Lenhardt, W.A. (1988), Seismic damage studies at a deep level African gold mine. Proc. 2nd Int. Symp. Rockbursts and Seismicity in Mines, Minneapolis, pp. 555-567.

MacDonald, P. (1988), Personal communication.

McGarr, A.R., Green, W.E. and Spottiswoode, S.M. (1981), Strong ground motion of mine tremors: some implications for near-source ground source parameters. Bull. Seismol. Soc. Am. vol. 71, pp. 295-319.

Ortlepp, W.D. (1969), An empirical determination of the effectiveness of rockburst support under impulse loading. Int. Symp. Large Permanent Underground Openings, Oslo.

Roberts, M.K.S. and Brummer, R.K. (1988), Support requirements in rockburst conditions. J. South African Inst. Min. Met. vol. 88, No. 3, pp. 97-104.

Spottiswoode, S.M. (1984), Underground seismic networks and safety. In: Monitoring for Safety in Geotechnical Engineering, SANGORM, Johannesburg.

Wagner, H. (1982), Support requirements for rockburst conditions. 1st Int. Symp. Rockbursts and Seismicity in Mines, Johannesburg, S. African Inst. Min. Met.

8. DESTRESS BLASTING

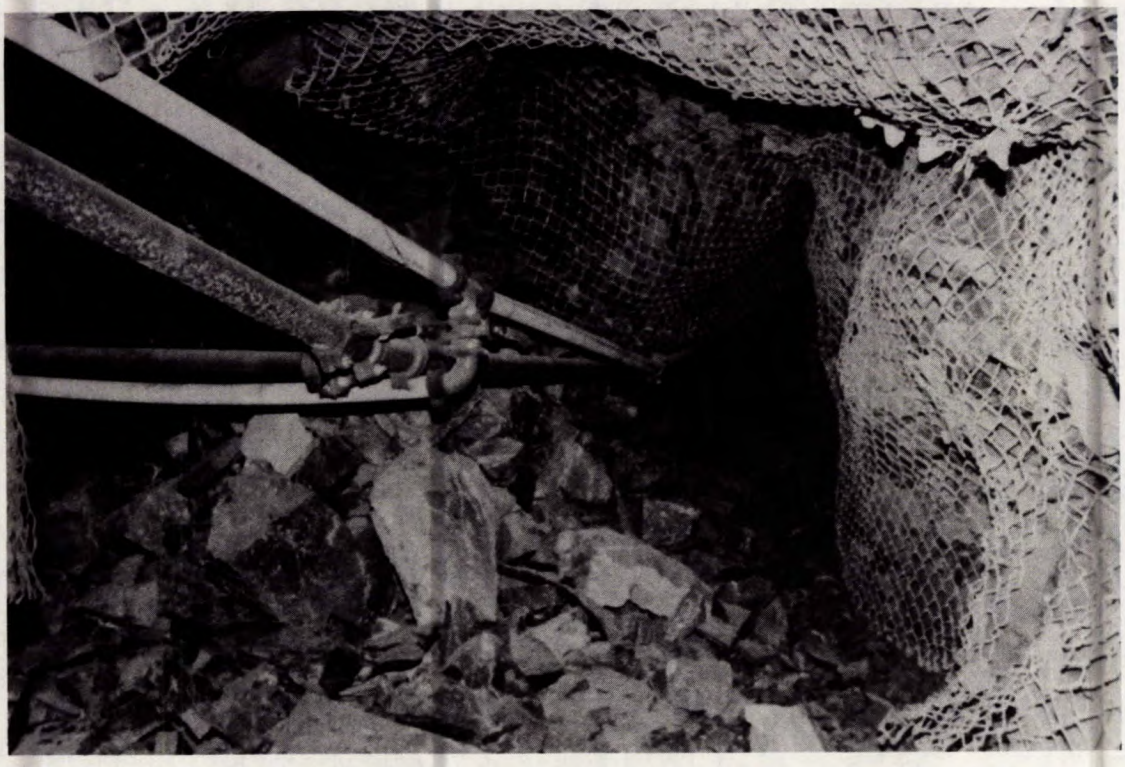

Damage to a drift at Macassa Mine about one year after destressing adjacent pillar.

Damage to a ramp at Strathcona Mine prior to initiating destress blasting.

8. DESTRESS BLASTING

8.1. Introduction

Destress blasting has been used for a number of years to overcome problems of highly-stressed ground and rockbursts. It was generally considered that the blast fractures the rock and reduces its stiffness which in turn transfers stress to the adjacent rock mass.

The first known instances of destress blasting were at the Lake Shore Mine at Kirkland Lake in the early 1950s. Cook and Bruce (1983) reported the use of destressing techniques in pillars prior to their extraction. Also on another occasion, the ground between advancing stope faces and a major rockburst-prone fault was destressed using 30 m long holes with apparent success.

The first systematic destress trials were done in a South African gold mine in the mid-1950s. The purpose was to create a fractured zone in front of a longwall face. It was reported (Roux et al., 1957) to be successful in reducing the number and severity of rockburst incidents. There was also a reduction in the number of casualties and lost days of production. Hanging wall conditions improved, and there was a significant decrease in the number of bursts occurring on-shift. However, the practice was discontinued apparently because of the problems of drilling relatively long holes and loading explosives in highly stressed ground. Later it was reported that the energy liberated in a destress blast was no greater than the energy in the explosive itself (Cook et al., 1966). Seismic recordings of rockbursts had indicated that two-thirds of the liberated energy was in the vertical shear wave component. Similar recordings of destress and conventional blasts indicated that most of the energy was in the radial compression wave and a negligible amount in the vertical shear wave. In the late 1980s destress blasting was again re-evaluated for the South African gold mines (Rorke and Brummer, 1988), and trials conducted underground (Rorke et al., 1990).

In North American mines, destressing is more widely practiced and apparently more successful. Destressing of sill pillars is done on a regular basis in the mines in the Coeur d'Alene district of northern Idaho. Instrumented field

trials have been reported by Blake (1972) and Board and Fairhurst (1983). Normally, destressing takes place when the sill pillars have been reduced to 10-12 m thickness and are highly stressed. Another concept is rock preconditioning where drilling and blasting are done before stoping takes place, and hence the rock is under its lowest stress condition. It has been reported that preconditioning significantly reduced seismic activity during mining (Blake, 1982).

In Canadian mines, destressing is normally practised in sill pillars in thin, steeply-dipping orebodies such as those at Campbell Red Lake Mine, Dickenson Mine, Falconbridge Mine (Moruzi and Pasieka, 1964), and Kirkland Lake (Cook and Bruce, 1983). At Inco's Creighton Mine, destress blasting is in regular use in driving development openings, and in pillar and stope faces during the first cut in cut-and-fill mining (Garrood, 1982, Oliver et al., 1987). Also at the Creighton Mine, a transverse slot was initially extracted across a large crown pillar which is a form of preconditioning (MacDonald, et al., 1988).

Only recently has the concept of destressing faults been addressed (Brummer, 1988 and Brady, 1988). There are two options, either to inject high fluid pressure into a fault or set off explosive charges in the plane of the fault.

8.2 Rock Mechanics Concepts of Destressing

8.2.1 Pillars

Most investigations have concerned pillar destressing. There is a general consensus that destressing softens the rock and reduces its effective elastic modulus. There are conflicting views on the importance of reducing stress and the stored strain energy within the destressed rock.

Conditions of stress and strain, before and after destressing, were investigated by Crouch (1974). He postulated subcritical, critical and super-critical degrees of destressing as illustrated in Figure 8.1. After destressing, the final equilibrium stress-strain position is dependent on the intersection of the destress modulus line with the slope of the local mine stiffness. If this intersection lies within the stress-strain envelope (i.e.,

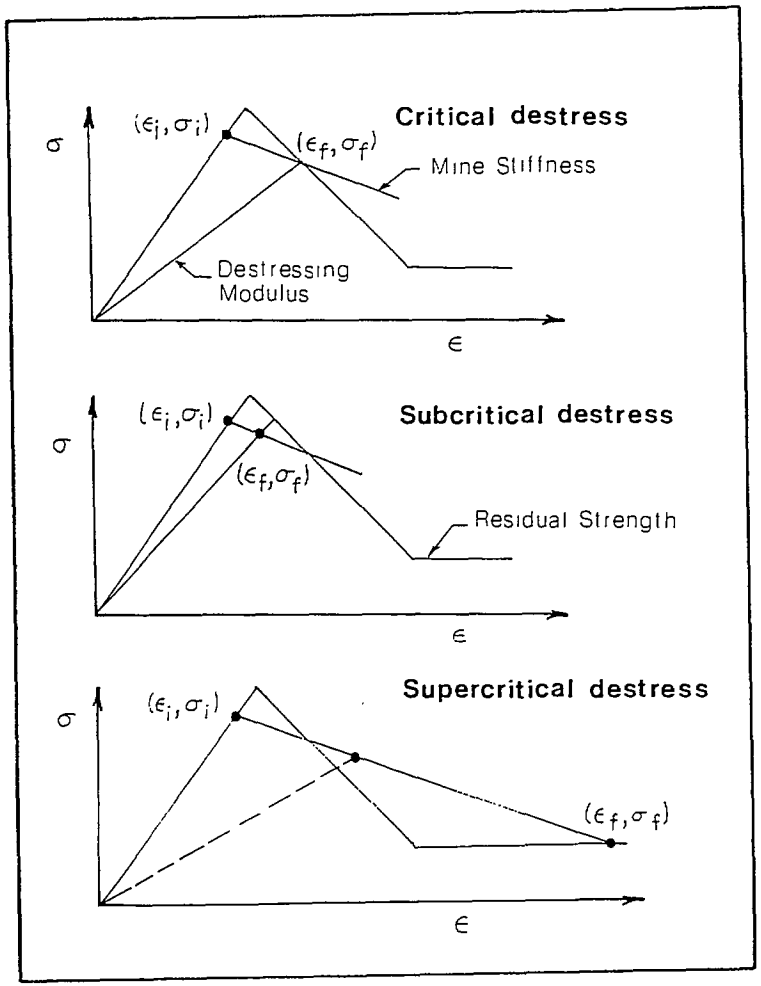

Fig. 8.1 - Different degrees of destressing (after Crouch, 1974).

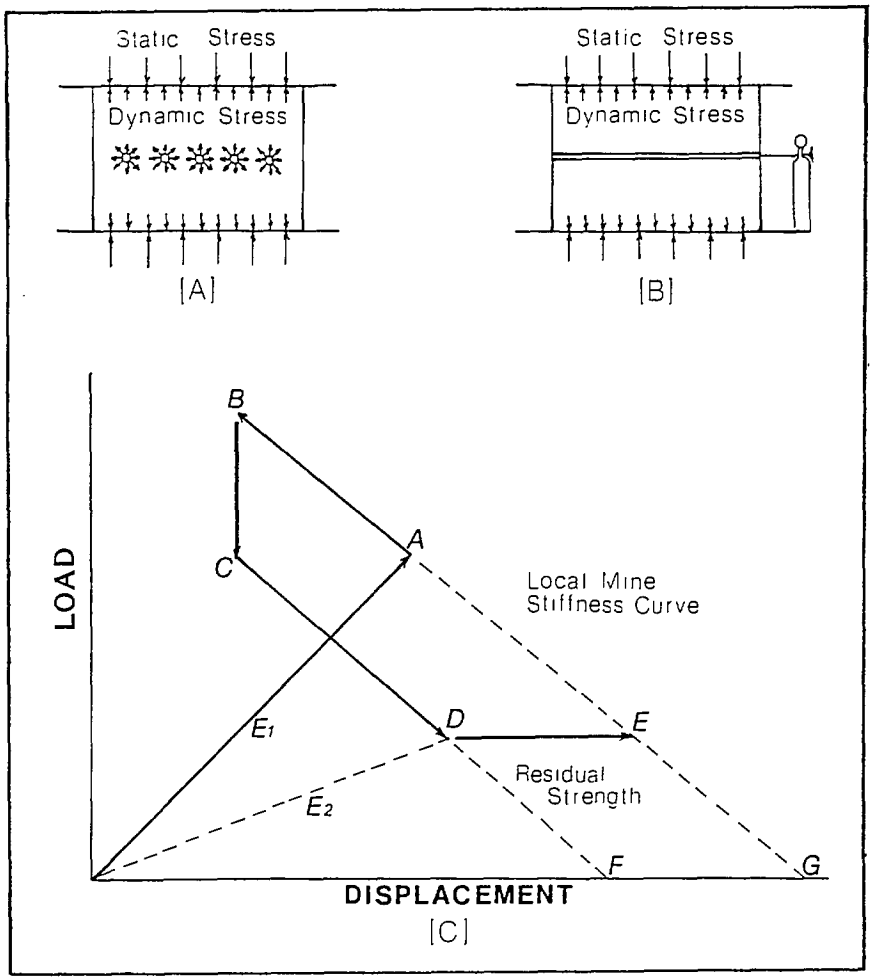

Fig. 8.2 - Stress-displacement history of a pillar during a destress blast.

subcritical), the destress blast will be ineffective. However, if the intersection lies outside the envelope (i.e., supercritical), excess energy will be released and eventually equilibrium will be achieved along the residual strength curve. Both Crouch (1974) and Blake (1972) state that destressing is most effective when the pillar is near its point of failure. Crouch (1974) also pointed out that the excess energy released in a destress blast or a rockburst is derived from the change in potential energy of the rock mass, not the stored strain energy in the pillar.

These studies have looked at the before and after effects of destressing, and not what happens during the blast itself. When an explosive is detonated in a borehole, a pressure or shock wave radiates outwards producing radial fractures around the hole. Expanding gases open and extend these fractures and physically displace (i.e., throw) the rock fragments. In a destress blast the explosive is confined and a free face is normally some distance away. Under these conditions, the shock wave is the major source of rock fragmentation and most of the gases are probably vented through the borehole collar. Generally, the seismic energy in the shock wave is 5-10% of the total chemical energy in the explosive (Duvall and Stephenson, 1966).

In an elastic medium, the increase in radial stress, $\Delta\sigma r$, can be expressed by:

$$\Delta\sigma r = P\left(\frac{r}{R}\right)^2 \qquad \text{Eq 8.1}$$

where, P = borehole pressure
r = borehole radius
R = distance from the borehole.

For commercial explosives, the borehole pressure is in the range of 200 to 8000 MPa (Coates, 1981). Equation 8.1 indicates that the change in radial stress decreases rapidly away from the borehole. When R = 10r the change in stress is only 1% of the borehole pressure. For typical hardrocks, the power coefficient is more likely to be 2.5 than 2, indicating greater attenuation of the shock wave.

The change in radial stress can also be expressed by:

$$\Delta\sigma r = \gamma \, Cp \, v \qquad \text{Eq 8.2}$$

where, γ = rock density

Cp = pressure wave velocity

v = particle velocity.

The velocity of crack propagation is only about 15 to 40% that of the pressure wave velocity (Coates, 1981). Hence, initially the pillar only experiences an increase in stress without a reduction in elastic modulus due to fracturing which occurs later.

The imposition of a dynamic load due to explosives on top of a static load can now be looked at in terms of load-displacement on a pillar as shown in Figure 8.2. Figure 8.2a) shows the pressure wave radiating from the destress boreholes. By the time these waves hit the hanging wall/footwall, they have probably coalesced into a straight front. Figure 8.2b) shows the mechanical equivalent of a destress blast with a thin flat jack at mid-pillar height which can be instantaneously pressurized. This is not an exact duplication since the explosive pressure wave is transient. Figure 8.2c) shows the load-displacement history of the hanging wall or footwall. The sequence of events during a destress blast are probably as follows:

- Just before the blast, the pillar is under static load-displacement conditions at point A with an elastic modulus E_1.

- After detonation, the pressure wave radiates outwards and increases the stress on the hanging wall and footwall similar to that obtained by pressurizing the flat jack. This internal pressure will force the hanging wall/footwall apart along the line AB which is the slope of the local mine stiffness curve.

- Fracturing occurs after the pressure wave, similar to rupturing of the flat jack. There will probably be a sudden load drop to point C after the pressure wave passes through, of magnitude probably equal to the increase

in load due to the explosive. This will be followed by a further load reduction as the hanging wall/footwall converge. The pillar will have a reduced elastic modulus E_2 due to fracturing which is reached at point D.

- Equilibrium has not yet been reached and displacement will continue along the residual strength curve until it intersects the local mine stiffness curve at point E.

- If it were a production rather than a destress blast, then unloading would continue along line DF until zero load is achieved. However, again, equilibrium is not reached until the hanging wall/footwall converge to point G which is the intersection with the local mine stiffness curve.

The energy components involved in the destress blast can now be examined. From Salamon (1974), the energy balance due to mining can be expressed by:

$$W_t + U_m = U_c + W_r \qquad \text{Eq 8.3}$$

where, W_t = change in potential energy
U_m = stored strain energy in mined material
U_c = increased strain energy in surrounding rock
W_r = released energy.

In the absence of any support, such as backfill, the released energy consists of the stored strain energy in the mined material, U_m, and seismic energy W_k, which vibrates the rock mass. In a destress blast, there will be additional energy components and Equation 8.3 becomes:

$$W_t + U_{m1} + Ex = U_c + U_{m2} + U_f + W_k \qquad \text{Eq 8.4}$$

where, U_{m1} = stored strain energy before destressing
U_{m2} = stored strain energy after destressing
Ex = explosive energy
U_f = energy consumed in fracturing the rock.

These energy components are illustrated in Figure 8.3. The net change in

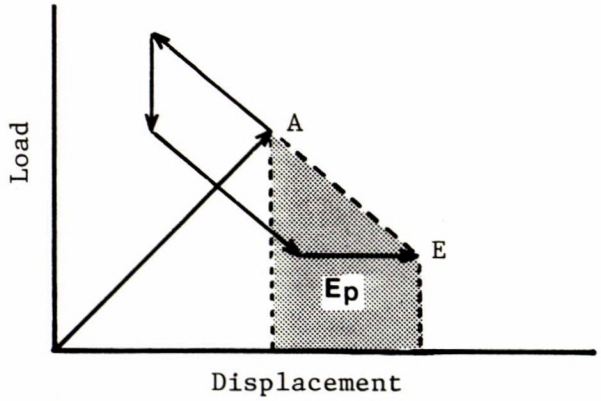

a) Net change in potential energy.

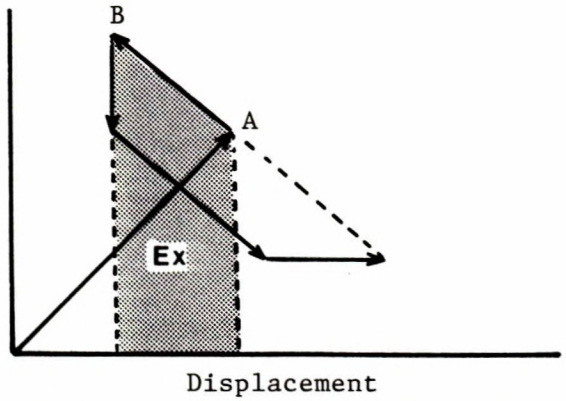

b) Explosive energy to push back walls.

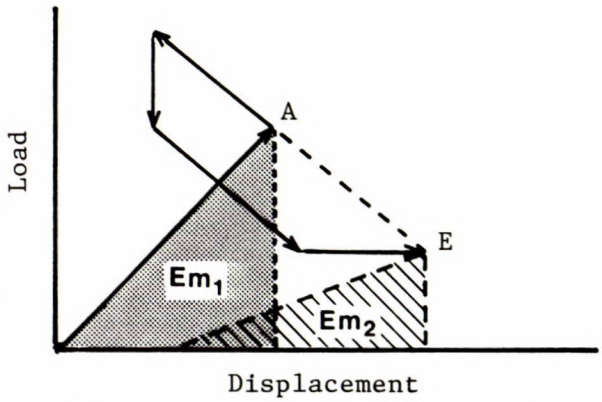

c) Stored strain energies before and after destressing.

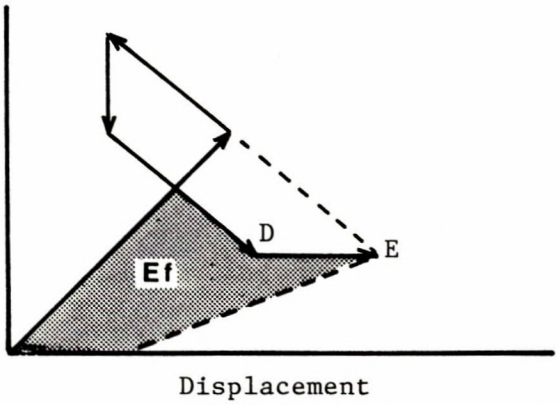

d) Energy consumed (excluding explosive) to fracture pillar.

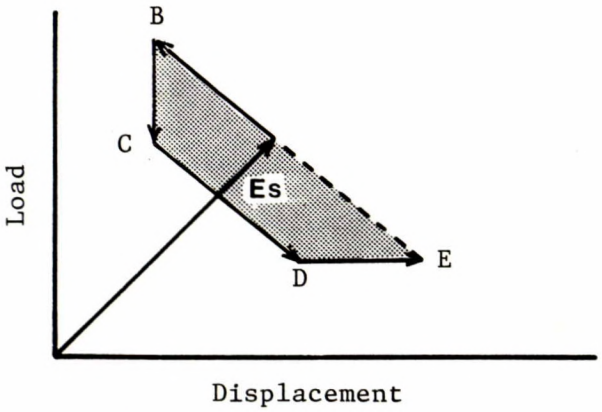

e) Seismic energy released.

Fig. 8.3 - Energy components during a pillar destress blast.

potential energy is the area under the AE line as shown in Figure 8.3a). Explosive energy used to push back the hanging wall and footwall is the area under the AB line as in Figure 8.3b). There is an additional explosive energy, such as in heat and expanding gases, which is not accounted for and does not affect the energy balance. Stored strain energies before and after destressing are shown in Figure 8.3c) and represent the load and elastic modulus at points A and E, respectively. The energy consumed in fracturing the rock is the area under the load-displacement envelope minus the stored strain energy remaining in the fractured pillar as shown in Figure 8.3d). The seismic energy released is the area outside the load-displacement envelope as shown in Figure 8.3e). It includes two components: that due to the explosive which pushed back the hanging wall/footwall, and that due to the change in potential energy of the rock mass.

Although this is a simplistic view of what happens during a destress blast, a number of fundamental deductions can be made from the stress-displacement history in Figure 8.2 and the energy components in Figure 8.3.

- The major function of destressing is to reduce the potential energy of the surrounding rock mass, which is the same conclusion as that reached by Crouch (1974). This is achieved by reducing the modulus and load on the pillar. In Figures 8.2c) and 8.3c), the reduction in potential energy is from point A to point E. A further reduction in potential energy will occur when mining the destressed pillar until point G is reached. The closer point E is to point G, the more effective is the destress blast although this must be balanced against the practical difficulties of mining extremely fractured ground.

- Irrespective of whether the pillar is destressed then mined, or is removed by production blasts, or has failed due to a rockburst, the endpoint is always the same (namely point G in Figure 8.2c)).

- The stored strain energy in the pillar is used in the fracturing process and is not released as seismic energy.

- The explosive as well as initiating the fracture process is used in pushing back the hanging wall/footwall.

- The seismic energy released is partly due to the explosive and partly due to the change in potential energy. It is released during the latter part of the cycle.

8.2.2 Development Openings

As mentioned in Section 3.5.1, high stress concentrations can cause bursting in the development opening, including shafts. One source of the released seismic energy is part of the stored strain energy in the rock as it goes from a triaxial to a biaxial or uniaxial stress condition. The purpose of destress blasting, in this case, is to transfer the high stress concentrations (and hence high stored strain energy) from where the sides of the opening are going to be. This concept is illustrated in Figure 8.4.

Figure 8.4a) shows a FLAC Mohr-Coulomb model of a 4 m by 4 m drift subject to a horizontal stress of 100 MPa, and a vertical stress of 50 MPa. Because of symmetry only one quadrant of the drift needs to be shown. An area 1 m in radius was positioned at each of the drift corners. Material properties (i.e., bulk and shear modulus, friction angle and cohesion) within this area were decreased to simulate a destress zone.

Figure 8.4b) shows the principal stresses around the drift with no destress zone. As expected, high stress concentrations occurred in the corners and back. Fig. 8.4c) shows the principal stresses after a successful destress blast. In this case, the high stress concentrations have been transferred about 2 m from the drift boundaries. To achieve this result, the cohesion in the destress zone had to be reduced to zero and the friction angle, bulk modulus and shear modulus halved in value. When a small cohesion and a friction angle of two-thirds was assigned to the destress zone, only partial destressing of the skin of the drift was achieved (Swan, 1991). These results imply that for the destress blast to be successful, the fractured zone around the destress hole must have zero cohesion, and that this fractured zone must intersect the opening.

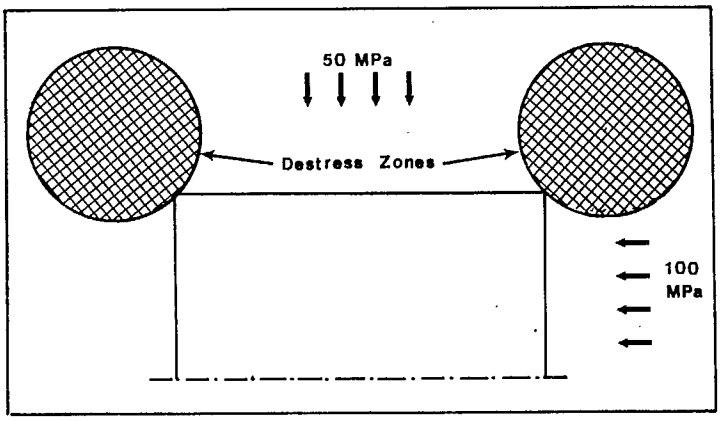

a) FLAC model.

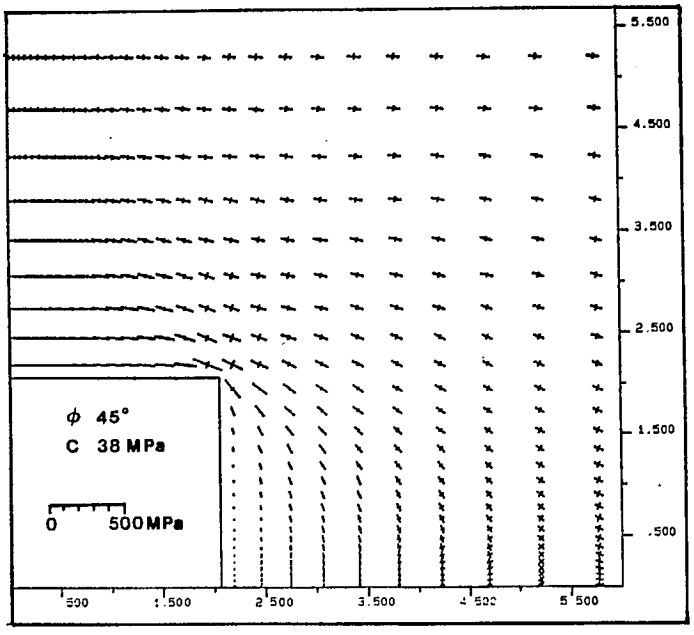

b) Without destressed zone.

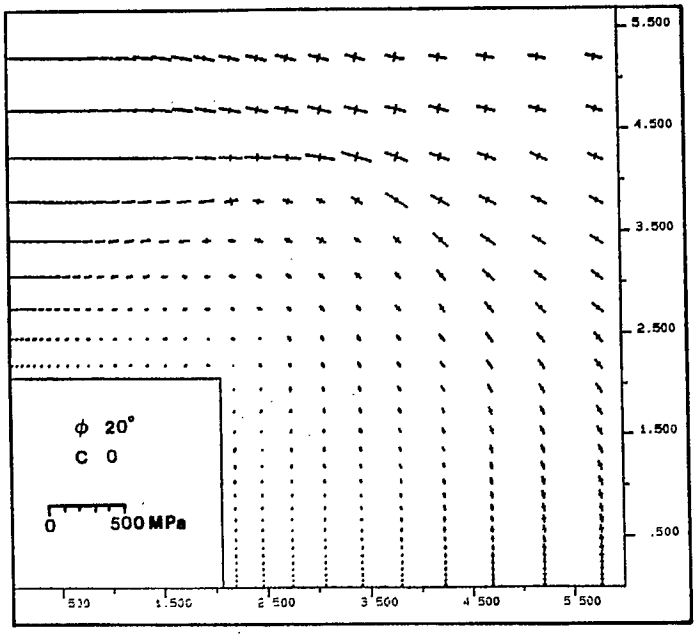

c) With destressed zone.

Fig. 8.4 - Model illustrating the transfer of stresses due to destressing.

8.2.3 Faults

The mechanics of slippage along a fault were presented in Section 3.5.3. The simplest model was described, that of a circular fault with only static and dynamic frictional properties. In most cases, faults will also have cohesional properties. Before slippage occurs the shear and clamping forces are in a stable condition:

$$\tau_s \leq C_s + \mu s \sigma n \qquad \text{Eq 8.5}$$

where, τ = shear stress
C = cohesion
μ = coefficient of friction
σn = normal stress

Subscripts 's' and 'd' denote static and dynamic. To initiate slippage means either increasing the shear stress or decreasing the cohesion, friction or normal stress. After slippage, equilibrium is re-established when:

$$\tau_d = C_d + \mu_d \sigma n \qquad \text{Eq 8.6}$$

and the stress drop is:

$$\tau_s - \tau_d = (C_s - C_d) + \sigma n(\mu_s - \mu_d) \qquad \text{Eq 8.7}$$

It is difficult to increase the shear stress, hence the only means of destressing faults is to reduce one or more of the clamping components. Fluid injection into the fault will reduce directly the normal stress by the amount of the fluid pressure. Fluid can also reduce the static coefficient of friction and cohesion by about 15% (Biskup and Kaiser, 1990). By controlling the fluid pressure and the flow rate, it may be possible to produce incremental non-violent stress drops on the fault. Brady (1988) and Brummer (1988) estimate that fluid pressures in the order of 20 to 50 MPa and flow rates of about 50 L/min would be required to trigger slippage on a fault.

The alternative is to detonate explosives in the plane of the fault. If the

boreholes are in the fault then the explosive pressure will directly reduce the normal stress. Otherwise for boreholes outside the fault plane, the tensile wave in the second half-cycle plus subsequent vibrations would reduce the normal stress, and to a certain extent, the friction and cohesion on the fault. Blasting is a one-shot method of trying to trigger slippage, perhaps violently, on a fault at a set time.

8.3 Pillar Destressing Practices

Pillar destressing is generally done in narrow steeply-dipping orebodies being mined by cut-and-fill techniques. The practice used at Placer Dome's Campbell Mine, Lac Mineral's Macassa Mine and Hecla's Lucky Friday Mine are described as well as the experience gained in mining a slot to precondition a large crown pillar at Inco's Creighton Mine.

8.3.1 Campbell Mine, Placer Dome Inc.

A series of steeply-dipping, gold-bearing orebodies, 2 to 12 m wide, are being mined to a depth of 1300 m at the Campbell Mine near Red Lake in Ontario. The upper levels, down to a depth of about 350 m, were predominantly mined using shrinkage stoping techniques. At deeper levels, overhand cut-and-fill methods are used with some undercut-and-fill of the crown pillars. The fill is classified tailings augmented with alluvial sand. Cement is added for working floors and sill plugs.

The mine has had a history of rockbursting since the early 1960s. Initially, these were associated with the boxhole and crown pillars of shrinkage stopes. In the cut-and-fill stopes, the crown pillars became critically stressed and burst prone when the pillar width approached 6 m, or at about 80% extraction. However, this critical dimension will likely increase with depth.

During the 1980s, four destress blasts were done with varying degrees of success (Neumann et al., 1987). The most successful was the destressing of crown and sill pillars on the 18 level. Figure 8.5 shows the layout of the destress blast. The 4.5 m wide crown pillar was drilled off with 44 mm holes at 1.8 m spacing, to within 1.5 m of the overlying drift, over a distance of

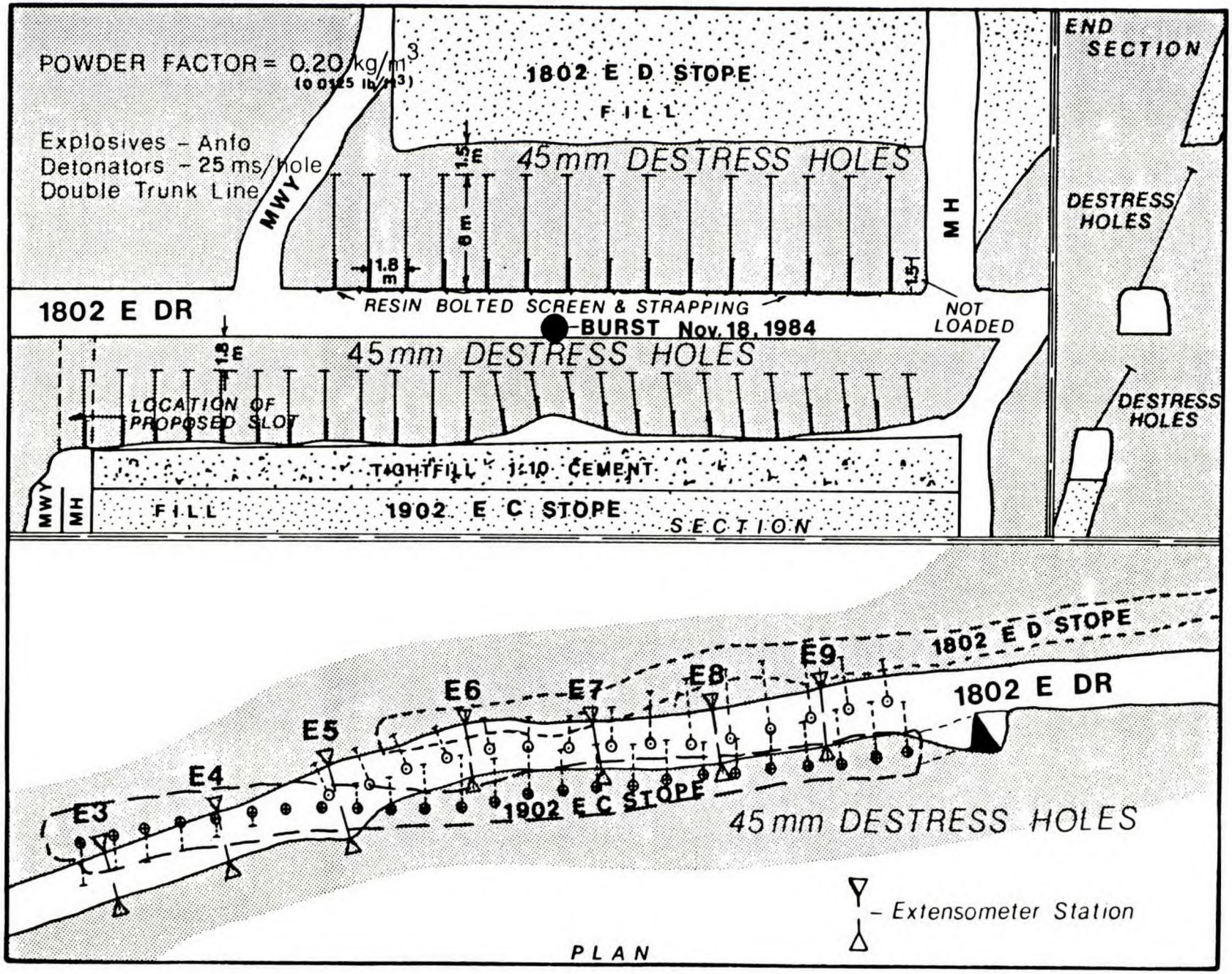

Fig. 8.5 - Layout of destress holes in the 1902 and 1802 crown and sill pillars at the Campbell Mine.

45 m. The sill pillar, above the level, was drilled off with a 6 m long hole again at 1.8 m spacing over a distance of 25 m. Prior to the blast the 18 level drift was reinforced with 1.8 m and 2.4 m long resin grouted rebar and welded mesh screen. Also the stope below was tight filled with 10:1 cemented tailings. ANFO was loaded into the destress holes with a powder factor of 0.2 kg/m^2.

The destress blast was followed by many small microseismic events. After 30 sec a rockburst occurred in the 1802 drift, as shown in Figure 8.5. Microseismic activity decreased over the next few hours. Inspection of the 18th level showed significant damage to the back and over 30 cm of broken rock covered the drift floor. Drilling in the crown pillar was difficult because of its fractured condition. After one production blast a small rockburst occurred in the pillar above the level, otherwise the remainder of the crown pillar was mined without further incidents. Although destressed, the pillar above the level was not mined, due to the unconsolidated fill above.

In another crown pillar destress blast a rockburst occurred in a boxhole pillar above the level, three days after the blast, without warning. Destressing of six boxhole pillars of a shrinkage stope may have contributed to instability in the area. Subsequently, this shrinkage mining zone was subject to a chain reaction of crown pillar failures with associated rockbursts over a two-day period.

8.3.2 Macassa Mine, Lac Minerals Ltd.

At Kirkland Lake, the gold bearing zones are associated with a prominent fault system known as the Main Break. At the Macassa Mine, the main ore bearing structure is the 04 Break which is sub-parallel to the Main Break. The planar orebody is 2 to 6 m wide and dips steeply at 75^{o}. At the west end of the mine, where most production is now concentrated, depth below surface ranges from 1400 m to 2150 m. Cut-and-fill is the predominant mining method. Prior to 1986, unconsolidated waste development rock was used exclusively as backfill. Since that time, cement rock fill was introduced and now accounts for almost 100% of the backfill poured.

Macassa Mine has had a history of rockbursts since 1935 and more than 400 have been reported (Arjang and Nemcsok, 1987). Approximately 70% of these bursts occurred in the ore zone or stopes and 10% of these were classified as heavy bursts with more than 50 tonnes of displaced rock and sometimes more than 1000 tonnes.

Crown pillars in the cut-and-fill stopes tend to become rockburst-prone when their width approaches 18 m and after 60% extraction. Figure 8.6 shows the destress layout in the 58-40 crown pillar (Hanson et al., 1987). Prior to the destress, three rockbursts had occurred in the pillar, in the raises at both ends, and in the back of the stope, displacing 20 to 100 tonnes of rock. The pillar was drilled off with 64 mm holes at 3 m spacing. Drilling indicated that the first 4 m had already fractured due to mining. ANFO was loaded into the destress holes with a powder factor of 0.15 kg/m^3 and 2.5 m of stemming. The holes were blasted in sequence, from borehole 1 to 14, using millisecond delays. Of these 14 holes, No. 1 could not be loaded properly because of squeezing ground near the collar, and hole No. 14 appeared to misfire.

A microseismic system with waveform recording had been installed around the crown pillar prior to the destress blast. Considerable microseismic activity, as shown in Figure 8.7, followed by the blast, mainly clustered around the crown pillar. However, some parts of the pillar were free of seismic activity, especially the east end of the pillar in the vicinity of hole No. 1, which was not fully loaded. Significant convergence of about 25 mm also occurred in the stope, except for only 6 mm adjacent to hole No. 1. Subsequent mining of the crown pillar triggered a small rockburst in the east raise, causing damage to the timber stalls; in addition convergence in this area increased to 33 mm. It was concluded that the initial convergence and microseismic activity was indicative of only partial destressing of the crown pillar.

About one year later, a series of rockbursts occurred after blasting in the crown pillar immediately above the destressed pillar. Damage amounted to about 1000 tons of displaced rock (see Section 10.3 for details). No damage occurred in the stope of destressed pillars but the adjacent drift to the east was severely damaged. This drift was above a waste pillar that had not been

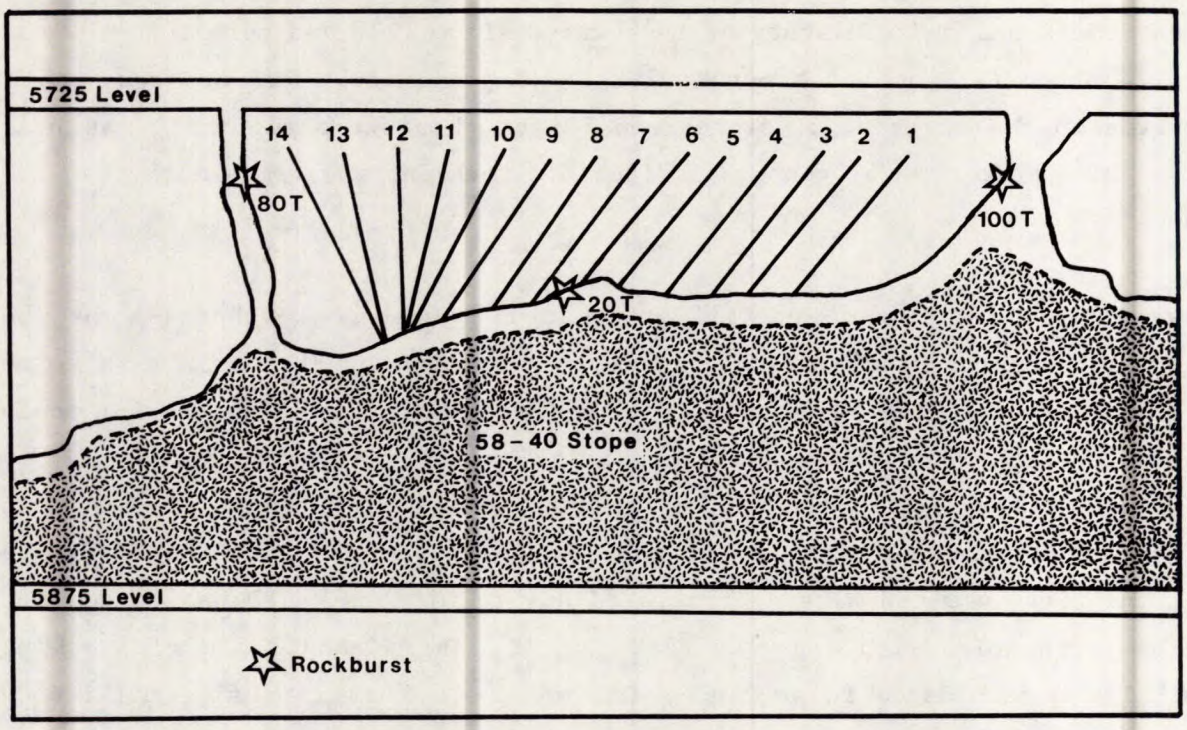

Fig. 8.6 - Layout of destress holes in the 58-40 crown pillar at the Macassa Mine.

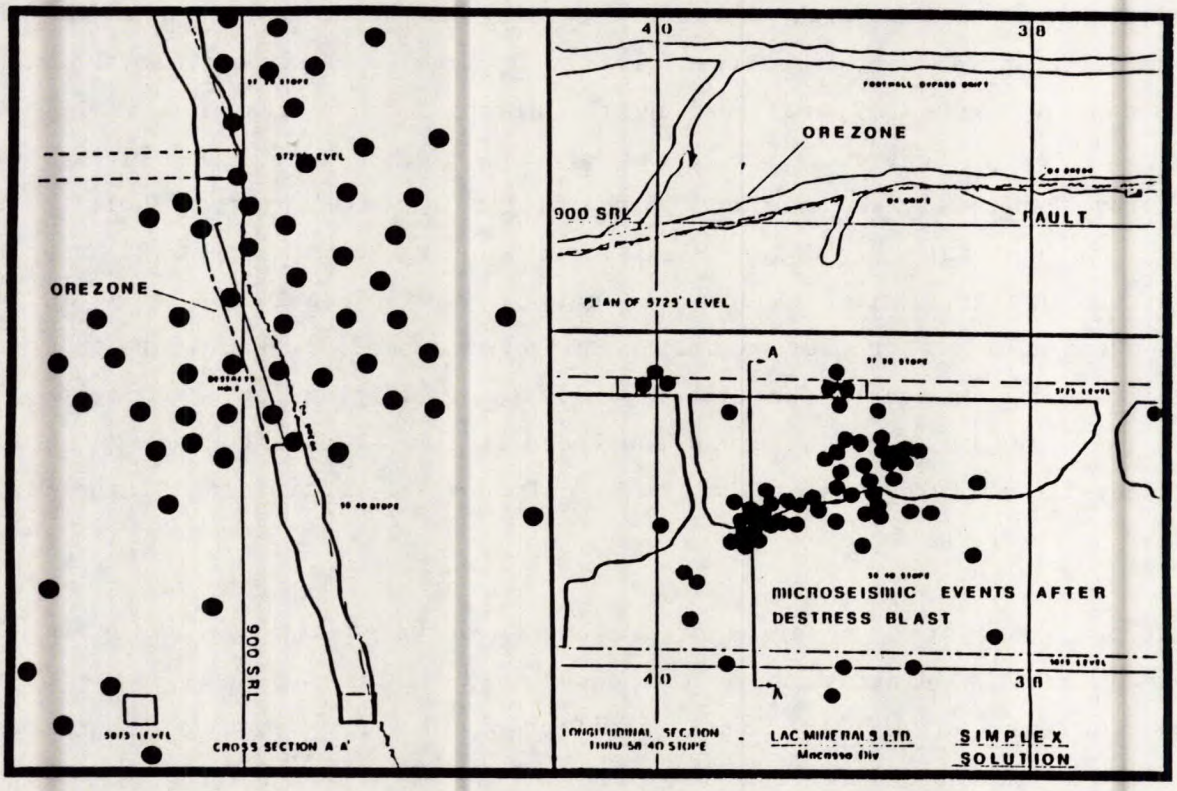

Fig. 8.7. - Location of microseismic activity following the destress blast.

destressed. In the final analysis, destressing of the 58-40 crown pillar probably improved conditions in the pillar itself but may have contributed to rockburst problems in the surrounding pillars.

The introduction of cemented rock fill and the conversion to predominantly undercut-and-fill have almost eliminated the need to destress blast at the Macassa Mine.

8.3.3 Lucky Friday Mine, Hecla Mining Company

The Lucky Friday Mine lies at the eastern most end of the Coeur d'Alene Mining District in Idaho. The lead-silver vein, 2 to 3 m wide, dips at about 80^{o} to a depth of 1620 m. Initially, overhand cut-and-fill methods were used. The mine has had a history of rockbursts since the 1960s. These generally occurred in the sill pillars as the stopes approached the mined-out level above. Destressing techniques, similar to those used at the Campbell and Macassa mines, were used in these sill pillars with moderate success.

In the early 1980s, Hecla conducted trials using undercut-and-fill techniques to recover the sill pillars (Bush et al., 1982). This eventually led to use of underhand techniques with 7:1 cemented tailings as the primary stoping method (Williams and Cuvelier, 1988).

One of these underhand stopes had progressed eight cuts (about 25 m) from the 4900 level when it was decided to destress the 28 m pillar beneath. Below the pillar was a previously-mined overhand cut-and-fill stope. During the mining of the first eight cuts, about 20 bursts greater than a magnitude 1.0 had occurred in the pillar or on the North Control Fault which is the eastern boundary of the stope.

The layout of the destress blast is shown in Figure 8.8. The stope extends about 180 m along strike and was drilled off with 140 mm holes, about 24 m long with an average spacing of 3 m. Continuous microseismic activity occurred during the two-month period of drilling the 58 destress holes, including a 2.5 magnitude burst which caused some damage to the floor. The bottom 15 m of each borehole was loaded with about 118 kg of powder (Apex 340)

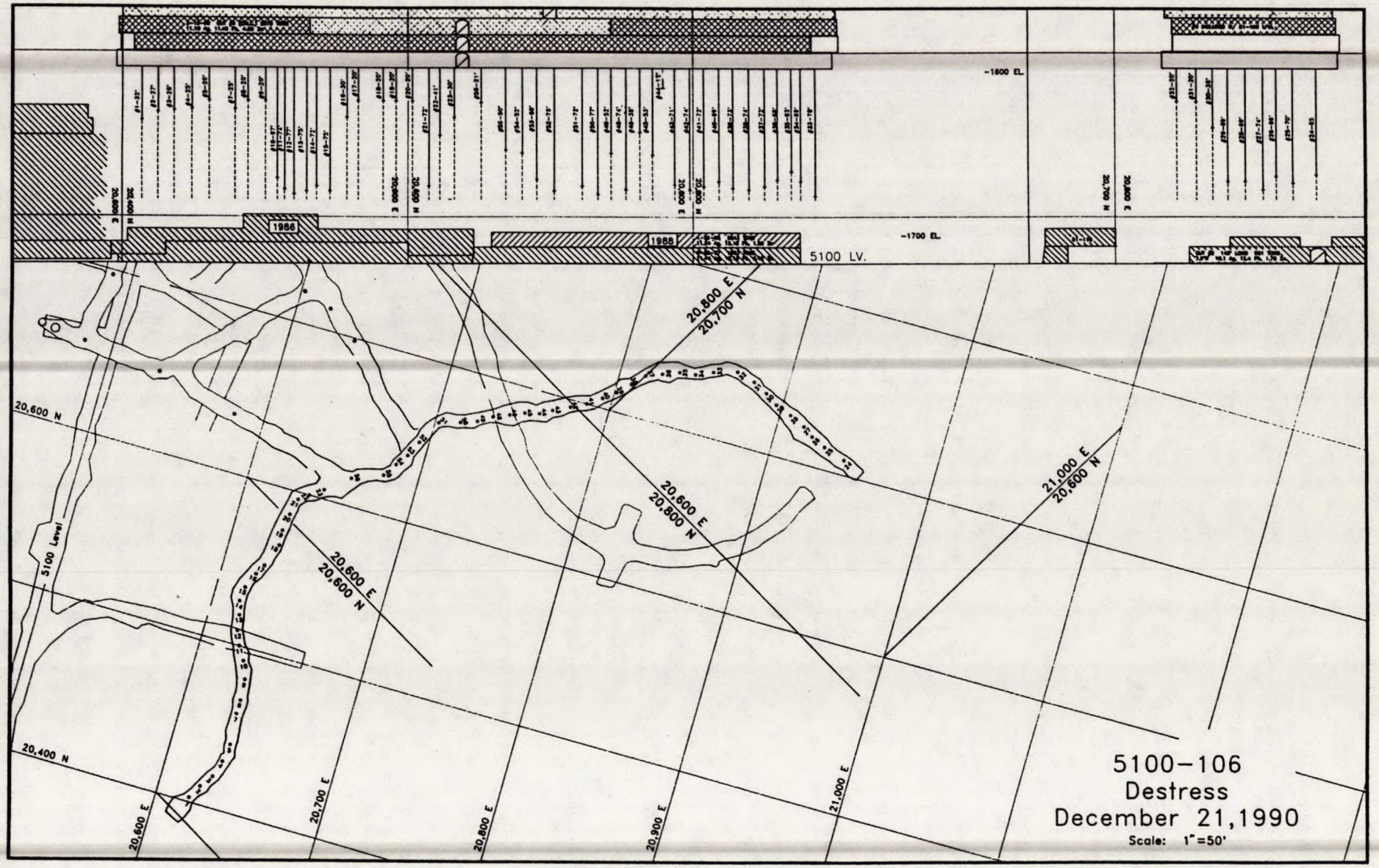

Fig. 8.8 - Layout of destress holes in an underhand longwall, Lucky Friday Mine.

with 6 m of stemming at the top of each borehole. Total explosive charge was 6,366 kg for an average powder factor of 0.6 kg/m^3.

The destress blast was detonated from west to east using millisecond delays between boreholes. A burst of magnitude 2.0 occurred in the middle of the blast. In the following 48 hours there was continuous microseismic activity in the destressed pillar, including an occasional low magnitude event. Since mining resumed, there have been several large events up to a magnitude of 2.8 which have all occurred along the North Control Fault zone, 30 m above to 30 m below the mining horizon (Blake, 1991). There has been no seismic activity in the vicinity of the vein or immediate wall rock, which appears to have been shattered.

8.3.4 Creighton Mine, Inco Ltd.

The 400 orebody at Creighton Mine is being mined to a depth of 2150 m. This orebody is about 230 m on strike, 65 m wide, with an overall dip of 65°. Levels are established at 60 m intervals. Initially, mining at depth was mechanized cut-and-fill starting at the lower level and advancing upwards. This created a crown pillar with the associated high stress problems, including rockbursts, when the pillar thickness was reduced to about 30 m.

It was decided to convert from mechanized cut-and-fill to vertical retreat mining to extract the crown pillar between the 6600 and 6800 levels. Rock mechanics studies indicated that mining a narrow transverse slot across the middle of the orebody would relieve the stress in the crown pillar and result in a significant release of potential energy (MacDonald et al., 1988). Hence, the major release of energy would occur at the beginning of the mining cycle rather than in the final stage.

Figures 8.9a) and b) show the layout of the destress slot on both a longitudinal section and plan. The 6 m wide slot was mined in a series of five panels, between June 1984 and May 1987, in the sequence shown in Figure 8.9b). Initially the crown pillar was 35 m thick, but in the three-year period taken to excavate the slot, mining continued in the cut-and-fill stopes below.

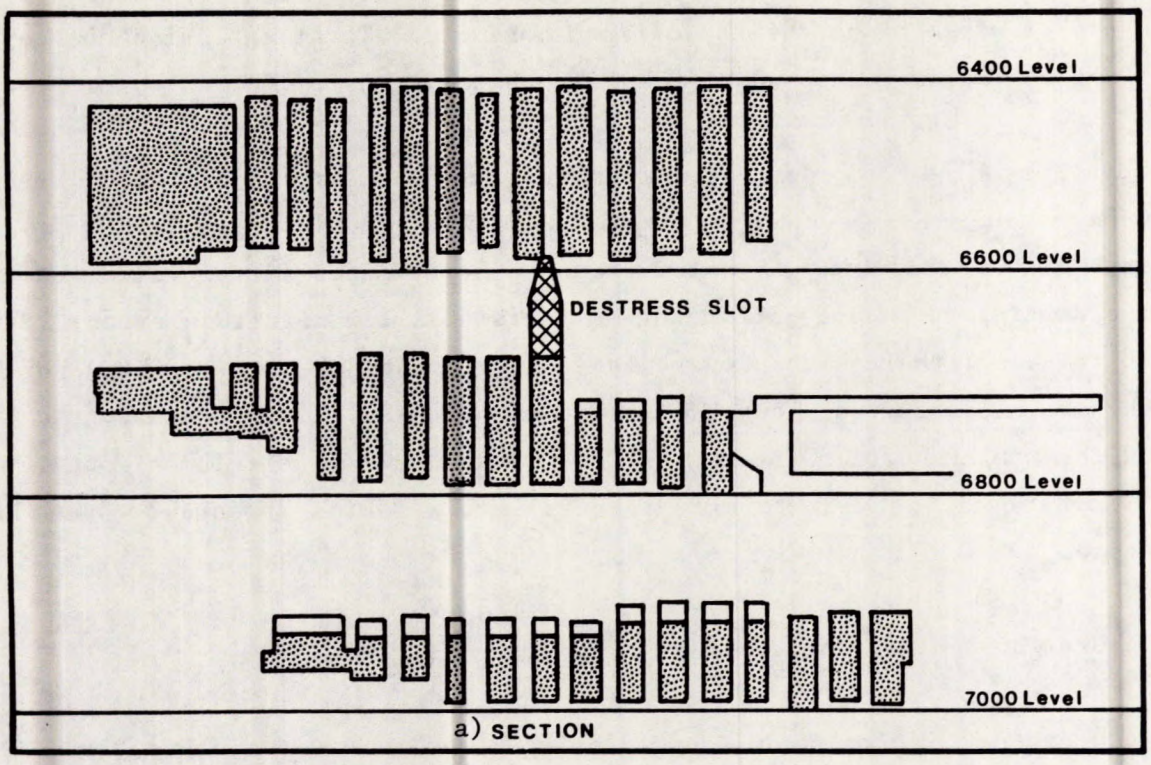

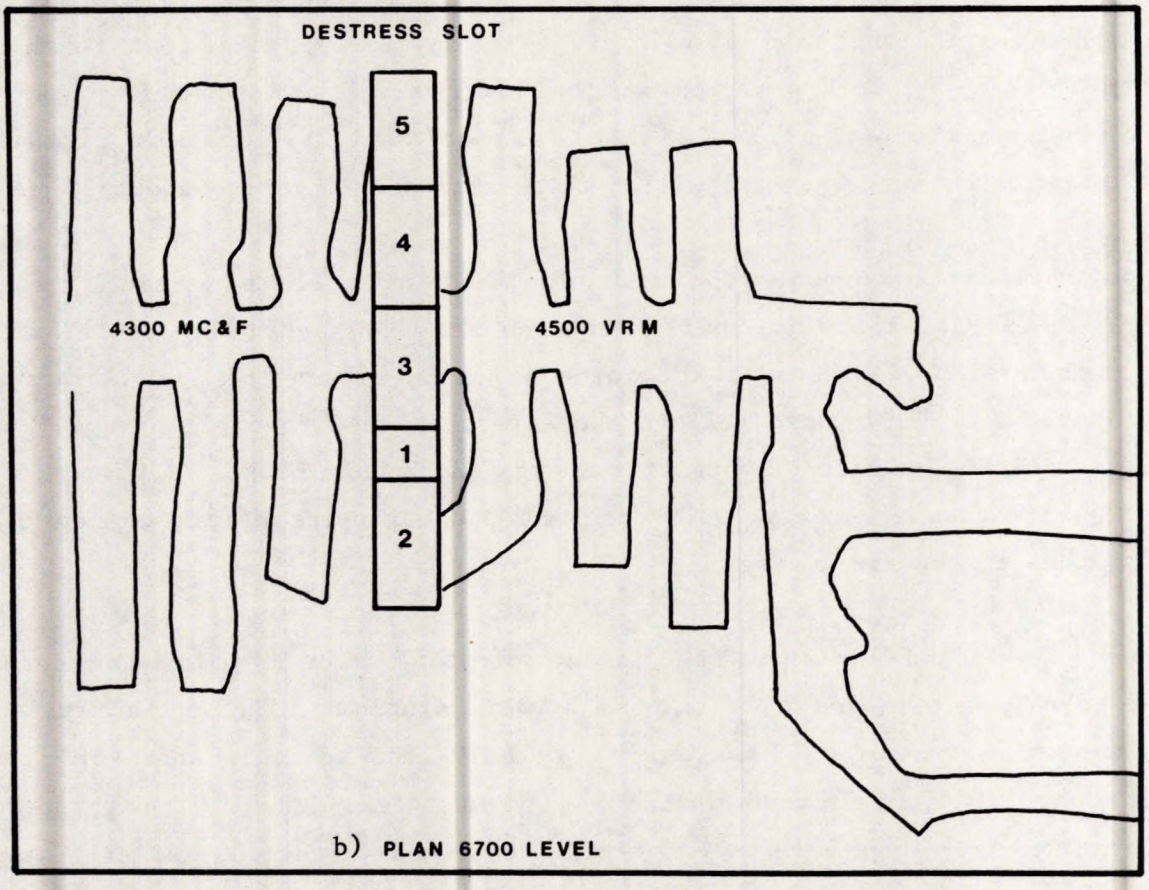

Fig. 8.9 - Layout of destress slot in the 6600-6800 crown pillar, Creighton Mine.

The first slot panel was 6 m by 6 m and drilled off with 159 mm boreholes at about 3 m spacing. Blasting started at the bottom and retreated upwards in 3 m slices. On completion the panel was backfilled with cemented tailings. Panel 2 was extracted in a similar manner, 15 m long towards the footwall, followed by panels 3, 4 and 5 towards the hanging wall.

Thousands of microseismic events occurred during mining of the slot, mainly in the crown pillar itself rather than in the cut-and-fill stopes above and below. Most of these events occurred within two hours after blasting. Three rockbursts were induced, up to a magnitude of 2.8 Mn, which caused damage to the drill sill and displaced some rock in the cut-and-fill stopes beneath.

Vertical retreat mining started in 1987 adjacent to the destress slot on the east side, followed in 1988 on the west side. A 'V' pattern has been established, retreating from the hanging wall. During this mining, microseismic activity continued in the crown pillar area. In addition two major 3.6 Mn magnitude events occurred on the 6800 and 6600 levels on the western abutment of the stoping-block. These events are thought to be associated with prominent fault structures. However, no damage occurred to the stopes.

8.4 Development Destressing Practices

Destressing of development openings, including shafts, is practiced on a regular basis at Inco's Creighton Mine (Dickout, 1962 and Oliver et al., 1987). In the early 1960s destressing techniques were first used on cross-cuts on the 5400 level (depth 1645 m). A single hole 67 mm diameter by 14 m long was drilled in the centre of the drift face. This hole was loaded with dynamite to within 3 m of the collar and blasted. Four 3 m face rounds were then taken before the next destress hole was drilled. Although successful in eliminating rockbursts, the drift advance had to be disrupted to set up a longhole machine to drill the destress hole.

The next development was to drill two 32 mm diameter holes double the round distance. These holes were loaded to the collar with ANFO and blasted with the round. Present day practice is illustrated in Figure 8.10 and is used

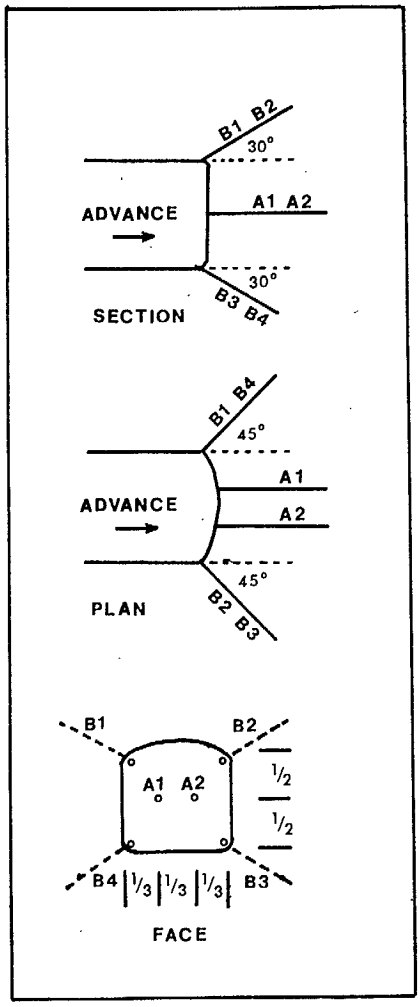

FACE DESTRESSING

Drill two holes A1, A2, halfway up on face and one third width in from walls. Drill holes flat. See chart for length.

WALL DESTRESSING

Drill four holes B1, B2, B3, B4, one in each corner of the face. Drill up and down at 30° and angle out at 45° from direction of advance. See chart for length.

REMARKS

Loading of destress holes: the bottom portion of each hole is to be loaded to depth shown in chart.

Blasting of destress holes: all destress holes must be fired before the first shots of the round.

Drift Advance	Face Holes A	Wall Holes B	Loading Depth
1.8 m	3.0 m	2.4 m	0.9 m
2.4 m	3.7 m	3.0 m	1.2 m
3.0 m	4.3 m	3.7 m	1.5 m
3.7 m	4.9 m	3.7 m	1.5 m
4.3 m	5.5 m	3.7 m	1.5 m

Fig. 8.10 - Standard destressing procedure for development headings at Inco's mines (courtesy of Inco Ltd.).

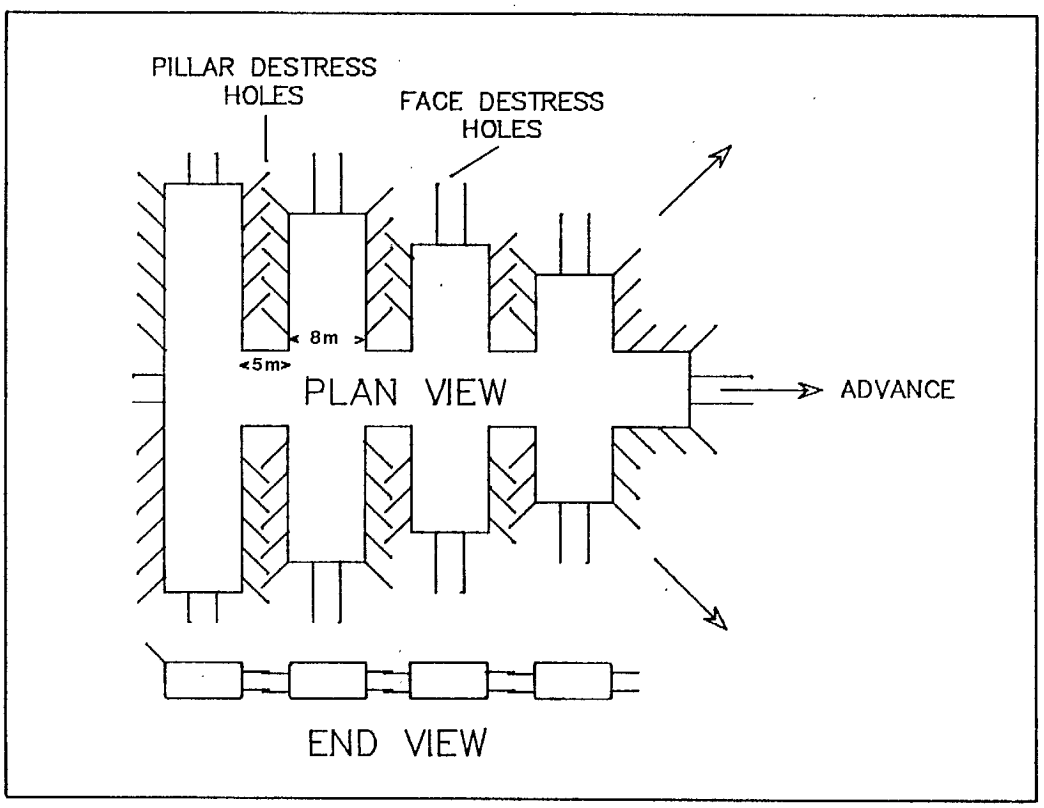

Fig. 8.11 - Destressing procedure for stope faces and rib pillars during silling operations (after Oliver et al., 1987).

exclusively below the 6000 level (1820 m) at the Creighton Mine. From the 6000 level down to the 7000 level (2130 m), the two holes in the face and the two corner holes in the roof are drilled. Below the 7000 level, the two extra corner holes in the floor are also drilled. Borehole size varies from 32 mm to 41 mm, depending on the type of drilling equipment being used in the heading. The length of the destress holes varies with drift advance as specified on the chart in Figure 8.10. The toe of the holes is loaded with ANFO and detonated first, just before the main blast.

Transverse mechanized cut-and-fill stopes are generally laid out with 8 m wide stopes and 5 m wide rib pillars. Above the 6400 level (1950 m), the rib pillars tended to yield non-violently on the second to fourth cut when the pillars were slender and relatively weak. On the 6600 level and deeper, rockbursts started to occur in the rib pillars during silling operation, when the pillars were squatter and much stronger. In these conditions, destressing is practiced in both the rib pillar and stope face as illustrated in Figure 8.11. Two 3 m holes are drilled into the side of the pillar and two 5.5 m holes into the stope face. The bottom of the holes is loaded with ANFO and detonated first, just before the main blast. This procedure did not stop rockbursts, but reduced their severity and caused most to occur shortly after the blast (Oliver et al., 1987).

8.5 Fault Destress Trials

Rockbursts generated by slippage along faults have been initiated by blasting (Morrison, 1987) and micro-earthquakes by fluid injection (Healy et al., 1968). However, these occurrences were unintended. Recently two trials have been conducted in South African gold mines to trigger slippage along specific faults, one by blasting in the plane of the fault (Brummer, 1988), and the other by fluid injection (Board, 1991).

8.5.1 Fault Destressing by Blasting

The first attempt to trigger slippage on a fault by blasting was done in a gold mine in the Klerksdorp area in 1987. Mining of the reef, at a depth of 2500 m, had already taken place on both sides of the fault. The fault which

dips at about 63° had displaced the reef by about 40 m.

Two-dimensional boundary element models were run as illustrated in Figures 8.12a) and b). For a cohesion of 80 MPa and a friction angle of 30°, the fault was locked. When the cohesion was reduced to 20 MPa, slippage occurred on the fault in the order of 200 mm.

From a tunnel which intersected the fault, twelve 20 m long boreholes, 60 mm in diameter were drilled in the fault plane in a semicircular fan. Only seven of the boreholes could be loaded with 50 kg of explosive for a total charge of 350 kg. Stemming was placed in the first 12 m of each borehole. The same electric delays were used to detonate the explosive.

The blast did not produce the expected fault slip nor generate any large seismic events. It was thought that the blast may have been too small or insufficiently confined. In addition, simultaneous detonation was not achieved.

8.5.2 Fault Destressing by Fluid Injection

The fluid injection trial was also done in a gold mine in the Klerksdorp area in 1990 (Board, 1991). Figure 8.13 shows a cross-section through a major fault that dips at 45° and has displaced the reef by about 45 m. Mining of the reef had already taken place on both sides of the fault except for an isolated pillar up against the fault, on the lower horizon. This pillar, at a depth of 675 m, was in the process of being mined.

Three boreholes 60 mm in diameter were drilled from the 26 X-cut to intersect the fault beneath the pillar. Casings 46 mm in diameter were fully grouted into the boreholes except at the borehole fault intersection. The pump had a capacity of 30 L/min up to 60 MPa pressure that was subsequently augmented with a second pump of 80 L/min capacity. A seven-channel microseismic system and a triaxial accelerometer for waveform recording were installed around the fluid injection area for event location.

Two- and three-dimensional computer models indicated that fluid pressure over

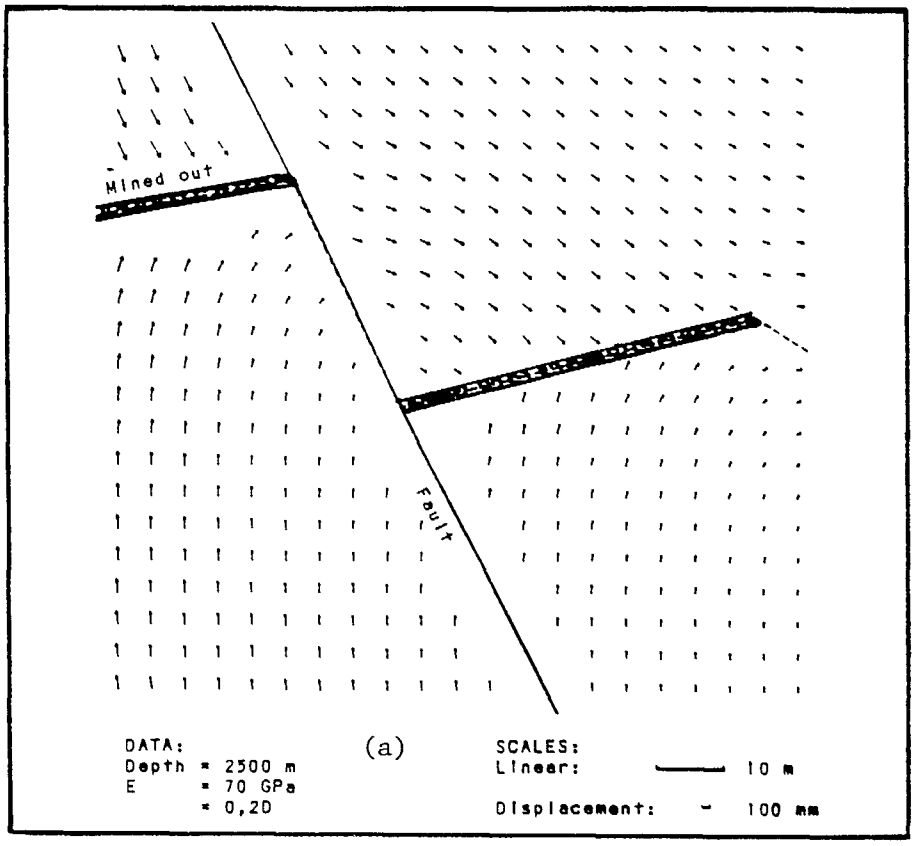

c = 80 MPa ϕ 30°

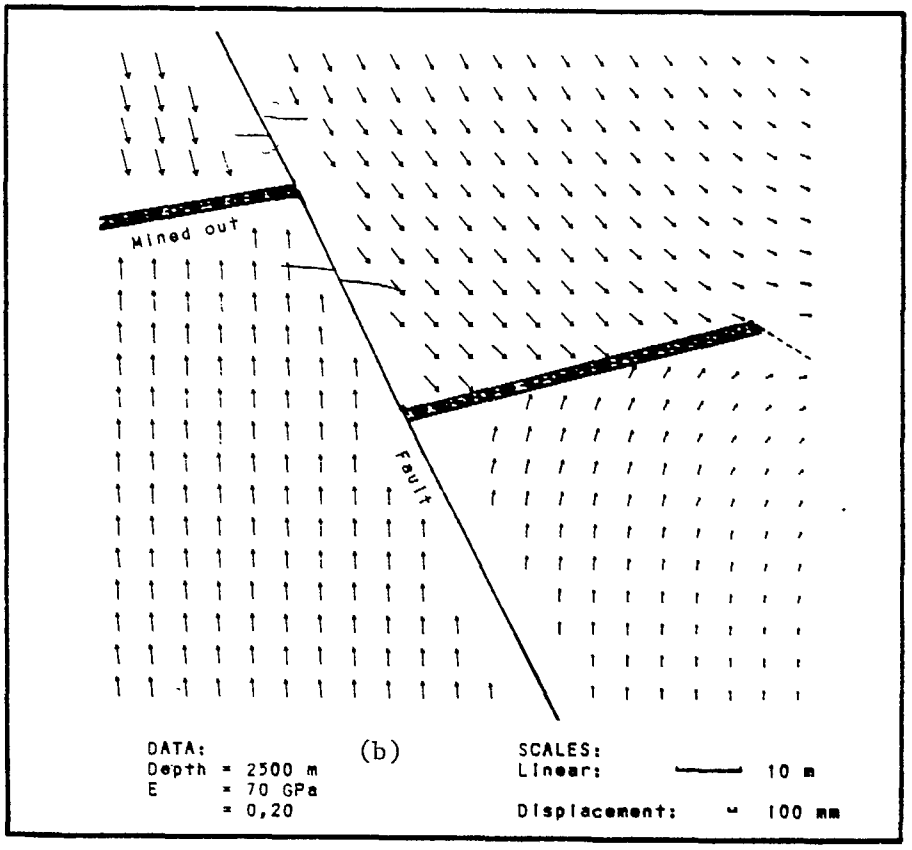

c = 20 MPa ϕ 30°

Fig. 8.12 - Displacement vectors before and after slippage on a fault (after Brummer, 1988).

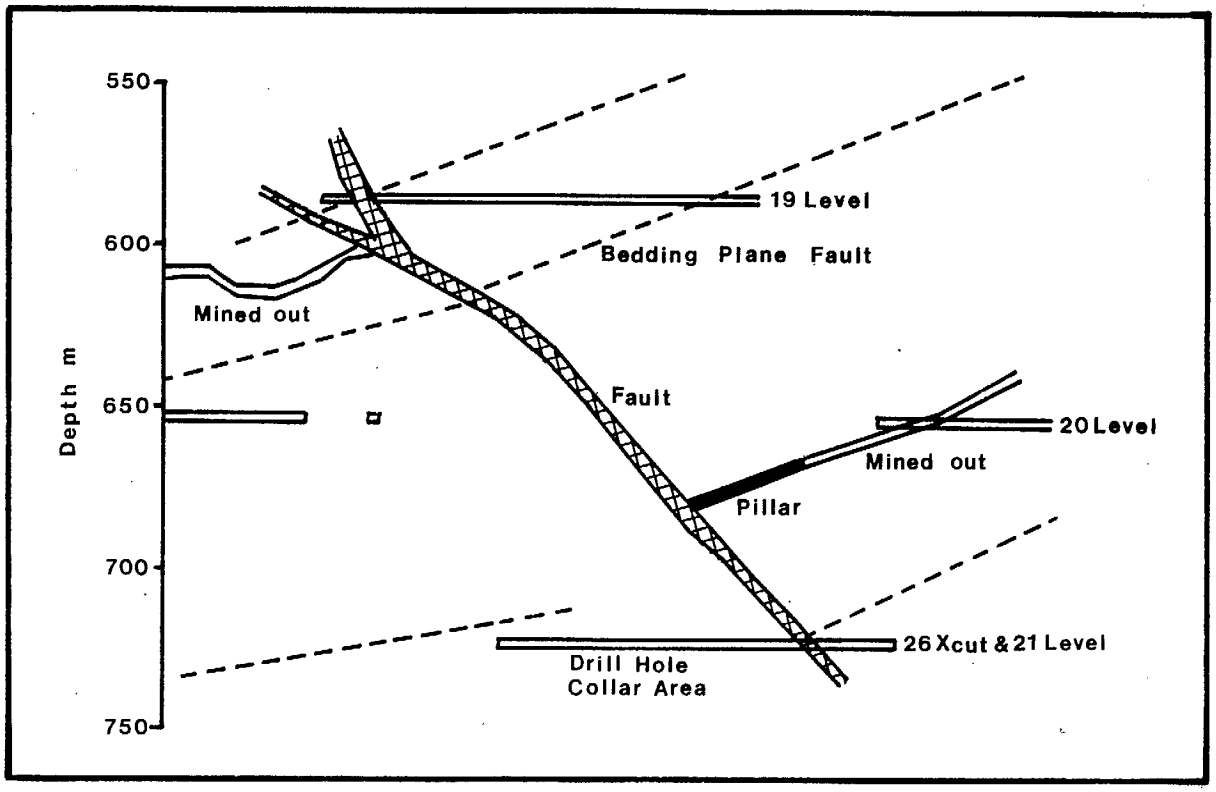

Fig. 8.13 - Cross-section showing the layout of a fluid injection fault destress trial (after Board, 1991).

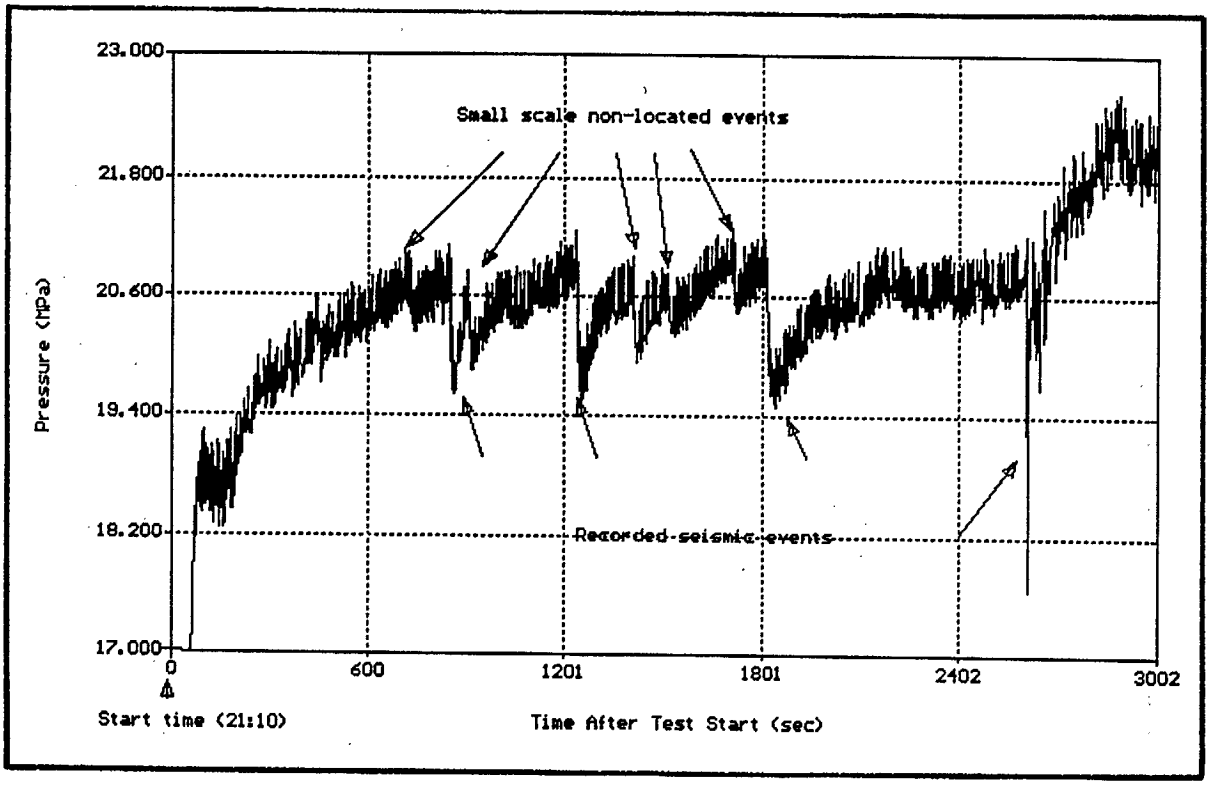

Fig. 8.14 - Record of pressure build-up and drops with associated seismicity during a fluid injection trial (after Board, 1991).

10 MPa could initiate significant slip and shear stress drop on the fault. Fluid pressures in excess of 20 MPa could open up the fault over portions of the injection surface.

In the first three injection trials, pressures of up to 18 MPa and 30 L/min were achieved. Pressure drops of up to 3.5 MPa occurred during the pumping accompanied by audible seismic activity. However, the sensitivity of the microseismic system was not great enough to record these events.

For the fourth test the sensitivity of the microseismic system was increased and a second pump was added to the circuit. Figure 8.14 shows the record of pressure build-up and stress drops and its relation to seismic activity. In this trial, 11 seismic events with magnitudes from -0.75 to -1.00 ML were located as were 200 smaller events. It was estimated that these magnitude events represented slippage over radii of 1 to 2 m. A maximum pressure of 25 MPa was achieved with observed leakage of the injection water indicating that the fault had opened.

Although controlled seismic activity was achieved by fluid injection, no anticipated events of magnitude of about 1.5 ML were induced. To achieve these larger seismic events would require slippage over larger areas of the fault.

8.6 References

Arjang, B. and Nemcsok, G., (1987), Review of rockburst incidents at the Macassa Mine, Kirkland Lake. Division Report MRL 87-21(TR), CANMET, Energy, Mines and Resources Canada.

Biskup, E. and Kaiser, P.K., (1990), Fault property determination at two Inco mines. Geomechanics Research Centre Report, Laurentian University, Sudbury, Ontario.

Blake, W., (1972), Rock-burst mechanics. Colorado School of Mines Quarterly, vol. 67, No. 1.

Blake, W., (1972), Destress test at the Galena Mine. Trans. SME-AIME, vol. 252.

Blake, W., (1982), Rock preconditioning as a seismic control measure in mines. Rockbursts and Seismicity in Mines, Johannesburg, S. Afr. Min. Met., Symp. Series No. 6.

Blake, W., (1991), Personal communication.

Board, M.P. and Fairhurst, C., (1983), Rockburst control through destressing - a case example. Symp. Rockbursts: Prediction and Control, IMM, London, pp. 91-102.

Board, M., (1991), Personal communication.

Brady, B.H.G., (1988), Rock stress, structure and mine design. Proc. 2nd Int. Symp. Rockbursts and Seismicity in Mines, Minneapolis, A.A. Balkema, Rotterdam, pp. 311-322.

Brummer, R.K., (1988), Active methods to combat the rockburst hazard in South African gold mines. CARE, Univ. Newcastle-upon-Tyne, Pub. IMM London, pp. 35-43.

Bush, D.D., Blake, W. and Board, M.P., (1982), Evaluation and demonstration of underhand stoping to control rockbursts, U.S. Bureau of Mines, Contract Report HO 292013, pp. 191.

Coates, D.F., (1981), Rock mechanics principles; Chapter 8 - Rock dynamics. Energy, Mines and Resources Canada, Monograph 874 (Revised).

Cook, N.G.W., Hoek, E., Pretorius, J.P.G., Ortlepp, W.D. and Salamon, M.D.G., (1966), Rock mechanics applied to rockbursts. J. S. Afr. Inst. Min. Met., May 1966, pp 435-528.

Cook, J.F. and Bruce, D., (1983), Rockbursts at Macassa Mine and the Kirkland Lake mining area. Symp. Rockbursts: Prediction and Control, IMM, London, pp. 81-90.

Crouch, S.L. (1974), Analysis of rock bursts in cut-and-fill stopes. Trans. SME-AIME, vol. 256, pp. 298-303.

Dickout, M.H., (1962), Ground control at the Creighton Mine of the International Nickel Company of Canada Limited. Proc. 1st Can. Rock Mech. Symp., McGill University, Montreal, pp. 121-139.

Duvall, W.I. and Stephenson, D.F., (1965), Seismic energy available from rockbursts and underground explosions. Trans. SME-AIME, pp. 235-240.

Garrood, P.S., (1982), Ground control aspects of the development at Creighton No. 11 shaft. 14th Can. Rock Mech. Symp., Vancouver.

Hanson, D., Quesnel, W. and Hong, R., (1987), Destressing a rockburst prone crown pillar - Macassa Mine. Division Report MRL 87-82(TR), CANMET, Energy, Mines and Resources Canada.

Healy, J.H., Rubey, W.W., Griggs, D.T. and Raleigh, C.B., (1968), The Denver earthquakes. Science, 161, pp. 1301-1310.

MacDonald, P., Wiles, T. and Villeneuve, T., (1988), Rock Mechanics aspects of vertical retreat mining at 2000 m depth at Creighton Mine. CARE Univ. Newcastle-upon-Tyne, Pub. IMM, London.

Morrison, D.M., (1987), Rockburst research at Falconbridge Limited. CIM Annual General Meeting, Toronto.

Moruzi, G.A. and Pasieka, A.R., (1964), Evaluation of a blasting technique for destressing ground subject to rockbursting. 6th U.S. Rock Mech. Symp., Rolla, Missouri.

Neumann, M., Makuch, A., Hedley, D.G.F. and Blake, W., (1987), Practical applications of pillar destressing at Campbell Red Lake Mine. 8th CIM Underground Operator's Conf., Elliot Lake, Ontario.

Oliver, P., Wiles, T., MacDonald, P. and O'Donnell, D., (1987), Rockburst control measures at Inco's Creighton Mine, Proc. 6th Conf. on Ground Control in Mining, West Virginia.

Rorke, A.J. and Brummer, R.K., (1988), The use of explosives in rockburst control techniques. Proc. 2nd Int. Symp. Rockbursts and Seismicity in Mines, Minneapolis, A.A. Balkema, Rotterdam, pp. 377-386.

Rorke, A.J., Cross, M., Van Antwerpen, H.E.F. and Noble, E., (1990), The mining of a small up-dip remnant with the aid of preconditioning blasts. Int. Deep Mining Conf., Johannesburg, S. Afr. Inst. Min. Met., Symposium Series S10, pp. 765-774.

Roux, A.J.A., Leeman, E.R. and Denkhaus, H.G., (1957), Destressing: a means of ameliorating rockburst conditions. Part 1: the concept of destressing and results obtained from its application. J. S. Afr. Inst. Min. Met., October 1957, pp. 101-127.

Salamon, M.D.G., (1974), Rock mechanics of underground excavations. Proc. 3rd Congr. Int. Soc. Rock Mech., Denver, Colorado, vol. 1, Part B, pp. 951-1099.

Swan, G., (1991), Personal communication.

Williams, T.J. and Cuvelier, D.J., (1988), Report on a field trial of an underhand longwall mining method to alleviate rockburst hazards. Proc. 2nd Int. Symp. Rockbursts and Seismicity in Mines, Minneapolis, A.A. Balkema, Rotterdam, pp. 349-354.

Blocked drift at edge of rockburst area at Campbell Mine.

Partial pillar failure at Denison Mine.

9. PREDICTION OF ROCKBURSTS*

9.1 Introduction

Rockbursts are a unique hazard associated with deep mining because it is seldom known when or where a burst will occur. This feature causes great anxiety to underground workers as well as to operating staff. For this reason a means of predicting rockbursts has been sought by mining companies and research organizations for more than 50 years.

The development of the microseismic method by the USBM in the late 1930s appeared to have great potential with respect to rockburst prediction. Unfortunately, extensive field testing of this technique in burst-prone mines in the 1940s failed to produce enough success to justify continued use of microseismic monitoring for rockburst prediction. Renewed interest in the use of microseismic monitoring in deep mines was aroused in the late 1960s when USBM research indicated that burst-prone mine structures could be identified by plotting the source locations of microseismic events on mine maps. Extensive use of microseismic monitoring in the 1970s, by both mining companies and research organizations, showed that while highly stressed mine structures could often be delineated, only in a few rare instances were rockbursts successfully predicted. Such monitoring was still being aggressively carried out in the 1980s utilizing much more sophisticated instrumentation and data analysis procedures. However, the low success ratio for rockburst predictions has not really improved.

Motivation for renewed and accelerated rockburst research in Ontario, including prediction, was brought about by the recent and unexpected occurrences of rockburst sequences at a number of mines, i.e., Quirke, Campbell Red Lake, Falconbridge, Creighton and Strathcona. Hence, the purpose of this chapter is to review and assess the state-of-the-art regarding rockburst prediction.

---

*Prepared by Wilson Blake

9.2 Prediction of Rockburst Location

While the ultimate goal of a successful rockburst prediction includes both its location and time of occurrence, it would be sufficient in most mining applications if just the location of an impending burst could be accurately determined. Knowledge of where a burst will occur allows time for strategies to be taken to deal with an expected burst.

9.2.1 Rockburst Location Based on Stress Concentration

Before the development of instrumentation or stress analysis techniques to delineate highly stressed zones, potential burst locations were identified based on past observations and mining experience. By the early 1900s, it was recognized in both India and South Africa that rockbursts occurred mostly in small pillars. Knowledge of where bursts were most likely to occur led to changes in mining geometries and sequences to avoid obviously highly stressed pillars. It was also recognized that mining and development openings were more burst prone when a geologic discontinuity was approached or intersected by an advancing face. Faults, dikes, contacts, and vein splits were identified as potential rockburst locations. Mining plans were often adjusted to minimize bursting when driving headings through such geologic features. However, despite utilizing past experience to predetermine or predict where rockbursts were most likely to occur for a given mining layout, subtle geologic differences or a different wallrock response to mining would result in unexpected bursting in unlikely locations, and often no bursting in likely locations.

Qualitative estimates of stresses resulting from mining geometries became much more quantitative in the 1960s as a result of the use of numerical methods for solving complex boundary value problems on digital computers. Mining layouts to minimize high stress concentrations, and resulting energy release rates (ERR) evolved from computer model simulations of mining carried out in South Africa.

Utilization of displacement discontinuity computer models to evaluate pillar stresses has been carried out in a number of burst-prone mines in Ontario.

Figure 9.1 shows results indicating expected failure zones or potential rockburst locations associated with mining of narrow orebody at the Macassa Mine. These types of models have been used to decide when to destress blast the sill pillars.

Finite element computer model simulations of mining in the Coeur d'Alene mining district of Idaho showed that areas of high stress concentration surrounding a cut-and-fill stope coincided with rockburst locations determined by microseismic monitoring (Blake, 1972). Figure 9.2 shows stress contours for a typical stope and pillar geometry, as well as concentrations of microseismic activity and rockburst locations induced by stope mining. It is interesting to note that the initial bursts, which preceded the major pillar burst, were likely shear failures out in the walls around the bottom of the stope.

Besides being able to provide a quantitative estimate of the magnitude of stress concentrations resulting from complex mining geometries, and hence identify potential burst-prone areas in the immediate vicinity of an advancing face, stress analysis computer models can be modified to evaluate the potential for shear failure on pre-existing geologic features by calculating the excess shear stress (ESS) acting on a plane of weakness. Just as a high stress concentration in a pillar might indicate a pillar burst, a high ESS on a fault or geologic discontinuity would indicate likelihood for a fault-slip seismic event.

Most computer models used for stress analysis, that is, finite element, finite difference, displacement discontinuity, boundary element, assume that the rock is a solid mass with no fractures or faults. By varying material properties, these models can be used to represent the behaviour of fractured rock or planes of weakness. Where this representation is unsatisfactory, a discontinuum model can be used to evaluate the potential for slip on geologic structures. Inco has developed a three-dimensional boundary element model for studying mine designs that will minimize rockburst occurrences at Creighton (Wiles, 1988). Falconbridge has been using a three-dimensional discontinuum model to assess the potential for fault-slip rockbursts at the Strathcona Mine (Hart et al. 1988).

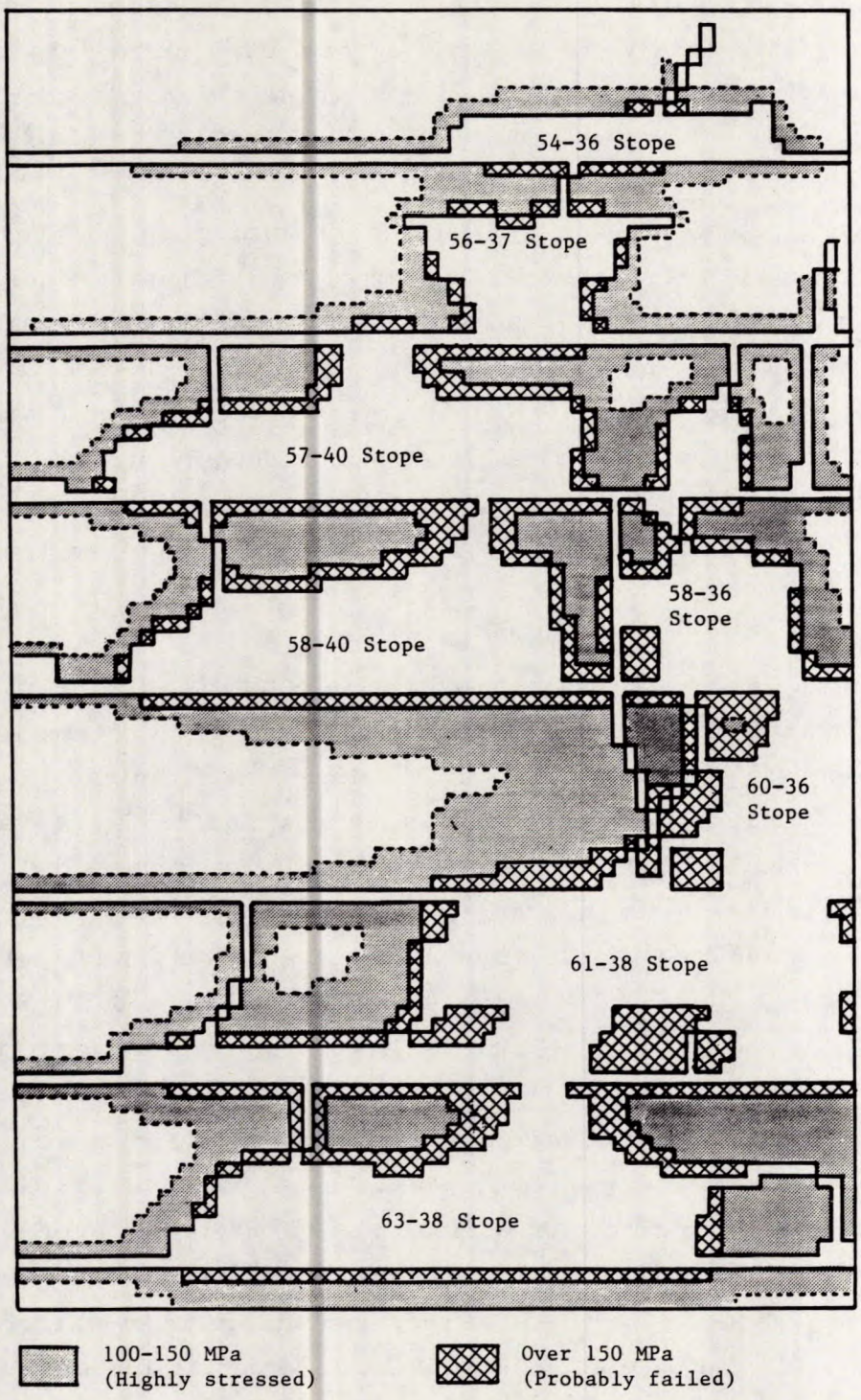

Fig. 9.1 - Computer model of Macassa Mine showing perpendicular stress distribution and area of expected failure and highly stressed ground (after Hanson, et al., 1987).

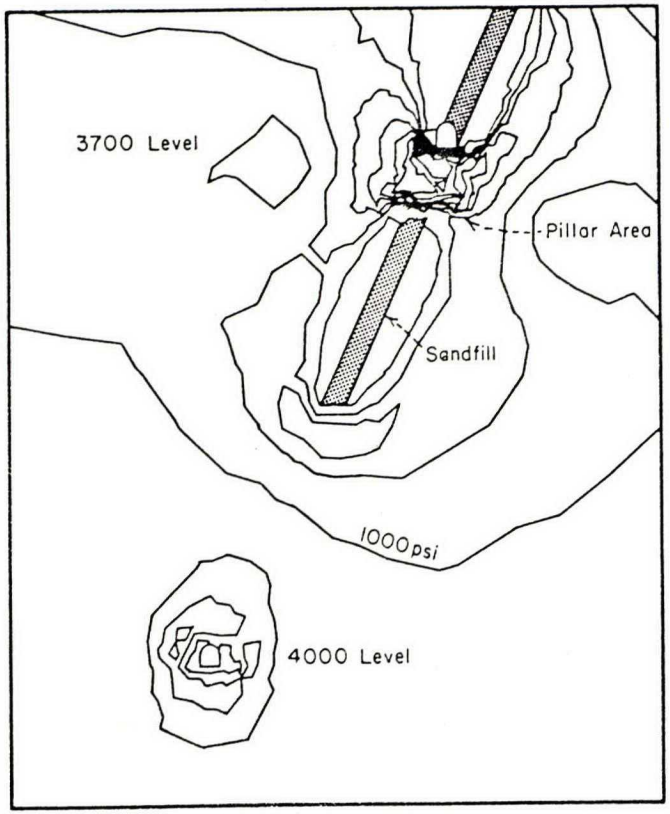

Maximum shear stress contour plots for 30 ft pillar, 1000 psi contour interval.

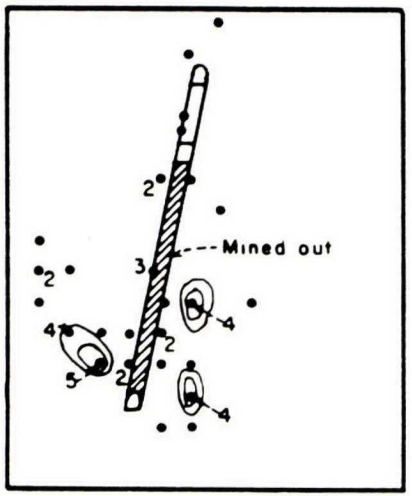

July 25 - July 9

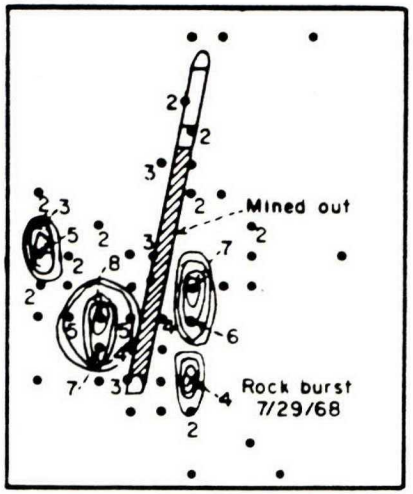

July 25 - July 29

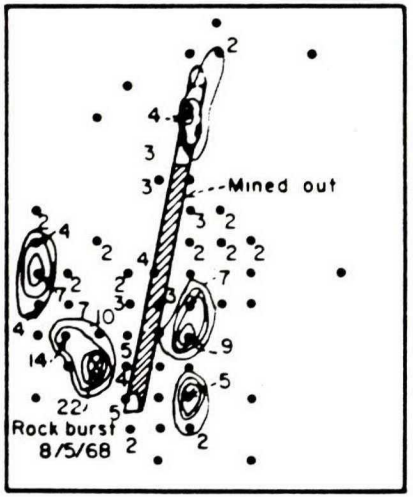

June 25 - Aug. 5

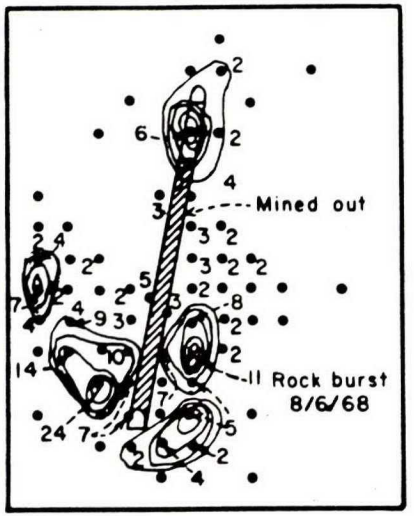

June 25 - Aug. 16

Cumulative plots of rock noise source locations 3400 to 3200 levels, Galena Mine (after Blake and Leighton, 1970).

Fig. 9.2 - Stress contours for pillar geometry and concentrations of microseismic activity (after Blake, 1972).

It should be pointed out that model results are more general than specific. That is, a high stress concentration, ERR or ESS indicates only that there is a potential for a rockburst, and not that a rockburst will in fact occur. Hence, computer model predictions for burst locations need to be supplemented by field observations, geologic data, seismic data and rockburst history in order to improve the reliability of such predictions.

9.2.2 Rockburst Location Based on Microseismic Activity

The USBM publication "Use of Subaudible Noise for Prediction of Rockbursts" (Obert, 1941) aroused great interest in mining camps experiencing rockbursts. It was hoped that use of microseismic monitoring would result in detecting areas of a mine that were about to burst. However, it was impossible with the original microseismic equipment to pinpoint specific burst-prone structures because the source of the microseismic activity could not be determined accurately. In addition, monitoring could be carried out only during quiet times in a mine, thereby excluding a great deal of important data.

Renewed interest in microseismic monitoring in burst-prone mines occurred again in the early 1960s as a result of field tests in South Africa (Cook, 1963). This work demonstrated that the source location of seismic events could be determined accurately using an array of geophones and first arrival time information. It was found that most of the seismic activity detected was occurring immediately ahead of or around an advancing face. Stimulated by this research, the USBM developed a multichannel microseismic monitoring system in the mid-1960s which demonstrated that burst-prone structures could be delineated in some mines (Blake and Leighton, 1970). Figure 9.2 shows development of burst-prone zones surrounding cut-and-fill mining. The USBM also demonstrated that it was possible to carry out microseismic monitoring around the clock automatically (Blake, 1971), that led to the development by mining companies of computer-controlled microseismic data acquisition and analysis systems (Langstaff, 1974).

By the end of the 1970s, rockburst monitoring systems were available commercially and were being installed in burst-prone mines throughout the world. While rockburst prediction may not have been the principal goal of

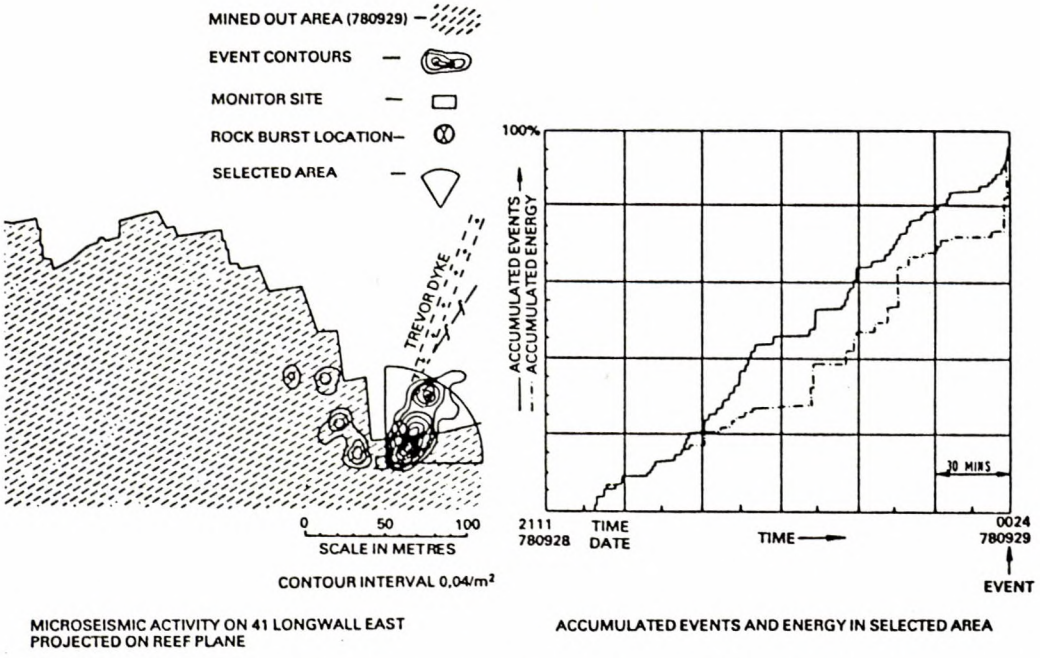

Microseismic events precursive to seismic event at 00h24 on 29-9-78.

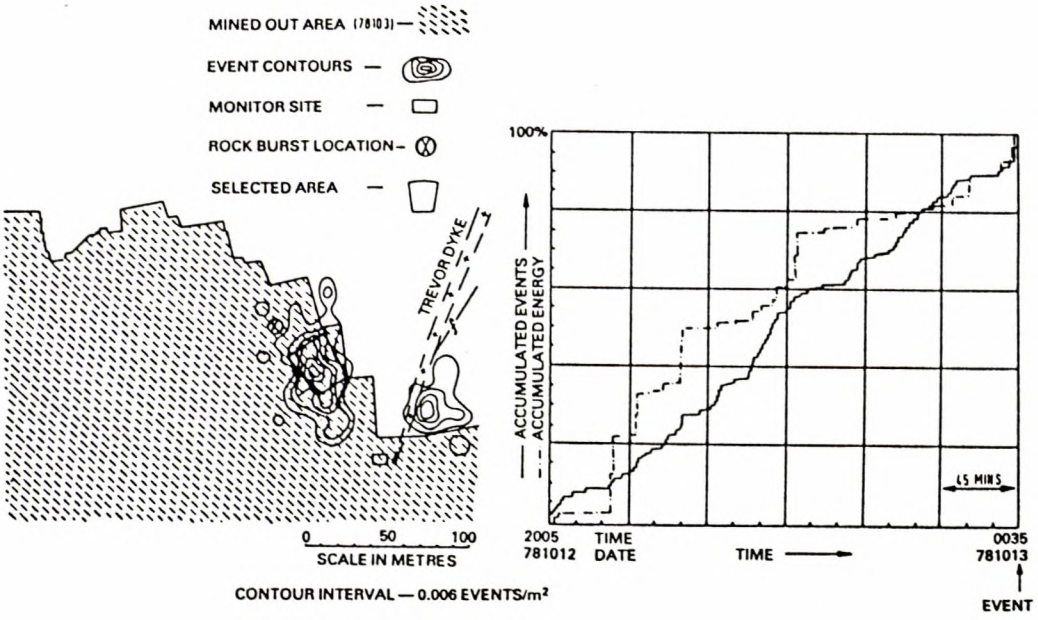

Microseismic events precursive to seismic event at 00h35 on 13-10-78.

Fig. 9.3 - Anomalous microseismic activity associated with longwall mining (after Brink, 1984).

this monitoring, it was given a high priority and did produce encouraging results regarding the delineation of burst-prone mine structures.

In the Coeur d'Alenes, microseismic monitoring is routinely used to identify burst-prone sill pillars or highly stressed headings that might require destressing. The success in delineating burst-prone pillars is to a large extent due to overhand mining with a goal of 100% extraction. Some fault structures have been identified based on microseismic data, but precursor patterns prior to a fault-slip rockburst on a specific structure have not been recognized.

Detailed microseismic monitoring at Western Deep Level Mine in South Africa has indicated that some rockbursts ahead of an advancing face have been preceded by anomalous microseismic activity that clearly delineated the burst-prone structure (Brink, 1984). Figure 9.3 shows the longwall front and the concentration of microseismic activity in the eventual burst location. The percentage of bursts preceded by such a well-defined precursor pattern is unknown.

Microseismic monitoring in Canada has been carried out in most burst-prone mines since the mid-1980s. Identification of burst-prone structures has only rarely been achieved. At the Quirke Mine, there was a build-up in seismic activity in the months preceding the major rockburst incidents in September 1984. However, in the hours preceding the first rockburst, there was no build-up in seismic activity. Microseismic monitoring in the F-2 zone at the Campbell Mine showed that a small burst in a boxhole pillar was preceded by a concentration of microseismic activity as shown in Figure 9.4 (Neumann and Makuch, 1984). Rockbursts in remnant pillars in other mining zones at Campbell have not been preceded by precursory microseismic activity. Microseismic monitoring at the Falconbridge Mine indicated that the microseismic activity was occurring in the footwall on geologic structures, but did not delineate any of the fault structures that burst (Davidge, 1984). Microseismic monitoring at the Strathcona Mine appears to indicate movement on some specific structure as shown in Figure 9.5 (Morrison, 1989). While it is not yet clear whether subsequent bursting occurred on microseismically

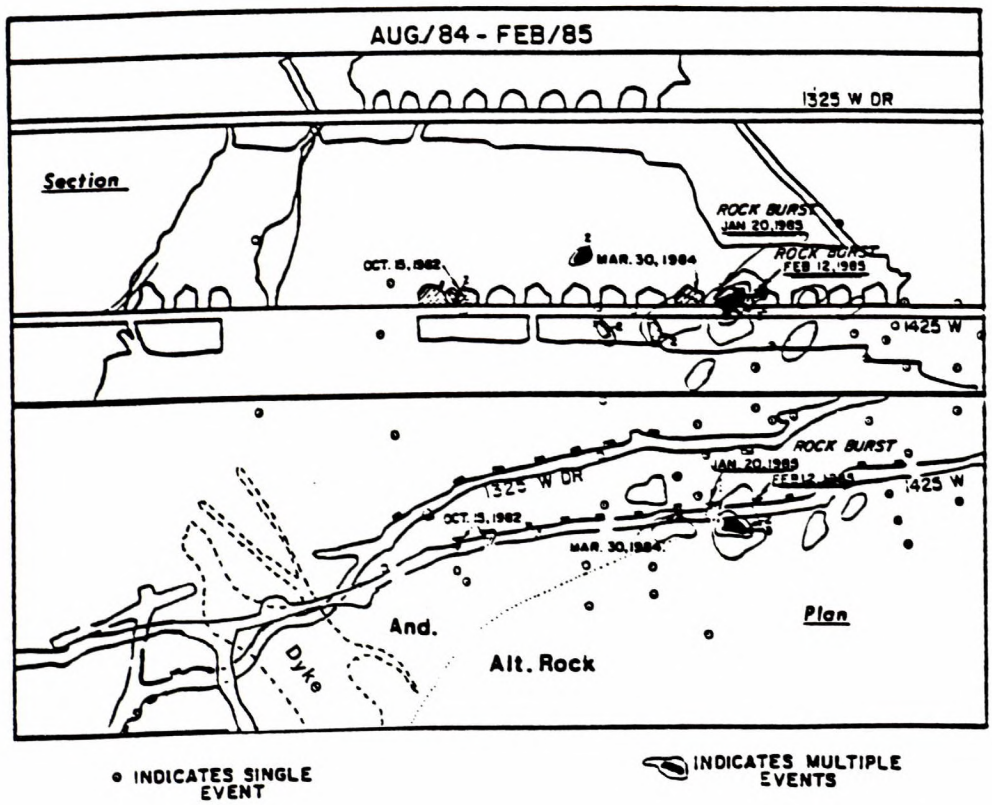

Fig. 9.4 - Anomalous microseismic activity at the Campbell Mine (after Neumann and Makuch, 1984).

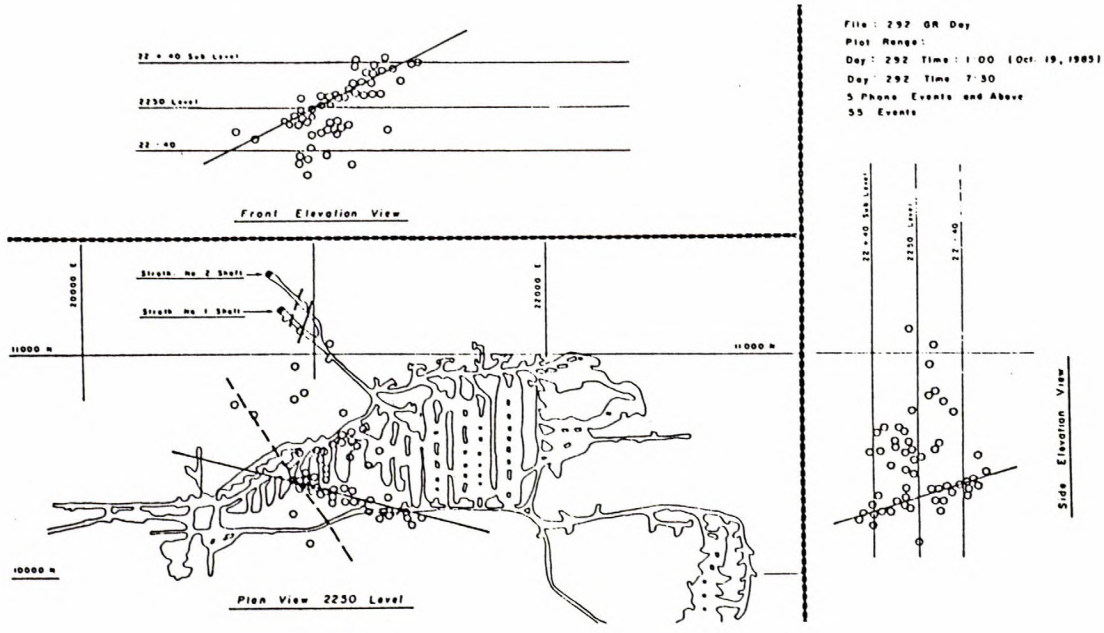

Fig. 9.5 - Anomalous microseismic activity at the Strathcona Mine (after Morrison, 1989).

identified structures, it is clear that the microseismic trends at Strathcona do indicate areas where fault-slip bursting is more likely.

Microseismic monitoring has resulted in locating burst-prone areas in mines throughout the world. However, successful predictions of where a burst will occur are not common. The microseismic data often indicate specific mine or geologic structures that are burst-prone, but these data by themselves are generally not sufficient for making reliable rockburst predictions. And, many bursts occur in or along structures that are not identified by anomalous microseismic data.

9.3 Prediction of Rockburst Timing

While there have been some notable successes in predicting rockburst locations, there has been much less success associated with predicting the time of a rockburst. This should not be surprising considering that many of the factors that contribute to the occurrence of a burst are poorly understood. Also the prediction of earthquakes is in a similar predicament.

9.3.1 Distribution of Rockburst Occurrences

Since rockbursts are mining induced, it is instructive to look at hourly and daily distributions of bursting for correlation with mining parameters. Figure 9.6 shows daily and weekly distributions of seismic activity for typical mines in South Africa and in the Coeur d'Alenes, and Figure 9.7 shows the same distributions of seismic activity for the Quirke Mine. The influence of day-to-day mining and face advance is very similar in South Africa and the Coeur d'Alenes, but has essentially no effect on seismic activity at Quirke.

These data imply that most of the bursts in South Africa and the Coeur d'Alenes are due to local mining geometry changes, whereas the bursting at Quirke is not affected by local mining geometry and is likely due to overall mining geometry. It is also clear that in South Africa and the Coeur d'Alenes, greater than half the bursting can be expected to occur with or shortly after blasting. Further, bursting is more likely to occur after mid-week on a weekly basis. These data suggest that it might be easier to predict

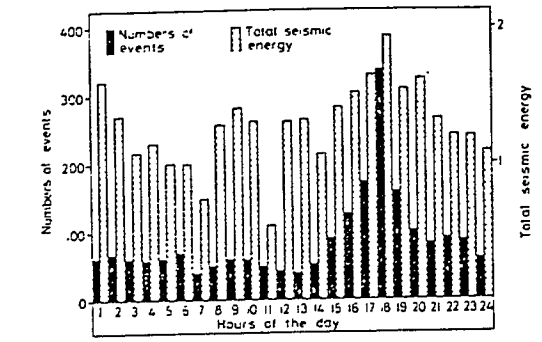

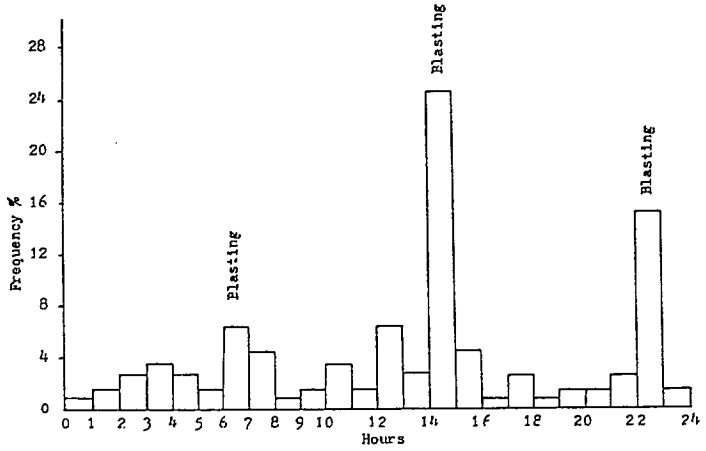

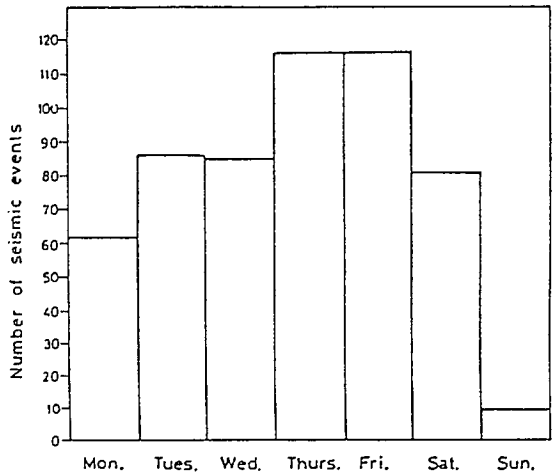

South Africa

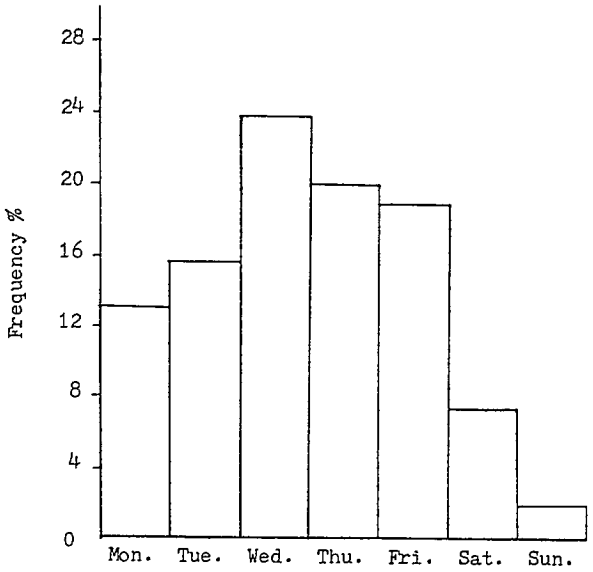

Coeur d'Alenes

Fig. 9.6 - Daily and weekly distribution of seismic activity associated with mining.

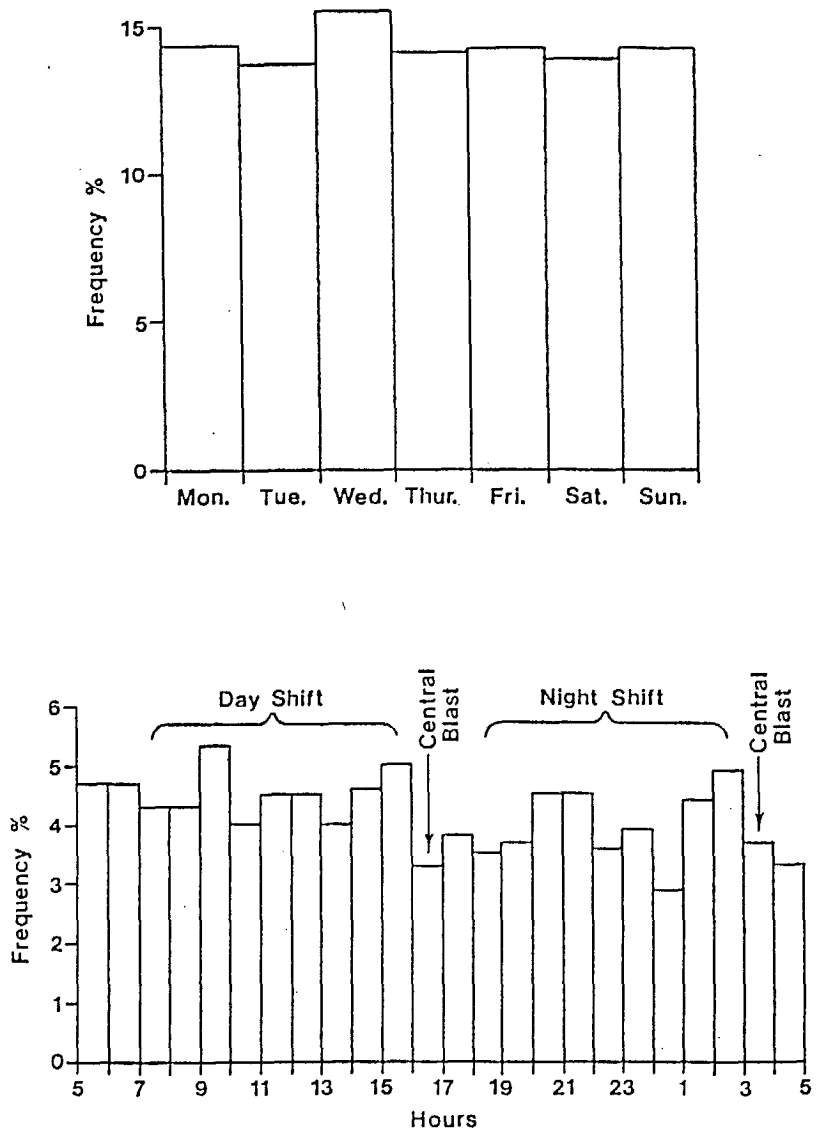

Fig. 9.7 - Daily and weekly distribution of seismic activity at the Quirke Mine.

rockburst timing in South Africa and the Coeur d'Alenes than it would be in cases similar to Quirke (i.e., rockbursts in abandoned areas of mines).

Because of increased bursting at Kirkland Lake and Sudbury during the late 1930s and early 1940s, and the apparent success reported by the USBM, the microseismic method was tested in these mining districts during a four-year period starting in 1942 (Hodgson, 1958). These investigations were much more extensive than the USBM research at the Ahmeek Mine, but the results were much less encouraging. No precursory phenomena were found to precede any of the many bursts that occurred at Kirkland Lake, some of which destroyed operating microseismic geophones. Bursts could not be predicted and potential burst locations could not be identified. Very similar results were found in the Sudbury district except that one burst was predicted based on an increased microseismic rate coupled with a simultaneous increase in the frequency of vibration. However, it was reported that microseismic monitoring with portable units did delineate some burst-prone areas in the orebody, but the time of occurrence of a burst could not be predicted. It was also concluded that the mine was too mechanically noisy for monitoring to be effective, and it was impossible to tell where the microseismic noise originated. Use of microseismic monitoring was apparently discontinued at the end of the test period.

9.3.2 Microseismic Precursor Phenomena

Microseismic and seismic precursor phenomena have been recognized prior to the occurrence of rockbursts. The most often reported are:

- a twofold or more increase in the microseismic rate or event count;
- a sudden increase in the microseismic rate or event count followed by a seismically quiet period;
- a sudden increase in the microseismic energy being released;
- a sudden increase in the average energy per event ratio; and
- an increase in the time it takes a burst-prone structure to quiet down or reach equilibrium following a face advance blast in the structure.

To evaluate these phenomena, three years of microseismic data from Hecla's

Star Mine were analyzed (Blake, 1984). During this period, some 49 rockbursts were induced by the mining of the two stopes monitored. A summary of the results of evaluating the precursor phenomena is presented in Table 9.1.

These data suggest that at the Star Mine only some 30% of bursts are preceded by recognizable microseismic precursor phenomena, whereas some 60% of all recognizable precursor phenomena are not followed by bursts. These results indicate a low reliability with respect to using microseismic precursors to predict the time of occurrence of rockbursts. No accurate rockburst predictions were made during the course of this study.

9.3.3 Recent Rockburst Prediction Studies

The USBM continues to carry out research directed towards rockburst prediction. Based on an analysis of laboratory tests, selected microseismic data preceding a few rockbursts and selected earthquake data, a means of predicting the time of a failure, including a rockburst, was proposed (Brady, 1978). The basis for determining the time of the failure is related to the time to form an areal extent of a well-defined microseismic build-up. While these criteria have been used to make some 'hindsight' rockburst and earthquake time of occurrence predictions, they have not yet resulted in a successful 'live' prediction. However, during the course of USBM research in the Coeur d'Alenes, miners have been removed from or held out of a stope prior to a burst because of a sudden and obvious increase in microseismic activity around that stope during shift, or failure of a stope to settle down microseismically between shifts. The reliability of such predictions is very low compared to the number of times crews have been removed or held out of stopes.

The rockburst prediction group at Western Deep Level Mine in South Africa has been working on developing a predictive capability based on microseismic precursor phenomena since 1978. To date the most reliable microseismic precursor has been found to be the change in microseismic rate for a specific volume of rock or mine structure (Brink, 1988). Figure 9.8 shows precursive activity prior to a rockburst. As a result of the increased microseismic rate on September 12, 1985, a rockburst was predicted and the crew was prevented

Table 9.1 - Evaluation of precursor phenomena preceding 49 rockbursts.

Recognized	Increased Rate of Event Count	Increased Rate Quiet Period	Increased Energy Release	Increased Energy/ Event	Increase in Time to Settle Down
Recognized precursors prior to a burst	12	3	15	4	15
Percentage bursts preceded by precursors	24%	6%	31%	8%	31%
Recognized precursors not followed by a burst	16	-	19	7	25
Percentage of precursors not followed by a burst	57%	-	56%	64%	63%

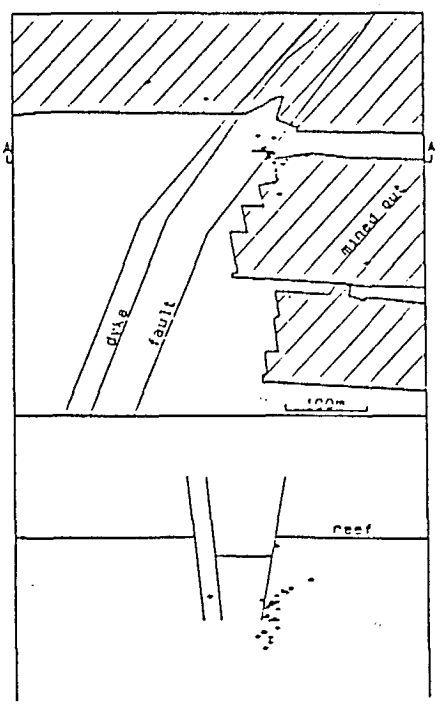

A plan and sectional view (A-A) of the first 4 minutes of aftershocks after a M_l = 0.6 seismic event on 12/9/85 at 11H32.

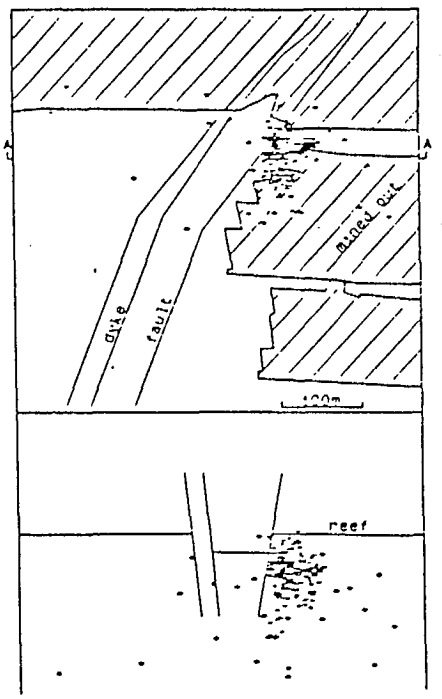

A plan and sectional view (A-A) of the first 4 minutes of aftershocks after a M_l = 2.4 seismic event on 14/9/85 at 15H34.

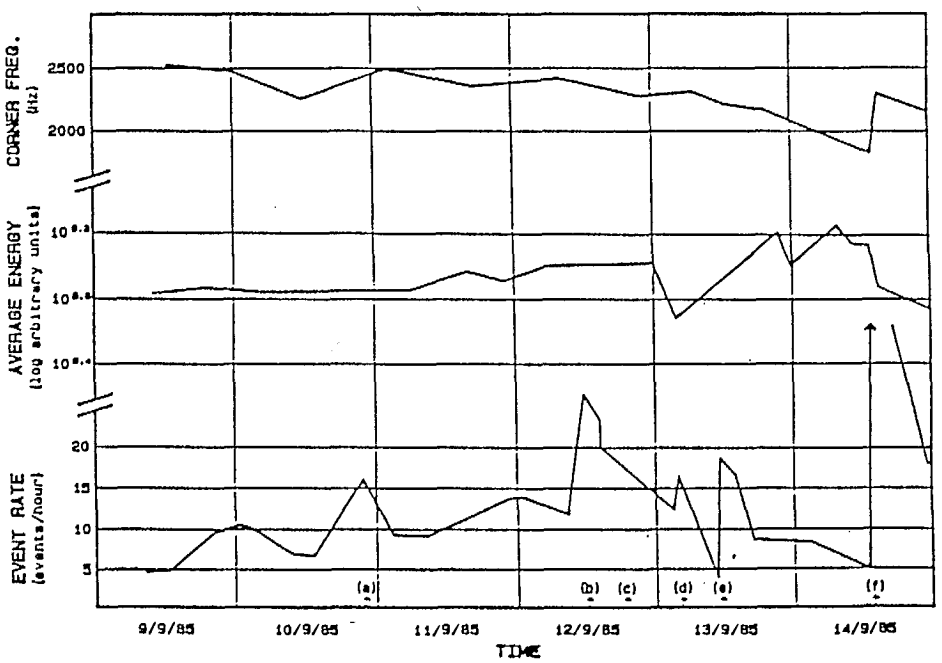

Fig. 9.8 - Development of precursive activity before a rockburst at Western Deep Level Mine (after Brink, 1988).

from entering the stope that afternoon and the next morning. The burst did not occur and it was presumed that it would not until the face was blasted. The burst occurred approximately two hours after blasting on September 14, 1985. During a nine-month period, nine bursts were reported, four of which were predicted based on microseismic precursive activity. It was concluded that a pending rockburst can often be recognized with reasonable success, but that it is not yet possible to accurately determine if a burst will occur unless it is triggered by additional mining. To improve rockburst prediction reliability, microseismic event source parameters are being studied.

Since the early 1980s, considerable effort has been made to utilize high frequency microseismic activity (signal frequencies $\geq$35,000 Hz) to predict rockbursts. Initial field investigations reported no success (Welch, 1984; Kanduth, 1984), but a recent field investigation utilizing different equipment has revealed success in being able to detect increasing stress in a pillar adjacent to pillar recovery mining that induced a rockburst (Calder et al. 1988). While it is apparent that an expected stress increase was detected in the pillar being monitored, it is not clear that a burst would be expected in the adjacent pillar. More field research is required to establish precursive relationships based on high frequency microseismic monitoring.

9.3.4 Rockburst History

Recognition of rockburst precursors implies that rockbursts are frequent occurrences and have occurred over a sufficient length of time to establish rockburst history. While rockbursts have occurred in Ontario mines for more than 60 years, the present rockburst incidence in Ontario is very low when compared to other rockburst-prone mining districts. Rockburst incidences in South Africa and the Coeur d'Alenes are in the range of 0.1 to 1.0 bursts per each 1000 t mined. In Ontario, where 50 to 100 bursts are now reported each year, the rockburst incidence is only from 0.003 to 0.006 bursts per 1000 t mined. This implies that it may take a longer time to establish precursor patterns in Ontario mines.

9.3.5 Precursive Phenomena

Considerable research has been carried out utilizing electrical resistivity and electromagnetic emission as rockburst precursors. Anomalous changes in electrical resistivity prior to small seismic events have been reported as a result of field investigations at the Lubin Copper Mine in Poland (Stopinski and Dmowska, 1984). The USBM has been monitoring electromagnetic emission in conjunction with both laboratory and field investigations to determine if these phenomena can be recognized prior to a rockburst (Powell et al. 1981; Hanson, 1982). While there has been some success in laboratory specimens loaded to failure, no success in recognizing electromagnetic emissions prior to a rockburst has yet been reported. Much more research is required to establish the potential of electrical phenomena with respect to rockburst prediction.

9.4 Rockburst Triggering Mechanisms

A number of active mining parameters as well as some passive non-mining parameters have been reported to trigger rockbursts.

9.4.1 Mine Blasting

As was shown in Figure 9.6, mine blasting is responsible for triggering a large percentage of the rockbursts that are induced by mining. It is not really the blast vibrations that trigger the bursting, but rather the face advance as a result of the blast. The greater the face advance, the greater the stress redistribution and hence, the likelihood of triggering a burst. Centralized blasting appears to be more effective than random blasting because stress readjustments are taking place simultaneously throughout the mine, and hence stress interactions may increase the likelihood of triggering bursts. While it is often reported that the stress wave from a blast triggered a rockburst at a distant location, there are no documented cases to support such a triggering mechanism.

In addition to normal mine blasting, destress blasting frequently results in triggering a rockburst. Almost all mines that have carried out destress

blasting have reported triggering rockbursts as a result of such blasting. The goal of microseismic monitoring in many mines is to recognize burst-prone structures so that the burst can be triggered by destress blasting. Recently, consideration has been given to using water injection to trigger bursting as an alternative to blasting.

9.4.2 Mine Drilling

While it is common for face drilling to trigger small scale seismic activity, popping and spitting, there are a number of reported cases where drilling has resulted in triggered bumps, small bursts and even a major pillar burst. Numerous longhole drilling operations for destressing in the Coeur d'Alenes have resulted in bumping at the bottom of the hole which violently shook the drill set-up and shook down loose rock. At least two major pillar bursts at the Galena Mine occurred during face drilling in the pillar, and a major pillar burst at the Lucky Friday Mine occurred while longhole destress drilling of the pillar was being carried out. Drilling for rockbolting during renovation of boxhole pillars at the Campbell Red Lake Mine has resulted in immediate 'working ground' and the subsequent occurrence of small bursts.

9.4.3 Mine Mucking

The extraction of broken ore from shrinkage stopes at the Campbell Red Lake Mine has triggered rockbursts in boxhole pillars in two different ore zones. The removal of wall support and the increased load on the pillar was sufficient to induce bursting.

9.4.4 Rockbursting

The occurrence of a rockburst often triggers continued bursting. This has been reported at a number of mines throughout the world, and in Canada at the Quirke, Campbell, Falconbridge, Creighton and Strathcona Mines in Ontario. Stress transfer due to failed pillars and/or displacement readjustments as a result of a fault-slip displacement resulted in burst sequences that continued for up to several months. Also at Quirke Mine there is evidence that the

dynamic stress pulse emanating from large rockbursts initiated seismic activity 500 m away.

9.4.5 Non-Mining Mechanisms

For years underground miners have expressed the opinion that rockbursts were triggered by phases of the moon - coincidental with increased gravitational pull. While this has never been documented, an in-house investigation of rockburst occurrences and phases of the moon at the Lucky Friday Mine revealed that there was no correlation.

Changes in the weather or changes in seasons have also been proposed as triggering mechanisms for rockbursts. After the hanging wall fractured above the main rockburst area at Quirke Mine, there was generally an increase in seismic activity during the spring run-off. A strong correlation between weather systems and the occurrence of rockbursts in the Sudbury Basin has been suggested. Such correlations need to be based on in-mine measurements and other mine data in order to be substantiated. There does, however, appear to be some correlation between the seasons and large mining-induced seismic events at the potash mines in Saskatchewan. While these local earthquakes have never resulted in any observed underground damage and appear to be related to overall mine design, the majority of these events have occurred during winter or cold weather months (Gendzwill, 1989).

9.5 Conclusions

Determining potential rockburst locations based on microseismic monitoring and/or computer modelling are standard practice at most mines with rockburst problems. The difficulty is in delineating those locations that will actually fail in a rockburst. The computer results and the microseismic data are not yet able to indicate whether a failure may take place seismically or aseismically. It is apparent that while the computer models and microseismic equipment have become much more sophisticated, our understanding of the complex wallrock reactions to mining and stress transfer have not sufficiently improved to allow for more reliable rockburst location predictions. The exception is in the sill pillar situations in narrow steeply-dipping vein

deposits, such as the Campbell and Macassa Mines. In these mines, rockburst problems are regularly encountered when the sill pillars reach a critical size.

Predicting the time of occurrence of a rockburst has been done only in a small number of instances, mostly under research conditions, i.e., well funded, well staffed, long-term projects focused on a small number of specific areas in a mine. Because of the lack of understanding of the field behaviour of a rock mass and its geologic structure, it is not likely that our ability to predict the time of occurrence of a rockburst will improve significantly in the near future. It also appears that the more complex the geology, the more difficult is any prediction.

The majority of rockbursts in Ontario during the past five years have occurred in old mined-out areas rather than being associated with day-to-day mining. Most of the mining in Ontario is also associated with massive sulphide deposits rather than narrow vein mining. Hence, there has not been much success in applying rockburst prediction technology based on narrow vein mining and total extraction. And further, with a greatly reduced incidence of bursting compared to other burst-prone mining districts, it appears that rockburst prediction in Ontario will not have as much success as has been attained in other more rockburst-prone mining districts.

The conclusions reached by the rockburst committee of the Ontario Mining Association some 40 years ago are still valid; "the prediction of the time of occurrence of a rockburst is of little actual value to a mine operator and it would be far more useful to be able to delineate areas predisposed to bursting and to apply means to inhibit and control the burst".

9.6 References

Blake, W. (1971), An automatic rockburst monitor for mine use. Proc. Conf. Underground Mining Environment, University of Missouri.

Blake, W. (1972), Rock burst mechanics. Colorado School of Mines Quarterly, vol. 67, No. 1.

Blake, W. (1984), Evaluation of some rock burst precursor phenomena. Proc. 3rd Conf. Acoustic Emission/Microseismic Activity in Geologic Structures and Materials. Trans Tech Publications.

Blake, W. and Leighton, F.W. (1970), Recent developments and applications of the microseismic method in deep mines. Rock Mechanics - Theory and Practice. AIME.

Brady, B.T. (1978), Prediction of failure in mines - an overview. USBM Report of Investigation RI 8285.

Brink, A.V.Z. (1984), Rock burst prediction research-development of an early warning system. Proc. 3rd Conf. Acoustic Emission/Microseismic Activity in Geologic Structures and Materials. Trans Tech. Publications.

Brink, A.V.Z. (1988), Application of a microseismic system at Western Deep Levels. Proc. 2nd Symp. Rockbursts and Seismicity in Mines, University of Minnesota.

Calder, P.N., Archibald, J.F., Madsen, D. and Bullock, K. (1988), High frequency precursor analysis prior to a rockburst. Proc. 2nd Symp. Rockbursts and Seismicity in Mines, University of Minnesota.

Cook, N.G.W. (1963), The seismic location of rockbursts. Proc. 5th U.S. Rock Mech. Symp., University of Minnesota, Pergamon Press.

Davidge, G.R. (1984), Microseismic monitoring at Falconbridge Mine. In: Microseismic Monitoring in Canadian Mines, Proc. CANMET sponsored workshop, Sudbury, Ont., August 1984, CANMET Division Report MRP/MRL 85-23, CANMET, Energy, Mines and Resources Canada.

Gendzwill, D.J. (1989), Personal communication.

Hanson, D.R. (1982), Electromagnetic radiation from rock failure. USBM Report of Investigation RI 8594.

Hanson, D., Quesnel, W. and Hong, R. (1987), Destressing a rockburst prone crown pillar - Macassa Mine. Division Report MRL 87-82 (TR), CANMET, Energy, Mines and Resources Canada.

Hart, R.D., Board, M., Brady, B., O'Hearn, B. and Allen, G. (1988), Examination of fault-slip induced rockbursting at the Strathcona Mine. In: Key Questions in Rock Mechanics, Proc. 29th U.S. Symp. (University of Minnesota), A.A. Balkema.

Heunis, R. (1987), Rockbursts and the search for an early warning system. Mining Magazine, vol. 136, No. 2, pp 83-89, Feb. 1977.

Hodgson, E.A. (1958), Dominion Observatory rockburst research 1938-1945. Publication Dominion Observatory, vol. 20, No. 1, Ottawa, p. 248.

Kanduth, H. (1984), Evaluation of the 'stress alert' rock stress monitor in Noranda group mines. In: Microseismic Monitoring in Canadian Mines, Proc. CANMET sponsored Workshop, Sudbury, Ont., August 1984. CANMET Division Report MRP/MRL 85-23. CANMET, Energy, Mines and Resources Canada.

Langstaff, J.T. (1974), Seismic detection system at the Lucky Friday Mine. World Mining, Oct. 1974.

Morrison, D.M. (1989), Rockburst research at Falconbridge Limited. CIM Bull. April 1989.

Neumann, M. and Makuch, T. (1984), Case study of microseismic monitoring of the 'F-2' zone at Campbell Red Lake Mine Limited; In: Microseismic Monitoring in Canadian Mines, Proc. CANMET sponsored Workshop, Sudbury, Ont. August 1984. CANMET Division Report MRP/MRL 85-23.

Obert, L. (1941), Use of subaudible noise dose prediction of rock bursts. USBM Report of Investigation RI 3555.

Obert, L. and Duvall, W.I. (1957), Micro-seismic method of determining the stability of underground openings. USBM Bulletin 573.

Powell, G.A., Brady, B.T., Yoder, L.P. and Hanson, D.R. (1981), Precursors of laboratory rock failure, fracture mechanics methods for ceramics, rock, and concrete. ASTM STP 745.

Stopinski, W. and Dmowska, R. (1984), Rock resistivity in the Lubin (Poland) Copper Mine and its relation to variations of strain field and occurrences of rockbursts. In: Rockbursts and Seismicity in Mines. South African Inst. Min. & Met. Symp. Series No. 6.

Welch, B.J. (1985), Evaluation of the McPhar Model RM-1 rock monitor. In: Microseismic Monitoring in Canadian Mines, Proc. CANMET sponsored Workshop, Sudbury, Ont. August 1984. CANMET Division Report MRP/MRL 85-23. CANMET, Energy, Mines and Resources Canada.

Wiles, T. (1988), Comparison of several numerical modelling techniques applied to three-dimensional mining geometries. Proc. 6th Int. Conf. on Numerical Methods in Geomechanics, Innsbruck.

10. CASE HISTORIES

Result of fracturing through to surface above the rockburst area at Quirke Mine.

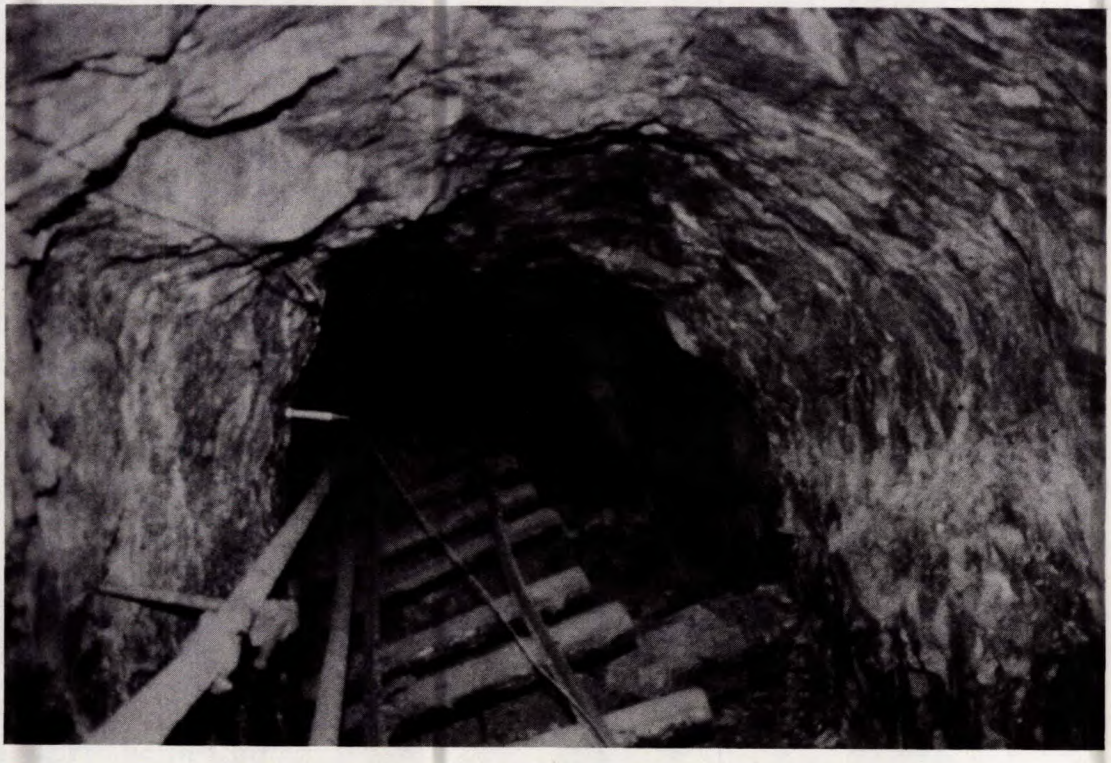

Floor heave due to rockbursts at Campbell Mine.

10. CASE HISTORIES

10.1 Rio Algom's Quirke Mine, Elliot Lake

10.1.1 Summary

The rockburst incidents at Quirke Mine were a classic example of a chain reaction of pillar failures. Over a five-year period, more than 160 seismic events, up to a magnitude of 3.5, were recorded by the Eastern Canada Seismic Network. An area larger than 70 ha was affected underground. Seismic activity substantially decreased when the hanging wall above the affected area fractured through to surface. This appeared to relieve the pressure on the abutments and the area stabilized.

10.1.2. Geology and Mining Methods

The uranium-bearing, quartz-pebble conglomerate reefs at Elliot Lake are in the form of a syncline. At Quirke Mine, the reefs 2 to 5 m thick dip at about 20^{o} to the South from just below surface to a depth of 1000 m. Massive quartzite forms the footwall and hanging wall of the reefs.

Two variations of a stope-and-pillar mining method are employed. In the main reef, rib pillars are systematically laid out on dip at 25 m centres, with crown and sill pillars on strike at the top and bottom of the stopes, typically 100 m long. Jack legs are used for drilling and slushers transport the broken ore to boxholes connected to a haulage level 6 m beneath the sill drift.

In the upper reef, about 35 m above the main reef, a trackless mining method is employed. To accommodate the trackless equipment rib pillars, up to 150 m long, are laid out at an apparent angle to dip to ensure a gradient of less than 10^{o}. The two reefs only partially overlap.

10.1.3 Rockburst Sequence

A plan of the eastern part of the main reef at Quirke Mine is shown in Figure

10.1.1. This area was mined in the 1970s with about 80% extraction. Near the centre of the area, between the 7 and 8 levels, a local roll in the orebody produced a flat lying area. It was difficult to recover the ore at the top of the stopes using slushers. Consequently, the top of these stopes were converted into a trackless panel as a trial, prior to the introduction of this method in the upper reef. The 3 m wide rib pillars were laid out at an angle of about 45° to true dip to accommodate the equipment. Mining started in the trial trackless area in 1977 and was completed in 1978 with no significant ground control problems.

By 1981 the stopes on the 9 level, immediately down dip, had been completed and mining had started on the 10 level stopes. By this time, deterioration was noticed in the trial trackless area and the 7 sill drift immediately up-dip. It took the form of pillar spalling and floor cracks. During the next year, the deterioration intensified accompanied by audible microseismic activity and broken rock bolts. By March 1982, an area 250 m in diameter centered on the trial trackless area was affected.

The first rockburst, which was felt on surface, occurred in the evening of March 12, 1982. This was followed within an hour by four more large rockbursts, the largest having a magnitude of 3.0 Mn. Inspection of the area revealed that both the 7 sill and haulage drifts were blocked off over a distance of 360 m adjacent to the trial trackless area. A more thorough inspection, a few months later, indicated that the violent rockburst type failures were confined to the relatively squat sill and crown pillars on the 7 level. Typically, the broken rock was in small fragments, dusty in appearance and scattered over large distances. The slender rib pillars in the stopes, and especially in the trial trackless area, appeared to have failed non-violently, since large blocks had sloughed from the sides of the pillars, with no scatter. No damage was observed to the roof, except where a mud-coated, low-angle thrust fault intersected one of the stopes. However, literally hundreds of broken rock bolts were found, coming from the roof. Floor cracks and heaving were observed, especially in the trial trackless area, with cracks up to 20 cm wide by over 2 m deep (Hedley et al. 1984).

A 16-channel microseismic system was installed around the affected area in

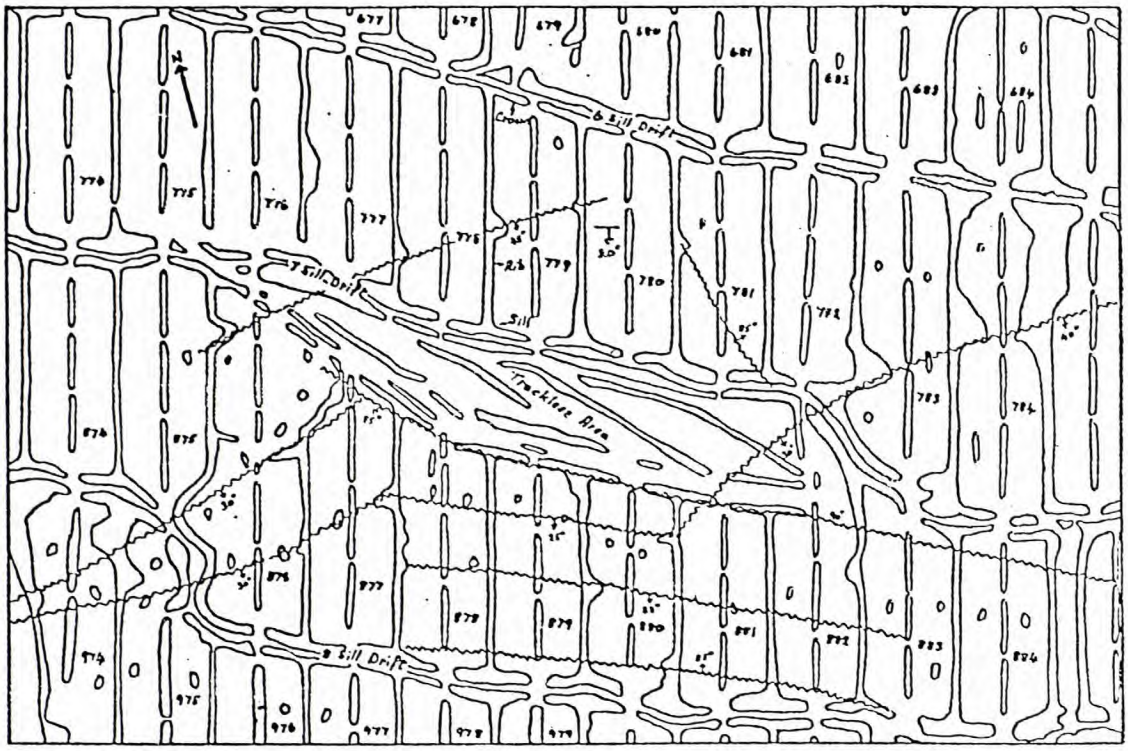

Fig. 10.1.1 - Stope and pillar layout in main reef at Quirke Mine.

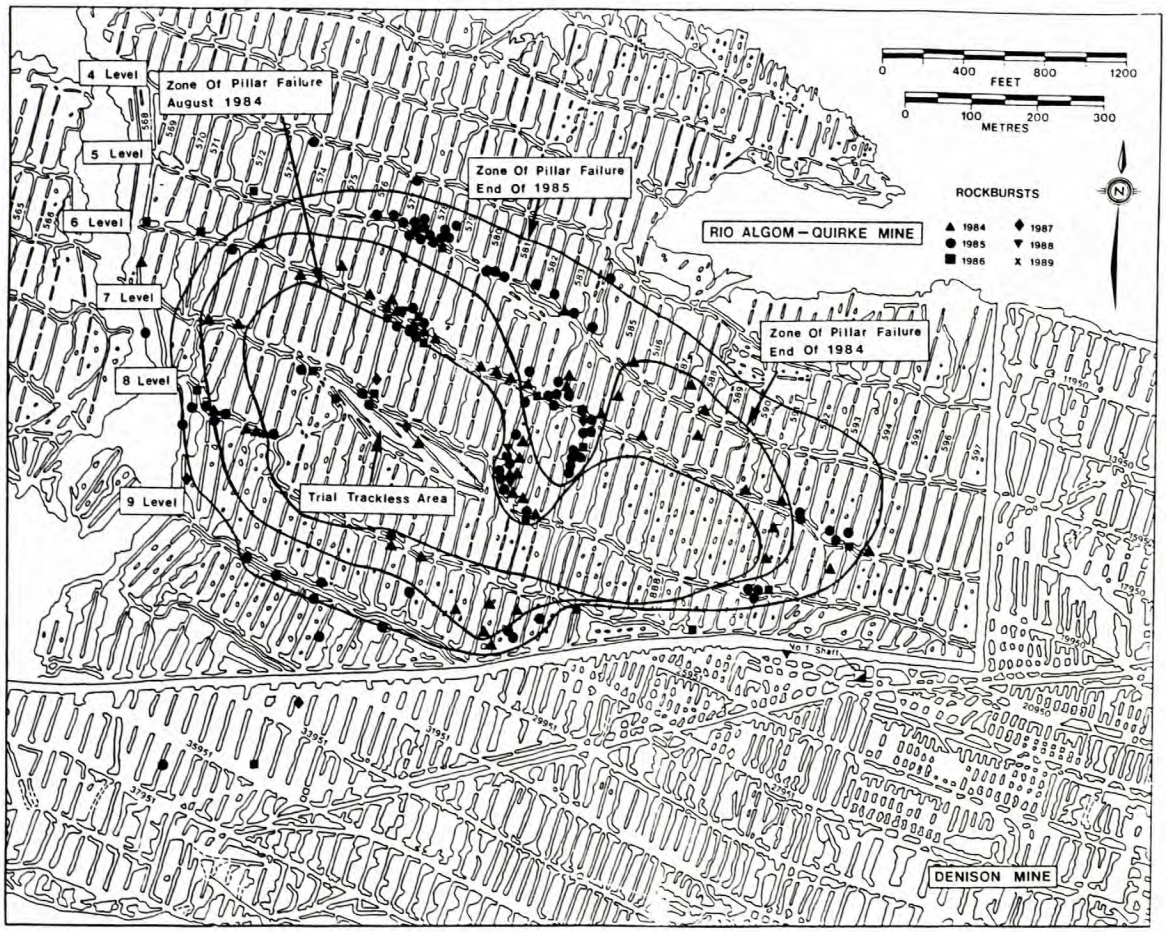

Fig. 10.1.2 - Location of rockbursts and expansion of affected area at Quirke Mine.

August 1982 (MacDonald and Muppalaneni, 1983). This system was subsequently expanded to 32 channels with 8 of the sensors on the Denison side of the boundary pillar to provide better coverage of this area. Numerous convergence stations were also installed around the periphery of the affected area.

Between March 1982 and September 1984, the affected area gradually expanded without major rockbursts (the level of detectability at that time was a magnitude of 2.2 Mn, subsequently decreased to about 1.0). Microseismic activity was cyclic with peaks occurring in June 1982, March 1983 and September 1983. More often than not an accelerating convergence rate preceded an increase in microseismic activity and an expansion of the affected area. During this period, access was lost to most of the 7 level and part of the 8 level directly below the trial trackless area. By August 1984, the zone of pillar failure extended about 870 m on strike by 300 m on dip as shown in Figure 10.1.2.

Major rockburst activity again occurred in September 1984 and over a 12 month period 154 large seismic events were recorded by the Eastern Canada Seismic Network, the largest having a magnitude of 3.4 Mn. The locations of these events are plotted in Figure 10.1.2. In September 1984, most of the seismic activity was concentrated on the 6 sill level directly above the trial trackless area. In December 1984, activity shifted to some large pillars just north-east of the trackless area, then to the eastern boundary just north of Denison's No. 1 shaft. By February 1985, the 5 sill level was destroyed followed by the 9 sill level in August/September 1985. At the end of 1985, the final zone of pillar failure extended about 1100 m on strike by 600 m on dip, as shown in Figure 10.1.2.

During this period of major rockburst activity, the main pattern was failure of the pillars at the edge of the affected zone. However, some events were located in the centre of the trial trackless area, where the pillars had already failed. It was suspected that these events occurred in the hanging wall and were caused by slippage near vertical faults or along bedding contacts. At the same time (April 1985), water flow into the rockburst area suddenly increased to 1000 L/min, and the water level in a small lake directly above the area dropped by about 4 m. This evidence points to fracturing of

the hanging wall through to surface. Subsequently, diamond drill holes from surface into the rockburst area encountered lateral displacement at bedding contacts, gaps of up to 150 mm wide, loss of circulating water at numerous horizons, and air being sucked down the boreholes into the mine.

Since the hanging wall fractured through to surface the level of microseismic activity has substantially decreased, as illustrated in Figure 10.1.3. The number and magnitude of the large events have also decreased. The affected area has stopped expanding and has stabilized essentially, with very little further damage being reported.

10.1.4. Analytical Studies

The history of rockbursts at Quirke Mine raises several questions including:

- What initiated the rockbursts?
- Why did squat pillars fail so violently and slender pillars non-violently?
- Why did the chain reaction of pillar failures occur over a 4-year period rather than hours or days?
- What was the mechanism of the hanging wall breakdown?

Both analytical and numerical models were used to investigate these aspects.

Cause of rockbursts

Two factors can be identified as contributing to pillar failures and rockbursts:

i) the pillars were highly stressed due to the depth and an extraction rate of 75 to 80%;
ii) pillars were in different orientations which resulted in some being weaker than others, or they were less effective in transmitting stress through them.

Of these, the high pillar stresses were a prerequisite. However, pillars in other areas of the mine were equally highly stressed but did not initiate

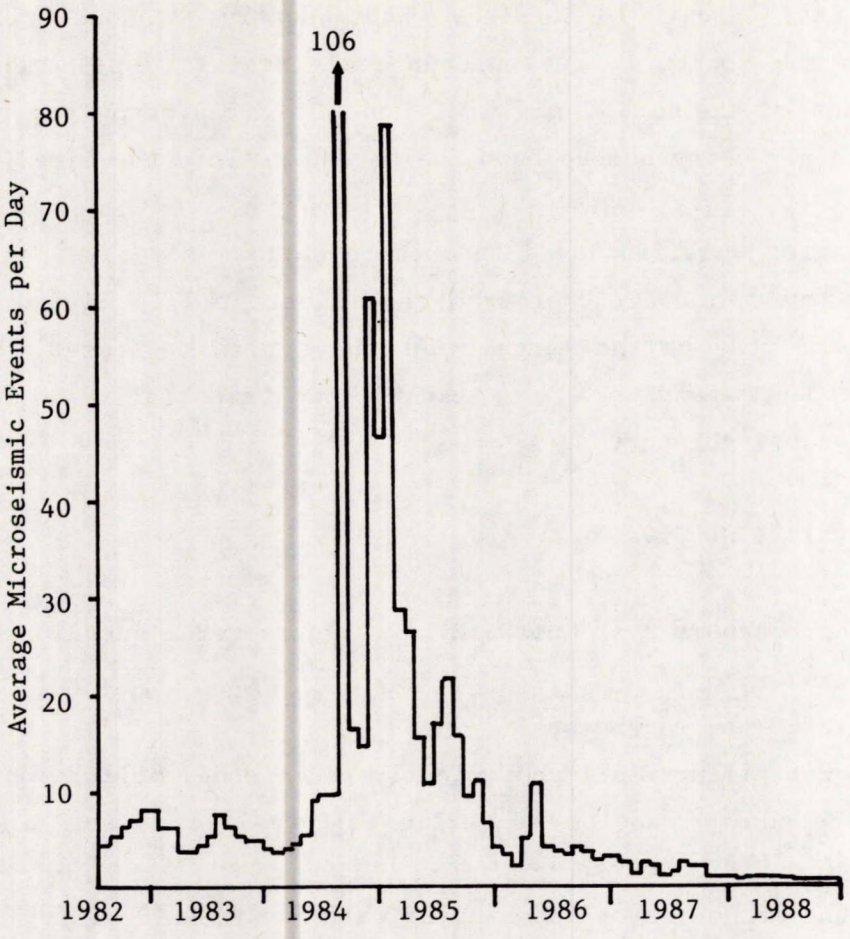

Fig. 10.1.3 - Level of microseismic activity 1982-1988 at Quirke Mine.

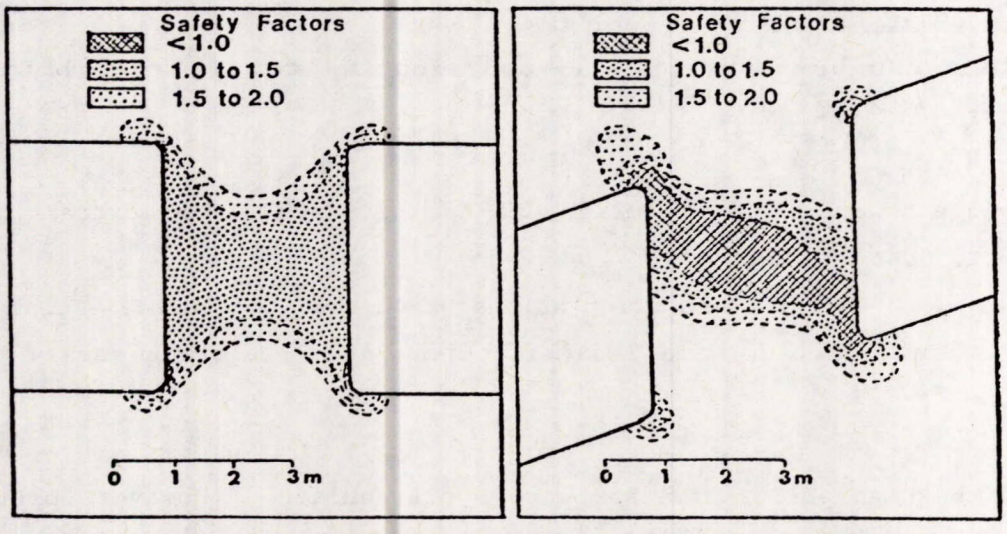

a) Dip Rib Pillar b) Strike Rib Pillar

Fig. 10.1.4 - Stability of rib pillars aligned on dip and strike.

rockbursts. Consequently, the weakness of the rib pillars in the trackless area is considered to be the cause of the rockbursts.

An elastic displacement discontinuity computer model was run to estimate average pillar stresses around the trial trackless area. Estimates of pillar strength were obtained from an empirical equation developed for the Elliot Lake mines by Hedley and Grant (1972), where:

$$Q = 133 \frac{W^{.5}}{H^{.75}} \qquad \text{Eq 10.1.1}$$

where, Q = pillar strength, MPa
W = pillar width, m
H = pillar height, m.

This analysis indicates a safety factor of 1.0 for the rib pillars in the trackless area, 1.3 for the rib pillars in the normal stopes, 1.7 for the crown pillars, and 2.1 for the sill pillars.

A boundary element model was used to illustrate the effect of pillar orientation on its stability. Figure 10.1.4 shows two identical rib pillars at the same depth and extraction ratio with one pillar being aligned on dip and the other on strike, where the dip is 20^{o}. The rib pillar on dip is stable and across the centre line the safety factor averages 1.2, whereas in the pillar on strike failure extends across the complete pillar width. This confirms that the rib pillars in the trial trackless area were weaker than those in the regular stopes.

Violent and Non-Violent Failure

The violent failure of squat pillars against the non-violent failure of slender pillars can be explained in terms of pillar stiffness compared to loading stiffness. As discussed in Section 3.5.2, the loading stiffness is controlled by the areal extent of the mine workings, the extraction ratio and the elastic properties of the rock mass. For a large mined-out area such as Quirke Mine, the loading stiffness is very soft and approaches dead-weight loading system (i.e., zero stiffness). In the displacement discontinuity model a single pillar was removed in the centre of the mining area to obtain

local mine stiffness. A value of 2 MPa/mm was obtained, confirming a soft loading system.

Pillar stiffness is controlled by the width/height ratio of the pillars, which in turn affects their strength. At Quirke Mine there is a range of slender to squat pillars, and hence a range of pillar strengths. Similar to the multiple specimen test described in Section 3.5.2, the weak slender pillars would fail first non-violently and transfer load to the adjacent stronger squatter pillars. Failure of the squat pillars would then be violent. This mechanism would explain the initial non-violent failure of the rib pillars in the trial trackless area followed by the rockburst failure of the 7 level sill pillars, immediately up-dip. Subsequently, the rib pillars in the regular stopes failed non-violently followed by the violent destruction of the sill and crown level pillars.

Chain Reaction

The relatively uniform layout of small pillars allowed the affected area to gradually expand until it reached more substantial abutments. However, there was still sufficient difference in pillar size and strength which prevented a rapid chain reaction of pillar failures. Swan (1985) examined the distribution of pillar strengths in the affected area. The frequency distribution is shown in Figure 10.1.5. Mean compressive strength is 75 MPa, with a standard deviation of 24 MPa, however, there are a number of pillars with strengths exceeding 100 MPa. It is these pillars which prevent a spontaneous pillar collapse.

A computer model which incorporates post-failure behaviour of the pillars (i.e., NFOLD model of Golder Associates) was run to estimate the possible future extent of the affected area.

This model distributes stress from the failed to the intact pillars, using an iterative process, until the whole model achieves equilibrium. The iterative procedure is a pseudo representation of time. It was observed that only a few iterations were required to fail the slender rib pillars, whereas failure of the sill pillar on the levels took many iterations. This model supports the slow chain reaction and cyclic nature of the pillar failures observed

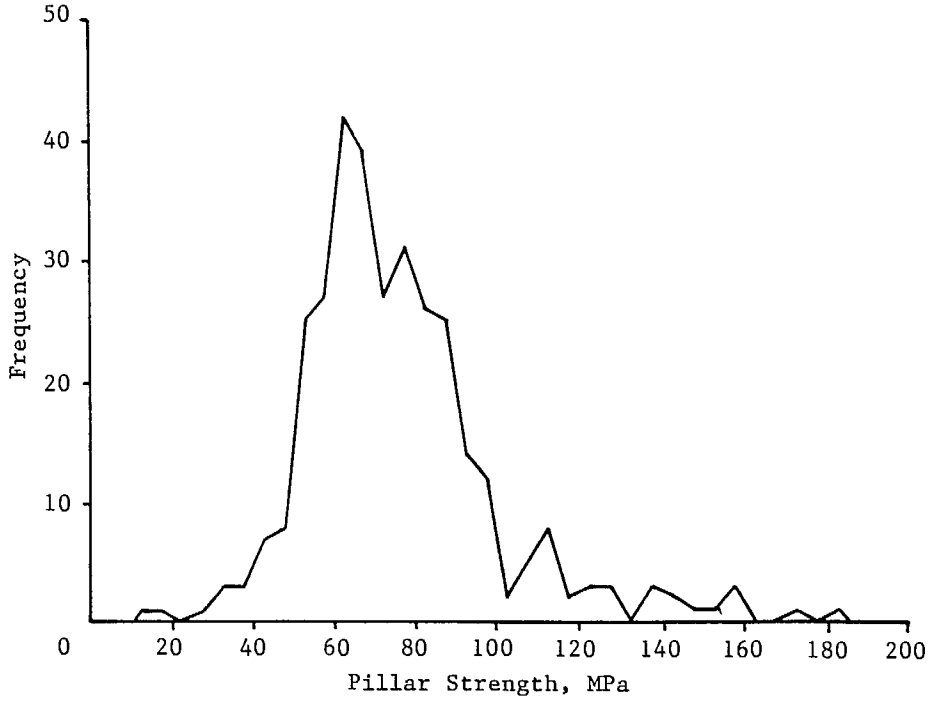

Fig. 10.1.5 - Pillar strength distribution in the affected area at Quirke Mine (after Swan, 1985).

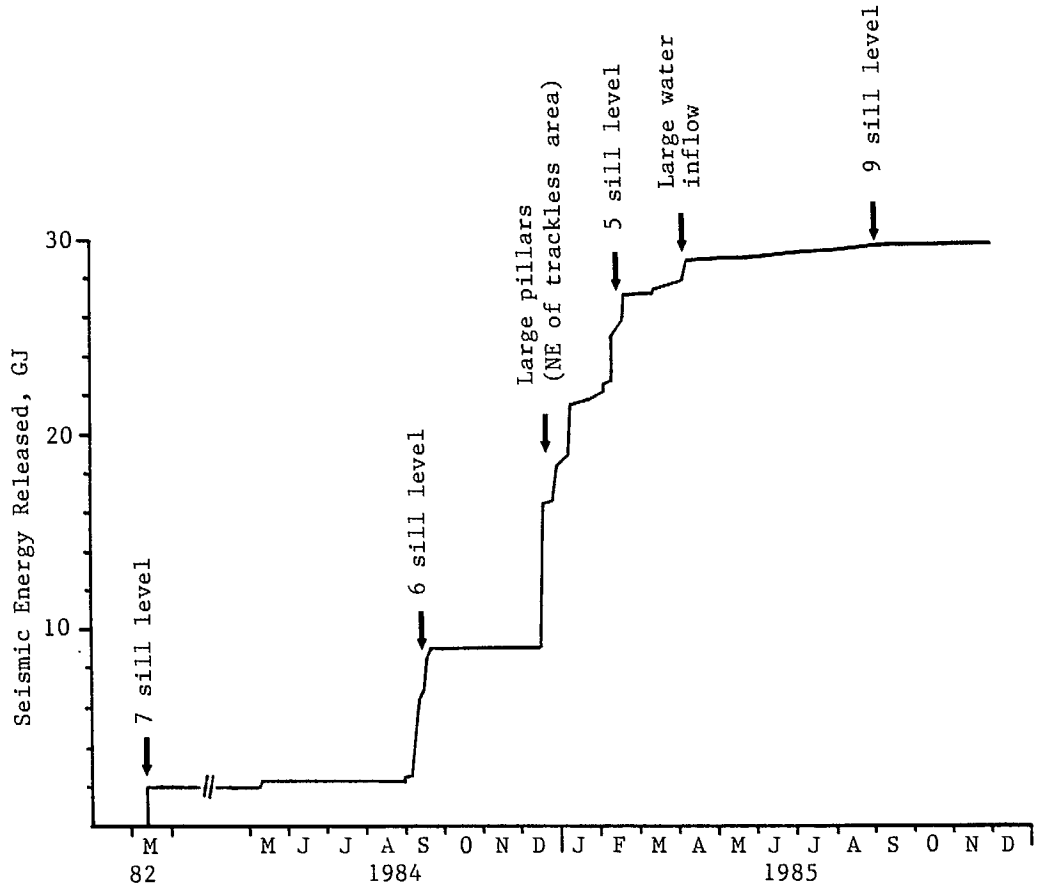

Fig. 10.1.6 - Temporal release of seismic energy at Quirke Mine.

underground. The model also indicated that the pillars in the affected area were in a condition of unstable equilibrium. Only minor changes of 10% in the peak and residual strength of the pillars would cause either run-away failure or stabilize the area.

Hanging Wall Failure

Overall hanging wall stability is controlled by the critical span. When this span is exceeded, stress can no longer be transferred from the failed pillars, in the centre of the area, to the pillars on the abutments. Failure can be either by shearing over the abutments or tensile failure at the centre of the area.

Two simple models were used to analyze possible modes of hanging wall failure. A laterally loaded beam will fail when the bending stresses, which are tensile, overcome the tectonic horizontal compressive stresses. This would allow near vertical faults and joints to slip near the centre of the affected area and for the hanging wall to unravel. This type of failure would likely be gradual and relatively non-violent.

An alternative model is to represent the hanging wall strata as a linear arch. Failure occurs when the compressive stresses exceed the rock strength over the abutments. In this case, failure would likely be sudden and violent.

In the analysis, the beam or linear arch was taken as the immediate 40 m thick quartzite bed with a 45 m thick argillite bed resting on top of it. The tectonic horizontal stress was taken as 18 MPa, and the compressive strength of quartzite as 100 MPa. The laterally loaded beam achieved zero horizontal stress or confinement at a span of 310 m, whereas the linear arch exceeded the compressive rock strength at a span of 430 m. In both cases the beam or arch was unsupported, whereas underground the failed pillar provided some partial support.

The evidence from the water inflows and the location of the rockbursts near the centre of the affected area suggest that the hanging wall acted as a laterally loaded beam. The first breakdown of the roof occurred when the partially supported span on dip was 420 m, and accelerated when the span

increased to 520 m. Critical span appears to be in the order of 400 m for a depth of 500 m. Seismic events located in the central zone, and thought to be occurring in the hanging wall, have had magnitudes of 1.6 to 2.2 Mn and have been relatively non-violent. They also tended to be concentrated during the spring run-off, probably due to lubrication of the vertical faults and bedding contacts.

10.1.5 Seismic Studies

Since March 1982, the magnitudes of the larger seismic events at Quirke Mine have been calculated by the Geophysics Division of the Geological Survey of Canada. Figure 10.1.6 shows the cumulative release of seismic energy between 1982 and 1985. The largest releases of energy occurred for short periods at specific times which correspond to the destruction of the sill level pillars, specifically the 7, 6 and 5 sill levels. However, the largest release of energy occurred when the large pillars failed north-east of the trackless area.

From Figure 10.1.6, the last major release of seismic energy occurred in April 1985, which coincided with the increase in water flow into the mine. Failure of the 9 sill level in August 1985 produced very little seismic energy. The total amount of seismic energy liberated is estimated to be in the order of 30 G.J which is equivalent to one rockburst of magnitude 4.8 Mn using Equation 5.10, i.e., $\log W_k = 1.3\ Mn - 1.75$ in MJ.

10.1.6 Discussion

Lessons learned from the rockburst experience at Quirke Mine should be directly applicable to other mines at Elliot Lake and perhaps other room-and-pillar hardrock mines.

- The rib pillars in the trackless area were the cause of the rockburst problem. They were the same width as the rib pillars on dip in the conventional stopes, but their orientation on apparent dip reduced their effective strength. It should be noted that no problems were encountered

during the mining of the trial trackless area, but only four years later when this block was near the centre of the mine workings.

- When rockbursts occur in a room-and-pillar layout, they are difficult if not impossible to control. At Quirke Mine, the relatively uniform layout of the small pillars resulted in a gradual expansion of the affected zone. However, there was still sufficient difference in pillar size which prevented a rapid chain-reaction type of pillar failure. Barrier pillars at regular intervals are a better method of containing and isolating areas of pillar failure. Subsequent to these events at Quirke Mine, the deepest mine at Elliot Lake, Stanleigh Mine of Rio Algom Ltd., was designed using a barrier pillar concept.

- In a uniform layout of pillars, the failure zone will expand until substantial abutments are reached or the hanging wall exceeds a critical span and fails. At Quirke Mine, the critical span was about 400 m at a depth of 500 m, giving a span/depth ratio of 0.8. In addition fracturing reached through to surface which was inconceivable prior to the rockburst problem because of the massive quartzite beds above the orebody.

10.1.7 References

Hedley, D.G.F. and Grant, F. (1972), Stope and pillar design for the Elliot Lake uranium mines. CIM Bull, vol. 65, No. 723, pp. 37-44.

Hedley, D.G.F., Roxburgh, J.W. and Muppalaneni, S.N. (1984), A case history of rockbursts at Elliot Lake. 2nd Int. Conf. Stability in Underground Mining, Lexington, Kentucky.

MacDonald, P. and Muppalaneni, S.N. (1983), Microseismic monitoring in a uranium mine. Rockbursts: Prediction and Control, Inst. Min. Met., London, pp. 141-145.

Swan, G. (1985), Strength distributions and potential for multiple pillar collapse. Division Report MRP/MRL 85-127, CANMET, Energy, Mines and Resources Canada.

10.2 Falconbridge Mine

10.2.1 Summary

The Falconbridge Mine had a history of minor rockbursts since 1955. By the mid-1980s over 90% of the orebody had been mined and production was concentrated in a few strategic pillars. In June 1984, a series of large rockbursts occurred that unfortunately resulted in four fatalities and closure of the mine. For Canadian mines, this was the first clear evidence of rockbursts being produced by slippage along prominent faults. After the mine closed seismic activity declined substantially with only sporadic larger events.

10.2.2 Mining Background

The Falconbridge Mine is located on the south-east rim of the Sudbury Basin and has been in operation since 1929. The tabular orebody strikes east-west for about 2000 m on surface and extends to 1800 m in depth, as shown on the longitudinal section in Figure 10.2.1. It dips steeply to the north down to 1200 level (265 m), then reverses and dips steeply south at depth. The orebody pinches and swells with an average width of 5 m. At depth the hanging wall greenstones, and especially jasperoid inclusions, are the strongest and most brittle rocks, followed by the footwall norites, with the massive sulphide orebody being the weakest rock.

The mine is serviced by two main shafts: No. 5 shaft extends from surface to the 4200 level, while the hoist room for the No. 9 shaft is on the 3850 level and this shaft extends down to the 6050 level. Levels are established at 53 m vertical intervals. Initially, square-set mining was the major extraction method, but was superseded by longitudinal cut-and-fill techniques with cemented tailings. Sill pillars, below the levels, were recovered using undercut-and-fill methods. In 1982, the mine was shut down for six months and when it reopened, production was decreased and undercut-and-fill became the main mining method. By 1984, about 94% of the orebody had been extracted and the major remaining ore reserves were in a pillar around the hoist room on the 3850 level, as identified in Figure 10.2.1.

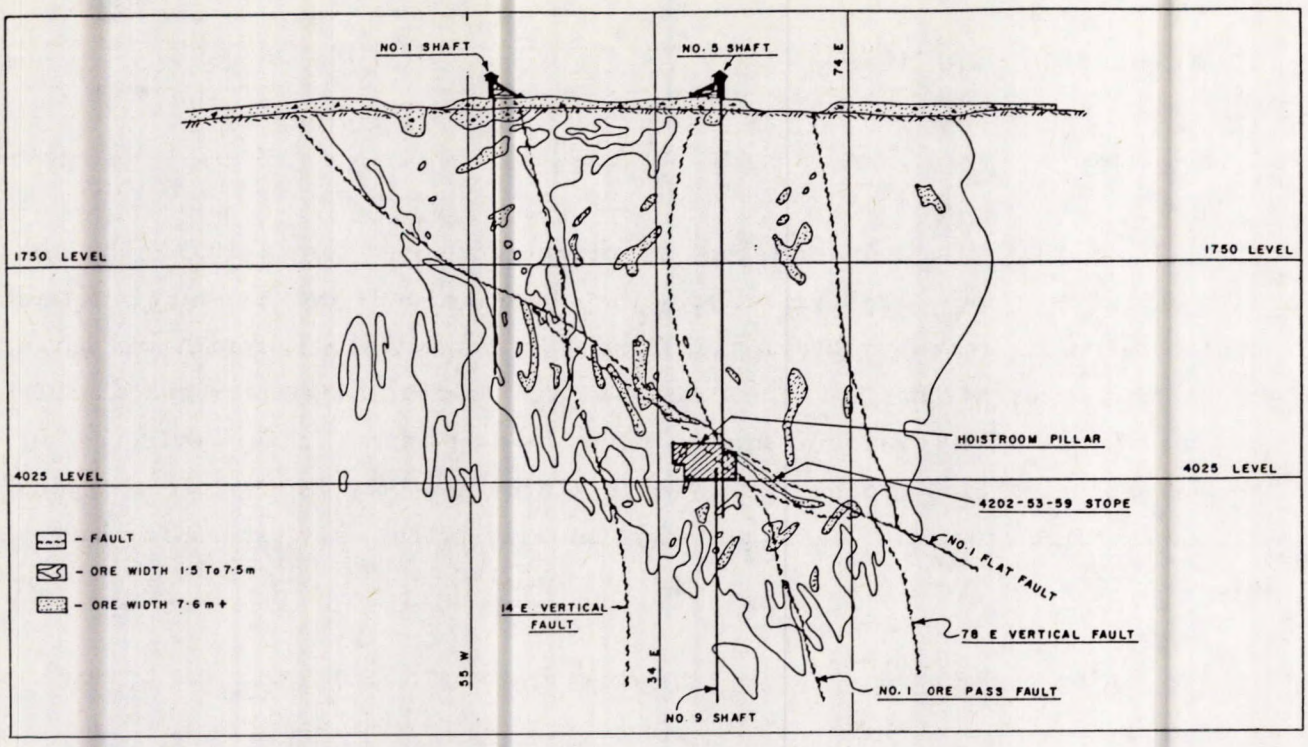

Fig. 10.2.1 - Longitudinal section of the Falconbridge Mine (after West, 1985).

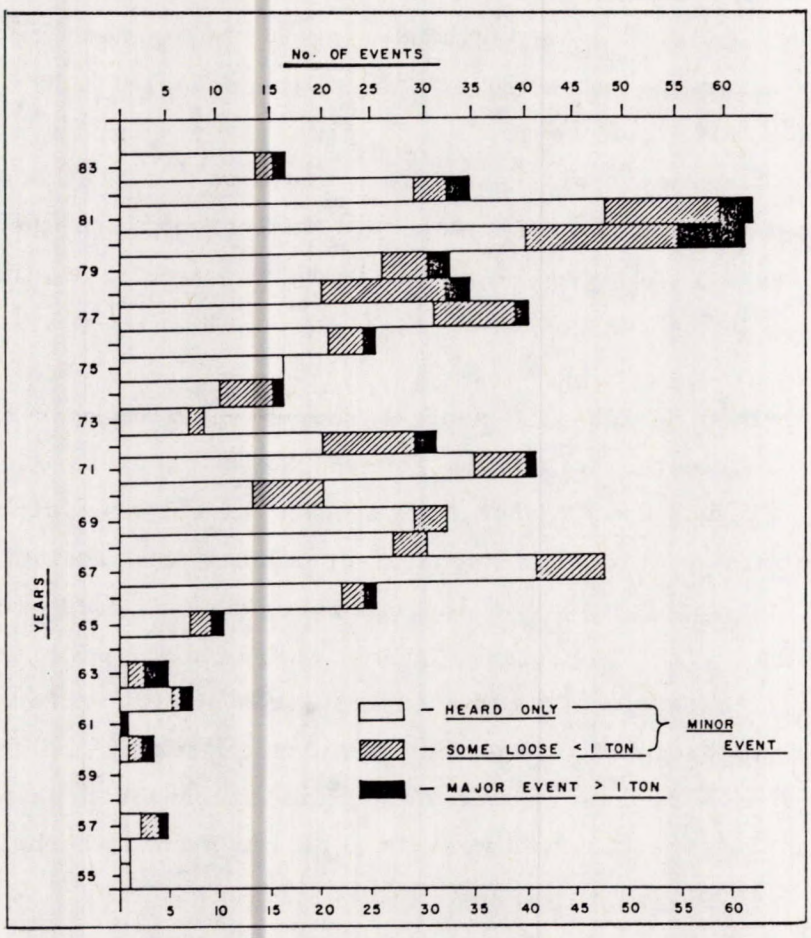

Fig. 10.2.2 - Distribution of recorded seismic events at the Falconbridge Mine (after West, 1985).

A number of major fault structures intersect the orebody, which itself is on the Main Fault. The characteristics of the faults were outlined by Vongpaisal et al. (1980).

The Main Fault occurs at the contact between the breccia sulphides and the norite. The fault zone is composed of gouge material up to 1 m thick. Where there is a deviation of the contact, tangential shears break away from the fault into the hanging wall.

The No. 1 Flat Fault dips at about 45^{o} to the north-east and extends across the whole mine. Gouge on this fault varies from a few centimetres to half a metre wide in thickness.

The Ore Pass Fault also extends across the whole mine and is comprised of a faulted and sheared zone of up to 15 m wide. It is steeply dipping and intersects the orebody at an acute angle.

All these faults intersect the orebody in the same area: just east of the hoist room pillar on the 4025 level.

10.2.3 Previous Rockburst Experience

The first reported rockburst at the Falconbridge Mine occurred in November 1955. A reporting procedure was developed based on underground observations and whether the vibrations were felt underground and on surface. In general, two categories were used. A rockburst was defined as a violent failure of rock causing engineering problems, whereas a shock disturbance causes no engineering problems. Figure 10.2.2 shows the distribution of reported events from 1955 to 1983 (West 1985). Of the 600 reported events only 31 or 5% were rockbursts causing damage. Some of the shock disturbances were felt at the townsite on surface and probably had a magnitude of more than 2.0 Mn. Since no damage was found, it is likely these events were caused by fault-slip somewhere in the wall rocks.

Based on location and the amount of damage, the cause and mechanism of rockbursting was investigated (Vongpaisal et al. 1980). Faults and other

geological structures accounted for 54% of the bursts and the mining of island, sill and remnant pillars for the other 46%. It was also observed that 78% of all seismic events occurred below the No. 1 Flat Fault and 85% below the 2450 level (750 m depth). Although faulting was recognized as the cause of many rockbursts, the mechanism was seen as a build-up of stress on one side of the fault due to the weak gouge material being unable to transmit stress through it. The concept was that slippage on the fault could be the mechanism and source of the liberated energy was not considered. This was because only the stored strain energy in rock was considered as the source of the released energy, rather than a change in potential energy.

Based on the compressive strength and elastic modulus, the rock types were classified on their proneness to bursting. Jasperoid was the most rockburst-prone rock followed by greenstone, with norite being the least likely to burst. This led to a program of destress blasting of jasperoid inclusions in the hanging wall during the 1960s (Moruzi and Pasieka, 1964). These blasts appeared to reduce the severity of bursting in sill and remnant pillar situations. However, with the installation of a microseismic system in 1981, it was found that seismic activity was predominantly concentrated along geological structures in the footwall norites, and the destress blasting program was largely discontinued.

10.2.4 Microseismic Monitoring

By the early 1980s one of the few remaining blocks to be mined was the hoist room pillar near the centre of the mine. Ground control problems including rockbursts were anticipated during the recovery of this pillar and an Electrolab MP-250 microseismic system was installed around the hoist room pillar prior to any mining. Initially eight geophones were installed, with the processing unit being located underground on the 3850 level, connected to the printer on surface (Davidge, 1984).

The background noise from mining equipment was relatively high and seismic monitoring and analysis were eventually confined to off-shift and weekends. Typically microseismic activity averaged 3 to 4 events per day. Most seismic activity was occurring in the footwall norites near prominent faults and

especially the Ore Pass Faults. Some seismic activity occurred around development openings in the hanging wall greenstones and jasperoid, but there was very little activity in the orebody. In September 1983, the system located a large rockburst of magnitude 2.8 in the footwall, about 70 m from the orebody and on the 3325 level. Damage was observed on this level and the one above.

10.2.5 Rockburst Sequence

On June 20, 1984 at 10:12 EDT, the first of a series of major rockbursts occurred. Over a 24-hour period, about 250 seismic events were recorded by the microseismic system. Rockbursts recorded by the Eastern Canada Seismic Network are listed in Table 10.2.1 (also included are events in 1983 and 1985) and their locations are plotted on a longitudinal section in Figure 10.2.3. Those rockbursts near the 4025 level are plotted on this level plan in Figure 10.2.4, which also shows the location of the major faults.

The first rockburst of magnitude 3.4 Mn occurred, without apparent warning, on the No. 1 Flat Fault on the 4025 level. Unfortunately, this was about 20 m from where four miners were working in an undercut-and-fill stope. Shock waves from this rockburst caused the overlying mat to collapse entrapping the miners in backfill. The next major rockburst, 3.5 Mn, occurred two hours later on the Ore Pass Faults between the 4025 and 4200 levels, followed 8 min later by a 3.2 Mn event on the same faults and on the 4200 level. For the rest of June 20 and 21, seismic activity was restricted mainly between the 4025 and 5325 levels and over a distance of 200 m on strike. Most of this activity appeared to be associated with the No. 1 Flat Fault, the Ore Pass Faults, and the Ropeway Dyke, as shown in Figure 10.2.4. During June 22 and 23, seismic activity moved up dip and one rockburst of 2.5 Mn, occurred on the 3675 level again on the Ore Pass Faults. The last of this sequence of rockbursts, 2.2 Mn occurred on July 5, 1984 on the 3500 level and on the No. 1 Flat Fault.

Visual inspection of the mine workings confirmed damage between the 4025 and 4375 levels (1225 and 1335 m depth) with approximately 1000 to 2000 tonnes of displaced rock. Slight damage, such as extension of fresh cracks and loose

Table 10.2.1 Rockburst sequence, magnitude and location

Date	Time	Magnitude	Depth, m	Fault System
Sept. 14/83	14:32	2.8	1015	Ropeway Dyke or No. 7 Shaft
June 20/84	10:12	3.4	1220	No. 1 Flat Fault
" "	12:12	3.5	1240	Ore Pass
" "	12:20	3.2	1280	Ore Pass
" "	12:38	2.0	1265	Ropeway Dyke
" "	13:00	1.5	1305	Ore Pass
" "	14:57	<1.5	1220	No. 1 Flat Fault
" "	20:59	<1.5		Location uncertain
June 21/84	05:15	<1.5	1250	Ropeway Dyke
" "	09:08	<1.5		Location uncertain
June 22/84	00:47	2.5	1115	Ore Pass
July 5/84	17:48	2.2	1065	No. 1 Flat Fault
April 17/85	01:20	2.0	1540	Ore Pass
" "	01:23	1.7	1455	Ore Pass

Table 10.2.2 Fault slip parameters

Magnitude Mn	Seismic Moment Mn.n	Radius m	Ave. Slippage mm	Stress Drop MPa
3.4	32,800	200	35	7.2
3.5	40,700	180	53	12.2
2.2	2,440	70	5	3.1

Table 10.2.3 Peak particle velocity and damage

Magnitude	Distance m	Peak Particle Velocity, m/s	Damage
3.4	20	2.15	Backfill mat collapsed
3.5	50	0.56	More mat collapsed
3.5	15	3.86	Severe failure overlying drift
3.5	50	0.56	Minor shake down cross-cut

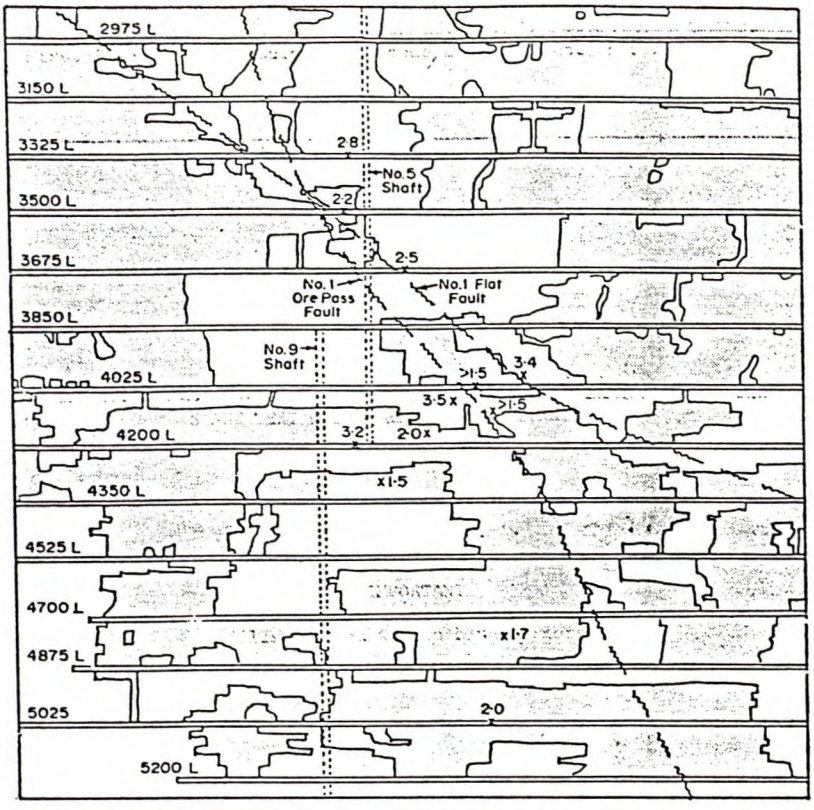

Fig. 10.2.3 - Longitudinal section showing location of major rockbursts.

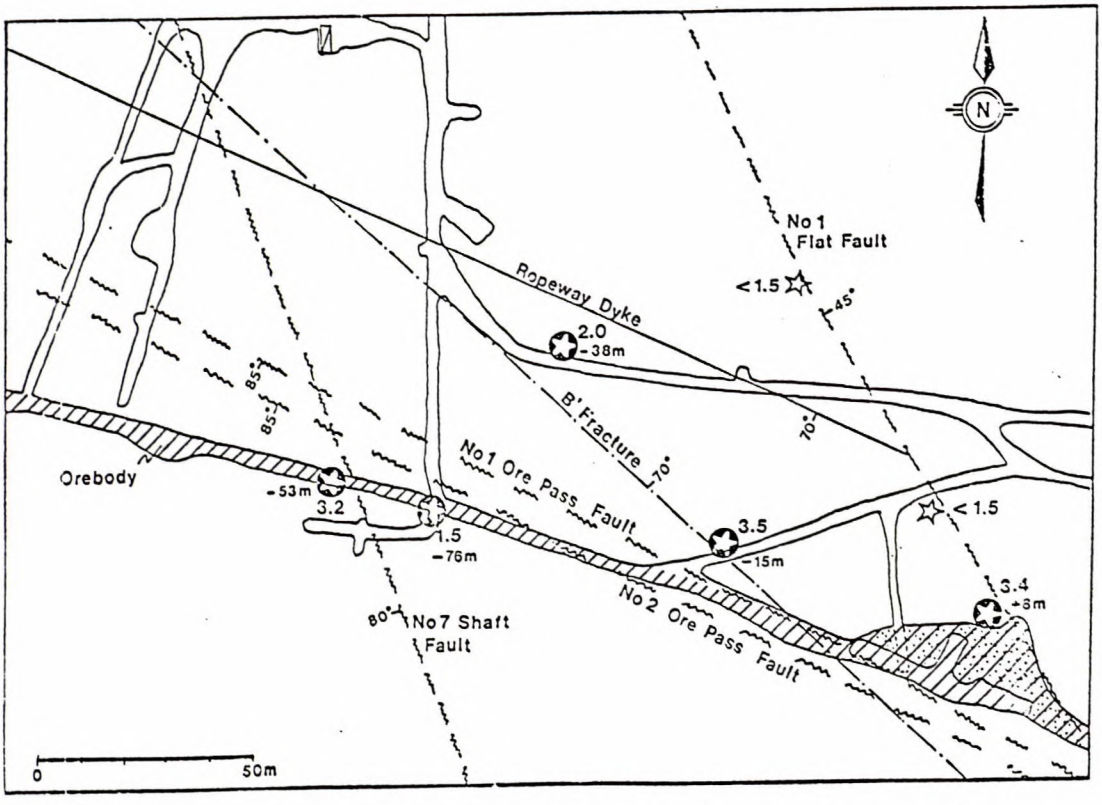

Fig. 10.2.4 - Plan of the 4025 level showing faulting and rockburst locations.

shake down, was observed over a circular area of radius 150 m centered on the 3.5 Mn event.

The location of the rockbursts from the microseismic system plus visual observations point to a fault-slip failure mechanism. This was confirmed for the rockburst on July 5, 1984, where there was no observed damage, and from striation marks on the gouge of the No. 1 Flat Fault on the 3500 and 3675 levels, the west side of the fault had moved laterally 1 to 2 cm towards the orebody.

After July 5, 1984 minor seismic activity continued sporadically. In the same month, it was decided to close the mine as a direct result of the rockburst incidents. In 1985, two rockbursts occurred within 3 min of each other on April 17. These were located on the Ore Pass Faults on the 5025 and 4700 levels. This is much deeper than the previously recorded rockbursts.

10.2.6 Seismic Investigation

After a major rockburst, the pattern and distribution of the aftershocks sometimes gives an indication of the area over which the fault slipped. Microseismic aftershocks in a one minute period following the first two major rockbursts of magnitude 3.4 and 3.5 were analyzed. As shown in Figure 10.2.5, all the microseismic events occurred in the footwall in a quadrant configuration of the radius 180 to 200 m, centered on the location of the major bursts.

No seismic waveforms were obtained from these events, consequently, spectral analytical techniques could not be used to estimate source parameters such as stress drop and average slippage. However, it is possible to estimate these parameters using the general seismology equations given in Chapter 5.

In the Canadian Shield, seismic moment M_o is related to magnitude Mn by Equation 5.13.

$$\log M_o = 0.94\ Mn + 1.32 \text{ in GN.m} \qquad \text{Eq } 10.2.1$$

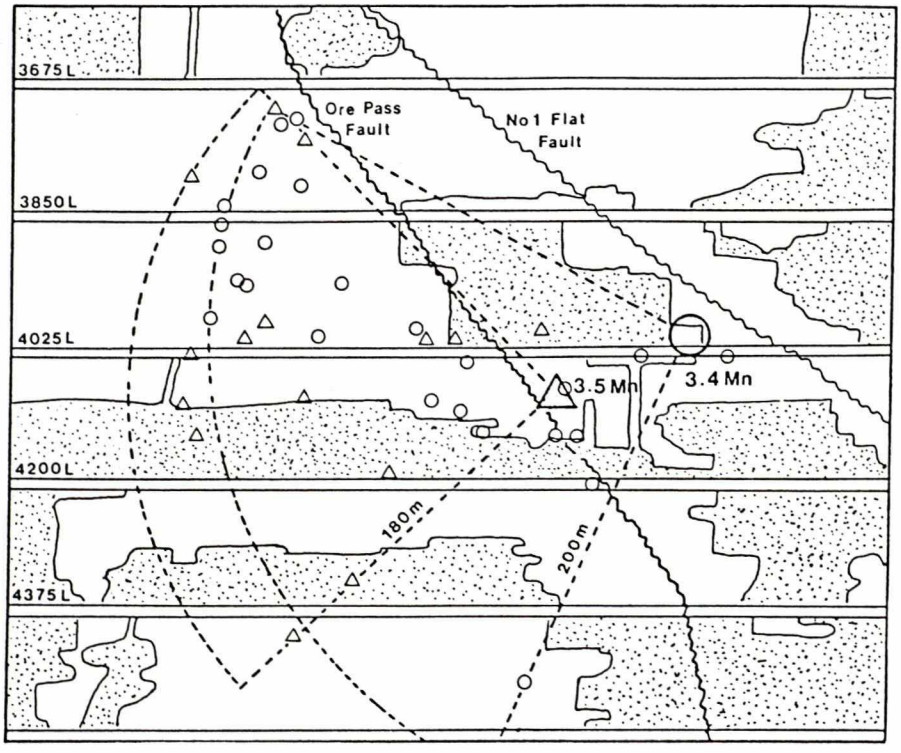

Fig. 10.2.5 - Aftershock patterns following the first two major rockbursts.

Seismic moment is also the product of the average slippage, ψa, shear modulus, G, and area. For a quadrant model:

$$M_o = \psi a . G \cdot \Pi/4 \; r_o^2 \qquad \text{Eq 10.2.2}$$

Also average slippage is related to the stress drop $\Delta\tau$ by Equation 5.19

$$\psi a = \frac{16 \Delta\tau \; r_o}{7\Pi \; G} \qquad \text{Eq 10.2.3}$$

Using these Equations, plus the radius of the aftershock patterns, the average slippage and stress drops were calculated for the first two rockbursts. These parameters are listed in Table 10.2.2, along with those from the 2.2 Mn event of July 5, 1984 where slippage was observed on the No. 1 Flat Fault 70 m from the source.

The radius over which slippage occurs, based on aftershock patterns, is in reasonable agreement with the 150 m radius of observed damage. Estimated stress drops of 3.1 to 12.2 MPa are feasible considering that the measured stresses in the hoist room pillar were from 40 to 90 MPa. Average slippage for the first two rockbursts also seem reasonable, although the 5 mm for the 2.2 event is lower than the 10 to 20 mm observed from striation marks on the No. 1 Flat Fault.

Some estimates can be made on damage criteria based on peak particle velocity and observations of the rescue crew who were operating 50 m away when the 3.5 Mn event occurred. Peak particle velocity, $\hat{V}$, as related to magnitude, M, and distance, R, is based on a number of measurements in Ontario mines (Hedley, 1988), where:

$$\hat{V} = 4000 \left(\frac{R}{10^{M/3}}\right)^{-1.6} \quad \text{in mm} \qquad \text{Eq 10.2.4}$$

The relevant parameters are listed in Table 10.2.3. The initial rockburst subjected the backfill mat in the undercut-and-fill stope to 2.15 m/s which caused it to collapse. Similarly, a velocity of 0.56 m/s from the 3.5 rockburst caused more of the mat to collapse. This second rockburst also

caused severe damage in the drift 15 m above, with an estimated velocity of 3.86 m/s, but only minor damage in a cross-cut 50 m away.

10.2.7 Discussion

The first rockburst of magnitude 3.4 Mn on the No. 1 Flat Fault was probably caused by mining in the adjacent undercut-and-fill stope. Since there was no microseismic activity prior to the burst, the triggering mechanism was probably a reduction in the clamping stress rather than an increase in the shear stress. Once movement occurred on the No. 1 Flat Fault, it allowed the other faults, noticeably the Ore Pass Faults, to become active. This resulted in the wedge of rock in the footwall below the No. 1 Flat Fault, and the orebody to move towards the mined-out stopes.

The amount of damage associated with this series of rockbursts was not large compared to similar pillar bursts (e.g., at Quirke and Macassa Mines). Most of the damage seemed to be associated with critically loaded structures, such as the backfill mat, being subject to high velocities and consequently high transient stress pulses.

As illustrated in Figure 10.2.4, both the No. 1 Flat Fault and the Ore Pass Faults intersected the orebody in the same area. One of the strategies developed in Ontario mines in the 1940s was to mine against major faults as soon as possible, then to retreat away from them. In this case, more than 90% of the orebody had already been mined. However, slippage along these faults could also have occurred if the adjacent stopes had been mined earlier, but the magnitudes of the rockbursts may have been less because of the reduced areal extent of mining.

The role of the hoist room pillar in the rockburst problem is unclear. It served its purpose of protecting the hoist room until the early 1980s. By that time, the pillar was heavily stressed, cracks were appearing around the edge, and both the shaft and hoist motor were indicating slight movement. The microseismic system indicated a concentration of seismic activity in the footwall norites behind the pillar, probably caused by minor adjustments on

the fault structures. However, none of the major rockbursts in the June 20, 1984 sequence were located in the hoist room pillar.

10.2.8 References

Davidge, G.R. (1984). Microseismic monitoring at Falconbridge Mine, Falconbridge, Ontario. CIM Bull., vol. 77, No. 868, pp. 45-49.

Hedley, D.G.F., Bharti, S., West, D. and Blake, W. (1985). Fault-slip rockbursts at Falconbridge Mine. Proc. 4th Conf. on Acoustic Emission/ Microseismic Activity, Penn. State University.

Hedley, D.G.F. (1988). Peak particle velocity for rockbursts in some Ontario mines. Proc. 2nd Int. Symp. Rockbursts and Seismicity in Mines, Minneapolis, pp. 502-512.

Moruzi, G.A. and Pasieka, A.R. (1964). Evaluation of a blasting technique for destressing ground subject to rockbursts. Proc. 6th U.S. Rock Mech. Symp, Rolla, Missouri.

Vongpaisal, S., Owen, D.L. and Freelandt, V.W. (1980). Rockburst analysis Falconbridge Mine: historical review and analysis. Falconbridge Internal Report.

West, D. (1985). A case history of rockbursts at Falconbridge Mine. CIM Rockburst Seminar, Sudbury, Ontario.

10.3 Lac Mineral's Macassa Mine, Kirkland Lake*

10.3.1 Summary

The Kirkland Lake Mining Camp has had a strong history of rockbursting. The rockbursts at Macassa, the only remaining producer in the camp, were previously associated with failure of crown pillars and these events were high energy seismic disturbances. In the last four years, the mine has changed from using unconsolidated waste rockfill to cemented rockfill as the main type of backfill.

The use of cemented rockfill and subsequent new mining methods have resulted in an apparent reduction in the rockbursting frequency from eight bursts per year down to one. This reduction has occurred in parallel with an increase in production of 65% and with mining depths approaching 2150 m. The current seismic activity has been downgraded from a pillar-type energy system to the more non-violent strain-type bursts.

10.3.2 Rockburst History

This case history is a summary of the implementation of a stiff backfill, cemented rockfill, for the regional control of rockbursts at the Macassa Mine, a division of Lac Minerals Ltd. Since the introduction of cemented rockfill at the mine, overall working conditions have improved as a result of an apparent reduction in the rockburst frequency. In addition, the cost of the post burst rehabilitation of drifts and stopes has been reduced.

The mine has experienced both strain bursts during development and pillar bursts during the mining of stope crown pillars (Cook and Bruce, 1983). Arjang and Nemcsok (1986) have indicated that from 1935 to 1985, more than 400 reported rockbursts have occurred at the mine. Approximately 70% of these bursts occurred in the ore zone or stopes, and 10% of these events were classed as heavy bursts with displacement of more than 50 tonnes of rock.

---

*Prepared by W. Quesnel and R. Hong, Lac Minerals Ltd.

Prior to the use of cemented rockfill, the larger bursts were associated with the crown pillar of cut-and-fill stopes. The largest burst magnitude, recorded by the National Seismograph Network was 3.1 Mn with a rock displacement of more than 1,000 tonnes. The majority of the bursting generally occurred with or shortly after production blasting.

10.3.3 Mining Background

The Macassa Division of Lac Minerals Ltd., has been in production since 1933 with a total gold production of 3.0 million ounces. The mine is now accessed by a 2207 m deep single lift shaft completed in 1986. The levels are spaced approximately 46 m apart.

The main mining horizons are now located between the 4750 level (1448 m) and the 7050 level (2150 m), and the orebody still remains open at depth. The majority of the active stoping areas are presently located between sections 32W to 42W or a strike length of 305 m. This strike length and the presence of a 61 m wide shaft pillar requires strict adherence to mine sequencing.

Overall mine sequencing is referenced to the shaft pillar. All mining east of the shaft is advanced towards the pillar and the mining west of the shaft is advanced away from the western shaft pillar boundary line. The final eastern and up dip limits of the shaft pillar will be based on monitoring results as mining progresses towards the pillar line.

The mining widths range from 1.5 m to 15 m. The majority of extraction has occurred along a strike fault, which is referred to on the '04 Break'. This major structure, on average, strikes N65^{o}E and has a dip of 75^{o}S. Recently, a comprehensive diamond drill program has located new horsetail '04' hanging wall vein structures. These H/W veins, which are sub-parallel to the 04 Break, are presently being developed for mining.

In addition, a new 05 Break has been located 450 m north of the 04 Break. This zone is still in the exploration stage with development and diamond drilling.

In situ stress determinations were conducted by CANMET on the 5300 and 6300 levels. The overcoring technique (CSIR and CSIRO) was used, and the following average stress gradients were measured.

Vertical Stress	= 0.026 MPa/m
Horizontal Stress (perpendicular to strike)	= 1.62 x Vertical Stress
Horizontal Stress (parallel to strike)	= 1.14 x Vertical Stress

Translating these stress gradients to the presently deepest mining level results in calculated pre-mining principal stresses in the order of 90 MPa.

The rock units have laboratory compressive strengths that range from 170 MPa to 345 MPa. The laboratory modulus of elasticity for the ore and wall rocks can range from 34.5 GPa to 80 GPa. Locally, the ore can be stiffer than the surrounding wall rocks.

The properties of cemented rockfill have been mainly studied under laboratory conditions. Uniaxial compression tests using 457 mm x 914 mm cylinders have given the following 28-day strengths and modulus of elasticity values.

Cement Binder	Uniaxial Compressive Strength (MPa)	Modulus GPa
5%	4	N/A
7%	7.2	4.1

It is interesting to note that the modulus for 7% cemented rockfill is in the order of 40% of medium strength concrete.

The actual batching of cemented rockfill consists of underground slurry mixing stations fed by 1.5 ton tote bags which contain Portland Type 10 cement. The cement is mechanically mixed at a pulp density of 55% and is delivered either by gravity or pumping to the dump point. The slurry is then mixed with waste development rockfill. The cement binder ranges from 5 to 7% by weight of rockfill.

10.3.4 Mining Methods

Since 1986, the Macassa Mine has evolved its mining methods from mainly overhand cut-and-fill with recycled, unconsolidated, waste development as backfill to underhand cut-and-fill, and underhand benching methods with cemented rockfill (CRF). In addition, some stopes are mined with overhand cut-and-fill utilizing CRF.

There has been a major reduction in the overall seismic activity and major rockburst frequency associated with the implementation of CRF and subsequent development of new mining methods. The following subsections describe the mining methods used before and after the implementation of CRF.

10.3.4.1 Mining Methods - Pre-CRF

The major mining method employed over the years at Macassa was overhand cut-and-fill with recycled waste development as backfill. Shrinkage stoping was also used in the upper levels.

The cut-and-fill stopes were mined from level to level or 46 m in height and had average strike lengths of 61 m. The stope would be advanced with uppers drilling utilizing hand held drills and slushers. The stope would be mined with cut-and-fill methods to within 15 to 18 m of the overlying strike drift. The remaining crown pillar would then be mined by longwall using uppers and horizontal blastholes. The backfill would follow, as tight as possible, to the advancing longwall face.

The backfill would be transported to the stopes using motors and 2-tonne cars. The fill would be dumped down the central raise and would be reslushed into the stope. The main ground support in the stope was mechanical rockbolts installed on a random pattern. Timber support was used along the tramming levels to support the unconsolidated backfill.

10.3.4.2 Mining Methods - Post-CRF

Details of the evaluation of new mining methods utilizing CRF have been given in the paper by Quesnel, de Ruiter and Pervik (1989). The two most successful

methods to date, for the rockburst control and improved ore recoveries are:

Underhand cut-and-fill
Underhand benching-and-fill

Underhand benching is generally used for ore widths in the order of 7.5 m. Both methods use cable slings for support of the CRF mats.

The underhand cut-and-fill method uses breasting techniques while the underhand benching method utilizes downholes. CRF is conveyed to the stopes using ore cars or 1.0 m^3 and 0.4 m^3 electric LHD units. The fill is dumped either directly into the stope, down previously installed backfill culverts or down raise bored fill/slot raises. The employment of LHDs has increased the overall backfill placement rate.

In addition, combinations of underhand and overhand mining methods with CRF are used for some stope blocks. To date approximately 80% of active stoping areas are using CRF. The depletion of ore reserves in the upper mining block, the increased mining depths and mining of parallel ore zones indicates that utilization of CRF will eventually approach 100%.

10.3.5 Rockburst Mechanisms

The two types of rockbursts that have occurred at the mine are pillar type bursts and strain bursts. The strain bursts were generally low to intermediate energy events with displacements in the range of 1 to 50 tonnes with assumed magnitudes of less than 2.0 Mn. The pillar type bursts were high energy events with magnitudes as large as 3.1 Mn. The rock displacements can vary from 50 to greater than 1,000 tonnes. To date, there has been no evidence of strike-slip bursts at the mine and this is believed to be because of the high horizontal stresses which provide substantial clamping forces across the major discontinuities at the mine.

The highest frequency of strain bursts has occurred along geological contacts between rock units with varying stiffness or near major discontinuities in stiff rock units (LeBel et al., 1987). These types of bursts were commonly

located in development headings or in stopes with irregular backs. These bursts are believed to be the result of the stress readjustment, concentration and removal of confined conditions during excavation. Hedley (1987) has indicated that certain strain bursts can be the result of released stored strain energy in the rock mass. This energy release occurred when the rock suddenly changed from a triaxial to either a biaxial or uniaxial stress state. The energy release or seismic efficiency of a strain burst can be much lower than a pillar burst. Hedley (1987) has indicated that strain bursts have a seismic efficiency of 30 to 60%, while pillar bursts can be in the range of 70 to 90%.

Pillar-type bursts have generally occurred when cut-and-fill stopes have been advanced to within 15 m of the floor elevation of the overlying strike drift. Numerical modelling work (Hanson et al., 1987) has indicated that when stope crown pillars approach this critical geometry, the applied stresses approach the estimated in situ compressive strength of the ore. The occurrence of a pillar burst under these conditions is then dependent upon the degree of convergence of the stope sidewalls and the relative stiffness between the ore and sidewall rock types (mine stiffness).

Salamon (1984) has indicated that for critical instability, the following inequality, in part, governs the potential for a violent rockburst to occur.

$$K + \lambda < 0 \qquad \text{Eq 10.3.1}$$

where, K = Mine stiffness (sidewalls)

λ = Ore stiffness.

Equation 10.3.1 can be used to explain the occurrence of crown pillar bursts at the mine when the ore stiffness is greater than the sidewall (H/W and F/W) or mine stiffness. Once the stresses approach the crown pillar strength and failure occurs, the ore stiffness, λ, becomes negative. In narrow vein stopes where the crown pillar geometry results in rigid pillars and the stiffness of the ore exceeds the mine stiffness, the failure of the crown pillar will result in the remoulded ore stiffness to exhibit a large negative value, which exceeds the positive mine stiffness. This results in rapid closure of the

sidewalls and this energy release forms the damaging seismic waves of a rockburst.

The parameters affecting the level of energy release can best be explained by Salamon's Mining Energy Balance equation as shown below:

$$W_t + U_m = U_c + W_r \qquad \text{Eq 10.3.2}$$

where, W_t = change in potential energy due to wall convergence
U_m = stored strain energy in mined ore
U_c = stored strain energy transfer to wall rocks
W_r = excess energy released,

and knowing that for elastic conditions:

$$W_t = 2(U_m + U_1) \qquad \text{Eq 10.3.3}$$
$$W_r = U_m + U_1 = W_t/2 \qquad \text{Eq 10.3.4}$$

where, U_1 = is the increase in stored strain energy if the stress increase had occurred on unstressed rock.

From Equation 10.3.4, it can be concluded that the largest component causing excess energy release, W_r, is the potential energy W_t, due to convergence of the sidewalls of a stope. The source of the damaging seismic waves or liberated kinetic energy, W_r is then controlled by:

$$W_k = W_t - (U_c + W_s) \qquad \text{Eq 10.3.5}$$

where, W_s = energy absorption of the backfill.

Hedley (1984) has suggested that the stored strain energy, U_m, is used up in fracturing the rock, or in this case the crown pillar. Therefore, the magnitude of the released, damaging seismic energy (rockburst) is mainly governed by the degree of wall closure.

Since the change in potential energy, W_t, is a function of the principal

stress, S_o, and the volumetric convergence of the stope, ΔV, ($W_t = S_o \Delta V$), then regional control measures for pillar-type rockbursting have to reduce or minimize the overall mine convergence.

At Macassa Mine, this has been achieved with the introduction of a stiff backfill, CRF. The CRF not only limits wall convergence, W_t, but reduces the stored strain energy, U_m, as a result of energy absorption due to strain hardening of the backfill. All these factors contribute favourably, as can be seen by Equation 10.3.5, to reducing the released seismic energy, W_k, as the result of a rockburst.

10.3.5.1. Rockbursting Pre-CRF

Prior to the use of CRF as backfill, the mine had an average rockburst frequency of eight bursts per year. In this context, a rockburst has been defined as any seismic event which resulted in more than 5 tonnes of rock displacement. The larger events with magnitudes greater than 2.0 Mn were all associated with overstressed stope crown pillars. One of the largest bursts had a magnitude of 3.1 Mn and resulted in more than 1,000 tonnes of rock being displaced.

In general, single event rockbursts usually occurred during mining of the stope crown pillar. The rockburst would occur with or shortly after production blasting in the stope. Back analysis of these events using N-Fold models indicated that the crown pillars were near failure and the resulting new geometry formed by the production blast caused sudden failure of the pillar. This resulted in rapid differential closure of the sidewalls.

Incremental closure has been measured after intermediate rockbursts. In one case, 58-40 stope, (1745 m) a 25-tonne burst occurred (September 1986) after blasting a longwall face in the crown pillar of the stope. The measured convergence after the burst was 22 mm. It is interesting to note that only 29 holes, 2.4 m long, were blasted at the time of this burst. Examination of the stope after the burst showed the stulls in the backfill raise had cracked and mechanical rockbolts in the stope were pulled through the wooden headblocks. Damage was limited to the stope.

In the case of large single or multiple events, the measured incremental closure can be in the order of three times the convergence measured in the 58-40 burst and the ground displacement can take place over a greater area, as experienced during a series of rockbursts that occurred in 1987.

Figure 10.3.1 outlines the rock displacement that occurred after these bursts. Approximately 750 tonnes of rock were displaced which affected three main levels. These rockbursts were high energy events with magnitudes ranging from 1.7 Mn to 2.5 Mn.

The rockbursts affected an area of 30 m to 60 m wide by 100 m high. Closure measurements after these rockbursts showed a maximum convergence of 75 mm on the 5725 level. The sequence of events and subsequent ground damage are summarized below:

- The initial burst was initiated after blasting a longwall face in 57-38 stope. This burst occurred shortly after the blast and had a magnitude of 2.5 Mn.

- The next two bursts with magnitudes of 2.1 Mn and 1.7 Mn occurred during night shift within 13 minutes of each other.

- The fourth burst, with a magnitude of 1.7 Mn occurred approximately three days after the initial burst. This burst occurred during the shift.

- The damage from these bursts was extensive and resulted in partial collapse of the 5600 and 5725 levels. Unconsolidated rockfill filled part of the 5725 level because of the collapse of the timber support. Track heave in this area was as large as 0.6 m.

- Some portions of the drift that were supported with screen did not collapse even though the screen was heavily loaded with loose.

- A large proportion of the damage was centered around a large waste remnant known as the 36 waste pillar.

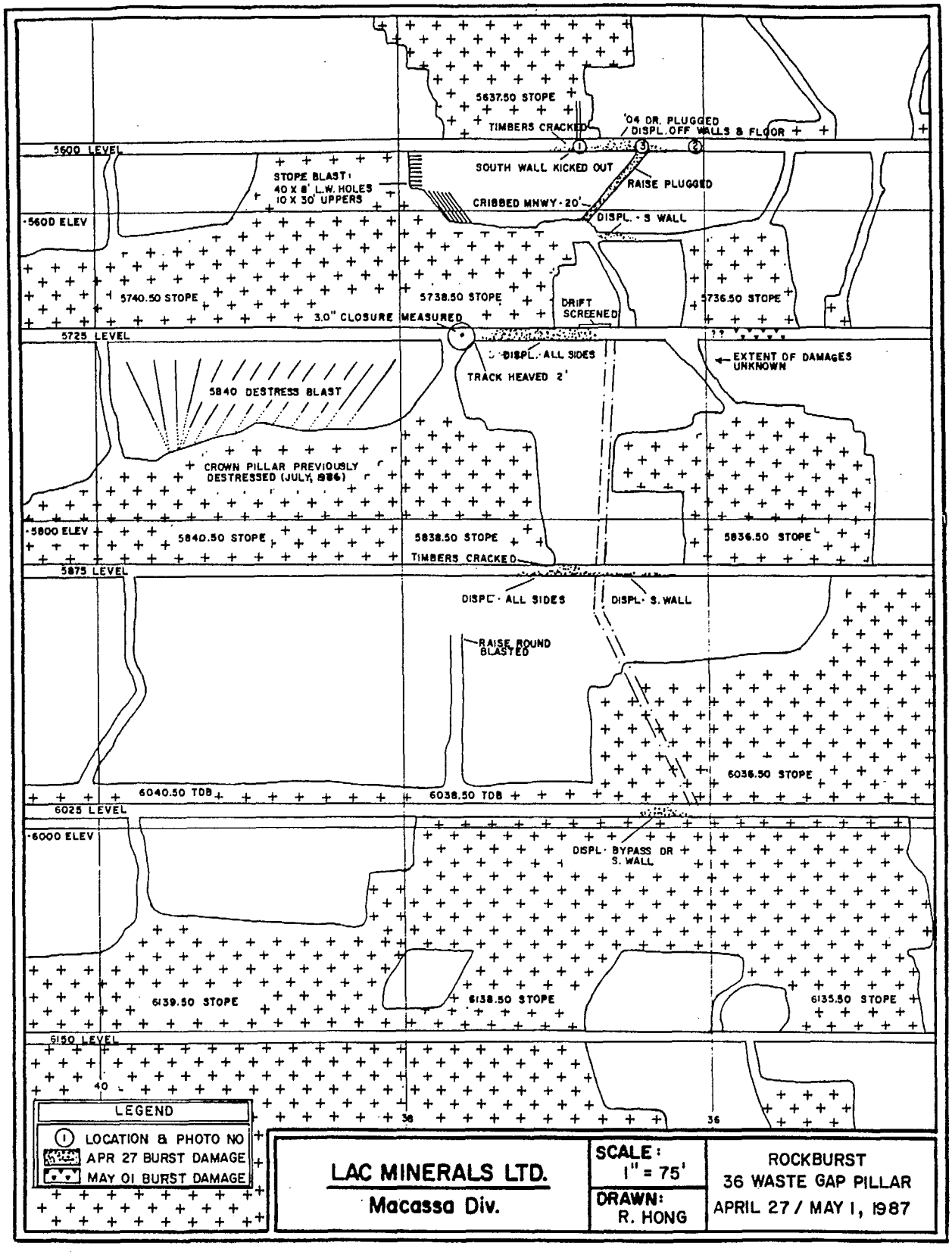

Fig. 10.3.1 - Longitudinal section showing location of damage caused by a series of rockbursts.

- Extensive mining had been completed in the affected area prior to the rockburst. Several crown pillars and ore remnants were located in the vicinity of these rockbursts. In addition, the 58-40 crown pillar had been previously destressed. This pillar was located approximately 30 m west of the center of the burst area. However, no damage occurred in this stope.

- All the stopes within the burst area had been backfilled with unconsolidated rockfill. The mined-out and backfilled area, west of the burst locations, extended to a vertical height of 140 m.

Based on the above observations and measured convergence, it was concluded that these rockbursts were a result of the overall reduction in mine stiffness due to the sequential failure of several crown pillars and ore/waste remnants. The initial burst was a result of the production blast and subsequent stress transfer to the metastable 57-38 crown pillar. The failure of this pillar resulted in a domino effect causing failure of the 36 waste pillar remnants above 5725 level and the 58-38 ore remnant. This caused a reduction in the local mine stiffness and resulted in extensive, sudden closure of the sidewalls. This situation could also have been further aggravated by the reduction in mine stiffness after the destressing of the 58-40 crown pillar (Hanson et al., 1987).

The above examples illustrate that the magnitude of the energy during a rockburst can be directly related to the degree of wall closure. The waste development backfill also appears to have very low absorption properties which can be related, in part, to the mining methods. Hedley (1984) has shown that the energy absorption of backfill in cut-and-fill stopes using uppers was lower than in cut-and-fill stopes using breasting techniques. This was due primarily to the fact that in stopes using uppers, the fill lags behind the back by one cut. In breasting the fill is generally brought to within less than 1 m of the back. The difference in backfill absorption between the mining methods can be significant.

10.3.5.2 Rockbursting - Post-CRF

In 1984, a test program was developed to study various backfills that could be used for rockburst control. Based on back analysis of rockbursting at the

mine, it was believed that the frequency of rockbursting would increase, as a result of proposed increases in production rates of 65% and deeper mining reserves centered around the 2150 level. It was felt that the only feasible method for improving the regional support of the mine was to implement a stiff cemented backfill. It was hoped that with a cemented backfill, changes to the mining methods and sequence could also be made.

The early test work centered around the use of concrete as backfill. A test stope, 47-04-3D, was mined at the 1400 m elevation using underhand cut-and-fill with concrete. Details of this initial test stope are given by de Ruiter and Hong, 1986, and Quesnel et al., 1989. The relevant conclusions from this test work are summarized below.

- The nature of the underhand cut-and-fill method used allowed for only 50% of the individual cuts to be filled. Convergence pins were installed between alternating layers of concrete.

- A total of five minor rockbursts occurred during mining of this stope. The largest burst displaced only 10 tonnes. This was surprising as the stope was located in an area of the mine that had a strong history of extensive pillar bursting.

- The bursts occurred in the footwall of the stope and were associated with a stiff band of tuff. There was no change in the trend or rate of wall closure after each burst. This indicated that no sudden or instantaneous closure of the sidewalls had occurred.

- It was concluded that these bursts were strain type events caused by the reaction of a stiff rock unit to the change in the mining stress state from confined to unconfined conditions.

- Although the use of concrete as backfill reduced the energy liberated during bursting, the increased mining costs would limit this backfill to a few select stopes.

Further research, using numerical modelling, indicated that if 100% of the

stope could be filled with a material having half the stiffness of concrete, the limits on volumetric closure would be similar to that in the 47-3D test stope.

Extensive test work began in 1986 utilizing minus 150 mm waste development rock and various cement binders. It was concluded that stiffness values in the order of 50% of that of concrete could be achieved with CRF having a cement binder between 5 and 7%.

To date 80% of the active stoping areas are now using CRF. It is felt that this ratio will increase to 100% within the next few years. Figure 10.3.2 shows that there has been an apparent reduction in the overall rockburst frequency associated with the implementation, as of 1987, of CRF as backfill. The frequency of bursting has been reduced from eight bursts per year to one. Figure 10.3.3 shows the total displacement of all bursts per year and the displacement and magnitude of the largest burst within the year. The total displacement and magnitude per burst have also been reduced and appear to be coincidental with the use of CRF.

It should be noted that the rockburst that occurred in 1989 with a magnitude of 3.1 Mn was centered around 60-36 stope. This stope had been mined with unconsolidated rockfill and had reached the crown pillar elevation. The stope adjacent to it, 60-38, was being mined with CRF. Very little damage occurred in the 60-38 stope.

At present, instrumentation is being installed in stopes using CRF to measure the convergence and determine more accurately the benefits of the backfill for rockburst control. However, with our experience to date, it can be stated that CRF has dramatically improved the overall regional mine stability by reducing the volumetric convergence due to mining. In addition, the energy liberated during a burst has been downgraded significantly resulting in minimal reconditioning of drifts after a burst. Also, the use of CRF has allowed a change in mining methods to utilize more effectively the energy absorption properties of the backfill. Underhand benching and underhand cut-and-fill allow for rapid tight filling directly above the next cut or bench.

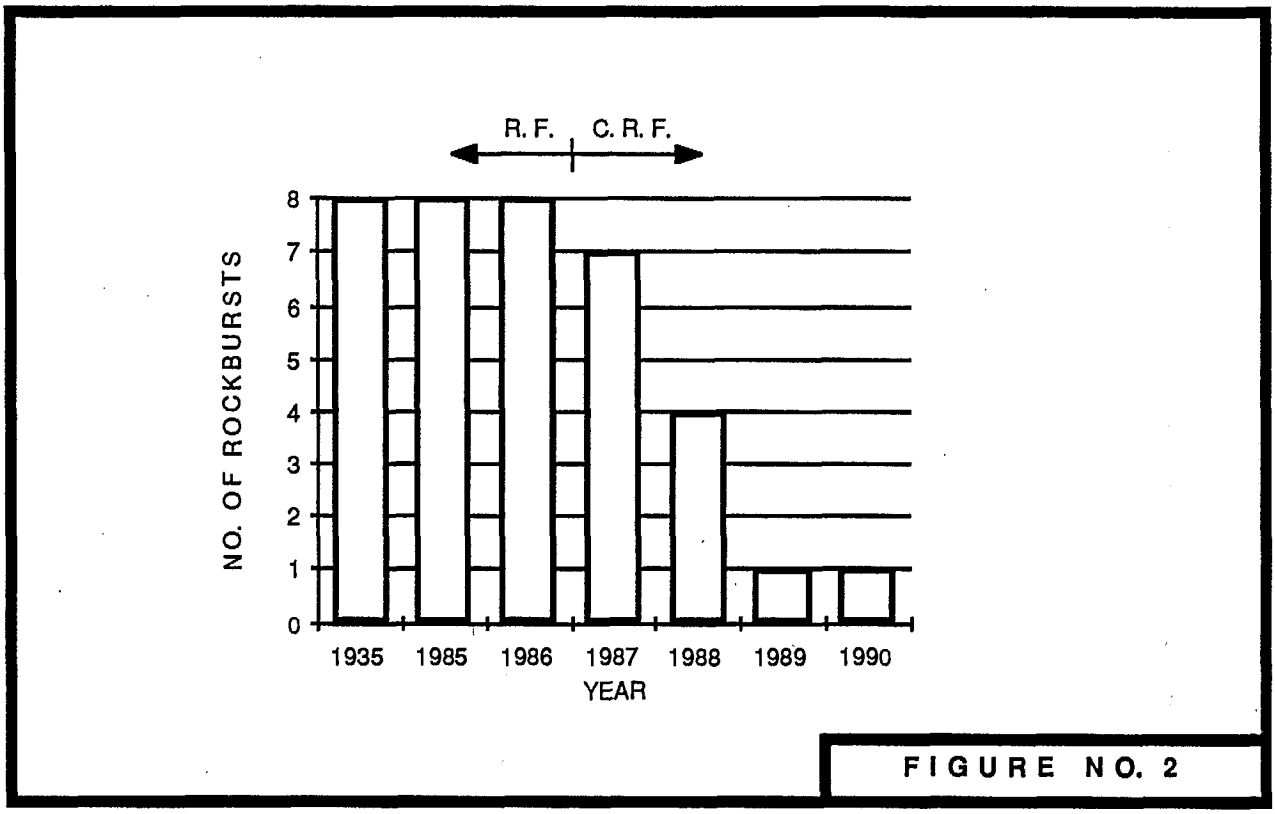

Fig. 10.3.2 - Frequency of bursting before and after introduction of cemented rockfill.

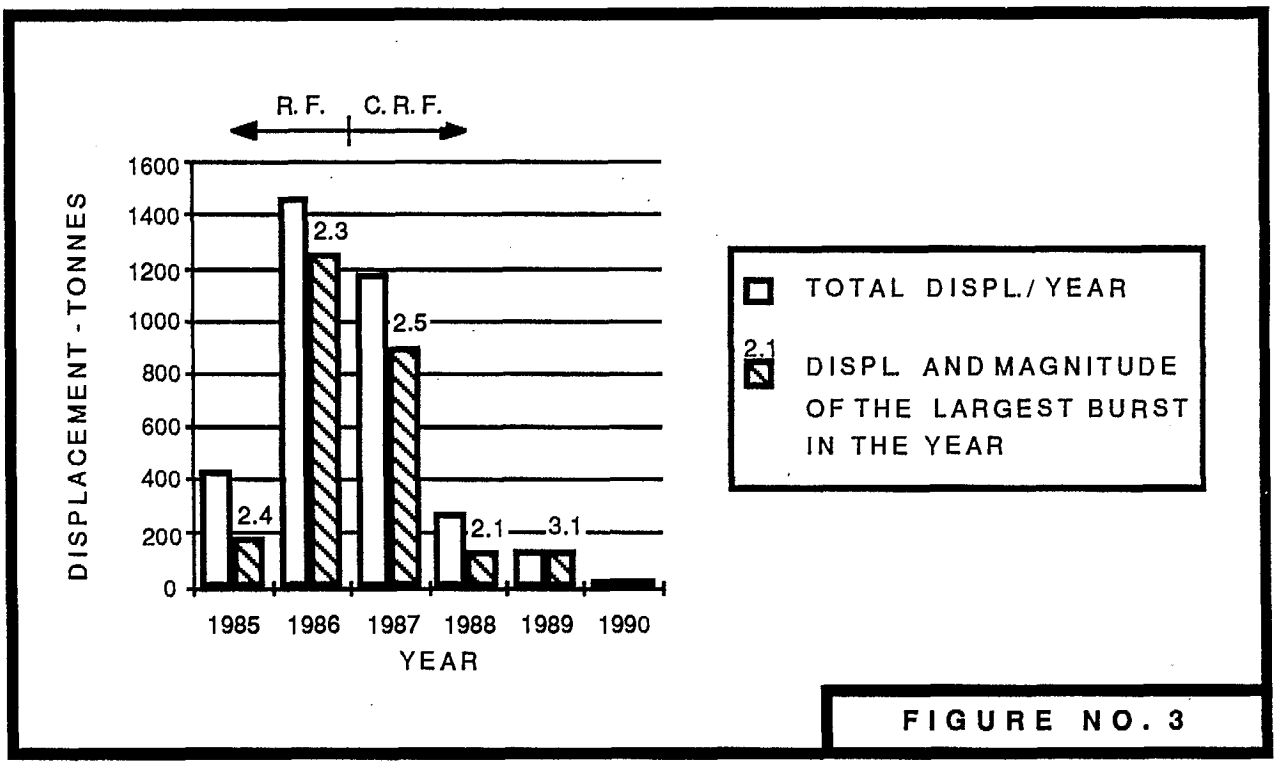

Fig. 10.3.3 - Damage caused by rockbursts before and after introduction of cemented rockfill.

10.3.6 Conclusions

- The magnitude of the energy release of pillar type bursts at the mine are related directly to the sudden convergence of the stope sidewalls.

- The occurrence of pillar bursts is associated with crown pillars that have a greater stiffness than the mine loading system.

- At depth (>1500 m), small incremental changes in stope volumes can cause significant rockbursting. This is especially valid where pillars are near peak strength, backfill is not kept tight to the advancing face, and the backfill material is not consolidated (i.e., low stiffness).

- In high extraction areas of mines susceptible to rockbursting, and that have used unconsolidated rockfill, special attention should be given to the sequencing of metastable pillars. The effects of incremental mining in one crown pillar on the stability of the surrounding ore and waste remnants should be determined with respect to the stress transfer and effects on the safety factors of the surrounding pillars. The effects of multiple pillar failure on the reduction of regional mine stiffness should be conducted to evaluate the rockburst potential.

- Backfill test work at the mine has shown that the energy released as a result of a rockburst can be reduced with the use of a stiff backfill. The stiffer the backfill, the greater the reduction in energy release.

- Since 1986, the mine has converted from using unconsolidated waste rockfill to cemented rockfill as the main type of backfill. An apparent reduction in the rockburst frequency has occurred coincident with the use of CRF. The rockburst frequency has been reduced from an average eight bursts per year to one. The total energy release of current bursting is much lower than bursting prior to the implementation of CRF.

- The use of CRF at the mine has allowed positive changes to be made to the mining methods. Underhand cut-and-fill and underhand benching methods are now used at the mine. These methods allow for rapid placement of the

backfill tight to the advancing face. This improves the overall energy absorption properties of the backfill which in turn reduces the overall stored strain energy in the rock mass.

10.3.7 References

Arjang, B. and Nemcsok, G. (1986), Review of rockburst incidents at the Macassa Mine, Kirkland Lake. Division Report MRL 87-21(TR), CANMET, Energy, Mines and Resources Canada.

Cook, J.F. and Bruce, D. (1983), Rockburst control through destressing - a case example. Rockbursts: Prediction and Control, pp. 81-91, IMM, London, U.K.

de Ruiter, H. and Hong, R. (1986), The use of underhand cut-and-fill with concrete support, Lac Minerals - Macassa Division. Presented at the Mine Backfill Design Seminar, McGill University, Montreal.

Hanson, D., Quesnel, W.J.F. and Hong, R. (1987), Destressing a rockburst prone crown pillar - Macassa Mine. Division Report MRL 87-82(TR), CANMET, Energy, Mines and Resources Canada.

Hedley, D.G.F. (1984), Utilization of backfill support in longitudinal cut-and-fill mining. Division Report 84-86(TR), CANMET, Energy, Mines and Resources Canada.

Hedley, D.G.F. (1987), Rockburst mechanics. Division Report MRL 87-118(TR), CANMET, Energy, Mines and Resources Canada.

LeBel, G.R., Quesnel, W.J.F. and Glover, W. (1987), An analysis of rockburst events during sinking of Macassa No. 3 shaft. Presented at 89th Annual General Meeting of the CIM, Toronto.

Quesnel, W.J.F., de Ruiter, H. and Pervik, A. (1989), The assessment of cemented rockfill for regional and local support in a rockburst environment, Lac Minerals Ltd., Macassa Division. Proc. 4th Int. Symp. on Mining with Backfill, Montreal.

Salamon, M.D.G. (1984), Energy considerations in rock mechanics: fundamental results. J. S. Afr. Inst. Min. Met., vol. 84, No. 8, pp. 233-246.

10.4 Placer Dome's Campbell Mine

10.4.1 Summary

Gold mines in the Red Lake area have a history of rockbursts dating back to the early 1960s. The most significant series of rockbursts occurred in the 'F' zone at the Campbell Mine at the end of 1983. This orebody had been mined by shrinkage stoping techniques, leaving boxholes and thin horizontal sill pillars. Over a 30-hour period 22 large rockbursts, up to a magnitude of 3.3 Mn, were recorded as well as numerous microseismic events.

The microseismic data, pillar stresses obtained from computer models and visual observations were used to reconstruct the sequence of events. Rockbursts started on level 10, near the centre of the orebody and quickly spread up dip to level 7, and down dip to level 13, covering an area of 450 m on strike by 300 m on dip. The cause of the rockbursts was the failure of the 6 m wide sill pillars on these levels. The mechanism of the rockbursts was a sudden change in potential energy as the hanging wall and footwall converged as a result of pillar failure. Stress levels of about 120 MPa appear to be critical for boxhole pillars, and 135 MPa for sill pillars.

At present (i.e., 1992), production has not been resumed in this orebody.

10.4.2 Mining Background

Campbell Mine is situated at Balmertown in the Red Lake District of Northwestern Ontario. Eight gold-bearing ore zones are found in steeply dipping faulted Precambrian volcanic rocks. There are two main vein structures: replacement veins of 0.6 to 9 m wide, and quartz carbonate fracture filled veins of 0.2 to 1 m wide. Andesite is the host rock for all veins.

The mine was brought into production in 1949 and daily tonnage is about 1,000 tonnes. The shaft is 1315 m deep with levels established at 45 m intervals. Most development drifts are driven in the ore zones. Initially all production was from shrinkage stopes but now most stopes below 600 m in depth use

overhand cut-and-fill techniques with deslimed tailings used as backfill. Present production is from a depth of 300 to 900 m and is 55% cut-and-fill, 35% longhole stoping, and 10% development.

10.4.3 Previous Rockburst History

As early as 1960, management suspected that two unlocated bursts had in fact occurred in the 'A' zone. In late September and early October there were five rockbursts in the adjacent Dickenson Mine. Both companies retained Professor Morrison of McGill University in 1961 to study the bursting problems. His recommendations follow:

- remove established sills and boxhole pillars as soon as possible;
- increase the size of sill pillars in shrinkage stopes presently being mined;
- eliminate boxhole pillars in favour of timbered backs in new shrinkage stopes;
- carry shorter stopes through in the vertical plane rather than long flat backs; and
- cut-and-fill mining methods should be adopted.

In the 'A' zone, these recommendations were followed. A transition from shrinkage to cut-and-fill was established on level 10 and sills began to be blasted on the upper levels. However in 1965, rockbursts were encountered on level 5. At this time, the stopes on level 6 and above had been mined out to a 4.6 m sill and these were being removed. Most of the 102 recorded bursts in the 'A' zone from 1962 to 1982 have occurred in boxhole pillars adjacent to the open face as the sill and boxhole pillars were being removed by long-hole blasts.

The 'A' zone ore is developed down to level 20 and a stepped sequence of mining has been established starting from the Dickenson boundary on level 20 and retreating westward. However, sill removal was stopped when it was found that most sill blasts were accompanied by rockbursts. Many ground problems and bursts were encountered on level 10 when the 1102 cut-and-fill stope was

being mined through. Although some of this stope was mined to level 10, it could never be completed.

10.4.4 Rockburst Sequence in the 'F' Zone

The 'F' zone is an isolated orebody to the west of the shaft. A generalized longitudinal section is shown in Figure 10.4.1. In the upper levels, the strike length is about 450 m and tapers down to 150 m on level 15. Ore thickness varies from 1.2 to 3.0 m with several offshoots also mined. Dip is generally 75^{o} to the south.

Mining of the 'F' zone began on the upper four levels in the 1950s and proceeded downward as the shaft was deepened. By 1974, all of the ore above level 10 had been mined using shrinkage methods with boxhole pillars and 6.1 m wide sill pillars.

Figure 10.4.1 shows the overall pattern of deterioration of the boxhole pillars prior to the major rockbursts in December 1983. The first burst occurred in July 1981 at the west end of level 11. Over a 30-month period, additional bursts were located in boxhole pillars between levels 7 and 14. These bursts were triggered either by drawdown of broken ore in the stopes, or renovation work in the levels, or in one case, destress blasting of boxhole pillars on level 14.

A renovation crew was removed from level 12 on December 20, 1983, because of seismic activity and visible deterioration of the boxhole pillars. Ten days later, the major sequence of rockburst occurred.

At 00:51 hours on December 30, the first violent rockburst was felt on surface, followed rapidly by other seismic events. The microseismic system indicated that bursting was confined to the 'F' zone, where no one was working. However, work crews in other parts of the mine felt the vibrations and were hoisted to surface.

The first visual inspection of the 'F' zone was done on January 5, 1984. It was found that levels 7 to 13 were blocked off near the eastern boundary of

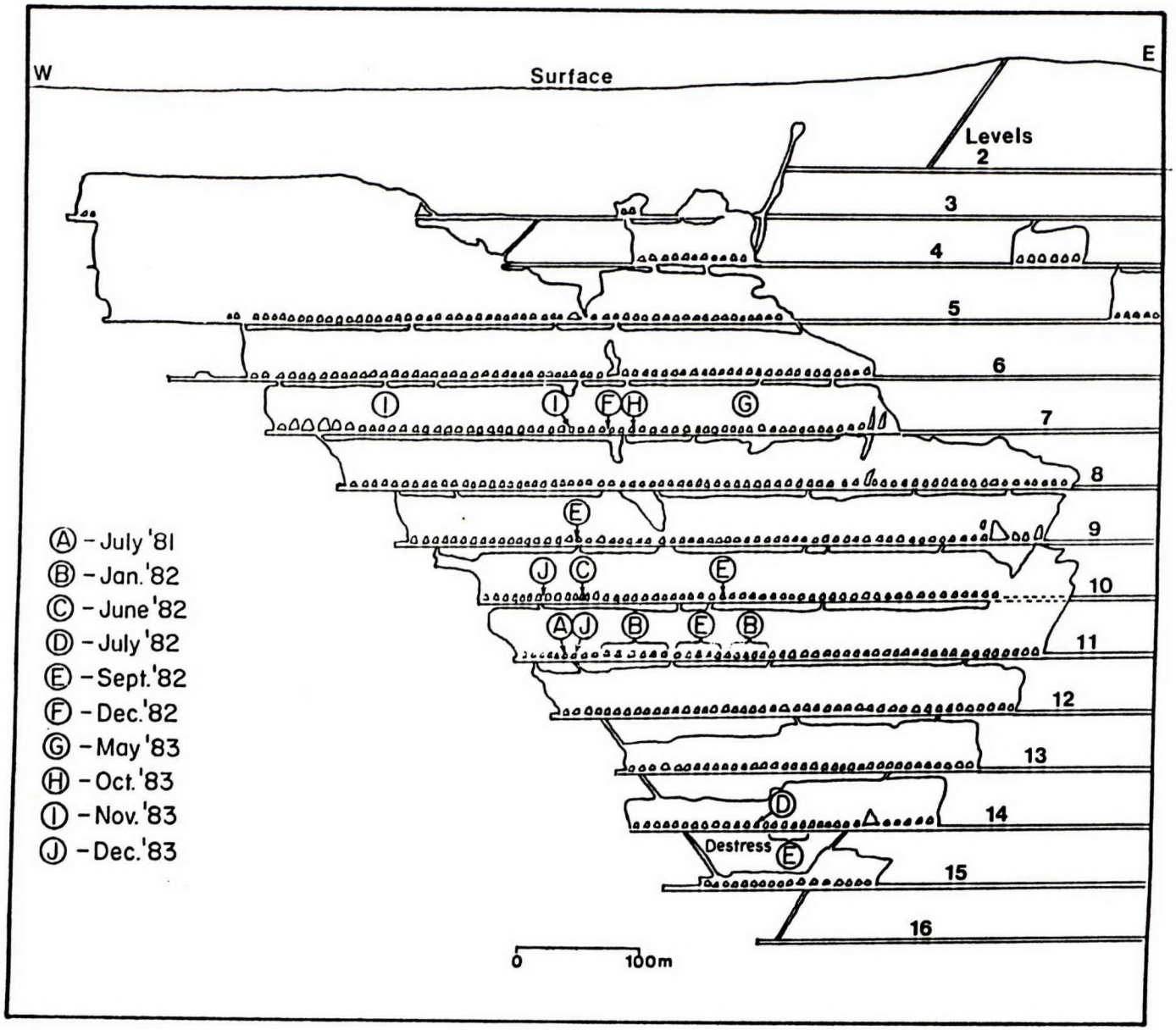

Fig. 10.4.1 - Generalized longitudinal section of the 'F' zone and sequence of deterioration of the boxhole pillars.

the orebody. Minor damage had occurred on level 14 and there was no change on level 15. Levels 4, 5 and 6 were open with some loose shaken down and fresh cracks.

In October 1984, an inspection was made of the west end of the 'F' zone on levels 12, 13 and 14. It was found that the west end of level 14 was relatively undamaged over a distance of 100 m. Similarly, the last 75 m of level 13 was relatively undamaged, whereas heavy spalling had occurred along the complete length of level 12. The top of the shrinkage stopes on levels 13 and 14 were open where they were 15 and 18 m thick, but showed signs of high stresses near where they narrowed down to 6 m thick.

10.4.5 Microseismic Monitoring

In August 1983, a 32-channel geophone network was installed through the mine to monitor seismic activity. Thirteen of these geophones were located around the 'F' zone. Figure 10.4.2 shows the number of events per day from November 1983 to January 1984. The sudden increase in activity on December 30 followed by the rapid decline is a classic example of main shocks followed by aftershocks.

Twenty-two of these seismic events were large enough to be picked up on the regional seismic network. The times, estimated magnitudes and locations within the 'F' zone of these 22 rockbursts are listed in Table 10.4.1. Figure 10.4.3 shows the location of these rockbursts and other major seismic events.

The progression of rockbursts can be identified and appears to fall into distinct time phases. Rockbursts were initiated on level 10 and within minutes had spread to level 11, and within one hour to level 9. By 08:40 hours on December 30, rockbursts had spread to level 8. During the rest of December 30, rockbursts were confined mainly to levels 8, 9 and 10, and after the flurry of rockbursts at 02:30 hours on December 31, activity ceased on these levels. For the rest of December 31 and January 1, activity was mainly on levels 7, 12 and 13. The extent of the rockburst areas, shown in Figure 10.4.3, closely matches the visible evidence of damage underground (i.e., levels 7 to 12 shut off). It is also interesting to note in Figure 10.4.3 that

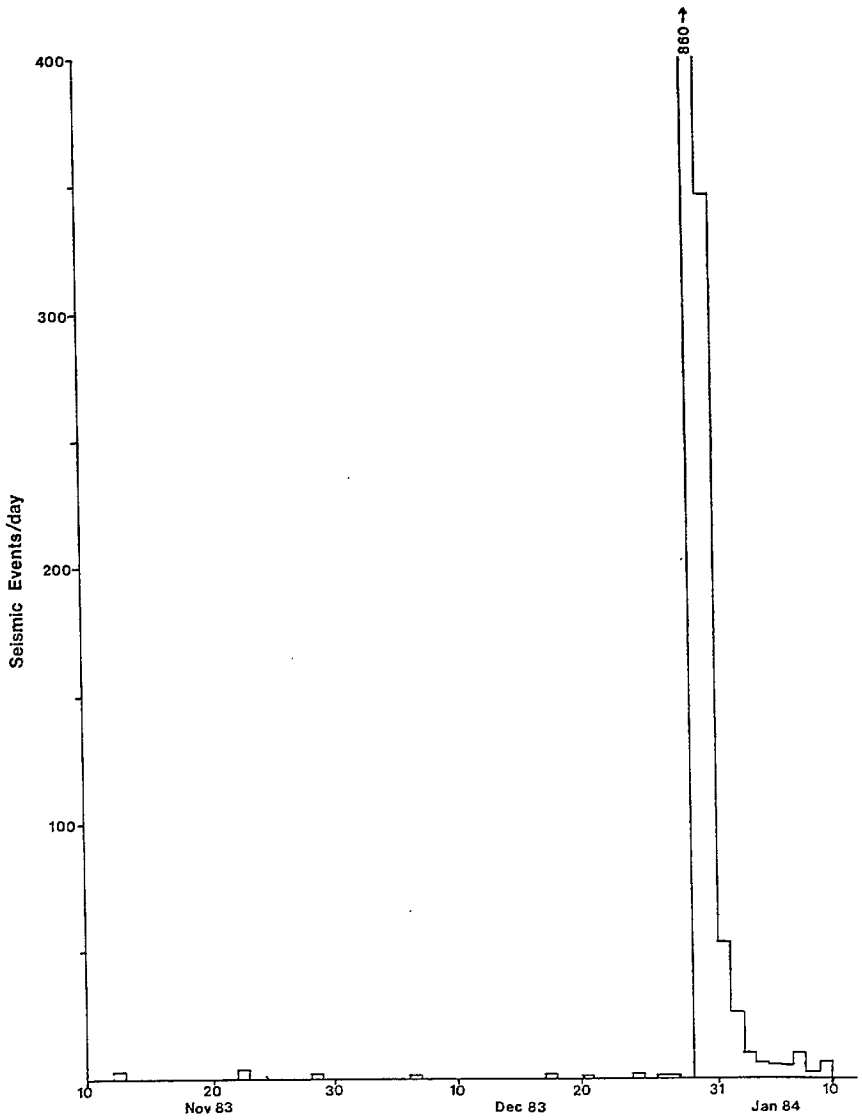

Fig. 10.4.2 - Frequency of seismic events.

Table 10.4.1 - Campbell Red Lake Mine, major rockbursts

No.	Date	Time	Mn	Mine Location
1	Dec 30	00:51	2.1	10 Level
2		00:56	1.3	11 Level
3		00:59	2.7	11 Level
4		01:36	2.4	11 Level
5		01:50	1.4	9 Level
6		04:20	2.2	10 Level
7		04:22	1.9	10 Level
8		07:44	2.6	9 Level
9		08:09	1.8	9 Level
10		08:18	2.2	9 Level
11		08:24	1.4	9 Level
12		08:40	1.4	8 Level
13		11:31	1.6	Power off
14		11:33	2.9	Power off
15		13:21	2.2	10 Level
16		13:46	1.6	9 Level
17		22:40	2.5	8 Level
18		22:41	2.1	8 Level
19	Dec 31	01:17	2.0	7 Level
20		02:30	3.3	8 Level
21		02:30	2.8	10 Level
22		05:11	2.2	12 Level

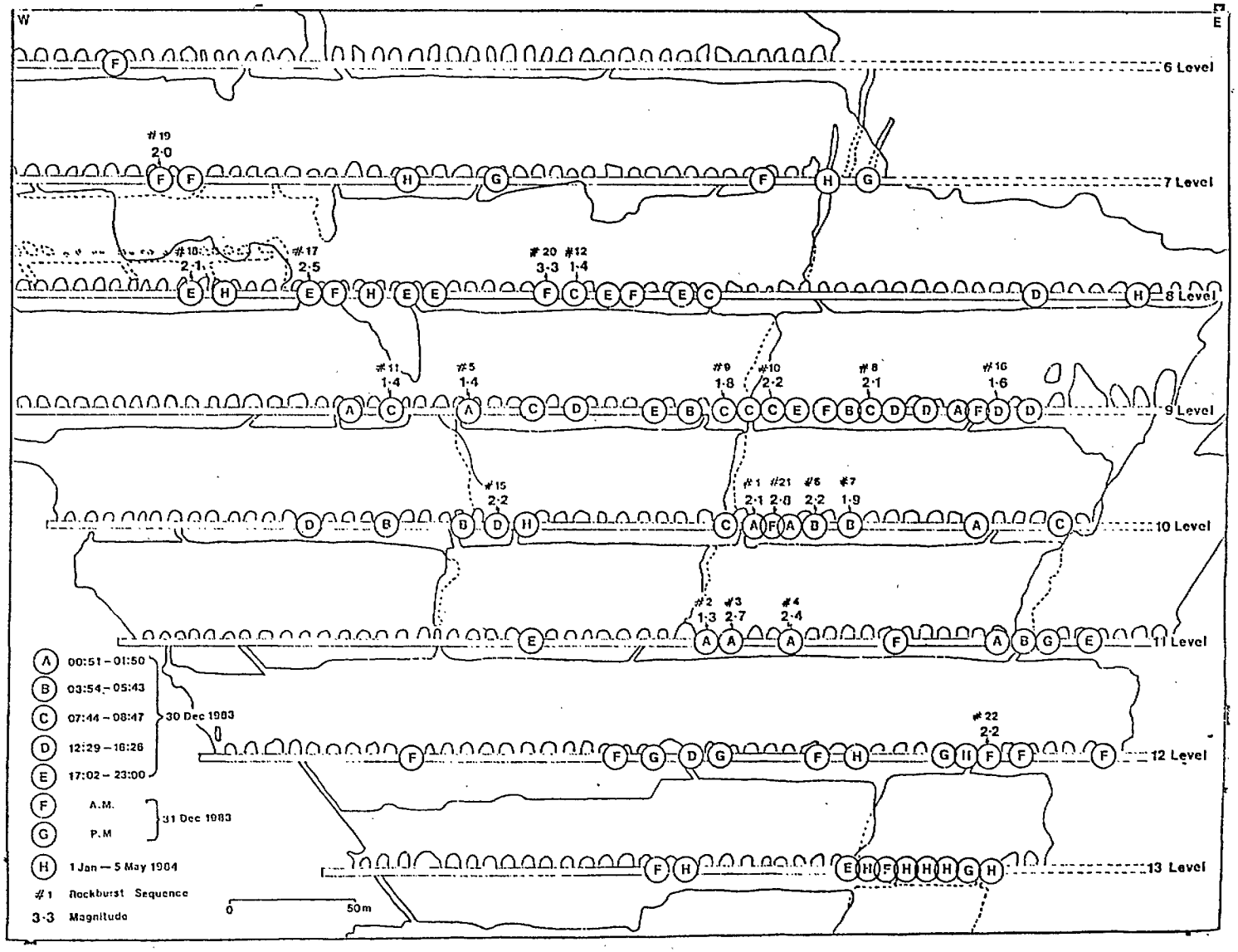

Fig. 10.4.3 - Location and sequence of major seismic events.

the vast majority of major seismic events occurred where the sill pillars are 6 m wide (on dip). Very few events occurred where the sills are 15 m wide.

10.4.6 Computer Modelling

The stresses and displacements around thin tabular orebodies, such as the 'F' zone, ideally are analyzed using displacement discontinuity models, which operate in the plane of the orebody. The perpendicular pillar stresses in the central part of the 'F' zone are illustrated in Figure 10.4.4 for elastic conditions. The boxhole pillars, especially on level 11, but also on levels 10, 12 and 13, are stressed very heavily (i.e., over 135 MPa). It is unlikely that these pillars could have supported these stresses and some had probably yielded prior to the start of rockbursting, and transferred some of the load to the adjacent sill pillars.

Estimates of strength of both boxhole and sill pillars were obtained using an Elliot Lake type of empirical relationship (i.e., Equation 10.1.1) where,

$$Qu = 100 \frac{W^{.5}}{H^{.75}} \qquad \text{Eq 10.4.1}$$

where, Qu = average pillar strength, MPa
W = least pillar width, m
H = pillar height, m.

The strength of a 1 m cube of andesite was taken as 100 MPa. Estimated strengths of various sizes of boxhole and sill pillars are listed in Table 10.4.2.

Using the model pillar stresses, and estimates of strength, safety factors were calculated for pillars on levels 7 to 13, which are listed in Table 10.4.3. For elastic conditions, all the boxhole pillars from level 9 down are subject to stresses higher than their estimated strength and have a safety factor of less than 1.0. The second column in the Table, under 'yielding pillars', assumes that the boxhole pillars yield and stabilize at a residual strength of 30 MPa (i.e., 25% of peak strength). The excess load is transferred to the sill pillar directly below. This is the likely condition

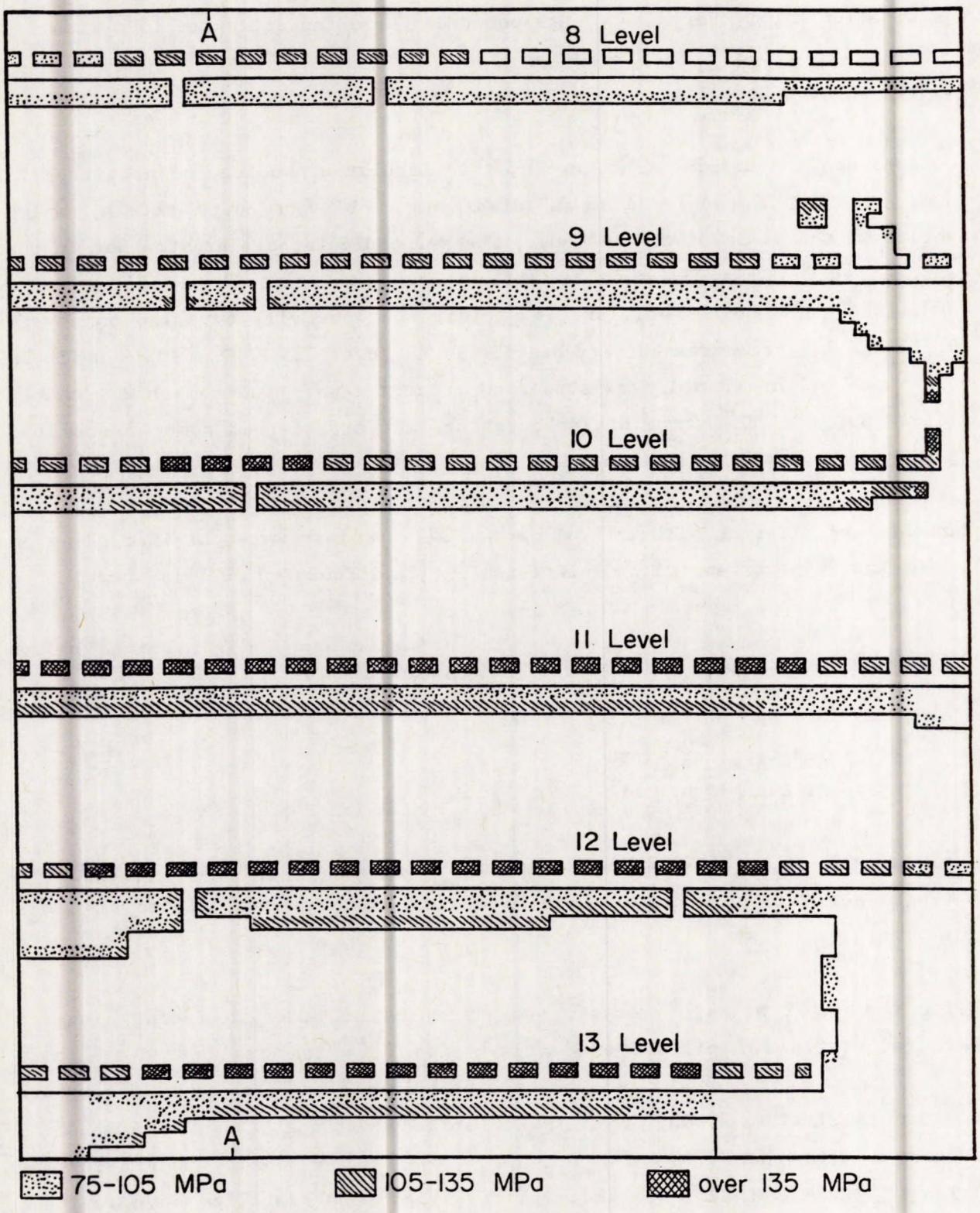

Fig. 10.4.4 - Perpendicular pillar stresses prior to rockbursts.

Table 10.4.2 - Estimated pillar strengths

Type of Pillar	Width, m	W/H Ratio	Strength, MPa
Boxhole	4.6	2.2	121
Sill	6.1	2.9	140
Sill	9.1	4.3	171
Sill	12.2	5.8	198

Table 10.4.3 - Estimated pillar stresses and safety factors (S.F.)

Level	Type	Pillar Width m	Elastic Stress MPa	Solution S.F.	Yielded Stress MPa	Pillars S.F.
7	Boxhole	4.6	87	1.40	87	1.40
	Sill	6.1	62	2.26	62	2.26
8	Boxhole	4.6	106	1.14	106	1.14
	Sill	6.1	77	1.82	77	1.82
9	Boxhole	4.6	123	0.98	30	Yielded
	Sill	6.1	88	1.58	119	1.17
10	Boxhole	4.6	137	0.89	30	Yielded
	Sill	6.1	97	1.45	132	1.05
11	Boxhole	4.6	147	0.82	30	Yielded
	Sill	6.1	103	1.36	142	0.90
12	Boxhole	4.6	145	0.83	30	Yielded
	Sill	9.1	77	2.22	103	1.67
13	Boxhole	4.6	139	0.87	30	Yielded
	Sill	12.2	75	2.65	93	2.12

just before the series of rockbursts on December 30, 1983. Results indicate that the sill pillars on level 11 had a safety factor just below 1.0, and on level 10 just above 1.0, followed by the level 9 sill pillars.

The microseismic system indicated that failure was initiated on level 10 sill pillar followed within a minute by the 11th sill, and within an hour by the 9th sill. Results from the computer model indicate that sill pillars on all three levels have a high degree of meta-stability.

10.4.7 Discussion

Based on the microseismic data, visual observations and computer modelling, the sequence of events in the 'F' zone is reconstructed as follows.

- Starting in 1981, and progressing through 1982 and 1983, minor bursts occurred in boxhole pillars between levels 7 and 14. The regional stability of the whole orebody was in a delicate balance at this time. There appears to be a direct relationship to the broken ore drawdown in level 12 stope, and subsequent boxhole pillar bursts on levels 11 and 10. The broken ore was probably acting as an uncemented rockfill which resisted closure of the hanging wall and footwall. When the ore was removed additional load was transferred onto the boxhole pillars in the level above triggering the bursts. Other minor activity such as the destressing blast in September 1982 was sufficient to cause a flurry of seismic activity. Even the scaling and drilling involved in rehabilitation of levels caused minor bursting.

- It is not known what triggered the series of large rockbursts on December 30, 1983. The microseismic network did not record any activity for at least a day before the first rockburst.

- Rockbursts began on level 10, and within minutes had spread to level 11, and within an hour to level 9. After about 8 hours, level 8 became affected and the following day rockbursts started to occur on levels 7, 12 and 13.

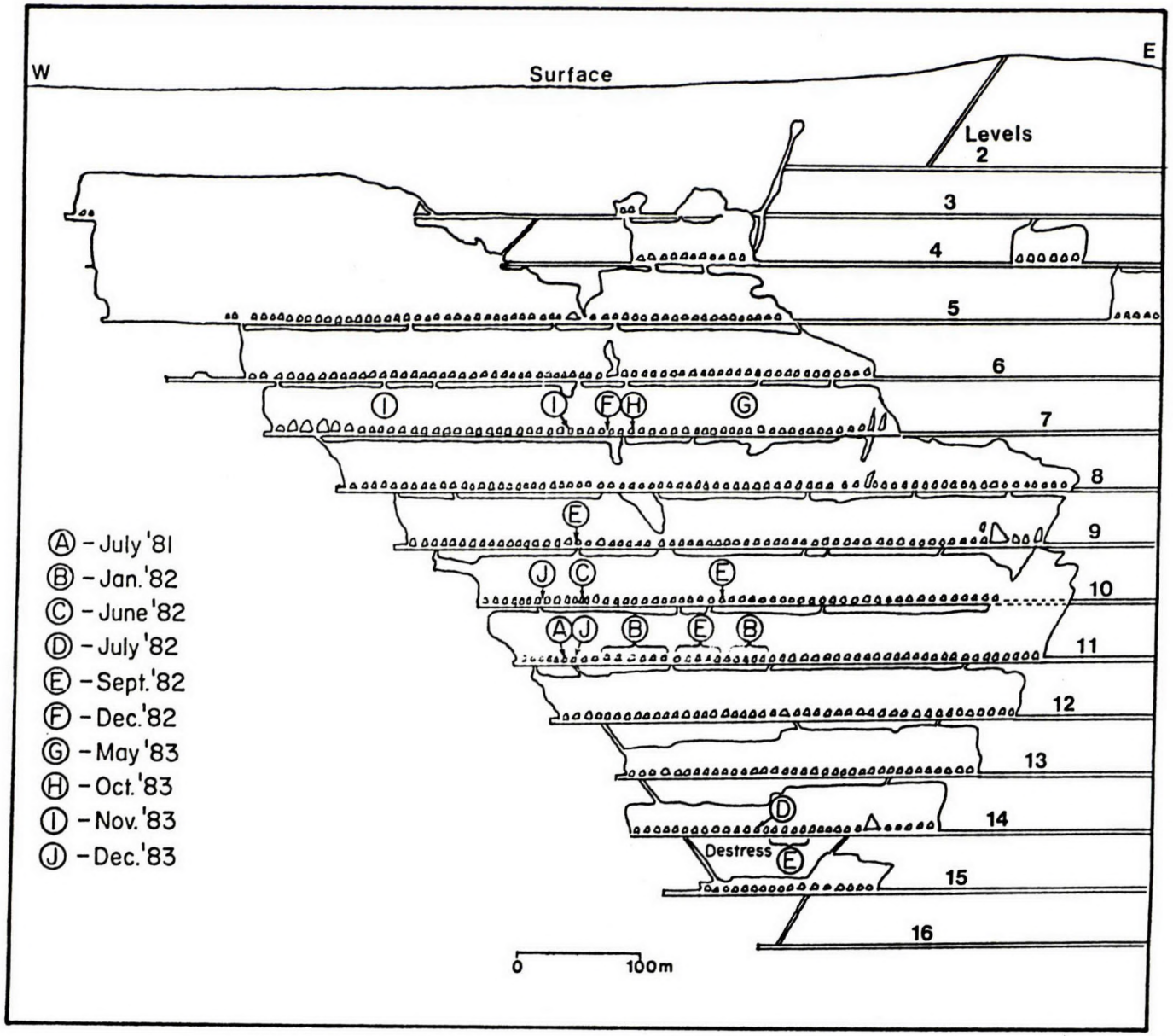

Fig. 10.4.1 - Generalized longitudinal section of the 'F' zone and sequence of deterioration of the boxhole pillars.

- From the analysis of pillar stresses and visual observations, where possible, the major rockbursts occurred in the sill rather than in the boxhole pillars. The major driving force appears to be the change in potential energy as the hanging wall and footwall suddenly converge.

- All the major rockbursts are confined to where the sill pillars are 6-m wide; only minor activity occurred where the sill pillars are wider than this.

- Analysis of pillar stresses indicates that boxhole pillars deteriorate at stress levels of 120 MPa or higher, and the 6 m wide sill pillars fail at stress levels of 135 MPa or higher. There is reasonable agreement between the areas of high pillar stresses from the computer model and observed damage underground. Computer modelling indicates high stress concentrations around raises in the sill pillars and many rockbursts were initiated at these locations.

- Once the broken ore is removed from shrinkage stopes, it becomes an open pit stope-and-pillar layout. Under these conditions, a certain proportion of the orebody has to be left as permanent pillars, as in room-and-pillar mines. An alternative is to convert to a cut-and-fill layout.

- The chain reaction of pillar failures at Campbell Mine occurred over a 30-hour period, compared to four years at the Quirke Mine. The area affected was smaller (i.e., 13 ha at Campbell, 70 ha at Quirke), and the pillars that failed were of a more uniform size.

10.5 Falconbridge's Strathcona Mine*

10.5.1 Introduction

Rockbursts became a significant concern at Strathcona Mine shortly after mining of the main sill pillar commenced in 1983. At that time, the sill ran the entire 500 m strike length of the orebody at an average depth of 720 m below surface. Prior to this time, as early as December 1973 in fact, rockbursting and bumping activity had been noted in the area of two diabase dykes between the 2750 level and 2625 level of the mine (Girard and Steele, 1974). The recommended treatment of ground problems at that time was to destress the footwall in active mining areas, to continue with the use of grouted rebar in loose, damaged rock, and to investigate instrumentation for continuous recording of rockburst activity. It is clear, however, that no consideration of a preferred mining sequence which might minimize the bursting risk or potential was made at that time. Indeed, even as late at 1984, the general opinion was being expressed that rockbursts were not (and by implication, would not) be a 'problem'. This was probably due to the fact that no sense of an increasing risk was considered likely, i.e., the problem was assumed to plateau at the then existing or slightly greater level and remain nothing more than a nuisance. In retrospect, this was an entirely reasonable assumption though incorrect.

Tracing the history of rockbursting at Strathcona Mine can be done most conveniently with reference to an extensive list of literature prepared by Falconbridge/Strathcona rock mechanics and engineering personnel together with consultants. In addition to Girard and Steele (1974), there are other references listed in chronological order: Singh (1975), Bharti, Udd and Cornett (1983), Bharti (1985), Morrison (1985), Blake (1985), Blake (1986), Morrison (1987), Hart and Board (1987), Davidge, Martin and Steed (1988), Blake (1988), Maxwell (1989), Semadeni (1989), Blake (1989), Tinucci and Hart (1990), Semadeni (1990), Maxwell, Urbancic and Young (1991). While this is by no means a complete list of reports, articles, reviews, memos, etc., written

---

*Prepared by G. Swan, Falconbridge Ltd.

on the subject, it will serve as an adequate source for the following summary of rockburst experience at Strathcona Mine.

10.5.2 Early History, 1971 to 1985

Strathcona Mine started production in 1968, and very quickly became Falconbridge's largest producing mine in the Sudbury Basin, with annual production rates of up to 2.1 million tonnes. Although originally developed as a cut-and-fill operation, by the mid-seventies increasing use was made of blasthole methods. By late 1984, when the incidence of rockbursts increased dramatically over previous levels, of the total 33.4 million tonnes of nickel-copper ore in reserve, approximately 27 million tonnes or 80% of the reserve had been mined out.

Prior to March 1985 and the installation of a basic 16-channel MP250 microseismic monitoring system, the only rockburst event records are those available from miners made known through daily production log books. According to these, for the period from 1971 to 1983, there was an average of 7 reports per year. During 1984, there was a tenfold increase to 74 reports. This increase may have been due in part to the rockburst incidents at Falconbridge No. 5 shaft in June 1984, and to a greater awareness of the rockburst problem as formal training in ground control for underground miners and supervision was begun in October 1984. Whatever the case, the severity of the problem in early 1985 can be judged by the decision to suspend mining in the affected areas of the mine (see Figure 10.5.1) until the microseismic monitoring system could be installed and a mining strategy could be developed with the help of various outside specialists. These included consultants, CANMET research scientists, and Ontario Ministry of Labour engineers. This strategy called for the reopening of some stopes and the closure of others. In addition, lunchrooms closest to the affected areas would be rebarred and cable-laced. Mining under the sill mat of the main sill would continue with strengthened timbering and with a blast design to minimize charge weights per delay. A monthly review of these actions was subsequently made by the mine supervision and ground control personnel.

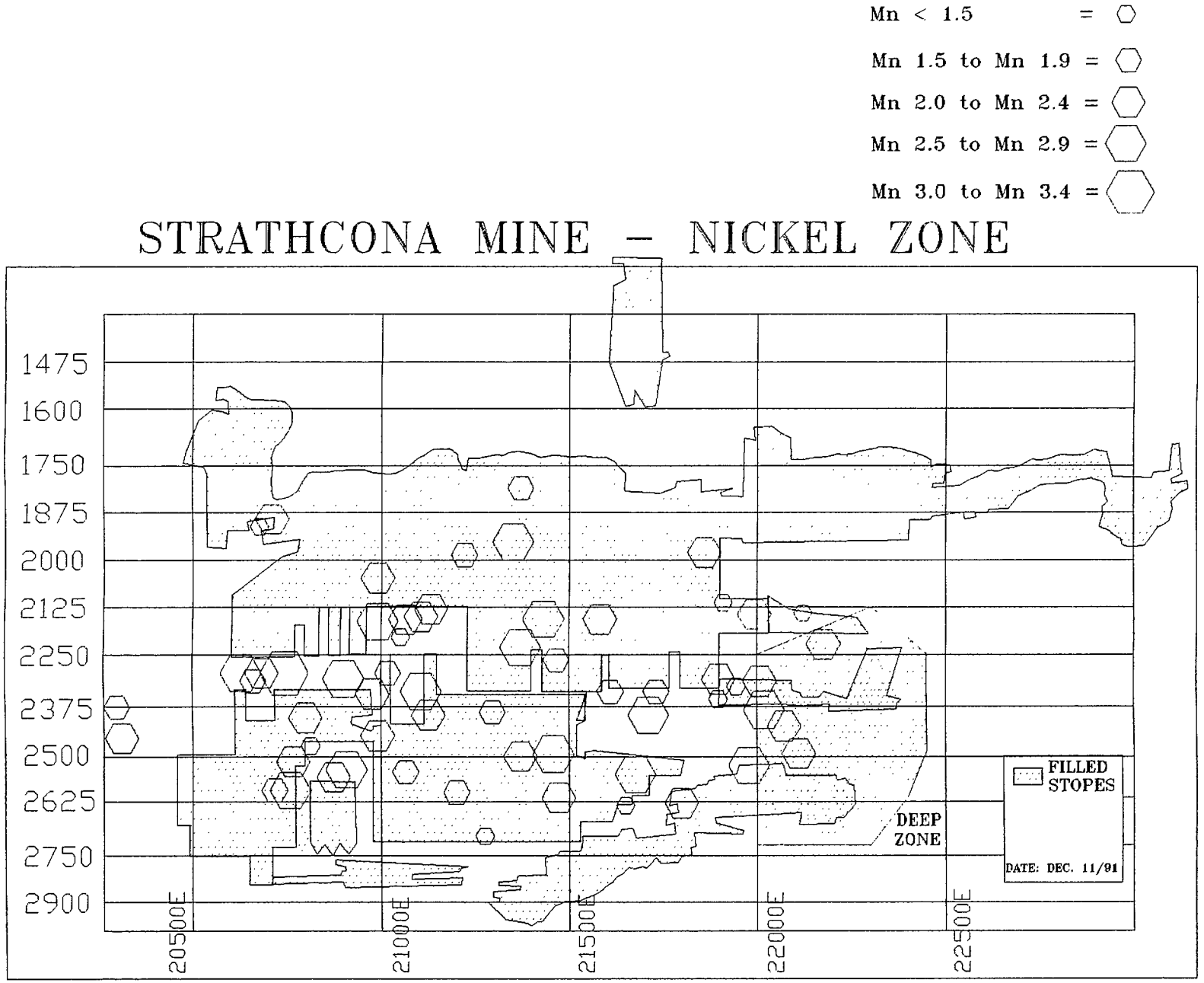

Fig. 10.5.1 - Longitudinal section, Strathcona Mine, showing partially mined main sill pillar and location/magnitude of major rockbursts from 1985 to 1991.

10.5.3 Developing a Strategy, 1985 to 1986

Throughout 1985, the rockburst incident rate continued to increase and focus in the main sill area of the mine, culminating in a 3.2 Mn burst on December 31. In order to keep pace, the microseismic system and data analysis software were continually upgraded and expanded to have 64-channel capability by early 1986. A special report form for the miners was devised and made available in all underground lunchrooms to be completed and submitted to ground control personnel at shift-end. With respect to ground control measures implemented at that time, the most notable were the introduction of expanded metal screens in drifts on intersections with olivine diabase dykes, and small-scale destressing of selected pillars comprising the sill. As a result of some NFOLD computer modelling, certain pillars were removed from the production plan and designated regional pillars. On the research side, two significant projects were initiated: development of a three-dimensional discontinuum model (3DEC) with ITASCA of Minnesota, and development of a full-waveform microseismic monitoring capability, including tomographic imaging of rock pillars, with the Engineering Seismology Group of Queen's University.

Following the event of 3.2 Mn, an assessment of damage on the 2200 level and 2300+40 level of the mine revealed a source of the activity to be violent slip on conjugate shear planes which connect with the diabase dykes referred to earlier. Most of the damage was confined to footwall areas of the main sill. Cable-lacing with cement grouted smooth bar eyebolts was now installed in critical footwall drift and ramp locations as part of the rehabilitation work of early 1986. The capacity of this support system to absorb seismic energy was demonstrated convincingly within six months of installation when a 3.0 Mn event occurred about 40 m away, following a production blast in the 23-226 blasthole stope. In unlaced areas, severe damage occurred with more than 1000 tonnes of displaced rock. In laced areas, the support system held and effectively contained the broken ground.

The mining strategy at this time was to adopt a conservative, flexible approach to ore recovery in the main sill, with high risk mining defined through increasing efforts to monitor and evaluate the seismic activity by the mine site Ground Control Department (comprising 3 people at that time) and

their consultants. This strategy was driven in response to the 32 recorded events in excess of 1.0 Mn which occurred throughout 1986 in the main sill area.

10.5.4. Rockburst Research, 1987 to 1990

Typical of the efforts made by late 1986 and in 1987 to evaluate and understand the rockburst mechanism was a discontinuum model of the 23-200 panel extraction sequence which included the various dykes and faults considered at the time to be associated with the problem. As a first attempt at applying complex three-dimensional discontinuum modelling to a mine design problem of this order, the findings were encouraging. For the first time, it was possible to investigate some of the mine-related factors which serve to enhance and to mitigate the mobilization of slip on identified structures.

A further example of research applied to the problem of rockburst mechanisms was the use of full waveform and seismic tomographic imaging techniques which began with the installation of the first Queen's Microseismic System (QMS) at Strathcona Mine in June 1987. This system was utilized during and after mining of the 23-233 and 25-143 blasthole sill pillars. The existing mine array of uniaxial accelerometers together with a special cluster of five triaxial accelerometers were used to monitor the activity. Examination of the full-waveform data showed that shear failure was the mechanism at the source of most events. Tomographic velocity images taken at intervals during the mining sequence showed small changes in velocity which appeared to correlate with microseismic activity.

For the period from 1987 to 1988, a total of 16 events in excess of 1.0 Mn were recorded in the main sill mining zones. By early 1988 annual production rates in the main sill had fallen from more than 1 million tonnes in 1986 to less than 350 thousand tonnes. This would likely account for the much reduced rate of 5 events in excess of 1.0 Mn for the first 5 months of 1988. In June, however, while developing the 23-233 blasthole overcut and mining the 25-143 blasthole stope, a widespread flurry of 20 relatively large seismic events (maximum 2.7 Mn) occurred. Damage to the overcut and access drifts was limited successfully by the cable-lacing in walls and backs. However, some

rehabilitation was necessary in areas where the support had sustained repeated hits from seismic events.

The June 1988 events were considered severe in the sense that a small mining change had produced a large, global response throughout the main sill. This conditionally stable state suggested the likelihood that further mining or reduction in load carrying area would cause renewed instability and uncontrolled bursting. On the other hand, it was also possible to argue that the June sequence, combined with past bursting, may have indicated that some areas of the main sill were now destressed and could be mined without inducing further bursting. This would most likely be the case in the long, slender pillars which remained in some parts of the sill.

In view of the perceived risks, no further mining of sill pillar zones was scheduled until a review of the problem has been completed by Falconbridge's Rock Mechanics Department in consultation with outside specialists and Ministry of Labour personnel. As part of this review process, a historical analysis of the complete MP250 database was made as a check on the integrity of event locations. Comparisons were made wherever possible with the Queen's Monitoring System full-waveform locations, that identified serious problems with non-events and erroneous arrival time picks with MP250 data. This work was important in giving greater confidence to the process of identifying spatial and temporal trends and patterns, in event activity. With respect to the modelling of these event trends and patterns a significant amount of work was still required before a calibrated and credible 3DEC simulation of the mining options could be achieved, if at all.

A modelling strategy was developed in early 1989 such that all identified major structures (10 in all) and an arbitrary division into 9 steps of previous sill mining activity, beginning late in 1984, would be incorporated into the 3DEC (Figures 10.5.2 a) and b)). Failure zones predicted by the model following each step would be compared with the reliable microseismic records. This strategy was reviewed by a panel of outside specialists well acquainted with Strathcona's rockburst problems, who agreed upon its validity as an acceptable calibration technique for assessing future mining options. The actual mining options to be evaluated by the model were provided by the

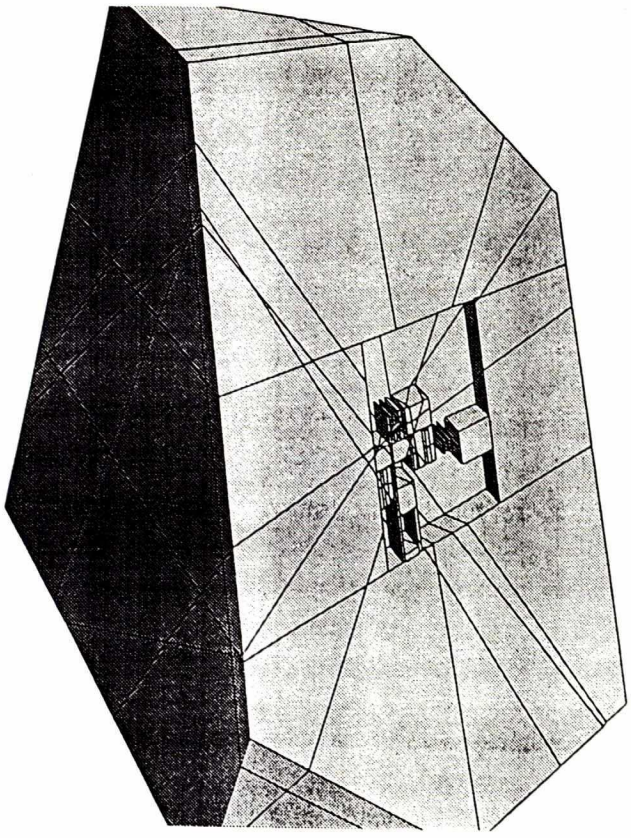

Fig. 10.5.2a - General 3DEC model of Strathcona Mine showing major fault and dyke sets.

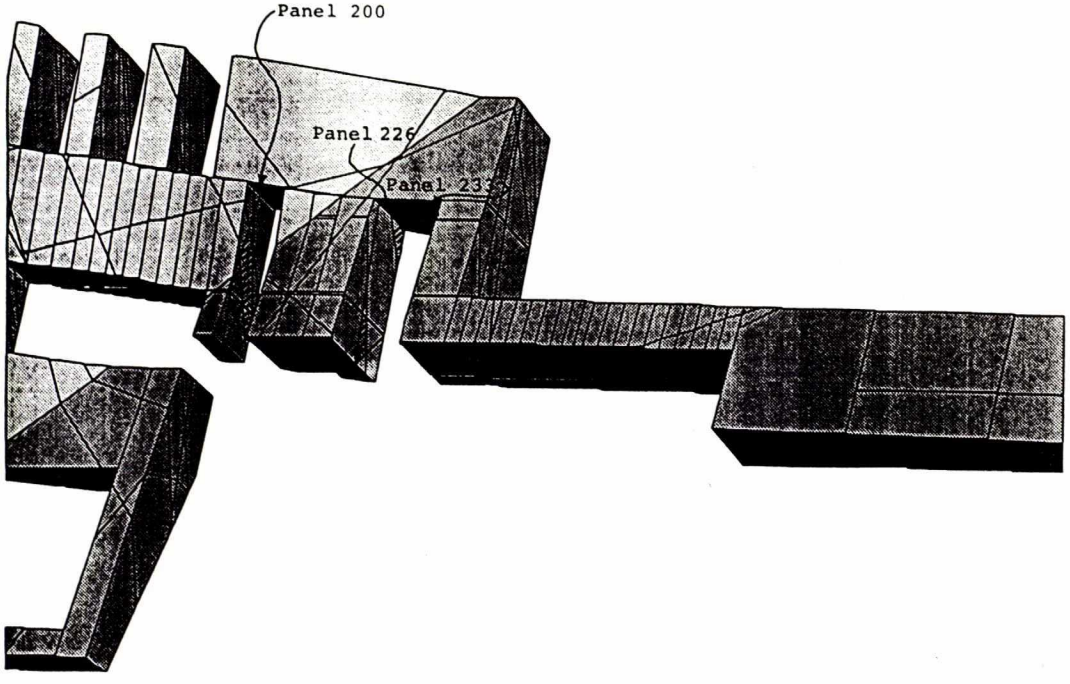

Fig. 10.5.2b - Detailed 3DEC model, central sill pillar area.

mine engineer on the basis of economics and mine design.

10.5.5 Final Recommendations, 1990 to 1991

Results from the 3DEC modelling work were made available in early 1990 in a report which concluded reasonably good success in the calibration process. However, while the model indicated that the sequence of proposed mining was important, the mechanisms influencing slip were not well enough known for the model to predict when features would slip. To some extent, answers to the mechanism question were being sought at this time in the microseismic data through research on fault-plane solutions and source mechanisms studies. Unfortunately, this is a long-term research subject with results requiring lengthy interpretation before application to a mine design exercise can be made. Of more immediate benefit to the sill mining decisions which Strathcona Mine faced at this time was the completion of a seismic velocity survey in March 1990 (Figure 10.5.3). This survey seemed to confirm the notion that areas in the sill which had experienced intense seismic activity in the past were, at the time of the survey, likely destressed, given that they consistently showed below average seismic velocities. Conversely, higher than average seismic velocities were seen in the footwall contact areas where microseismic activity was current. These observations together with the forward modelling capability of 3DEC offered a reasonable means of assessing the rockbursting potential of further sill pillar mining. This led to a decision in March 1990 to increase the mineable reserve by 40 thousand tonnes in the eastern regional pillar (25-39-D4 stope) with no change in the overall seismic risk of mining. The stope was subsequently mined and achieved budget in ore recovered before a 2.6 Mn rockburst occurred which forced a decision to shut down production permanently in the area.

By early 1991, a recommendation was available to proceed with mining in central pillars where all available evidence indicated a destressed state. These were specifically panels 25-207 to 25-220 in the lower main sill (Figure 10.5.2), and the western pillars nearby 25-143 stope. The fact that no further mining was attempted in these areas was a decision based more on economics than on risk for rockbursting. Unfortunately, at their current stage of development, the tools which were used at Strathcona Mine to evaluate

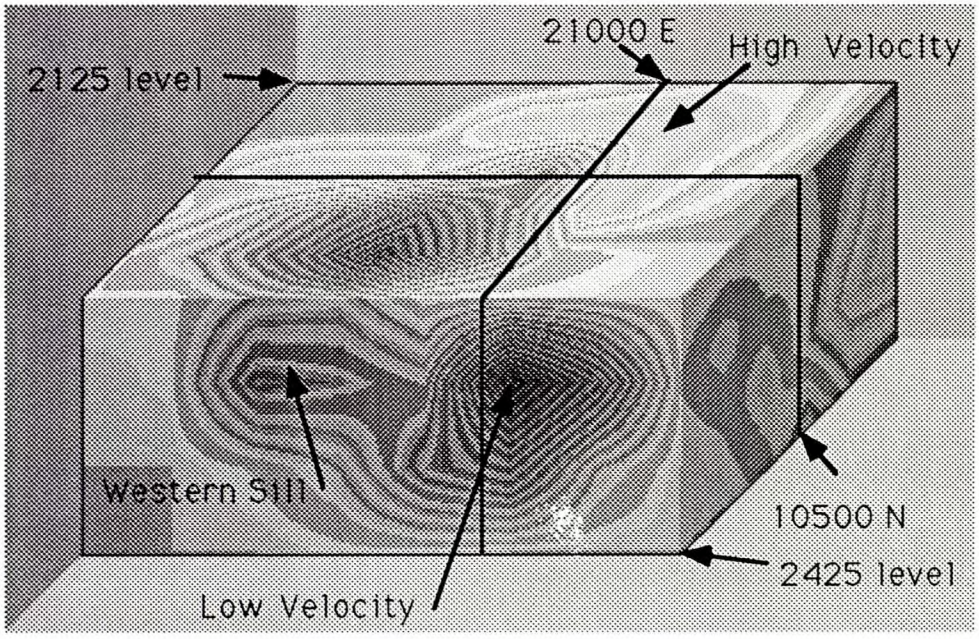

Strathcona Mine 3D Velocity Image

Queen's University, Engineering Seismology Laboratory

Fig. 10.5.3 - Three-dimensional isometric views of the main pillar velocity image. Velocities increase from dark (5.3 m/msec) to light (6.6 m/msec), Maxwell et al. (1991).

risk in mine design are extremely time-consuming. Every effort must now be made to improve on the efficiency of risk evaluation in order that decisions to mine or not to mine can be made on a time scale appropriate to production economics.

10.5.6 References

Bharti, S. (1985), Strategy to reduce the rockburst hazard at Strathcona Mine. Memo, dated February 19, 1985 to M. Musson and D.J. Cornett.

Bharti, S., Udd, J.E. and Cornett, D.J. (1983), Ground support at Strathcona Mine. CIM Symp. Underground Support Systems, Sudbury.

Blake, W. (1985), Visit report, Strathcona Mine, April 1985.

Blake, W. (1986), Visit report, Strathcona Mine, October 1986.

Blake, W. (1988), Visit report, Strathcona Mine, September 1988.

Blake, W. (1989), Visit report, Strathcona Mine, June 1989.

Davidge, G.R., Martin, T.A. and Steed, C.M. (1988), Lacing support trial at Strathcona Mine. Proc. 2nd Int. Symp. Rockbursts and Seismicity in Mines, Minnesota, June 1988.

Girard, N.A. and Steele, R.H. (1974), Rockburst and ground control at Strathcona Mine. Memo dated October 8, 1974 to K.H. Singh.

Hart, R. and Board, M. (1987), Development and testing of three-dimensional distinct element method - case study 1: Examination of fault slip induced rockbursting at the Strathcona Mine. Itasca Consulting Group report, October 1987.

Maxwell, S.C. (1989), Historical analysis of Falconbridge's Strathcona Mine microseismic activity. Report to Falconbridge Ltd.

Maxwell, S.C., Urbancic, T.I. and Young, R.P. (1991), Three-dimensional seismic tomography at Strathcona Mine. Final Report, Dept. Geological Sciences, Queen's University, February 1991.

Morrison, D.M. (1985), Review of seismic activity at Strathcona mine. Memo, dated January 16, 1985 to S. Bharti.

Morrison, D.M. (1987), Rockburst research at Falconbridge's Strathcona Mine. CIM Annual Meeting, Toronto, May 1987.

Semadeni, T.J. (1989), Minutes of sill pillar mining team meeting. Memo dated July 25, 1989.

Semadeni, T.J. (1990), Mining of eastern regional pillar at Strathcona Mine. Memo dated March 23, 1990 to D.J. Cornett et al.

Singh, K.H. (1975), Ground control and rockburst conditions at Strathcona Mine. Internal Report, Falconbridge Ltd., November 1984.

Tinucci, J.P. and Hart, R.D. (1990), Development and testing of the three-dimensional distinct element method - case study 5: Examination of mining-induced seismic events at the Strathcona Mine. Itasca Consulting Group report. January 1990.

Udd, J.E. (1984),Shock disturbances, rockbursts and falls of ground recorded at Strathcona Mine from November 1977 to date. Memo, dated April 12, 1984 to S. Bharti.

10.6 Inco's Creighton Mine, Sudbury

10.6.1 Summary

Creighton Mine has a history of rockbursts dating back to the early 1930s. In recent years the three largest magnitude rockbursts in Ontario have occurred in this mine. The orebodies at Creighton Mine are large and extend to a depth in excess of 2200 m, with high in situ stresses. At depth, mining was mainly by cut-and-fill techniques until recently with the conversion to vertical retreat mining with delayed backfill.

Rockbursts are a problem in crown pillar situations. However, some of the largest rockbursts have also occurred in the hanging wall and footwall, apparently along prominent geological structures. Rockburst control measures include destress blasting and sequencing of extraction to minimize the crown pillar problems.

10.6.2 Mining Background

Creighton Mine is located on the southern rim of the Sudbury Basin. Disseminated and massive sulphide orebodies are present in the lower sublayer of the hanging wall norites. Footwall rocks are mainly granite and gabbro. Quartz diorite and lamporphyre dykes are also encountered. The orebodies, although interconnected, are irregular in shape and size with an overall dip of 65° to the northwest. A generalized cross-section through the mine is illustrated in Figure 10.6.1, showing the major shafts and levels. Mining extends to a depth of about 2200 m, making it the deepest operating mine in Canada.

The mine began operations in 1901. Over its 90 years of production many mine methods have been used, including open pit, shrinkage, blasthole, panel caving, square set, overhand and undercut-and-fill, and vertical retreat blasthole methods. Present day production is concentrated between the 5000 and 7200 levels (1500 to 2200 m depth) and is almost totally vertical retreat mining with delayed backfill.

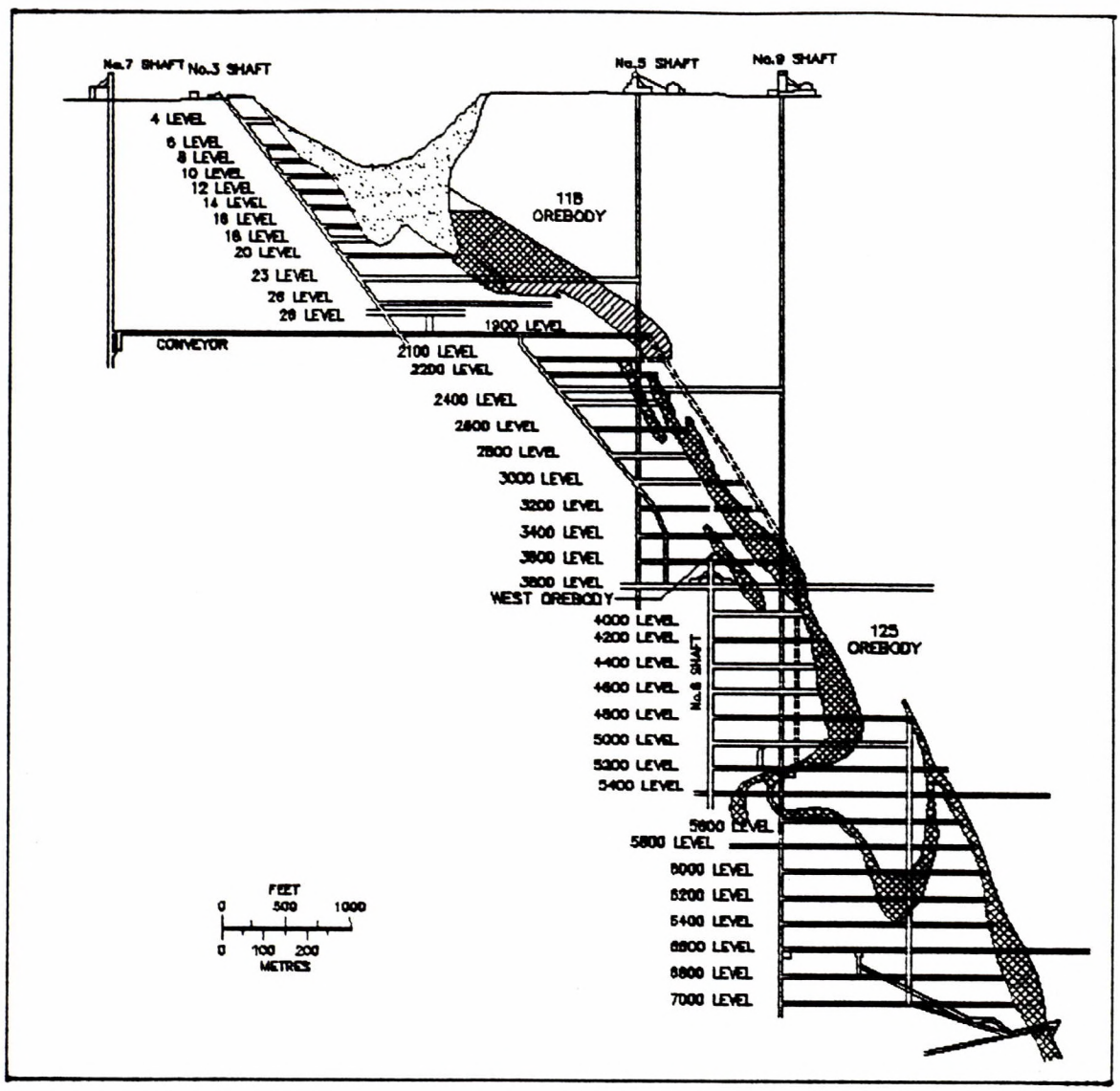

Fig. 10.6.1 - A general cross-section through Creighton Mine.

10.6.3 Rockburst History

The first recorded rockburst at Creighton Mine was in 1934 at a depth of 700 m. Three transitional zones for rockburst occurrences have been identified (Oliver et al., 1987). Below a depth of 700 m, bursts occurred in crown and remnant pillars. Bursts in isolated development openings began to occur below a depth of 1200 m. Finally, at a depth of 2000 m, bursts started in silling operations at the beginning of production from a level.

Rockbursts have also been classified into 'inherent' and 'induced' categories. Inherent, in that, in situ stresses were high enough to cause bursts during the development stage. Induced bursts were caused by the mining operations. These tended to occur in pillars after 60 to 70% extraction in a mining block. This was followed by induced bursts in adjacent development openings. Finally, near the end of mining in the block, induced unlocated bursts would occur in the wall rocks. Initially, these bursts were thought to occur on the periphery of major pressure domes, but more likely were occurring along geological structures.

Since 1934, the mine has recorded and investigated almost 1100 rockburst incidents. Since 1984, rockbursts have been classified by magnitude, similar to other mines in Ontario. During an eight-year period, there have been 71 rockbursts at Creighton Mine of magnitude 2.0 Mn or greater. Also during this time, the three largest rockbursts in Ontario mines, of magnitudes of 3.6, 3.7 and 4.0 Mn, have all occurred at the Creighton Mine.

In 1984, there was a multiple rockburst sequence at Creighton Mine during the summer shut-down. It was initiated by a 4.0 Mn event located a few hundred metres into the hanging wall between the 3400 and 4000 levels (1030 to 1220 m depth). In the following 90 minutes, five smaller rockbursts (2.1 to 2.5 Mn) occurred in the footwall development drifts on the 3200 to 4000 levels, and some several hundred metres from the first large event.

The other major rockbursts, since 1984, have all occurred in the lower levels around the active mining zones.

The frequency/magnitude relationship for rockbursts at Creighton Mine is shown in Figure 10.6.2, for the years 1984 to 1991. The gradient of the frequency curve is just under 1.0 and similar to that for naturally occurring earthquakes. This would suggest that a shearing mechanism, either along geological structures, or through intact rock, is the driving force. The recurrence time for rockbursts of varying magnitudes over the eight-year period is also plotted in Figure 10.6.2. On average, a rockburst of at least a magnitude of 2.0 Mn occurs about once a month, and a magnitude of at least 3.0 Mn occurs about once a year.

10.6.4 Seismic Monitoring

The first microseismic system in Ontario was installed at the Creighton Mine in 1980. It consisted of a 16-channel Electro-Lab MP-250 system. Subsequently, the system was expanded to 48 channels and covered the 5400 to 7000 levels. The series of rockbursts in 1984, at higher levels in the mine, resulted in a further expansion to 64 channels and an extended coverage to the 3200 level (Oliver and MacDonald, 1985). This system is called the mine-wide array, and on average, records 80 microseismic events per day, which reduces to half at weekends.

In 1989, a second 64-channel microseismic system was installed in a dense array covering the active mining workings between the 6600 and 7200 levels. This array generally records 300 events per day, which again reduces to half at weekends.

In addition to these microseismic systems, both CANMET and the Department of Geological Sciences at Queen's University have installed seismic systems to record complete waveforms. The former system is designed to record the larger seismic events, while the latter records smaller events.

The locations of the major rockbursts over a magnitude of 2.0 Mn, recorded in 1985 to 1991, are plotted on a cross-section of the lower levels in Figure 10.6.3. Most of these rockbursts have occurred in and around the 400 orebody. There is an especially heavy concentration which includes those over a magnitude of 3.0 in the crown pillars below the 6600 and 6800 levels.

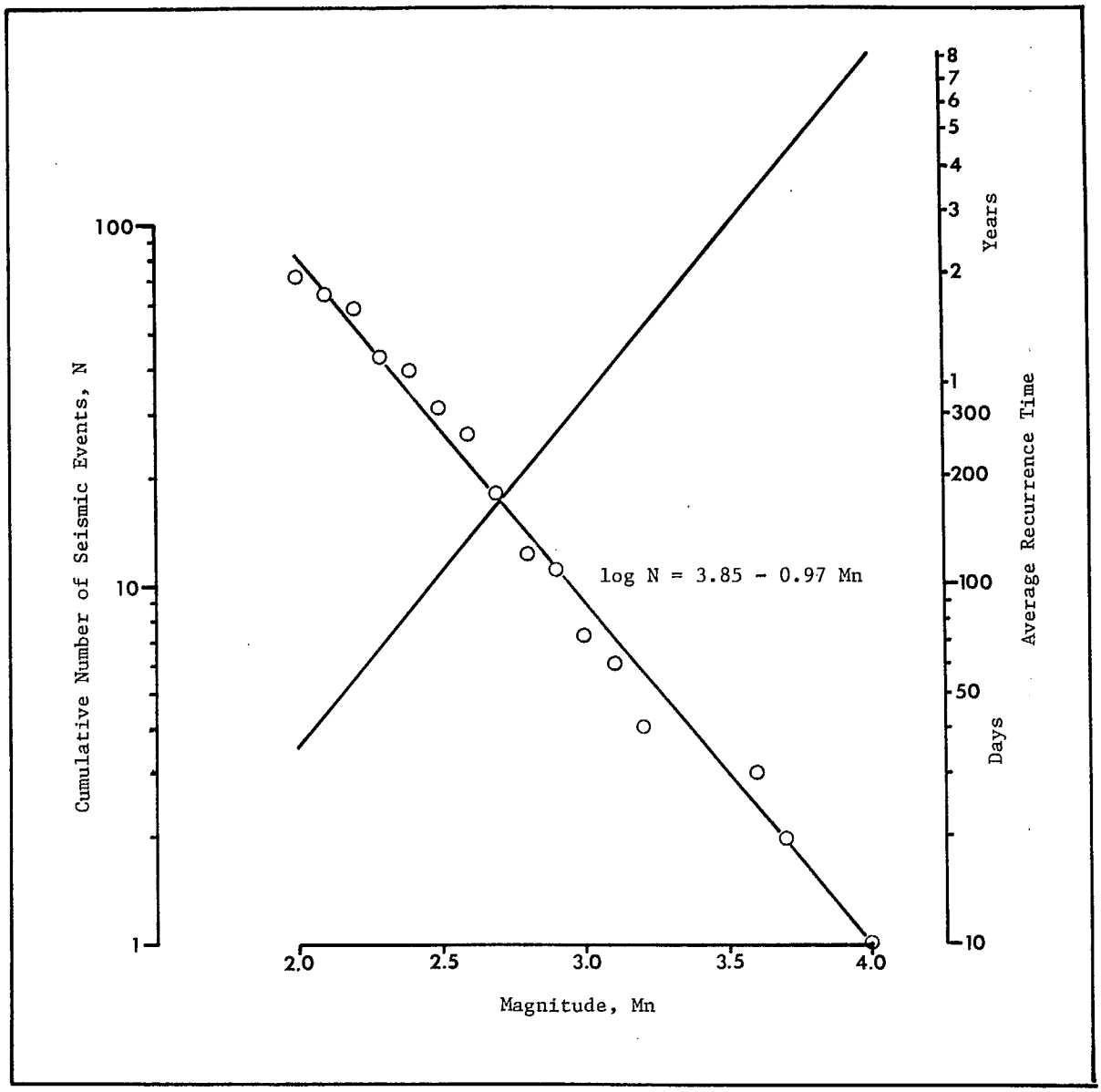

Fig. 10.6.2 - Frequency of occurrence and recurrence time relationships with magnitude for Creighton Mine over the period from 1984 to 1991.

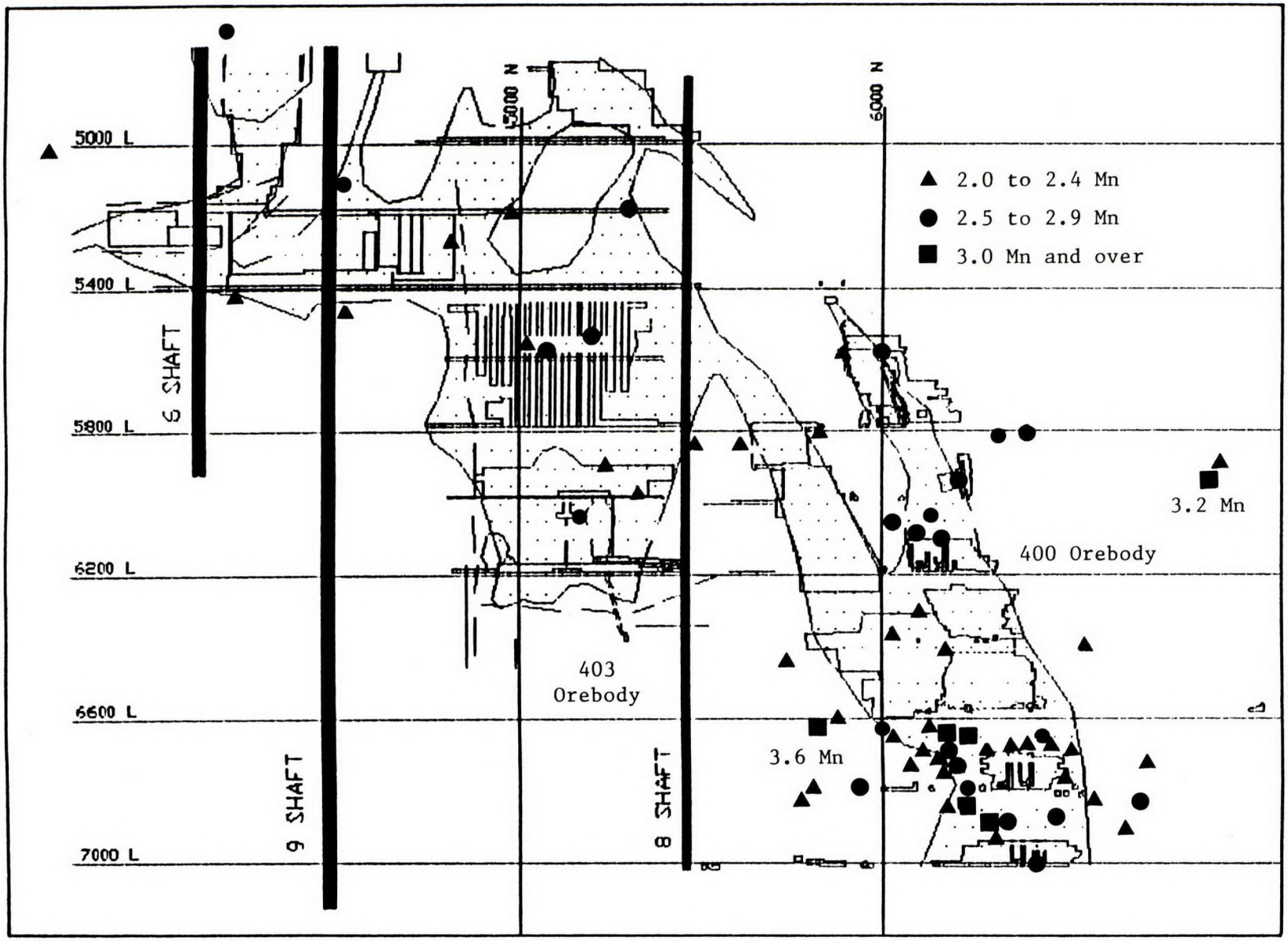

Fig. 10.6.3 - Generalized cross-section of the lower levels at Creighton Mine, showing locations of the major rockbursts from 1985 to 1991.

However, there are a number of events occurring out in the footwall and hanging wall, including two of magnitude 3.2 and 3.6 Mn. The 403 orebody, which is at right angles to the 400 orebody, is less seismically active, and the largest recorded rockburst had a magnitude of 2.7 Mn on the 5600 level.

10.6.5 Rockburst Control Measures

The measures developed at Creighton Mine to combat the rockburst problem, have been described by Dickout (1957 and 1962), and by Oliver, et al., (1987). They covered rockbursts in development openings, including shafts and stoping operations. The general concept was that, because of the high stress conditions, a skin of broken rock was required around mine openings to act as a cushion, and that pillars should be made weak so that they failed non-violently at low stress levels.

Initially, development drifts were supported with timber or steel sets with wood lagging between sets. This practice changed in the early 1960s with the introduction of steel mesh with rockbolts, destress blasting and the conversion from dynamite to ANFO. Steel mesh allowed the use of mechanical bolts to support the back and walls. The mesh contains the broken rock around the opening and prevents fly material from being ejected by rockbursts.

Destress blasting techniques in development openings has been described in Section 8.4. At Creighton Mine, below 6000 level, two destress holes were drilled in the face, and two angled corner holes in the roof. Below the 7000 level two additional corner holes were drilled in the floor.

When dynamite was being used, the charges were decoupled which resulted in a type of cushion blasting. This tended to leave relatively smooth unfractured and highly stressed walls. The hole is completely loaded with ANFO explosive which produces considerable fracturing of the wall rocks.

When rockburst problems were encountered in shafts, round lengths were decreased, the bottom of the shaft was blasted in a concave shape and bolts, mesh and concrete lining were kept as close to the bottom as possible. In one case a rectangular shaft was converted to a semi-elliptical shape. All recent

shafts are circular and are concrete lined. When rockbursts are encountered, benching is adopted, whereby one half of the shaft advances ahead of the other. Destress blasting has also been used.

A square-set method, with water-borne sand as backfill, was used when rockbursts became a problem in stoping operations. Major rockbursts tended to occur when the stopes approached the mined-out level above. An inverted 'V' sequence of extraction was developed, as illustrated in Figure 10.6.4a), whereby, a lead stope, near the centre of the orebody, was first advanced into the level above. This did not eliminate rockbursts, but reduced their severity. The other stopes could then be mined through to the level without undue problems. An inverted 'V' sequence was also followed in recovery of the rib pillars.

The introduction of cemented backfill in the 1960s eliminated the need for square-sets, although the sequence of extraction was still maintained. At that time the equipment was captive within each stope. In the 1970s, mobile mechanized equipment was introduced and several stopes were interconnected which meant that they had to be at the same elevation. A modified sequence of extraction was adopted, as illustrated in Figure 10.6.4b). Rockbursts in the crown pillars became a problem, especially when the orebody was less than 30 m wide, and the stopes had advanced within 20 m of the level above.

The concept of a lead stope was reintroduced below the 6600 level, as illustrated in Figure 10.6.4c). In this case, the mechanized cut-and-fill stopes from all the 6800 level were advanced about 30 m, then a vertical slot was blasted near the centre of the orebody, between hanging wall and footwall, using vertical retreat methods (VRM). The rest of the crown pillar was also mined by the same techniques, retreating from the central slot.

With the complete conversion from cut-and-fill to VRM mining, the initial slot from level to level is still located near the centre of the orebody. In addition, lacing support techniques are now being installed in burst-prone development openings and shotcrete is being used in stope development on the lower levels (i.e., 7000 and 7200).

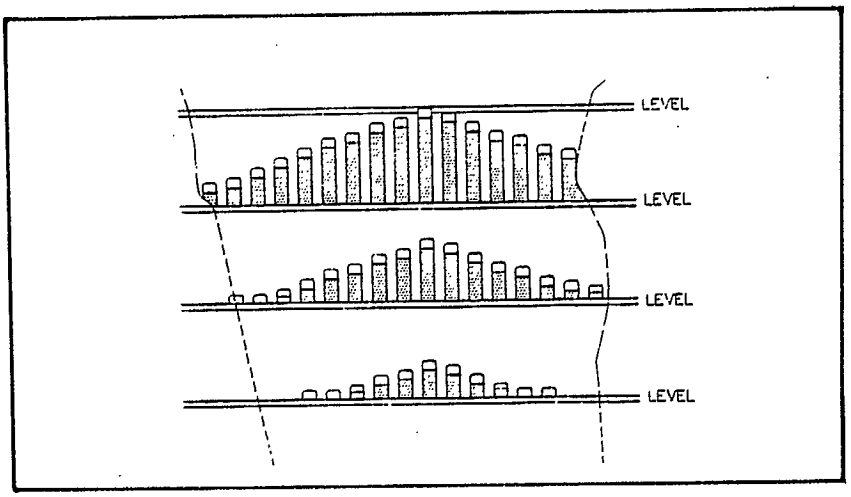

a) Inverted 'V' sequence for transverse cut-and-fill mining.

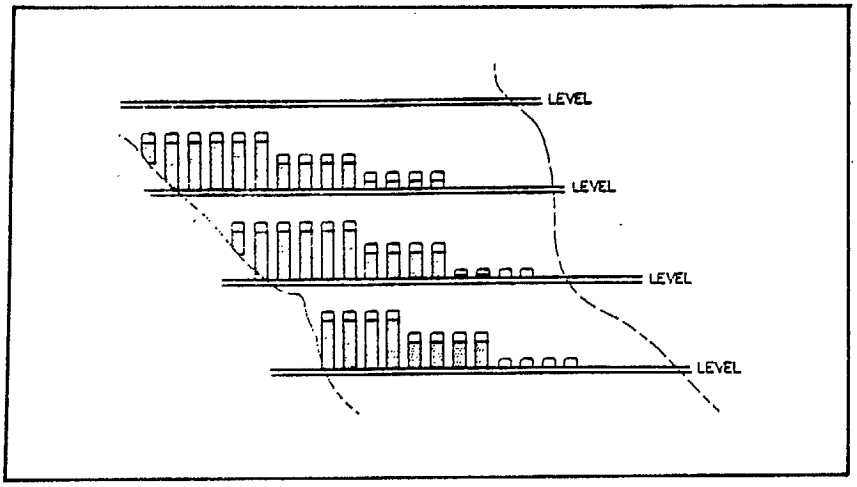

b) Modified sequence for mechanized cut-and-fill mining.

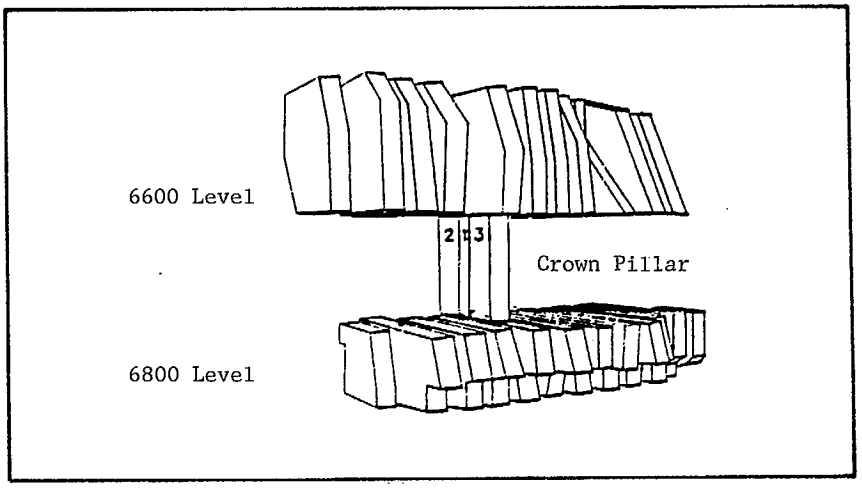

c) Central slot through crown pillar.

Fig. 10.6.4 - Variations in mining sequence at Creighton Mine (after Oliver et al., 1987).

10.6.6 References

Dickout, M.H. Rockburst control at the Creighton Mine of the International Nickel Company of Canada Limited; Proc. 6th Commonwealth Mining and Metallurgical Congr., Canada, pp. 385-388; 1957.

Dickout, M.H. Ground control at the Creighton Mine of the International Nickel Company of Canada Limited; Proc. 1st Can. Rock Mech. Symp., McGill University, Montreal, pp. 121-129; 1962.

Oliver, P.H. and MacDonald, P. The microseismic monitoring system at Creighton Mine, Inco Limited. Proc. 4th Conf. Acoustic Emission/Microseismic Activity, Penn State University; 1985.

Oliver, P.H., Wiles, T., MacDonald, P. and O'Donnell, D. Rockburst control measures at Inco's Creighton Mine; Proc. 6th Conf. on Ground Control in Mining, West Virginia; 1987.